

## PETROGRAPHIC EXAMINATION REPORT

---

<b>Client:</b>	Pennoni Associates, Inc.	<b>Client ID:</b>	PENN003
<b>Project:</b>	I-95 Viaduct Project	<b>Report #:</b>	SL0845-01
<b>Location:</b>	Delaware	<b>Dates Received:</b>	12/15/14, 01/07/15, 01/14/15
<b>Sample Type:</b>	Concrete cores	<b>Report Date:</b>	02/14/15
<b>Delivered by:</b>	Client (M. Padula)	<b>Petrographer:</b>	J. Walsh
		<b>Analyst:</b>	M. Pattie

---

**Page 1 of 34**

### Report Summary

- This report presents the results of petrographic examination and air-void analysis on six concrete core samples taken from viaduct structures along I-95 near Wilmington, DE.
- All examined concrete is similar in composition and appears to represent a single mix design. The material is a normal weight, portland cement concrete with no supplementary cementitious materials. Original water to cement ratios are estimated to have been moderate within the mid to high 0.4's. Cores 744NB-1P, 744SB-1P, and 745NB-1P are estimated at the higher end of this range. Five of the six cores exhibit air structures consistent with intentional air-entrainment. No air-entrainment is identified in Core 746SB-1P. The northbound cores have air structures with appropriate spacing factors and specific surfaces. The air in the southbound cores is considered somewhat deficient. Coarse aggregates include a variety of amphibolites and associated granofels as primary components. Granitoids or diorites are a lesser to minor constituent. Gradations are consistent with a No. 56 or No. 57. The fine aggregates appear identical and are identified as coarse-grained natural quartz sands with several percent ferruginous chert.
- All concrete materials are well mixed, cast, and consolidated. No obvious workmanship deficiencies are identified unless the variations in air-entrainment were caused by poor handling. It is also assumed that the concrete was designed with the moderate water to cement ratio and the mixtures were not overwatered at the job site. The only minor deficiency is the migration of bleed water and its partial entrapment below aggregate surfaces in Core 746SB-1P. The propensity for increased bleed may have been caused by the absence of entrained air in this sample.
- The concrete represents a moderate quality mixture suitable for many normal-duty, non-aggressive service environments. However, the poor air development in the southbound cores leaves this concrete susceptible to freeze-thaw distress. The only existing distress in the examined samples includes axial microcracking related to early stage alkali-silica reactions. These are noted throughout the full depth of Core 744SB-1P and the uppermost sections of Cores 745NB-1P and 746NB-1P. The offending aggregate includes the quartz-rich granofels as well as the granitoids. Isolated reaction is also identified in the chert present in the fine aggregate and this is observed in all cores even if only in trace amounts. The reactions have not compromised the integrity of the concrete and no imminent threat is suggested by the existing conditions. Though no mitigating factors are identified, the concrete may remain provisionally stable over the course of a normal life cycle. However, this cannot be guaranteed and continued reaction may proceed at a relatively slow rate.
- A more detailed discussion of these findings may be found in the "Petrographic Findings and Discussion" section on page 3 of this report.

## **1. Introduction**

On December 15, 2014, and January 7 and 14, 2015, Highbridge received a total of twenty-seven (27) concrete core samples from Mr. Michael Padula of Pennoni Associates, Inc. reported to have been taken from viaduct structures along I-95 near Wilmington, DE. At the client's request, testing is performed on the structural layers of all core samples. No testing is requested for any wear courses present. For each sample, petrographic examination is requested to identify constituents, evaluate condition, and investigate the potential causes of any observed distress. No specific emphasis is requested and a general comprehensive examination is performed. Quantitative air-void analysis is also requested for the same samples.

Results for six of the core samples are presented in this report. Results for other sample batches are presented under separate cover. This report presents the results for the following cores:

744NB-1P

744SB-1P

745NB-1P

745SB-1P

746NB-1P

746SB-1P

## **2. Methods of Examination**

The petrographic examination is conducted in accordance with the standard practices contained in ASTM C856. Data collection is performed by a degreed geologist who by nature of his/her education is qualified to operate the analytical equipment employed. Analysis and interpretation is performed or directed by a supervising petrographer who satisfies the qualifications as specified in Section 4 of ASTM C856.

Air-void analysis is performed in accordance with the point-count method of ASTM C457. Component point counts are performed on hand-lapped concrete slabs sliced parallel to the core axis. The analysis is performed at a magnification of 75x on a Bausch and Lomb Stereozoom microscope and a dedicated cross-slide table machined to produce 0.05 inch translations per count. Air-void percentages are presented as those whose two-dimensional cross sectional diameter are less than or greater than one millimeter. The one millimeter diameter is considered a reasonable distinction between voids that are entrained and those that are entrapped in concrete that has been air-entrained. It should be understood that this threshold is somewhat arbitrary.

## **3. Standard of Care**

Highbridge has performed its services in conformance with the care and skill ordinarily exercised by reputable members of the profession practicing under similar conditions at the same time. No other warranty of any kind, expressed or implied, in fact or by law, is made or intended. Interpretations and results are based strictly on samples provided and/or examined.

## **4. Confidentiality**

This report presents the results of laboratory testing requested by the client to satisfy specific project requirements. As such, the client has the right to use this report as necessary in any commercial matters related to the referenced project. Any reproduction of this report must be done in full. In offering a more thorough analysis, it may have been necessary for Highbridge to describe proprietary laboratory methodologies or present opinions, concepts, or original research that represent the intellectual property of Highbridge Materials Consulting and its successors. These intellectual property rights are not transferred in part or in full to any other party. Presentation of any or all of the data or interpretations for purposes other than those necessary to satisfy the goals of the investigation are not permitted without the express written consent of the author. The findings may not be used for purposes outside those originally intended. Unauthorized uses include but are not limited to internet or electronic presentation for marketing purposes, presentation of findings at professional venues, or submission of scholarly articles.

## **5. Petrographic Findings and Discussion**

### **5.1 - General Summary**

This report presents the results of petrographic examination and air-void analysis on six concrete core samples taken from viaduct structures along I-95 near Wilmington, DE. The study includes only the substrate concrete layers and not the 1.5" to 3" thick wear courses adhered to all of the samples.

All examined concrete is similar in composition and appears to represent a single mix design. The material is a normal weight, portland cement concrete with no supplementary cementitious materials. Original water to cement ratios are estimated to have been moderate within the mid to high 0.4's. Cores 744NB-1P, 744SB-1P, and 745NB-1P are estimated at the higher end of this range. Five of the six cores exhibit air structures consistent with intentional air-entrainment. No air-entrainment is identified in Core 746SB-1P. The northbound cores have air structures with appropriate spacing factors and specific surfaces. The air in the southbound cores is considered somewhat deficient. Coarse aggregates include a variety of amphibolites and associated granofels as primary components. Granitoids or diorites are a lesser to minor constituent. Some variations are found in these lithologies such that Cores 745SB-1P and 746SB-1P appear to contain a somewhat different batch of stone. The other four are more similar though some notable differences are found in Cores 744NB-1P and 744SB-1P. The first group has a gradation consistent with a No. 56. The others have gradations closer to a No. 57. The fine aggregates appear identical and are identified as coarse-grained natural quartz sands with several percent ferruginous chert.

All concrete materials are well mixed, cast, and consolidated. No obvious workmanship deficiencies are identified unless the variations in air-entrainment were caused by poor handling. It is also assumed that the concrete was designed with the moderate water to cement ratio and the mixtures were not overwatered at the job site. The only minor deficiency is the migration of bleed water and its partial entrapment below aggregate surfaces in Core 746SB-1P. The propensity for increased bleed may have been caused by the absence of entrained air in this sample.

The concrete represents a moderate quality mixture suitable for many normal-duty, non-aggressive service environments. However, the poor air development in the southbound cores leaves this concrete susceptible to freeze-thaw distress. The only existing distress in the examined samples includes axial microcracking related to early stage alkali-silica reactions. These are noted throughout the full depth of Core 744SB-1P and the uppermost sections of Cores 745NB-1P and 746NB-1P. The offending aggregate includes the quartz-rich granofels as well as the granitoids. Isolated reaction is also identified in the chert present in the fine aggregate and this is observed in all cores even if only in trace amounts. The reactions have not compromised the integrity of the concrete and no imminent threat is suggested by the existing conditions. Though no mitigating factors are identified, the concrete may remain provisionally stable over the course of a normal life cycle. However, this cannot be guaranteed and continued reaction may proceed at a relatively slow rate.

## 5.2 - Materials

All cores contain a siliceous crushed stone coarse aggregate estimated at approximately 35-40% by hardened concrete volume. Cores 744NB-1P and 746NB-1P have aggregate contents closer to the lower end of this range. The stone in all appears genetically related though Cores 745SB-1P and 746SB-1P should be set aside as having a slightly different lithology. Core 744SB-1P may also be considered slightly different than the other five. The predominant rock types are amphibolites that are interpreted to represent metabasites (i.e. metamorphosed gabbros or basalts). Grains that are best described as leucocratic schistose granofels exhibit a gradation of lithological characteristics that link them to the amphibolites. Subordinate igneous rocks are detected in all but Core 744NB-1P. These include medium-grained granitoids in Cores 744SB-1P, 745NB-1P, and 746NB-1P. In Cores 745SB-1P and 746SB-1P, diorites or quartz diorites are identified instead.

The amphibolites in four of samples are mostly amphibolite schists rich in either actinolite or hornblende (i.e. Cores 744NB-1P, 744SB-1P, 745NB-1P, and 746NB-1P). Plagioclase feldspar and strained quartz are also major components. Fewer particles represent lower metamorphic grade likely within the prehnite-pumpellyite facies. Only one grain observed petrographically in Core 744NB-1P contains relict orthopyroxene and clinopyroxene. Some microscopic vugs are detected in a single particle from Core 745NB-1P. These two trace textures suggest that the amphibolites are metamorphosed gabbros and/or basalts. Some epidotized material is present in all four samples. Minor sulfide phases are found in association with the amphibolites. These are more prevalent in Core 744NB-1P and not really significant in the other three samples. The sulfide is either pyrite or pyrrhotite but these are not differentiated in this study. A less abundant lithology associated with the amphibolites may be classified as a schistose granofels. This type of grain is relatively abundant in Core 744SB-1P. These are variable in appearance but tend to be rich in a fine-grained matrix of highly sheared quartz with or without distributed amphibole. Porphyroclasts of feldspar, quartzite, and micaceous material are also included in some grains.

Cores 744SB-1P, 745NB-1P, and 746NB-1P also contain a granitic rock as a minor component of the coarse aggregate. Feldspar and quartz are major components and the granitoid is unusually rich in interstitial material. The latter includes graphic intergrowths of quartz and feldspar as well as regions of strained quartz characterized by multiple fine subgrains. Accessory minerals in the granite include chlorite, biotite, amphibole, and epidote. None of the granitic material is positively identified in Core 744NB-1P.

Cores 745SB-1P and 746SB-1P have similar coarse aggregate types but clearly represent a different batch of material. The amphibolite schists in these samples are richer in chlorite and many represent lower metamorphic grade than those in the other four cores. Less of the purer amphibolite schists are present overall and the schistose granofels are much more common. Still, these tend to be richer in amphibole, chlorite, and minor biotite. Nonetheless, the sheared quartz matrix is still common. The granitoid lithologies are not present in these two cores. Instead, a more basic igneous rock is detected in trace abundance. In Core 745SB-1P, this is a quartz diorite including quartz and feldspar with accessory pyroxene, amphibole, and opaque phases. Some of the pyroxene appears to be replacing olivine. In Core 746SB-1P, the rock is a diorite rich in plagioclase feldspar. Orthopyroxene and possibly some relict olivine are present as accessories. Quartz is absent from this rock.

From a physical perspective, the stone in all six cores is considered hard, inelastic, and non-porous. Though the amphibolite schists have a strongly directed lineation, these are not identified as a significant preferential weakness. The lithological types are not among the list considered to be particularly alkali-silica reactive. Nonetheless, some evidence for reaction is noted in three of the samples. The strained quartz is likely the more reactive component within the stone. These features are discussed in greater detail below.

The coarse aggregate shapes are all angular to subangular. Grains are subequant on average with a moderate proportion of plate-like particles having aspect ratios in the 3:1 to 4:1 range. The presence of anisotropic grains is not significant and the particle shapes are suitable for aggregate to be used in portland cement concrete mixtures. The gradations cannot be quantified petrographically and the particle size distributions are estimated from two-dimensional cross sections of the concrete. It is noted that the darker amphibolites are more often at the coarser end of the gradation profile. The mottled granofels, granitoids, and diorites are somewhat finer on average. The northbound cores all have gradation profiles likely compliant with a No. 57 as specified by ASTM C33 though a No. 6 is also possible. The nominal top sizes are estimated at the 3/4" sieve with profiles that are rich over the 1/2" mesh and having relatively little passing the 3/8" sieve. The aggregate in Core 744SB-1P would likely comply with the same No. 57 or No. 6 gradation profile. However, a moderate proportion of

grains are estimated to pass the 3/8" sieve in this sample and the particle size distribution is broader. The aggregate in Cores 745SB-1P and 746SB-1P has a slightly different gradation than the other four and this is consistent with the different lithologies present in these two samples. The nominal top size is estimated at the 3/4" sieve with possibly greater than 85% of the material retained on the 1/2" sieve. A No. 56 gradation profile as specified by ASTM C33 is considered most likely for these samples. A No. 57 would require more than 25% passing the 1/2" mesh and this does not appear to be the case in either core.

In contrast to the subtle variations identified in the coarse aggregate, the fine aggregate observed in the six cores appears to be more or less identical in composition and quality. The material is a natural quartz sand estimated at 40-45% by hardened mortar fraction though likely at the lower end of this range. The material is predominantly monocrystalline quartz with lesser polycrystalline quartz and alkali feldspar. Mildly to moderately strained quartzite is a minor constituent. A minor but significant amount of ferruginous chert is included in all samples at several percent of the total sand volume. Some of the ferruginous particles appear to include siltstones or argillites as well. However, their texture under reflected light suggests that all are cemented by a cryptocrystalline silicification. Both the chert and the strained quartzite are more concentrated in the grain sizes coarser than the No. 8 sieve. Heavy accessory minerals are rare in the sand. Trace glauconite is only detected in Core 746NB-1P. No clay coatings or friable materials are identified. From a physical perspective, the sand is considered hard, inelastic, and non-porous. Chemically, the chert in the coarser sizes is considered potentially alkali-reactive and this could represent a modest durability concern.

The sand in all six samples consists of equidimensional particles that are subangular to subrounded in shape. Based on the qualitative petrographic observations, the particle size distributions are estimated to comply with the gradation requirements of ASTM C33. However, these are likely near the coarser size limits of the current standard. The nominal top sizes are estimated at the No. 4 sieve. In all cases, the particle size distributions are rich above the No. 30 sieve with little estimated to pass the No. 50 mesh.

Ordinary gray portland cement is identified as the sole binder in the six examined samples and no supplementary cementitious materials are present. Liquid admixtures cannot be identified petrographically though their influence on paste microstructure can often be detected. It is not clear whether or not any water-reducing admixtures had been added. The cementitious hydrate in Cores 744SB-1P and 745NB-1P has a microscopically "clotted" texture. This is usually attributed to cement particle flocculation in mixtures not containing plasticizers. However, the texture is not diagnostic. In fact, the clotting only occurs in the cores for which some alkali-silica reaction has occurred. This may indicate that the feature represents a secondary effect on the cementitious hydrate. The paste in the other four cores is more uniform at the microscopic scale. The size and distribution of spherical air-voids indicates that all but the concrete in Core 746SB-1P was intentionally air-entrained. There is some variability in the development and quality of the air system between these five samples.

All concrete is estimated to have been mixed at a moderate water to cement ratio (w/c). Though the ratios cannot be quantified petrographically, cement paste characteristics are consistent with w/c in the mid to high 0.4's. Based on minor differences in the microporosity of the hardened binder as well as subtle visual differences in color and luster of the hydrated paste, Cores 745SB-1P, 746NB-1P, and 746SB-1P contain concrete estimated to have been mixed with w/c closer to the mid 0.4 range. The other three concretes are interpreted to have been mixed at a relatively higher water content though the differences in most microstructural characteristics appear relatively minor. Nonetheless, it is interesting to note that the samples with lower estimated w/c coincide with the three core groups for which at least one sample yielded a compressive strength over 6000 psi. This is based on data provided by the client.

The characteristics used to estimate original water to cement ratio include the capillary porosity of the cured cementitious hydrate. The capillary pore structure is produced by the evaporable water present in the fresh mixture. As described above, Cores 744SB-1P and 745NB-1P have cementitious product that has a microscopically clotted texture with denser clots surrounded by paste with moderately high capillary porosity. Despite the lower porosity zones, the permeability is controlled by the more porous regions. Core 744NB-1P has a uniform hydrate but still one with a moderate to moderately high capillary porosity. The slightly higher capillary porosity in these three cores is the primary evidence used to interpret these as having been mixed with the higher mix water contents. In contrast, Cores 745SB-1P, 746NB-1P, and 746SB-1P have a uniform hydrate with moderate capillary porosity. Assuming the six cores were meant to represent concrete of the same design, the paste quality suggests some variability in mix proportioning. However, the differences are not major.

Calcium hydroxide is a primary phase of portland cement hydration and its size, morphology, and content can also be an indicator of original water contents when preserved. In this case, there are no obvious differences between samples though the characteristics are all consistent with moderate w/c. The hydroxide concentration is moderately high. The phase appears as fine to medium-grained crystal masses within the paste and as discontinuous deposits along aggregate interfaces.

Any differences in the presence of portland cement residuals between samples is quite subtle. All of the cement exhibits a high degree of hydration and very little if any of the hydraulic calcium silicate remains unhydrated. Residual grains include agglomerates of former calcium silicate with an interstitial matrix of residual iron-bearing ferrite. Isolated flakes of ferrite without obvious calcium silicate impressions are also observed. The three northbound samples have a moderate abundance of cement residuals though relatively few of these are well-defined agglomerates. The cement is fine to medium-grained with most estimated to pass a No. 200 sieve and relatively few approaching or retained on the No. 100 sieve. Some unhydrated material remains but only within the cores of the coarsest agglomerates. In Core 744SB-1P, the cement residuals are approximately the same size and texture as found in the northbound samples. However, the abundance is somewhat lower and even fewer remain unhydrated. Unhydrated material is rare in Cores 745SB-1P and 746SB-1P. The residual particles also tend to be finer in these two samples with grains rarely coarser than the No. 200 sieve. Finally, there is a tendency for the hydrated grains to have become filled with cementitious hydrate in the upper portions of each core section for these two samples.

The air content and microstructure in five of the six cores is indicative of intentional air-entrainment. A summary of the air contents, structural parameters, and qualitative distribution is presented in Table 5.2a. Details of the quantitative air-void analyses are presented in Section 6 below. The three northbound cores all have air structures that meet the generally accepted parameters for adequate freeze-thaw resistance. These include specific surfaces greater than 600 in.<sup>-1</sup> and spacing factors less than 0.008 in. The southbound cores do not meet these criteria. In fact, Core 746SB-1P exhibits no microstructural evidence for an air-entraining agent. Core 745SB-1P is deficient in voids with diameters less than one millimeter (at 1.8% by volume), but the sphericity and fineness of these voids suggests the use of an air-entraining admixture. Core 744SB-1P has a higher content of air-voids but a coarser size distribution that results in a lower specific surface and higher spacing. For all cores with entrained air-voids, these are mostly well distributed with depth in each core sample. There is some minor heterogeneity in Core 744NB-1P but this is considered inconsequential. For the most part, the voids are well dispersed at the microscopic scale and there is little to no clustering within the paste or along aggregate interfaces.

**Table 5.2a: Summary of Air Contents and Parameters**

Core ID	Total air (%)	Specific surface (in. <sup>-1</sup> )	Spacing factor (in.)	Remarks
744NB-1P	6.7	706	0.0061	The size distribution is good with adequate fine sizes. There is a slight tendency for increased air with depth (subtle). Very minor clustering is apparent but only within the paste and not along aggregate interfaces.
744SB-1P	6.4	421	0.0106	Possibly somewhat bimodal size distribution with a greater degree of void diameters over 0.25 mm. Homogeneous distribution with no clustering.
745NB-1P	3.5	764	0.0079	Sparse but evenly distributed in size. Homogeneous distribution with no clustering.
745SB-1P	4.0	342	0.0156	Air-entrained but deficient in fine air content. Homogeneous distribution with no clustering.
746NB-1P	4.7	651	0.0079	Good size distribution with high abundance of fine diameters. Homogeneous distribution with no clustering.
746SB-1P	1.1	136	0.0700	No evidence for intentional air-entrainment.

### **5.3 - Original Placement and Hydration**

Based on the core samples examined, the components of the structural concrete were well mixed in each core. There are no cement lumps, sand streaks, or rock pockets. It is not known whether the concrete was designed with the moderate water to cement ratios estimated for these cores. Therefore, it cannot be stated whether an inappropriate later addition was introduced on site. Nonetheless, the mix water appears to have been mostly well incorporated and there is no evidence for inappropriately late retempering. There was some bleed water migration in the concrete represented by Core 746SB-1P. However, this is not interpreted to have been the result of late watering. Assuming that all mixes were intended to have the same air structure, there are clearly some inconsistencies in the development of the entrained air. In fact, no entrained air structure is identified in Core 746SB-1P and the fine air is deficient in Core 745SB-1P. Only the northbound cores exhibit air structures with similar spacing factors. Generally speaking, it is not possible to isolate a particular cause for inadequate air development. Certainly these can be caused by admixture dosages. However, qualities of the mixing equipment, presence of incompatible materials, or environmental conditions may all result in air content variability.

All cores contain materials that are monolithic throughout the entire structural cross section and no cold joints are identified within the structural layers. The lower forming of the concrete is not evaluated as the cores do not include lower surfaces. In all samples, the structural concrete was well compacted and consolidated. There are no large void structures or honeycombing. Coarser air-voids are generally no more than several millimeters in size. Voids greater than one millimeter constitute up to a little over 2% of the total volume in any core sample (see Section 6). There is no evidence for excessive vibration. Coarse aggregate grains are homogeneously distributed throughout each concrete section without segregation. Though some grains are plate-like in shape, there are no preferential alignments of the stone due to excessive fluidity. The size, spacing, and location and steel reinforcement is outside the scope of a petrographic examination. Nevertheless, no reinforcement is included with the examined samples. It is not certain whether the original concrete surfaces are present below the wear courses. If they are, then there is no evidence for a weakened finish layer or other deficiencies that might be related to workmanship.

For most of the core samples, there is no evidence for excessive bleed water development. However, vertical bleed channels are identified throughout Core 746SB-1P. It is notable that this is the same core for which no air-entrainment is detected. Since entrained air can act to minimize bleed water, it may be that the lack of the entrainment is in part responsible for the migration. The bleed water left behind microscopic porous channels as it meandered upward throughout the concrete. These also tend to have deflected around aggregate grains reducing the quality of the paste-aggregate bond at these locations. Though the other five cores do not exhibit the bleed water features, the paste-aggregate bonds are only moderately well developed in these samples as well. Though not necessarily deficient, the moderate mix water contents result in a concrete that tends to fracture around rather than through aggregate grains.

As described above, the portland cement hydration is quite advanced in all samples. The hydration characteristics are mostly consistent throughout the full depth of each sample and there is no evidence for differential drying of the slab or loss of water near exposed surfaces. However, it is not certain that the original screeded surface is present in all of the samples.

All six samples have wear courses installed above the structural concrete. The wear courses are not part of the examination but are identified in a cursory manner. The total thickness of wear course ranges from 1.4" to 3.1". Only one material is identified in four of the cores. However, the Cores 746NB-1P and 746SB-1P both have two wear courses with the lower layers having thickness between 0.5" and 0.8". Microscopically, there is no debris identified at the contact between wear course and structural concrete. There is some "looseness" to the base of the wear course in Core 744SB-1P but none of the material appears to be foreign. The top of concrete appears mostly sound in all samples. Aggregate truncations are only positively identified in Core 745SB-1P and one of these exhibit shattering consistent with some type of scarification process. Based on the evidence, it is not certain if any surface preparation had been performed on the other five cores in advance of the wear course installation.

#### **5.4 - Condition and Durability**

The structural concrete examined for the six core samples represents a moderate quality mixture considered suitable for many normal-duty service applications. The notable issues identified in this report include a deficiency in air-entrainment in the southbound cores and the inclusion of potentially alkali-reactive materials in both the fine and coarse aggregates. Moderate permeabilities are also noted but are not considered a major deficiency in their own right. However, compressive strength results provided by the client indicate some variability. Where higher permeabilities are identified, it can be expected that these correlate with original water to cement ratios. By extension, these would correlate with variations in compressive strength. With respect to the current condition of the concrete, only limited axial cracking (most of which is microscopic) is identified in several of the samples. This is discussed at greater length below. Carbonation is limited to a thin veneer no greater than one millimeter thick at the top of the structural concrete. There does not appear to be any risk for pH-related depassivation of embedded steel if any is actually present in the concrete. All mineralizations identified are related to early-stage alkali-silica reaction (ASR) including the deposition of minor amounts of ettringite in pores and microcracks.

The moderate permeability of the concrete is a result of mix water contents that are perhaps a little higher than desirable for exterior applications. However, none of the concrete is considered to be excessively permeable. Nonetheless, the concrete should not be considered fully water-resistant and this can increase the susceptibility to any distress mechanisms that are associated with moisture infiltration. Of course, the possibility of denser wear courses could mitigate this susceptibility while any larger cracks going through the slab could promote increased infiltration of water. These last two are outside the scope of the examination.

Aside from the potential for chloride infiltration, the issue most closely tied to water permeability is freeze-thaw resistance. Assuming the wear courses are equally permeable, it should be expected that the structural concrete is capable of at least partial saturation if regularly exposed to moisture. The northbound core samples have entrained air structures that would be considered by most industry professionals to be sufficient for adequate freeze-thaw protection. Even though two of the northbound cores have fine air contents less than 4% (Cores 745NB-1P and 746NB-1P), the calculated spacing factors and specific surfaces are within industry accepted ranges. Specifically this includes spacing factors less than 0.008 in. and specific surfaces greater than 600 in.<sup>-1</sup>. The southbound cores do not meet these criteria. In fact, no entrained air is present in Core 746SB-1P. Despite some deficiencies, there is no significant evidence for freeze-thaw related distress in the structural concrete of any sample. The only possible feature is a trace level of incipient scaling within the uppermost millimeter of structural concrete in Core 744NB-1P.

Early stage alkali-silica reactions (ASR) are identified in several of the core samples. ASR is a reaction in which chemically unstable forms of silica react with alkalis normally found in the cement paste to produce a hygroscopic gel. Absorption of water into the gel causes the material to expand and this can often lead to significant expansive cracking. In these core samples, the reaction is restricted to the granitoids and the schistose granofels in the coarse aggregate. No reaction is observed in the purer amphibolites or the diorites. Both the granitoids and granofels include fine subgrains of strained quartz. Deformation in the quartz crystal matrix is responsible for the higher reactivity. Strained quartz exhibiting this level of deformation is usually considered only slowly reactive. The chert in the fine aggregate is also reactive and signs of internal cracking and gel development are found in these grains as well.

While still somewhat minimal, Core 744SB-1P exhibits the most significant reaction. It is notable that this particular core contains the greatest concentration of the schistose granofels that are rich in strained quartz matrix. This is interpreted to be the primary reason for the slightly more advanced reaction. In cross section, reaction rims are found along most of the mottled aggregate particles (i.e. those that are not amphibole-rich). Internal cracks are found in many of the granofels and granitoids with opening thicknesses mostly less than 50  $\mu\text{m}$ . An exception is found near the upper surface with a width of approximately 125  $\mu\text{m}$ . In some cases, these link up to form semi-continuous microcracks with an axial orientation. The core break located just below the wear course in the sample as received is also identified as an extension of these cracks. The spacing of the more continuous cracks is relatively wide at the inch-scale. ASR gel plugs are found at the intersection between reacted aggregate and adjacent cement paste. Reaction gel is also identified in air-voids that are in proximity to reaction sites. Chert in the fine aggregate also exhibits internal microcracks along with some gel plugs. However, these do not appear widespread when evaluated in full depth cross section.

Cores 745NB-1P and 746NB-1P exhibit a similar reaction but only within a limited depth at the uppermost portions of the structural concrete. Occurrences of ASR are rare and isolated at depth. In 745NB-1P, the reactions are limited to the uppermost 2" of the structural concrete with semi-continuous axial cracks only within the upper 1". The core break approximately 1" below the top of the structural layer is a manifestation of the reaction cracking. The chert within the fine aggregate also exhibits some well-developed cracking and gel formation within the upper section. In cross section, there are also instances of reaction gel having exuded from around chert particles after the section had been sliced and honed. In Core 746NB-1P, the coarse aggregate reactions are limited to the uppermost 0.5" of the structural concrete. Reactions in chert are identified but less prevalent than in Core 745NB-1P.

Only rare instances of trace ASR reaction are observed in Cores 744NB-1P, 745SB-1P, and 746SB-1P. These are exceptionally minor and include internal microcracks in chert fine aggregate and exudation of reaction gel around chert grains in freshly prepared cross section. No reaction is observed in the coarse aggregate of these samples. It is noted that the granitoids are absent from the coarse aggregate in all three of these cores. Additionally, the more granofels are less quartz-rich in Cores 745SB-1P and 746SB-1P.

There is no evidence to suggest that continued ASR development is mitigated by any particular feature of the concrete. ASR is sometimes controlled by the addition of supplementary cementitious materials or (more recently) lithium-based admixtures. The former are clearly not part of the mix design and the latter is unlikely though this can only be demonstrated chemically. Alkaline cement paste is one precondition for the initiation of aggregate dissolution. The lack of carbonation has allowed all concrete to maintain a high alkalinity throughout the full cross section of each core. Continued aggregate reactions can be expected even if somewhat slowly. Availability of moisture is also an important factor in the rate of ASR development and distress. Again, the concrete is not especially water-resistant even if the permeabilities are not excessive. Cores 744NB-1P, 744SB-1P, and 745NB-1P are estimated to have the higher permeabilities of the group and may be slightly more susceptible to water infiltration. Of course, exposure and drainage will also have an impact on the amount of water available and this cannot be evaluated in the laboratory.

Despite the lack of mitigating factors, the coarse aggregate is not considered to be among the most aggressively reactive rock types. Any reactions identified in this study are at an early stage and have not compromised the integrity of the represented concrete. It is quite possible that the concrete may remain provisionally stable over the course of a normal life cycle. The chert in the fine aggregate is considered to be significantly more reactive than the granofels and granitoids. However, the abundance may be too low to represent a significant threat. To be sure, the chert is present at several percent of the fine aggregate volume and this might be expected to produce unacceptable levels of expansion if the raw material were subjected to accelerated durability tests in the laboratory. Nonetheless, there is clearly no imminent durability threat produced by the chert alone. Of course, it must be stressed that while petrographic examination can identify potential durability threats, it cannot be fully predictive. Monitoring of concrete containing such components may be prudent. It is also possible that the concrete studied for this examination is not fully representative of all material on site. If other areas of the construction exhibit visible cracking not captured in the provided samples, these should be considered to have a potential association with the types of reactions described herein. Patterned cracking with a polygonal shape or "map-cracking" would be one possible indication of more advanced alkali-aggregate reaction as would the presence of white mineral exudates.

**6. Air-Void Analysis**

**Table 6.1: Point-Count Data**

Core ID	744NB-1P	744SB-1P	745NB-1P	745SB-1P	746NB-1P	746SB-1P
Aggregate nominal top size (in.)	0.75	0.75	0.75	0.75	0.75	0.75
Total traverse length (in.)	76	76.35	74.55	76.9	74.95	75.65
Total area (in. <sup>2</sup> )	12.8	12.8	12.8	12.8	12.8	12.8
Aggregate points	981	984	963	1059	992	1059
Paste points	437	444	456	418	437	437
Air points (less than 1 mm)	71	67	39	27	49	2
Air points (greater than 1 mm)	31	30	12	34	21	15
Crack points <sup>1</sup>	0	2	21	0	0	0
Total points	1520	1527	1491	1538	1499	1513
Air intercept	900	510	487	261	570	29

Notes:

1. Cracks are non-totaling and do not influence the air-void parameter calculation.

**Table 6.2: Calculated Volumes and Air-Void Parameters**

Core ID	744NB-1P	744SB-1P	745NB-1P	745SB-1P	746NB-1P	746SB-1P
Aggregate (volume %)	64.5	64.5	65.5	68.9	66.2	70.0
Paste (volume %)	28.8	29.1	31.0	27.2	29.2	28.9
Air less than 1 mm (volume %)	4.7	4.4	2.7	1.8	3.3	0.1
Air greater than 1 mm (volume %)	2.0	2.0	0.8	2.2	1.4	1.0
<b>Total air (volume %)</b>	<b>6.7</b>	<b>6.4</b>	<b>3.5</b>	<b>4.0</b>	<b>4.7</b>	<b>1.1</b>
Paste/air ratio	4.28	4.58	8.94	6.85	6.24	25.71
Voids/inch	11.84	6.68	6.53	3.39	7.61	0.38
Average chord length (in.)	0.006	0.010	0.005	0.012	0.006	0.029
Specific surface (in. <sup>-1</sup> )	705.88	420.62	763.92	342.30	651.43	136.47
<b>Spacing factor (in.)</b>	<b>0.0061</b>	<b>0.0106</b>	<b>0.0079</b>	<b>0.0156</b>	<b>0.0079</b>	<b>0.0700</b>

Respectfully submitted,

John J. Walsh  
 President/ Senior Petrographer  
**Highbridge Materials Consulting, Inc.**

**Appendix I: Visual Description of Petrographic Samples**

<b>Sample ID</b>	<b>744NB-1P</b>
Dimensions and Details	The sample consists of a 3.25” diameter core approximately 7” in length. The core is received as one intact piece. A wear course of approximately 1.4” thickness overlies the structural concrete. The wear course is tightly bound to the substrate along a roughly planar surface.
Top/Outer Surface	The top surface is roughly planar with low to moderate relief coarse aggregate exposure. Moderate soiling of the paste is also apparent. Remnants of linear scoring have an approximately 1/2” spacing.
Bottom/Inner Surface	The bottom surface is a clean, artificial drilling break intersecting few aggregate particles.
Core Circumference	Smooth with no differential erosion from coring. Some irregular wear is identified locally along a single friable aggregate particle intersected by the coring.
Embedded Items	No reinforcement is included in the sample.
Visible Cracks	No macroscopic cracking is visible in hand sample.

<b>Sample ID</b>	<b>744SB-1P</b>
Dimensions and Details	The sample consists of a 3.25” diameter core approximately 7” in length. The core is received in two contiguous pieces with a core break running mostly through the structural concrete at approximately 2.4” depth. The break refracts into the boundary between a wear course and the substrate along one edge of the core. A wear course of approximately 2.2” thickness overlies the structural concrete. The wear course is tightly bound to the substrate along a roughly planar surface in most areas.
Top/Outer Surface	The top surface is roughly planar with low to moderate relief coarse aggregate exposure. Moderate soiling of the paste is also apparent.
Bottom/Inner Surface	The bottom surface is a clean, artificial drilling break.
Core Circumference	Smooth with no differential erosion from coring.
Embedded Items	No reinforcement is included in the sample.
Visible Cracks	The core break is the only crack visible in hand sample. This may represent a pre-existing structure. However, the surface appears reasonably fresh with no soiling. Some possible mineralization is noted around coarse aggregate.

<b>Sample ID</b>	<b>745NB-1P</b>
Dimensions and Details	The sample consists of a 3.25” diameter core approximately 8” in length. The core is received in two contiguous pieces with a core break running through the structural concrete at approximately 4.2” depth. A wear course of approximately 3.1” thickness overlies the structural concrete. The wear course is tightly bound to the substrate along a roughly planar surface.
Top/Outer Surface	The top surface is roughly planar with low to moderate relief coarse aggregate exposure. Moderate soiling of the paste is also apparent.
Bottom/Inner Surface	The bottom surface is a clean, artificial drilling break that tends to deflect around aggregate surfaces.
Core Circumference	Smooth with no differential erosion from coring.
Embedded Items	No reinforcement is included in the sample.
Visible Cracks	The core break is the only major crack visible in hand sample. This may represent a pre-existing structure. However, the surface appears reasonably fresh with no soiling or mineralizations. Another hairline crack is identified along the upper surface of the wear course. The crack does not appear to penetrate the concrete to any appreciable depth.

**HIGHBRIDGE MATERIALS CONSULTING, INC.**

Pennoni Associates, Inc.; I-95 Viaduct Project

Report #: SL0845-01

Page 12 of 34

<b>Sample ID</b>	<b>745SB-1P</b>
Dimensions and Details	The sample consists of a 3.25" diameter core approximately 7.5" in length. The core is received as one intact piece. A wear course of approximately 2.7" thickness overlies the structural concrete. The wear course is tightly bound to the substrate along a roughly planar surface.
Top/Outer Surface	The top surface is roughly planar with low to moderate relief coarse aggregate exposure. Moderate soiling of the paste is also apparent.
Bottom/Inner Surface	The bottom surface is a clean, artificial drilling break intersecting few aggregate particles.
Core Circumference	Smooth with no differential erosion from coring.
Embedded Items	No reinforcement is included in the sample.
Visible Cracks	No macroscopic cracking is visible in hand sample.

<b>Sample ID</b>	<b>746NB-1P</b>
Dimensions and Details	The sample consists of a 3.25" diameter core approximately 7.5" in length. The core is received in two contiguous pieces with a core break running through the contact between structural concrete and an overlying wear course. Two wear courses totaling 2.9" thickness overlie the structural concrete.
Top/Outer Surface	The top surface is roughly planar with low relief coarse aggregate exposure. Moderate soiling of the paste is also apparent. Linear scoring has a 1.3" spacing.
Bottom/Inner Surface	The bottom surface is a clean, artificial drilling break. Aggregate is visible but coated with dried drilling slurry.
Core Circumference	Smooth with no differential erosion from coring.
Embedded Items	No reinforcement is included in the sample.
Visible Cracks	The core break is the only crack visible in hand sample. The crack is a clean adhesive failure between the structural concrete and the first wear course.

<b>Sample ID</b>	<b>746SB-1P</b>
Dimensions and Details	The sample consists of a 3.25" diameter core approximately 7" in length. The core is received as one intact piece. Two wear courses totaling 2.3" thickness overlie the structural concrete. The wear courses are tightly bound to each other and to the substrate along roughly planar surfaces.
Top/Outer Surface	The top surface is roughly planar with low relief coarse aggregate exposure. Moderate soiling of the paste is also apparent. Linear scoring has a 1.2" spacing.
Bottom/Inner Surface	The bottom surface is a clean, artificial drilling break.
Core Circumference	Smooth with no differential erosion from coring.
Embedded Items	No reinforcement is included in the sample.
Visible Cracks	No macroscopic cracking is visible in hand sample.

**Appendix II: Photographs and Photomicrographs**

Microscopic examination is performed on an Olympus BX-51 polarized/reflected light microscope and a Bausch and Lomb Stereozoom 7 stereoscopic reflected light microscope. Both microscopes are fitted with an Olympus DP-11 digital camera. The overlays presented in the photomicrographs (e.g., text, scale bars, and arrows) are prepared as layers in Adobe Photoshop and converted to the jpeg format. Digital processing is limited to those functions normally performed during standard print photography processing. Photographs intended to be visually compared are taken under the same exposure conditions whenever possible.

The following abbreviations may be found in the figure captions and overlays and these are defined as follows:

cm	centimeters	PPL	Plane polarized light
mm	millimeters	XPL	Crossed polarized light
µm	microns (1 micron = 1/1000 millimeter)		
mil	1/1000 inch		

Microscopical images are often confusing and non-intuitive to those not accustomed to the techniques employed. The following is offered as a brief explanation of the various views encountered in order that the reader may gain a better appreciation of what is being described.

**Reflected light images:** These are simply magnified images of the surface as would be observed by the human eye. A variety of surface preparations may be employed including polished and fractured surfaces. The reader should note the included scale bars as minor deficiencies may seem much more significant when magnified.

**Plane polarized light images (PPL):** This imaging technique is most often employed in order to discern textural relationships and microstructure. To employ this technique, samples are milled (anywhere from 20 to 30 microns depending on the purpose) so as to allow light to be transmitted through the material. In many cases, Highbridge also employs a technique whereby the material is impregnated with a low viscosity, blue-dyed epoxy. Anything appearing blue therefore represents some type of void space (e.g.; air voids, capillary pores, open cracks, etc.) Hydrated cement paste typically appears a light shade of brown in this view (with a blue hue when impregnated with the epoxy). With some exceptions, most aggregate materials are very light colored if not altogether white. Some particles will appear to stand out in higher relief than others. This is a function of the refractive power of different materials with respect to the mounting epoxy.

**Crossed polarized light images (XPL):** This imaging technique is most often employed to distinguish components or highlight textural relationships between certain components not easily distinguished in plane polarized light. Using the same thin sections, this technique places the sample between two pieces of polarizing film in order to determine the crystal structure of the materials under consideration. Isotropic materials (e.g.; hydrated cement paste, pozzolans and other glasses, many oxides, etc.) will not transmit light under crossed polars and therefore appear black. Non-isotropic crystals (e.g.; residual cement, calcium hydroxide, calcium carbonate, and most aggregate minerals) will appear colored. The colors are a function of the thickness, crystal structure, and orientation of the mineral. Many minerals will exhibit a range of colors due to their orientation in the section. For example, quartz sand in the aggregate will appear black to white and every shade of gray in between. Color difference does not necessarily indicate a material difference. When no other prompt is given in the figure caption, the reader should appeal to general shapes and morphological characteristics when considering the components being illustrated.

**Chemical treatments:** Many chemical techniques (etches and stains typically) are used to isolate and enhance a variety of materials and structures. These techniques will often produce strongly colored images that distinguish components or chemical conditions.



**Figure 1:** Photographs of the six concrete core samples used for petrographic examination and air-void analysis of the structural concrete layers. All are shown with their upper surfaces toward the left of each image. All contain wear course layers (WC) overlying normal weight structural concrete (SC). The arrows indicate core breaks present in three of the samples as delivered. These occur as cohesive failures within the substrate in Cores 744SB-1P and 745NB-1P and are interpreted to represent pre-existing axial cracks. The break in Core 746NB-1P is an adhesive failure between the wear course and substrate.

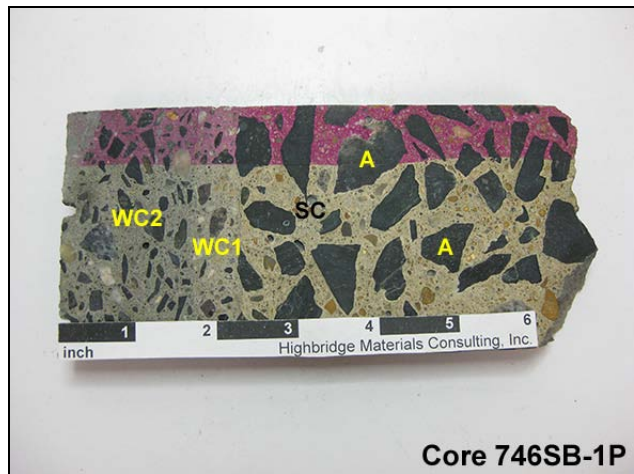
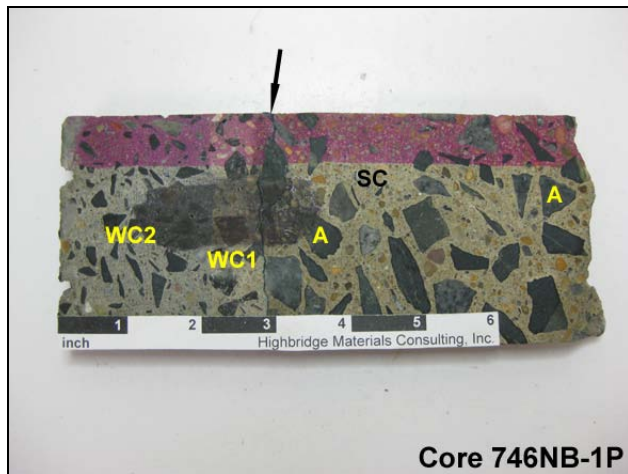
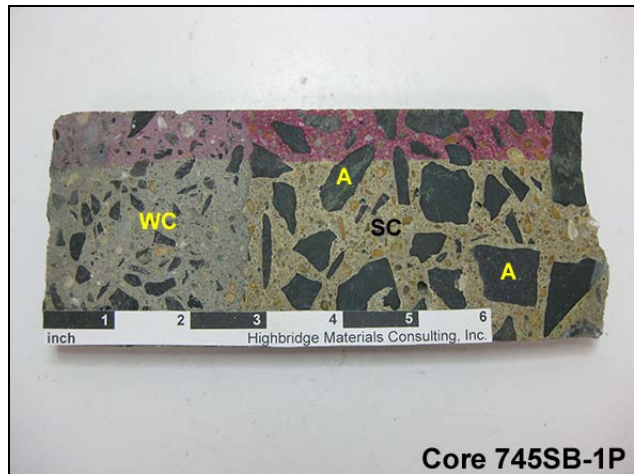
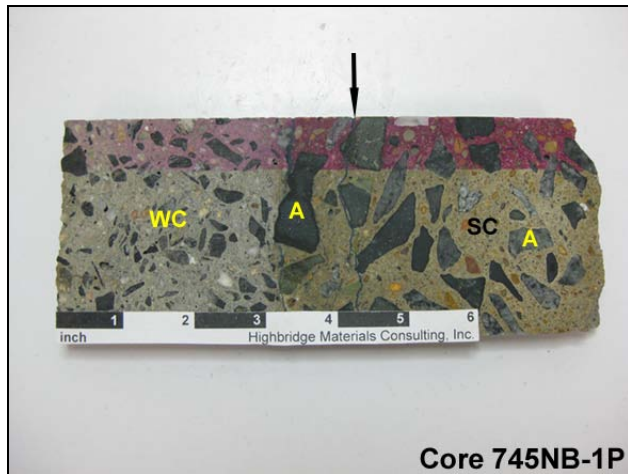
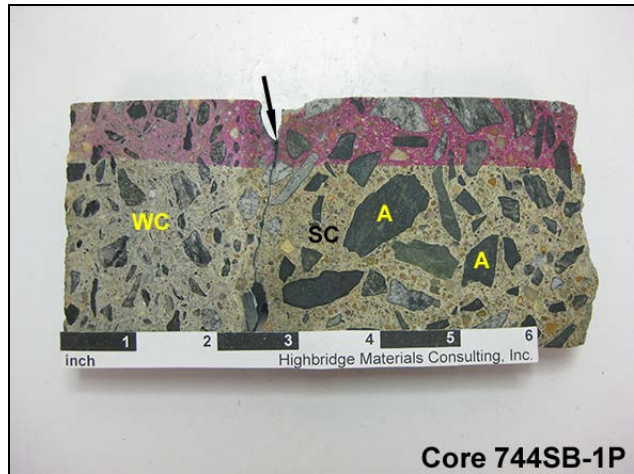
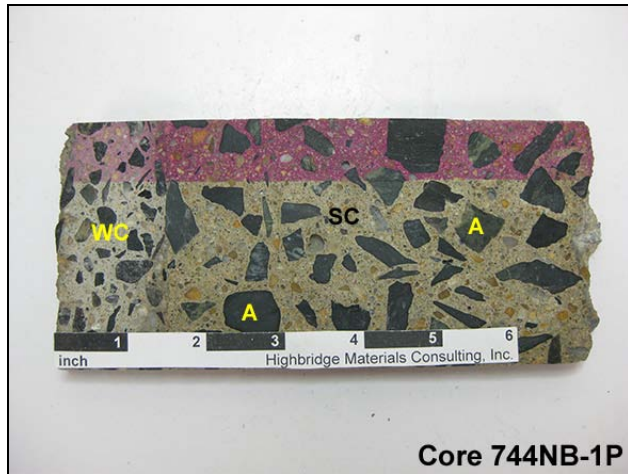


**Figure 2:** Photographs of honed concrete cross sections prepared for the full depth of each provided sample. The upper surfaces are shown to the left in each example. The arrows indicate where core breaks were epoxied together prior to honing. Wear courses (WC) overlie structural concrete (SC). Two wear courses are present in Cores 745SB-1P and 746SB-1P. The size and gradation of the crushed stone aggregate (A) can be observed in the structural layers. All cores have aggregate with a 3/4" nominal top size. The aggregate is well distributed and no segregations are identified. A portion of each core is treated with phenolphthalein indicator solution. The pink color indicates that the structural concrete is alkaline throughout all but a thin veneer along the upper surfaces. The blue patch in Core 746NB-1P is a different pH indicator. The high pH is indicative of the relative lack of carbonation within the structural layers. Steel embedded within the substrate concrete would not be at risk for depassivation at least within the upper portions represented here.

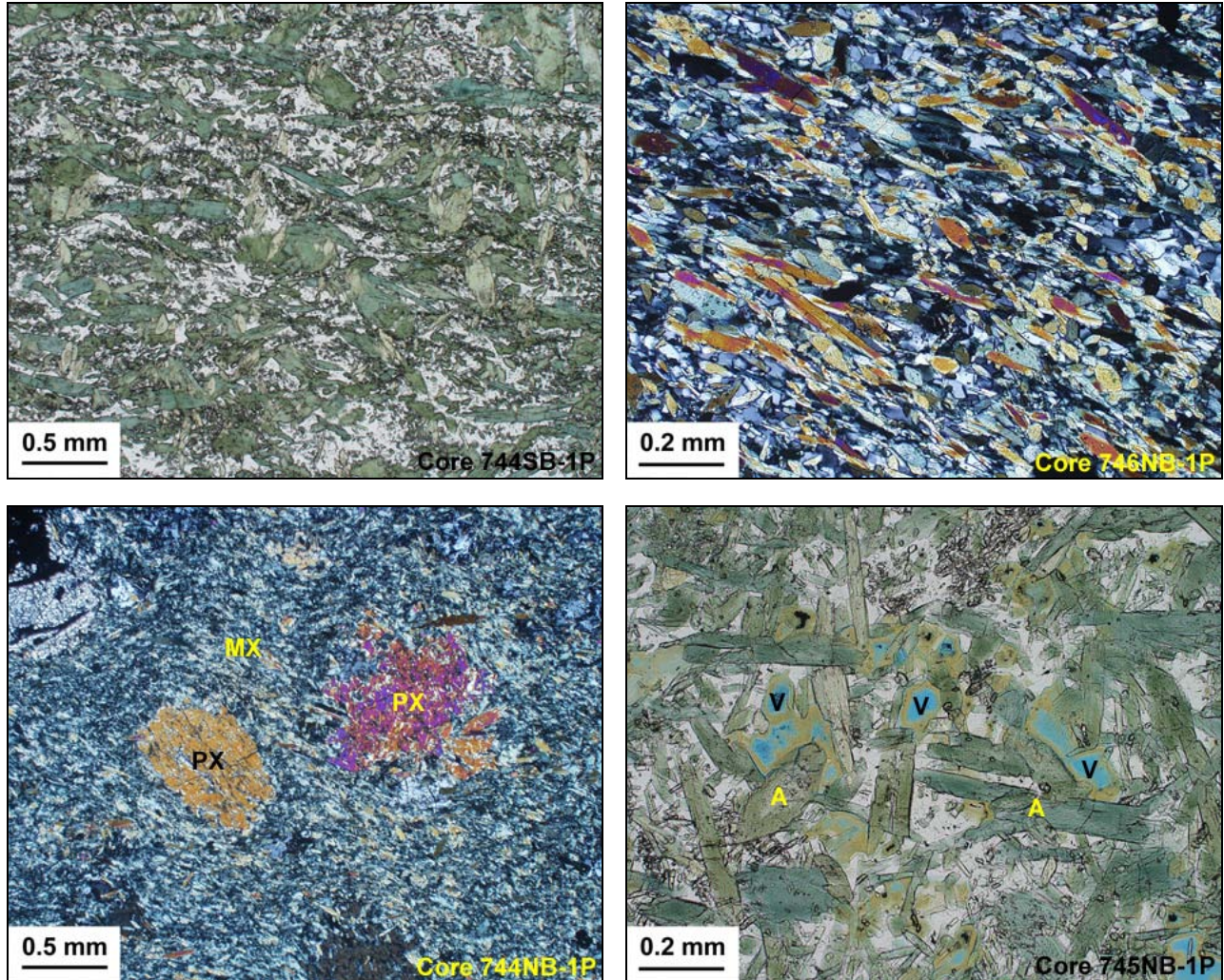


**Figure 3:** Amphibolite represents the major component in the coarse aggregate. Four of the core samples have similar amphibolite lithologies and examples of the range are shown in these photomicrographs. (Upper left PPL image) The green minerals are amphibole and these dominate the rock. The white areas are mostly feldspar. (Upper right XPL image) A similar grain is shown under crossed polars. The amphibole appears brightly colored in this image. Note the preferred orientation of the crystals. (Lower XPL image) Relict pyroxenes (PX) are embedded in a matrix of lower temperature phases (MX). The pyroxene suggests the amphibolites are the metamorphosed products of basic rocks such as gabbro. (Lower right PPL image) Microscopic vugs (V) are lined with a low-temperature phase and these are found between amphibole crystals (A). The open vugs suggest an original basaltic source for this particular lithology. Basalts and gabbros are related rock types.

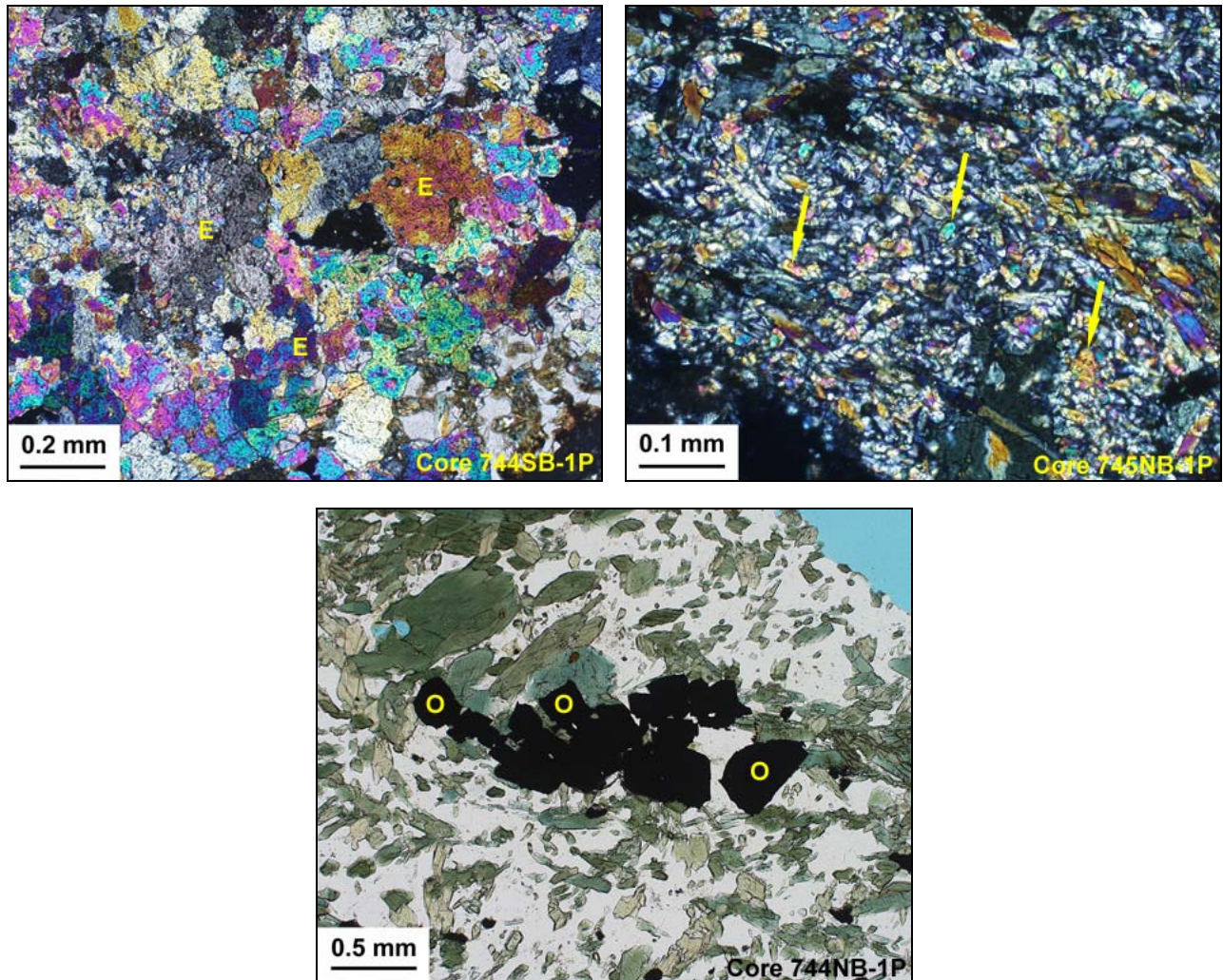


**Figure 4:** Photomicrographs illustrating other features of the amphibolite. Epidote is an alteration phase present in some of the amphibolite as shown in the upper XPL images. At left, large epidote crystals (E) dominate the grain. At right, the arrows indicate finer crystal agglomerates. Opaque phases (O) are shown in the lower PPL image. Many of these represent sulfide minerals but the abundance is not considered significant.

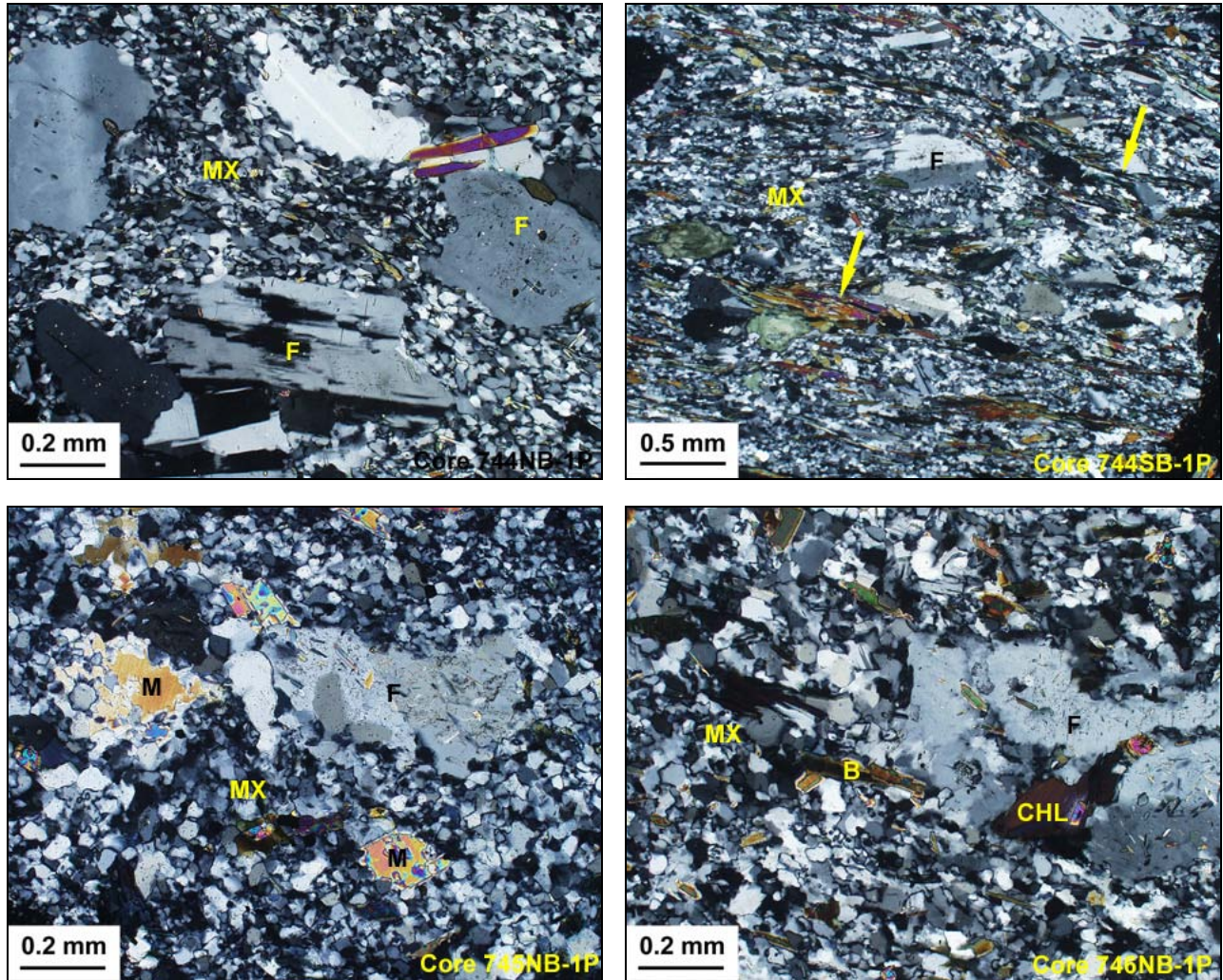


**Figure 5:** Schistose granofels are associated with the amphibolites in the four cores illustrated in Figure 3. Examples of the range of lithologies are shown in these XPL photomicrographs. In all cases, the stone is dominated by a matrix (MX) of fine-grained quartz subgrains. The matrix is essentially a strained quartzite. The deformation causes the stone to be alkali-silica reactive and much of the early stage reactions identified in this study are found in this lithology. Coarser porphyroclasts are entrained within the sheared matrix. Feldspar (F) is common. However, muscovite (M), biotite (B), and chlorite (CHL) are also identified. The arrows indicate thin laminae of amphibole. Though these rock types do not immediately appear similar to the amphiboles, increasing amounts of amphibole suggests that there may be a full gradation between these two lithologies. The gradation is better observed in Cores 745SB-1P and 746SB-1P.

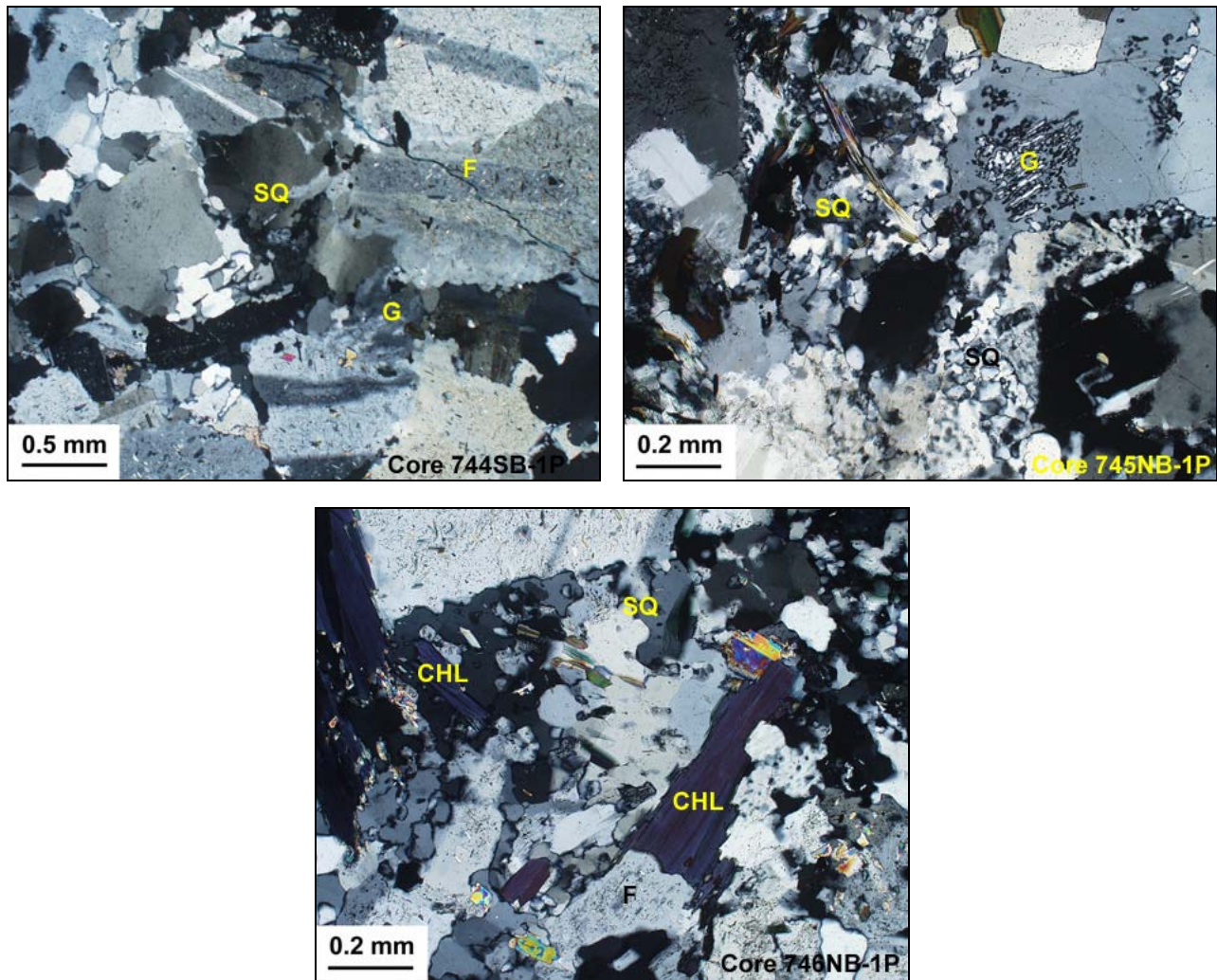


**Figure 6:** Granitoid lithologies are a minor portion of the coarse aggregate in Cores 744SB-1P, 745NB-1P, and 746NB-1P. Feldspar is dominant (F) and darker accessory minerals such as chlorite (CHL) are also observed in low concentration. More importantly, there is an abundance of fine interstitial matrix. This contains both graphic intergrowths (G) of quartz and feldspar as well as patches of strained quartz (SQ). The fine, deformed quartz is considered to be alkali-silica reactive and some of the early stage reactions observed in this study are found in these rocks.

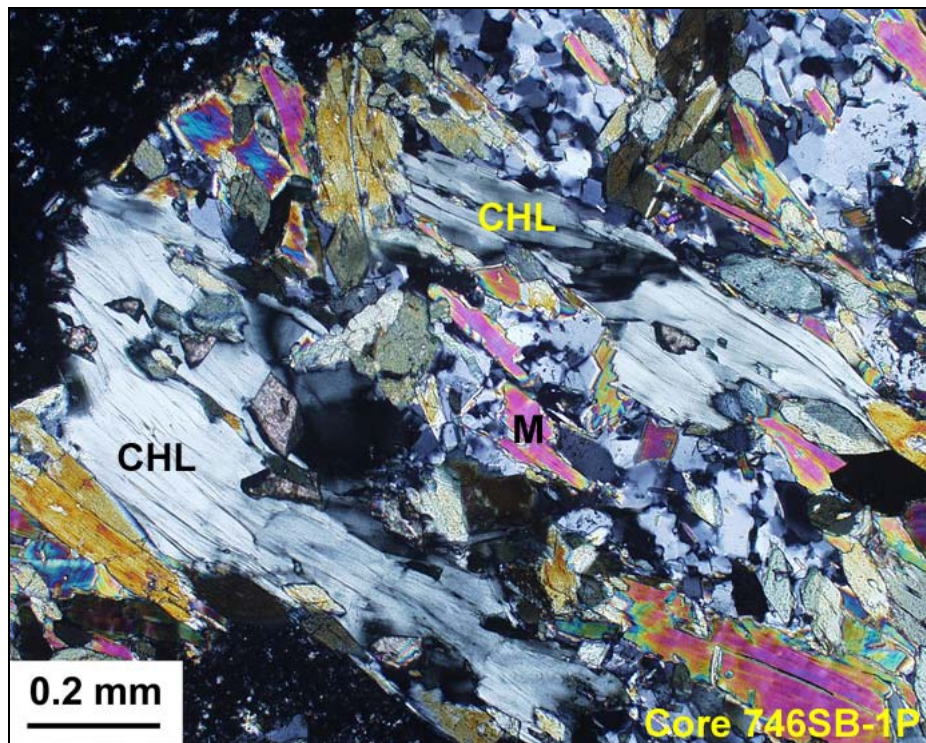
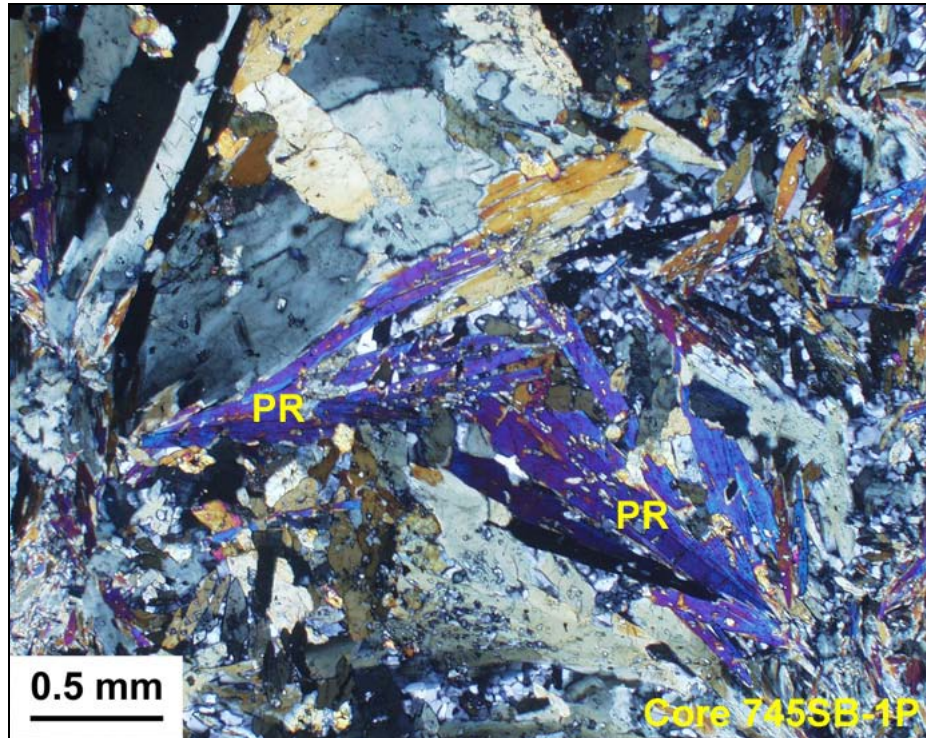


**Figure 7:** The amphibolites in Cores 745SB-1P and 746SB-1P are notably different than those of the other four cores. Two examples are shown in these XPL photomicrographs. In the upper image, prehnite crystals (PR) indicate a lower metamorphic grade. The grain in the lower image is rich in chlorite (CHL) as well as other micas (M).

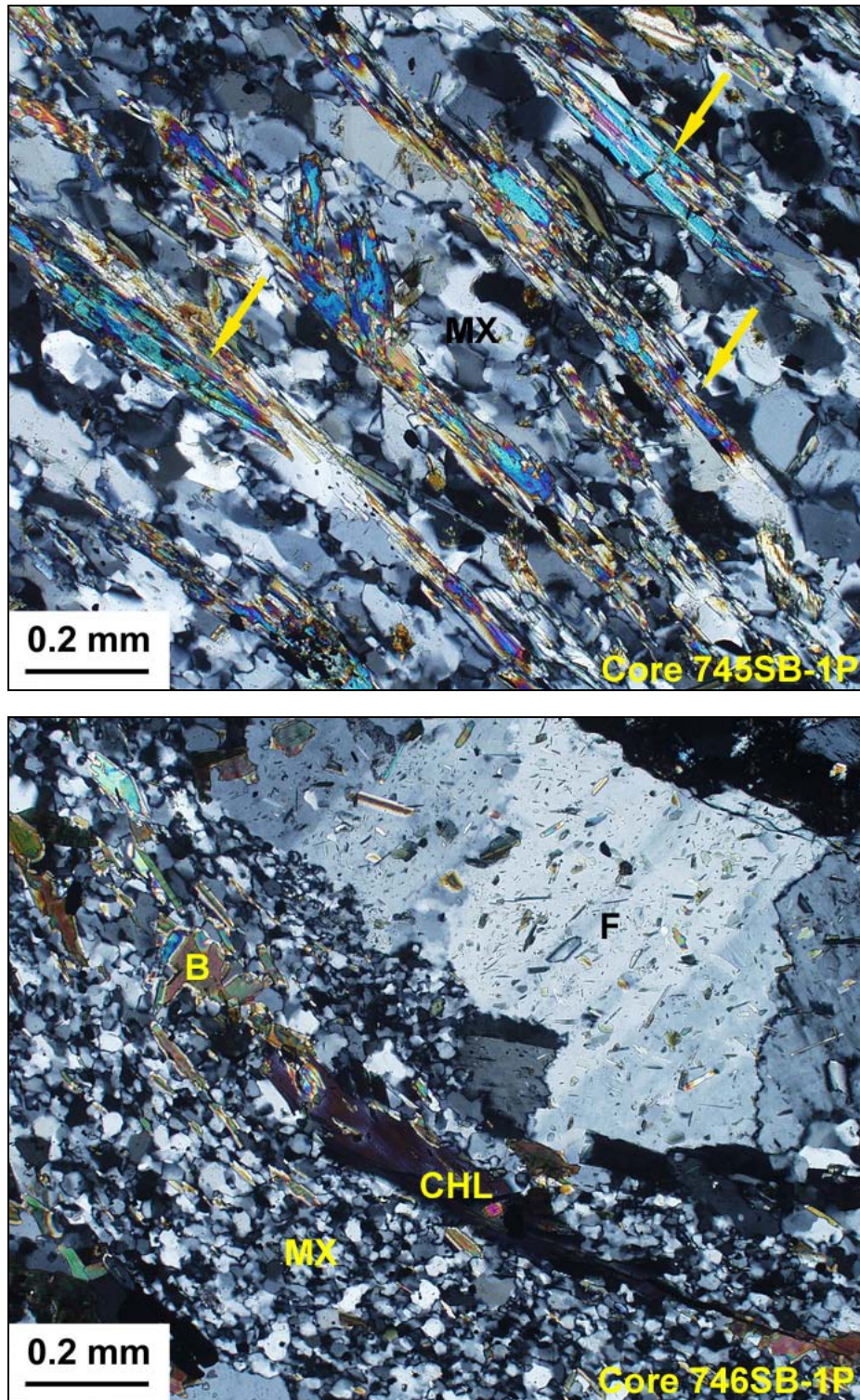


**Figure 8:** The coarse aggregate in Cores 745SB-1P and 746SB-1P also contain the schistose granofels and examples are shown in these XPL images. In both grains, the rock has a matrix of fine quartz subgrains (MX). In the upper image, the arrows indicate laminae of amphibole. In the lower image, porphyroclasts include feldspar (F), chlorite (CHL), and biotite (B).

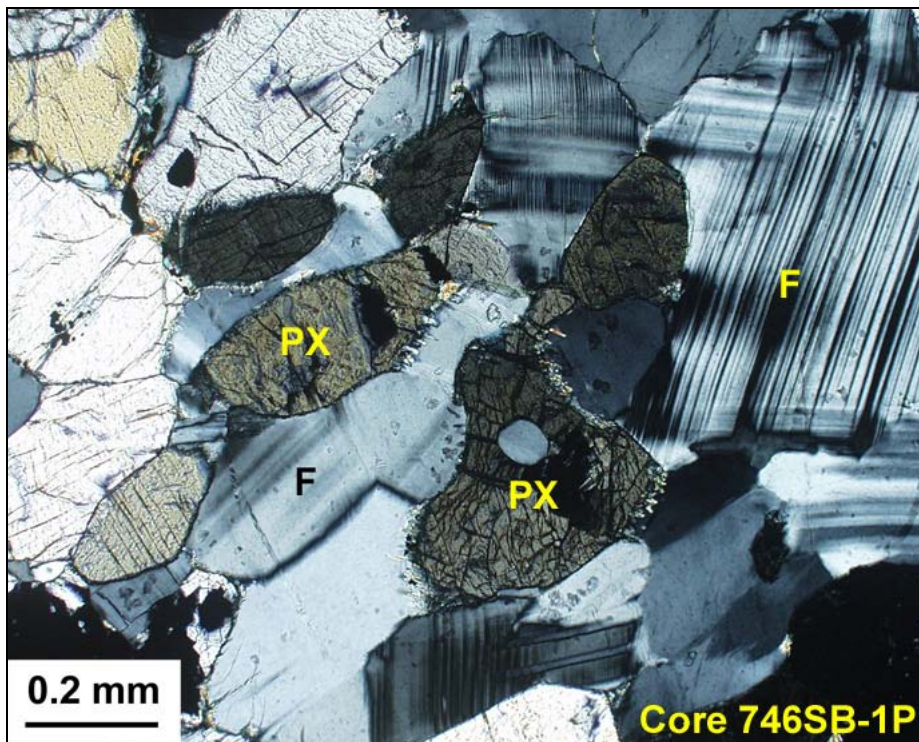
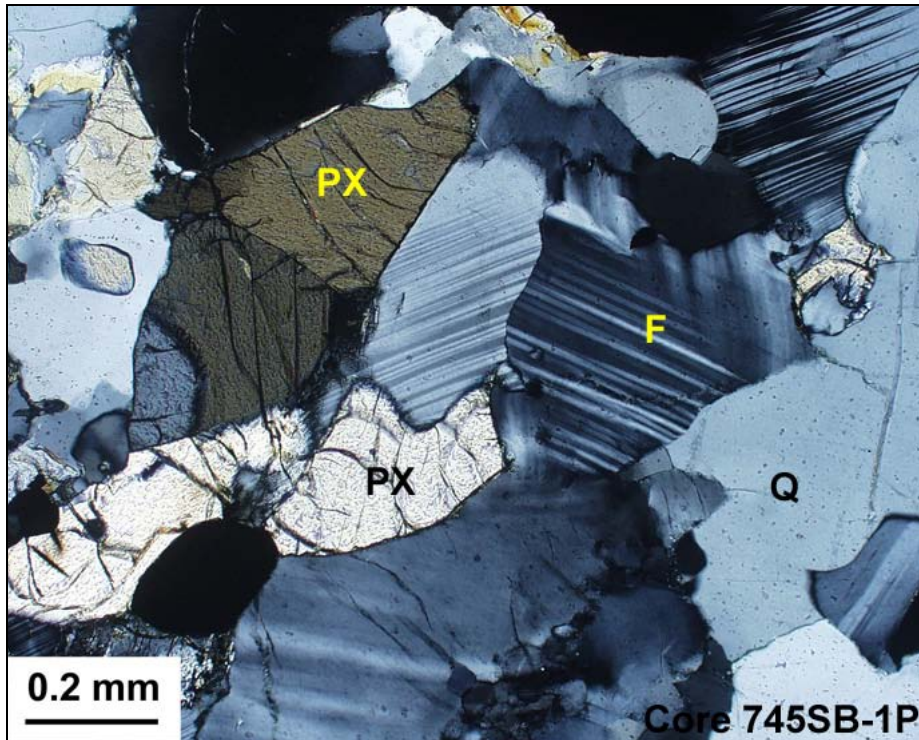


**Figure 9:** Diorites are a minor component of the coarse aggregate in Cores 745SB-1P and 746SB-1P as shown in these XPL images. The diorite has a granoblastic texture containing plagioclase feldspar (F) and orthopyroxene (PX). Quartz (Q) is only found in Core 745SB-1P.

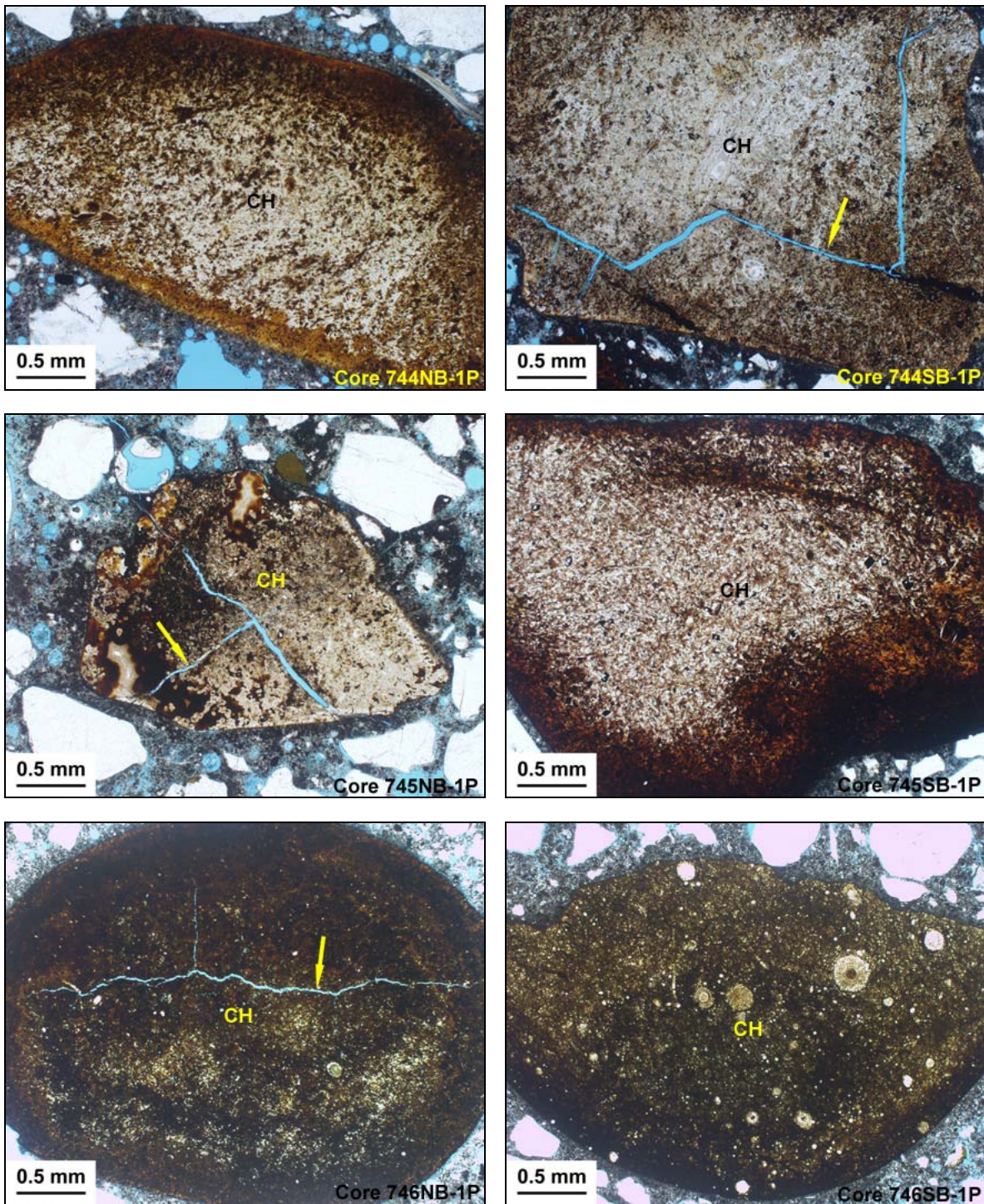


**Figure 10:** PPL photomicrographs. All cores contain ferruginous chert (CH) in the fine aggregate at about several percent by volume. Chert is considered to be one of the most highly alkali-reactive rock types. Traces of reaction are observed in this material in all cores. The internal microcracks shown by the arrows in these images represent one form of evidence for the reaction.

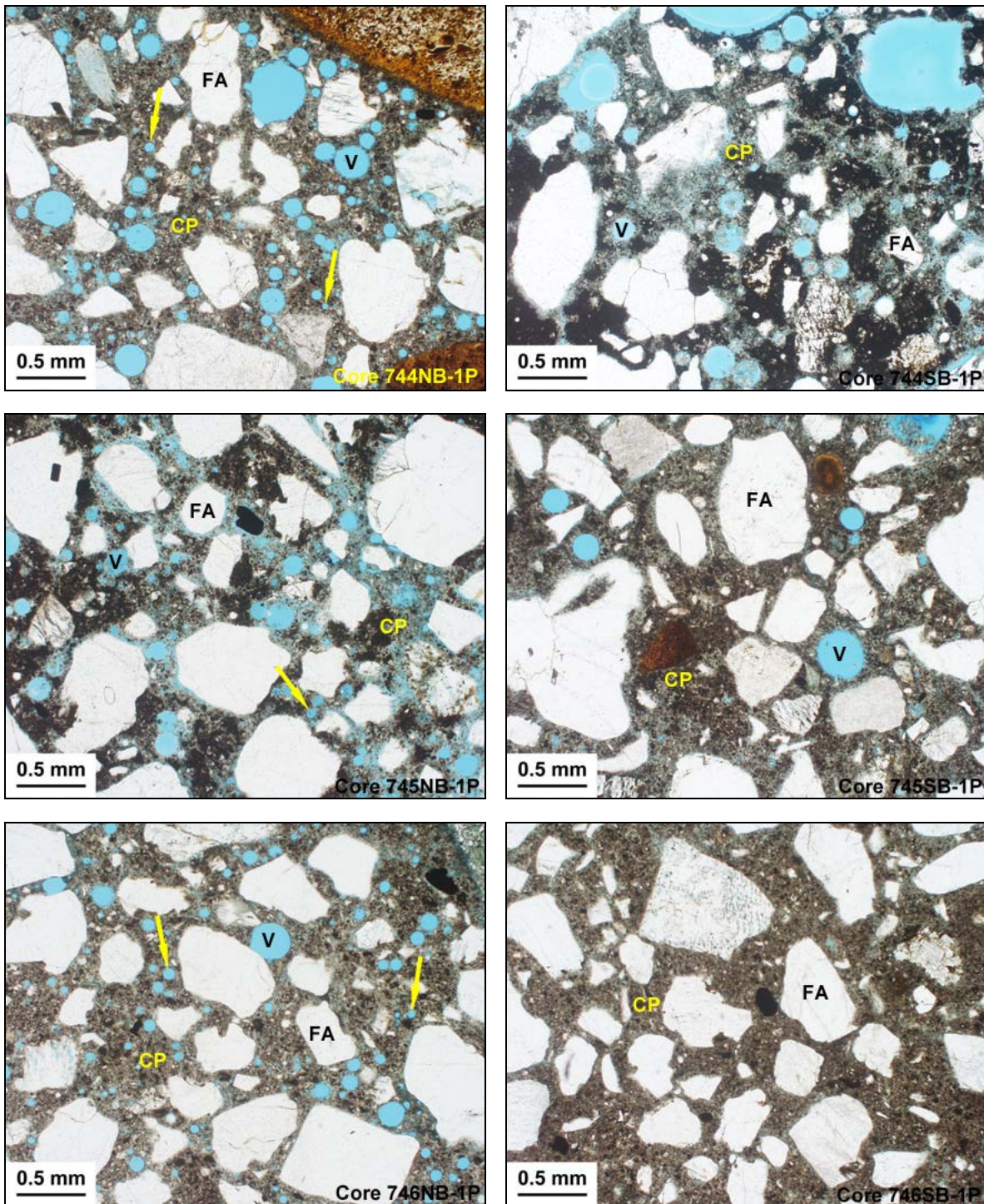


**Figure 11:** PPL photomicrographs illustrating the overall microstructure of the structural concrete. There is some variability in water contents and entrained-air development that result in some quality differences. In all of the examined samples, the cement paste (CP) is well-developed and relatively dense as indicated by the even brown coloration under plane light. Some mottling is identified in Cores 744SB-1P and 745NB-1P. This may represent a primary cement flocculation but could also have been a secondary effect of alkali-silica reaction. The samples are impregnated with a low-viscosity, blue-dyed epoxy in order to highlight cracks, pores, and voids. There is a moderate absorption of the epoxy consistent with moderate mix water contents. Note the lower absorption particularly in Cores 745SB-1P and 746SB-1P. The fine aggregate (FA) is well distributed throughout the matrix. The sand is somewhat coarse-grained but otherwise well graded. Fine, spherical voids (V) indicate intentional air-entrainment in all cores but 746SB-1P. The arrows illustrate very fine voids that are abundant in some of the northbound core samples.

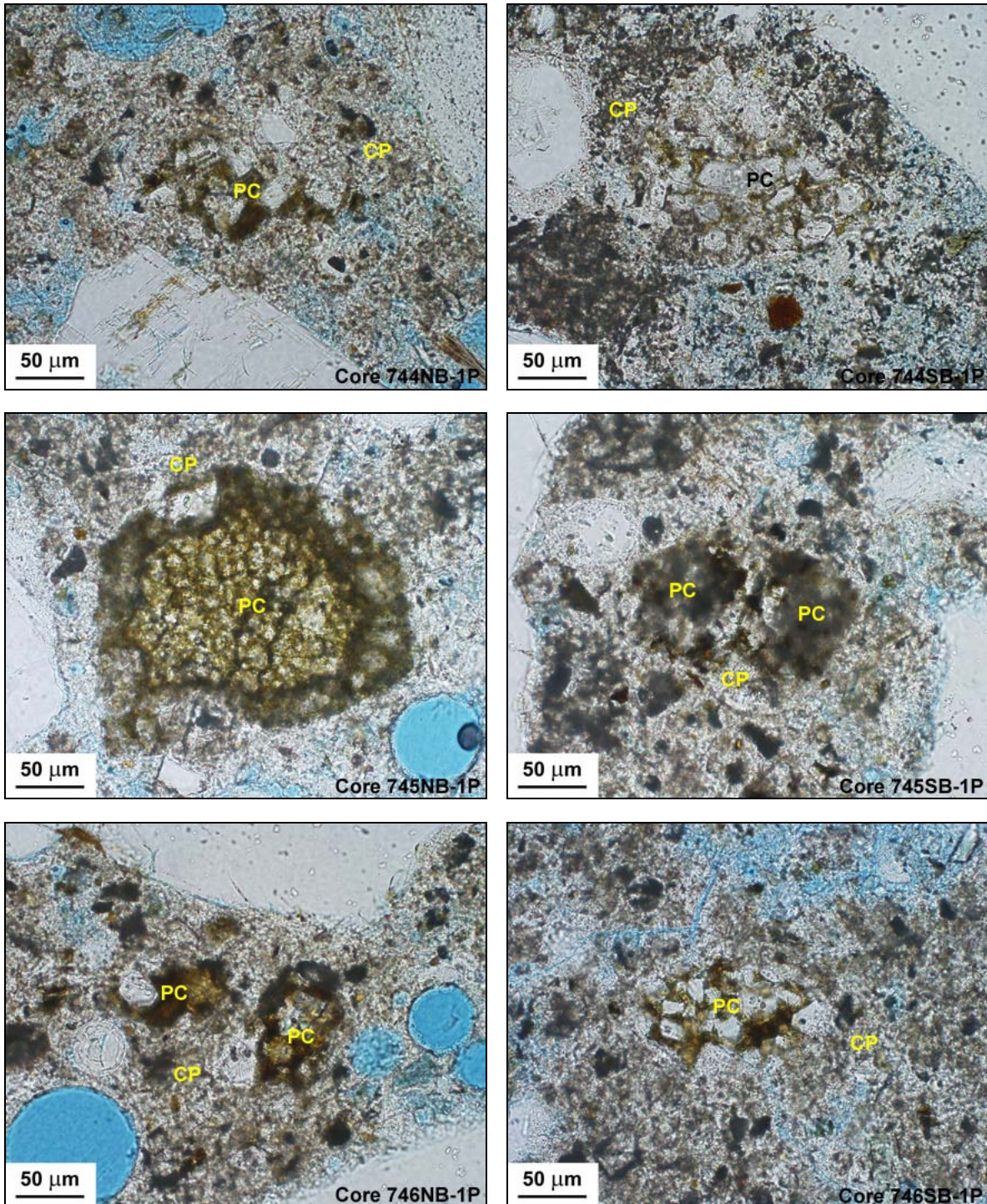


**Figure 12:** PPL photomicrographs illustrating the occurrence of residual portland cement (PC) in the examined concrete. The cement hydration is advanced and most calcium silicate is fully consumed. These appear as light-colored areas within the cement agglomerates. An exception is shown for Core 745NB-1P where belite remains unhydrated. For Core 745SB-1P, an area is shown where the empty pores are now filled with an amorphous cementitious hydrate. All of the cement residuals are fine to medium-grained agglomerates with brown-colored interstitial ferrite. The adjacent cement paste (CP) is well-formed in all samples.

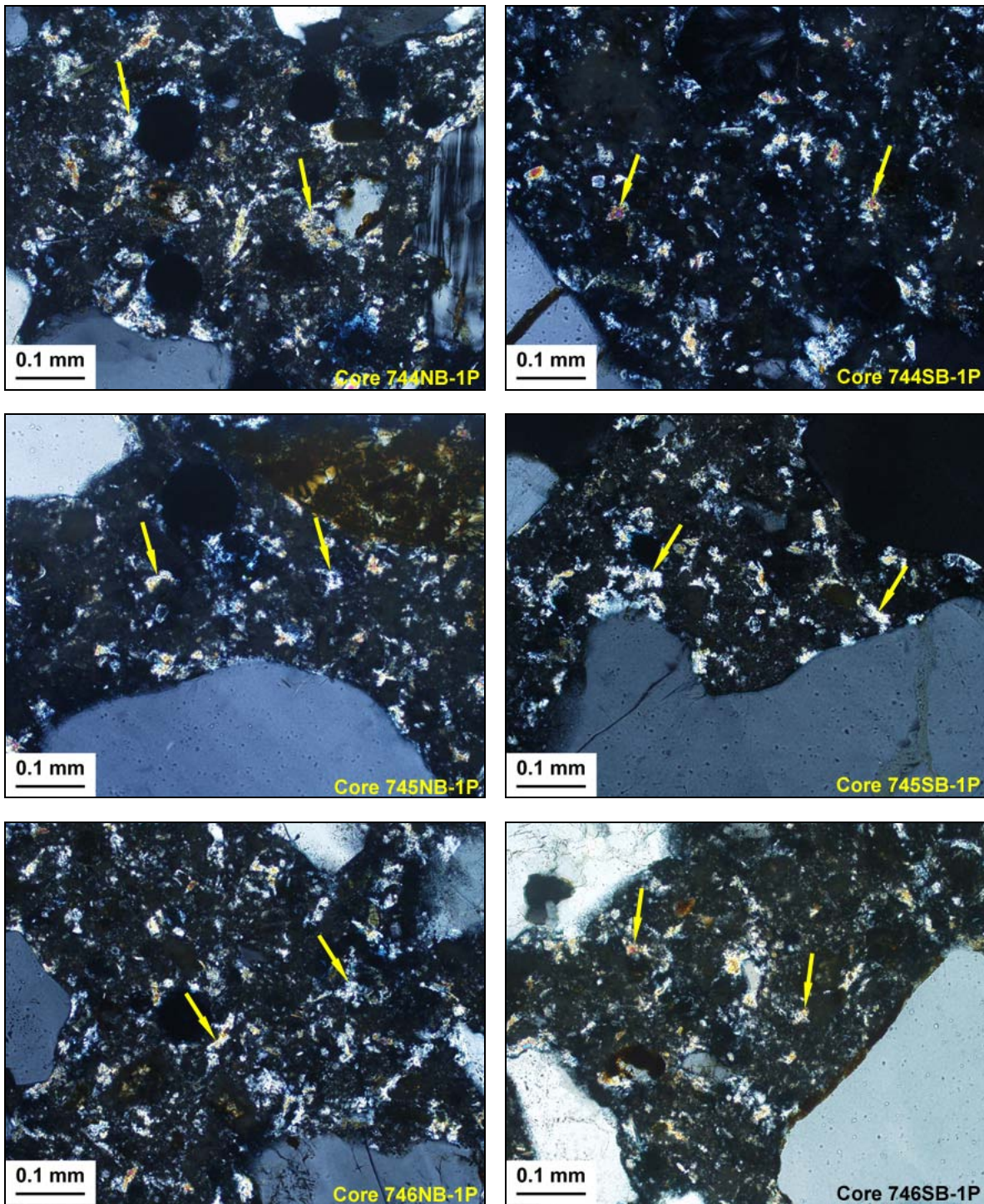


**Figure 13:** XPL photomicrographs illustrating the occurrence of primary calcium hydroxide produced during the cement hydration. The hydroxide (arrows) is distributed throughout the paste as medium-grained crystal masses with non-compact morphologies. The content and structure is generally indicative of moderate mix water contents.

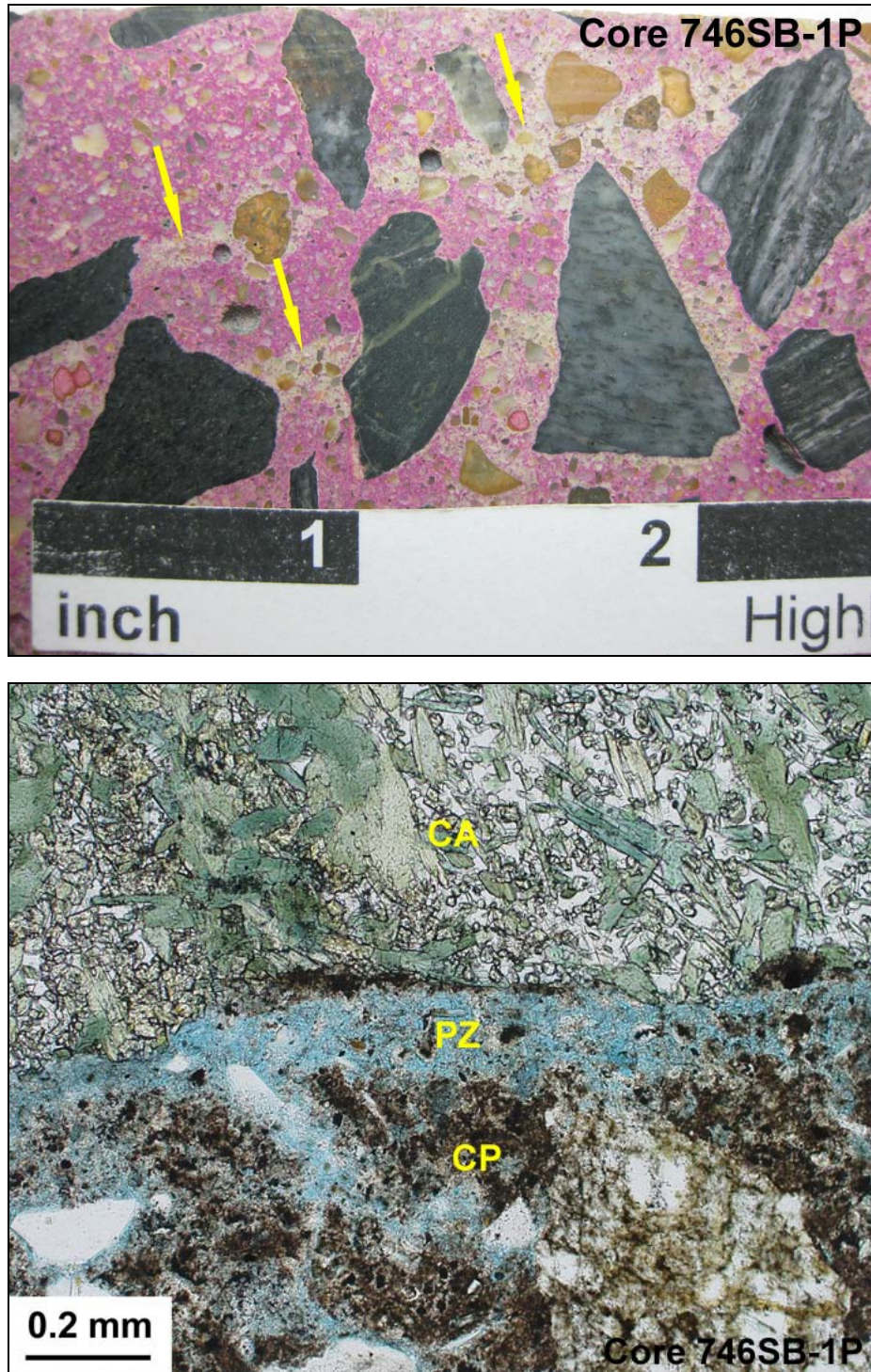


**Figure 14:** Evidence for bleed water migration and entrapment is found in Core 746SB-1P. The upper image is a close-up of the honed cross section treated with phenolphthalein indicator. The arrows indicate bleed water channels that show up as colorless bands. Note that the section is rotated on its side so that the channels appear horizontal rather than vertical. The lower PPL image illustrates a porous zone (PZ) between the cement paste (CP) and coarse aggregate (CA). This is caused by the local entrapment of mix water under the aggregate grain. The paste-aggregate bond is weakened as a result.

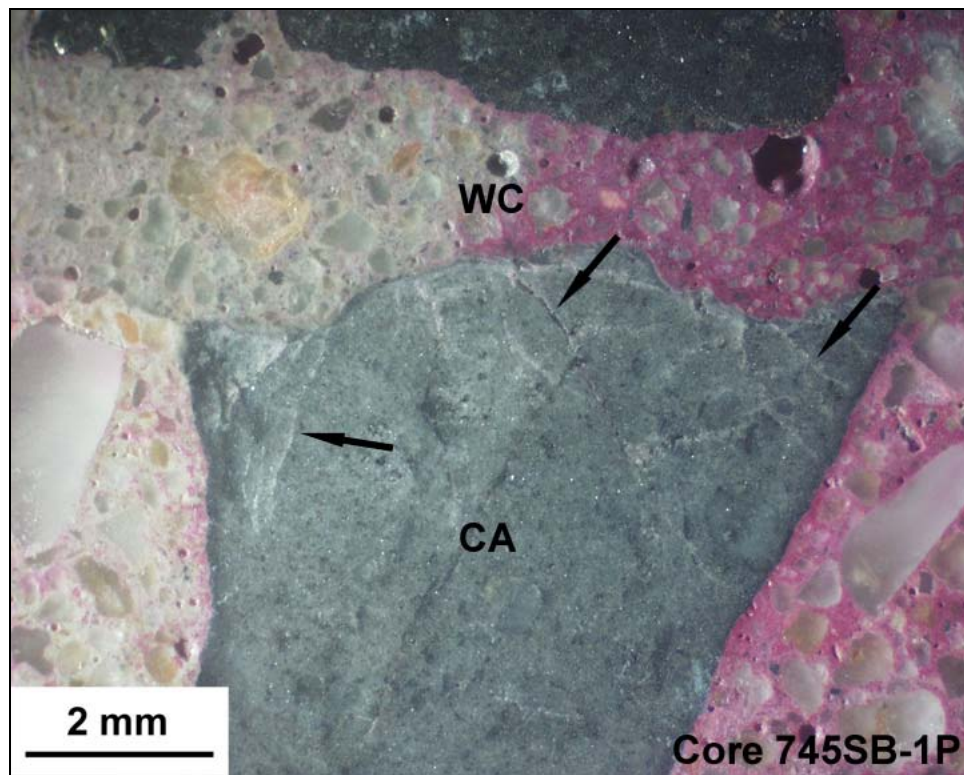


**Figure 15:** Reflected light photomicrograph of Core 745SB-1P. The wear course is shown directly over a truncated coarse aggregate grain in the structural layer (SC). The arrows indicate shatter cracks within the particle. The observations suggest a scarification process in advance of the wear course installation.

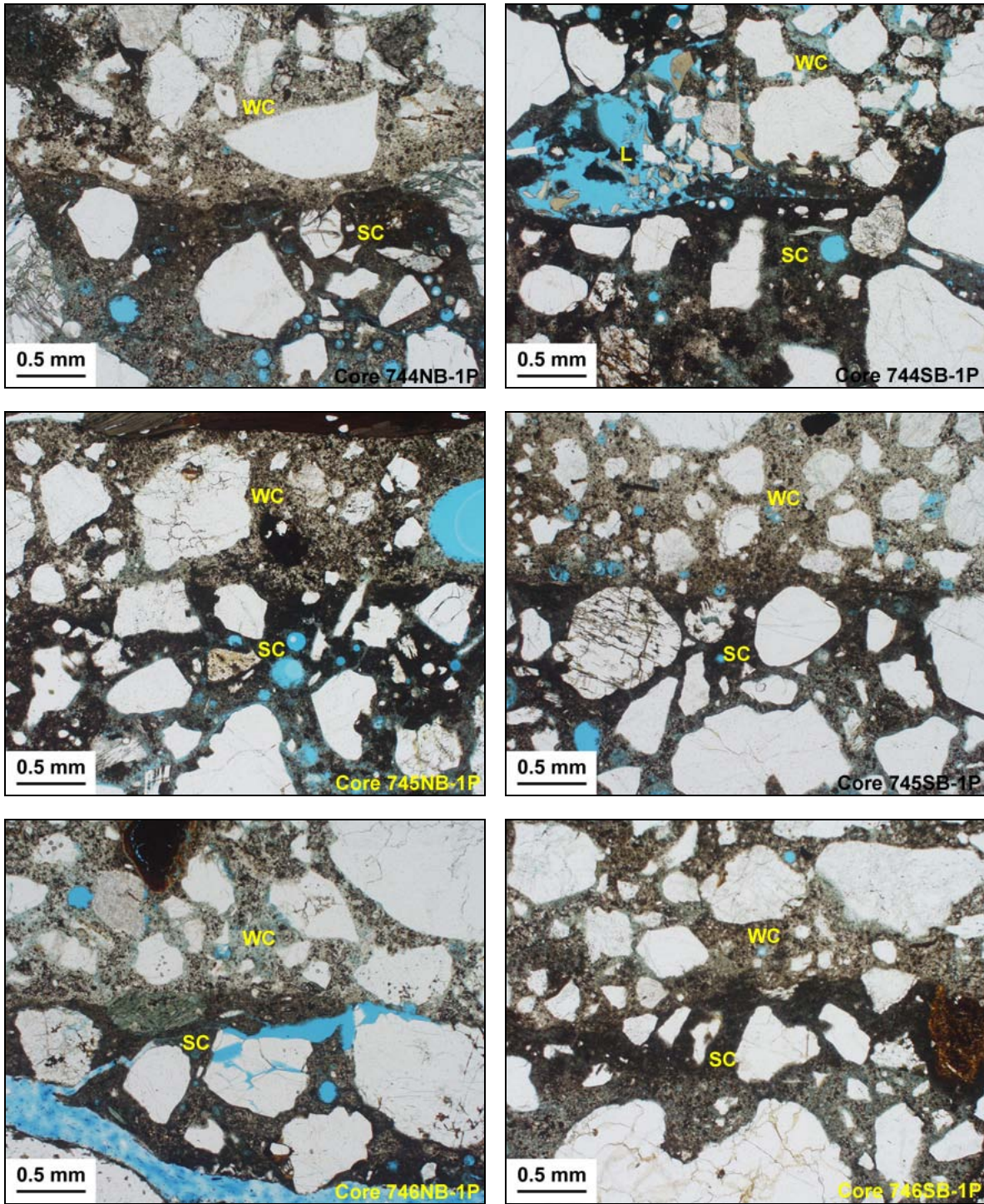


**Figure 16:** PPL photomicrographs illustrating the mostly tight contacts between wear course (WC) and structural concrete (SC). Some cracking is shown in blue for Core 746SB-1P. A patch of loose wear course material (L) is shown for Core 744SB-1P.

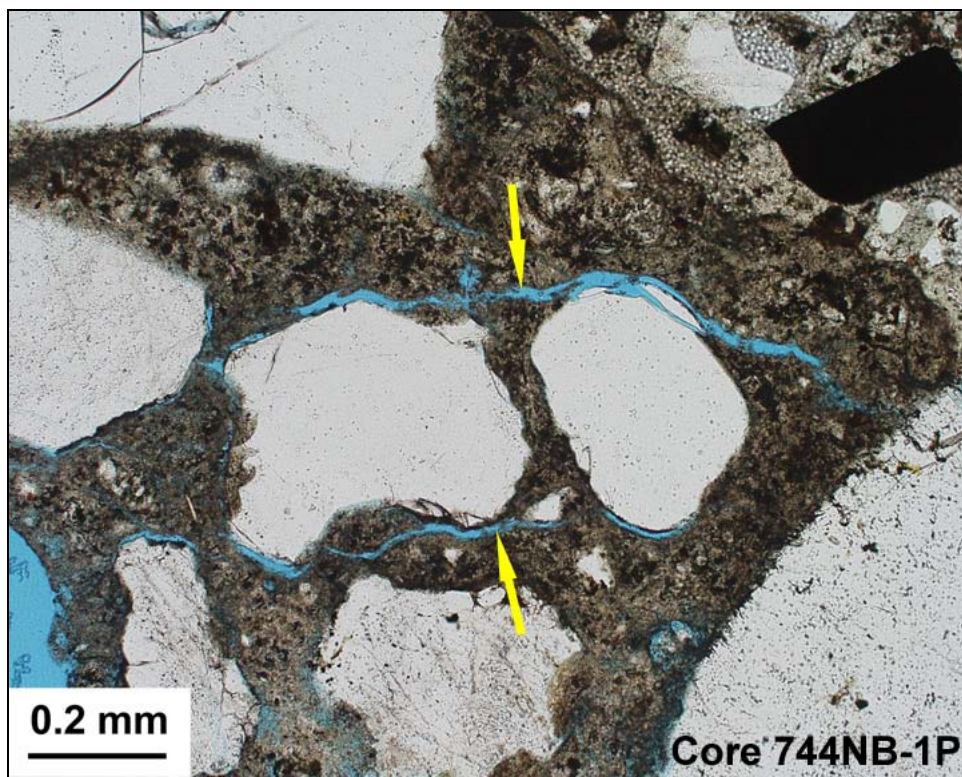


**Figure 17:** PPL photomicrograph of Core 744NB-1P. The arrows indicate minor surface-parallel microcracks just below the upper surface of the structural concrete. The cracking could be related to some freeze-thaw distress but the evidence is quite scant.

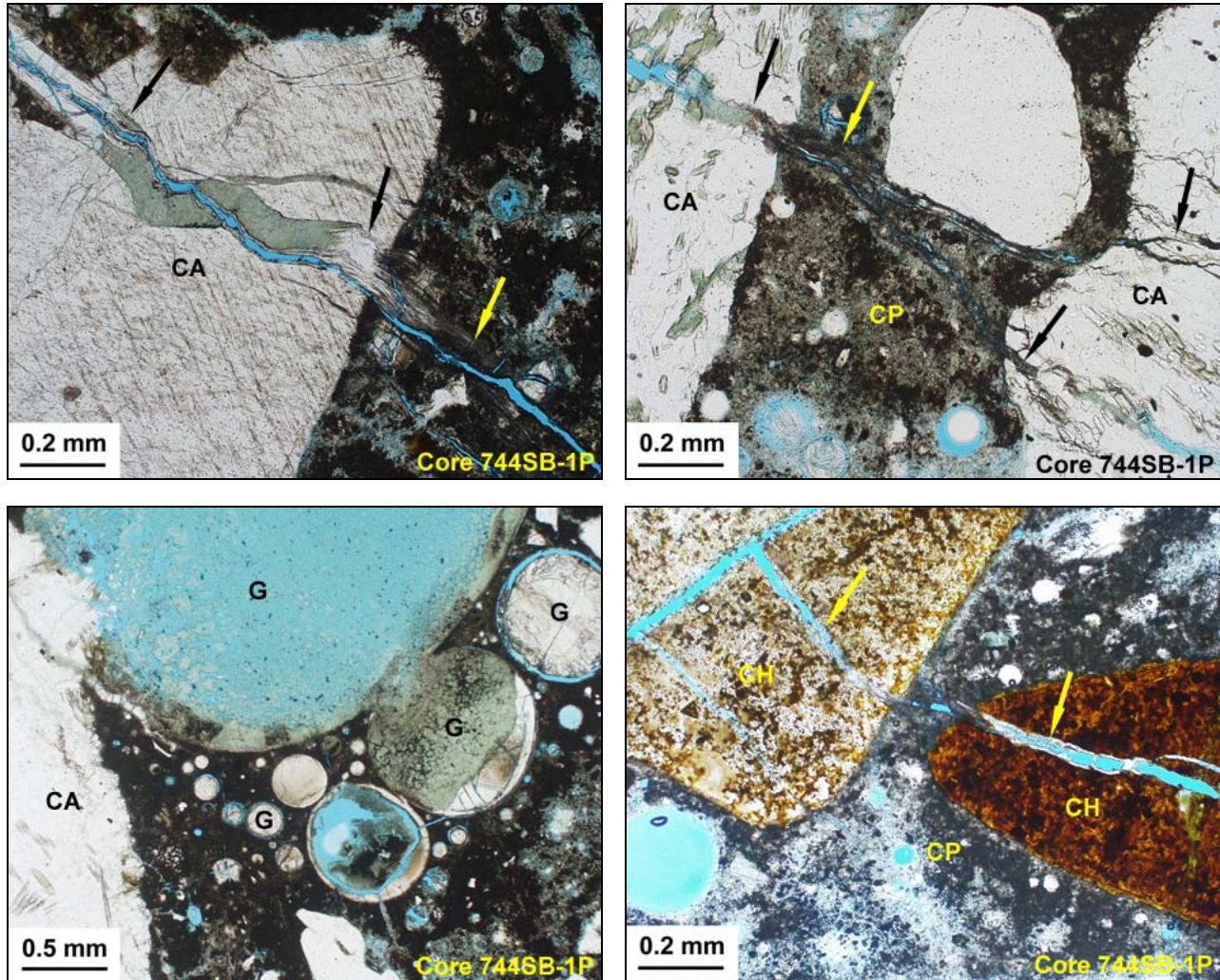


**Figure 18:** Core 744SB-1P exhibits the most well-developed alkali-silica reaction even if the reaction is only in its early stages. In the upper two PPL photomicrographs, the black arrows indicate reaction cracks within coarse aggregate grains (CA). The yellow arrows indicate where these have propagated into the adjacent cement paste (CP). ASR gel plugs are found at the periphery of the reactive stone. The reactive grain in the left image is a granitoid. The cracks span two granofels particles in the right image. Another granofels coarse aggregate grain (CA) is shown in the lower left PPL image. Alkali-silica reaction gels have deposited in adjacent air-voids (G). Chert (CH) in the fine aggregate is also reactive in this sample. In the lower right PPL image, the arrows indicate reaction cracks that are lined with ASR gel and link through the adjacent cement paste (CP).

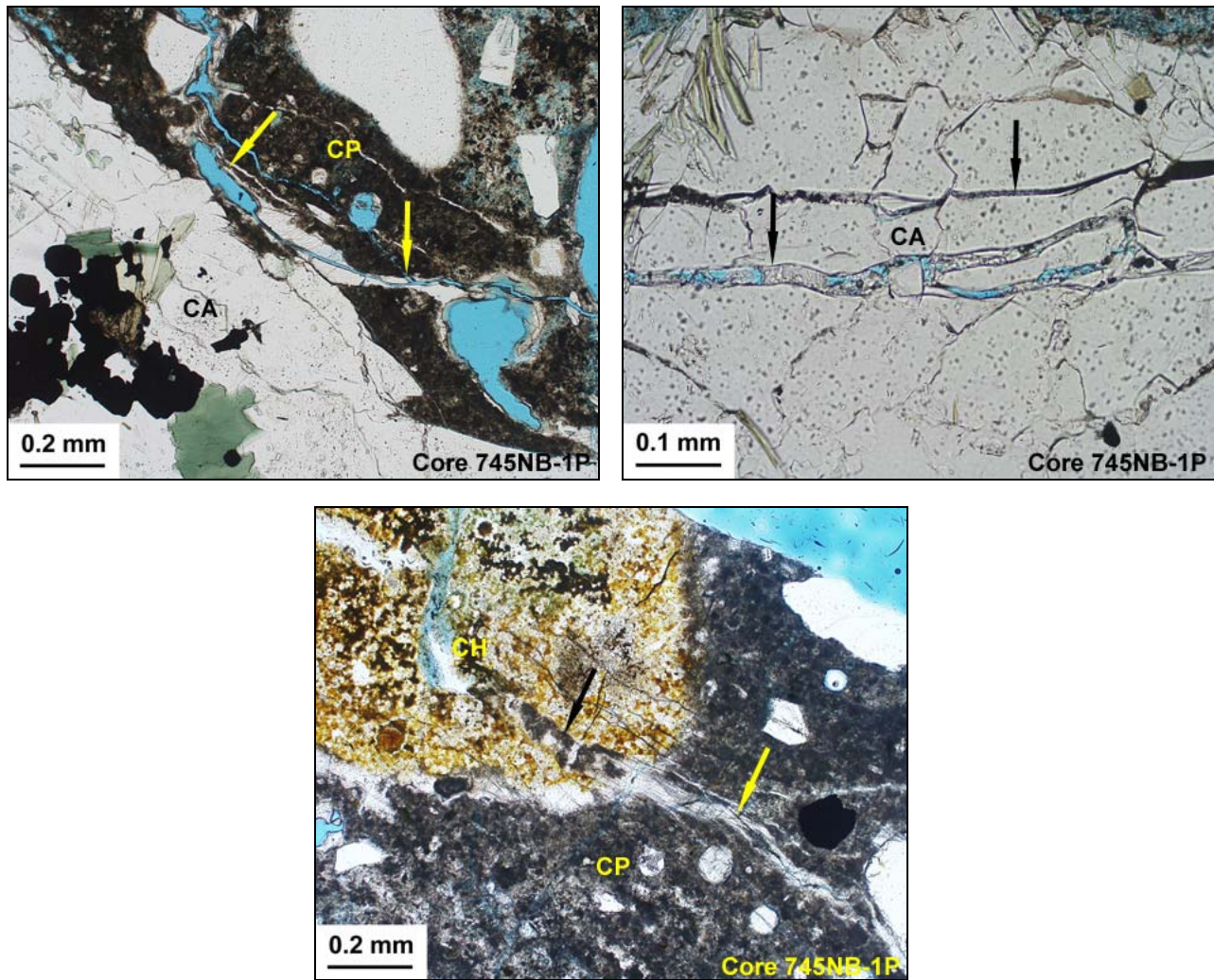


**Figure 19:** Early stage ASR reaction is also observed in Core 745NB-1P as shown by these PPL photomicrographs. (Upper left) The coarse aggregate shown (CA) is a granitoid. The arrows indicate cracks within the cement paste (CP) that are lined with well-developed ASR gels. (Upper right) The arrows indicate reaction cracks within another granitoid coarse aggregate particle (CA). (Lower image) The black arrow indicates a reaction crack within a chert particle (CH) in the fine aggregate. The yellow arrow indicates where this has propagated into the adjacent cement paste (CP). An ASR gel plug is found at the periphery of the reactive sand particle.

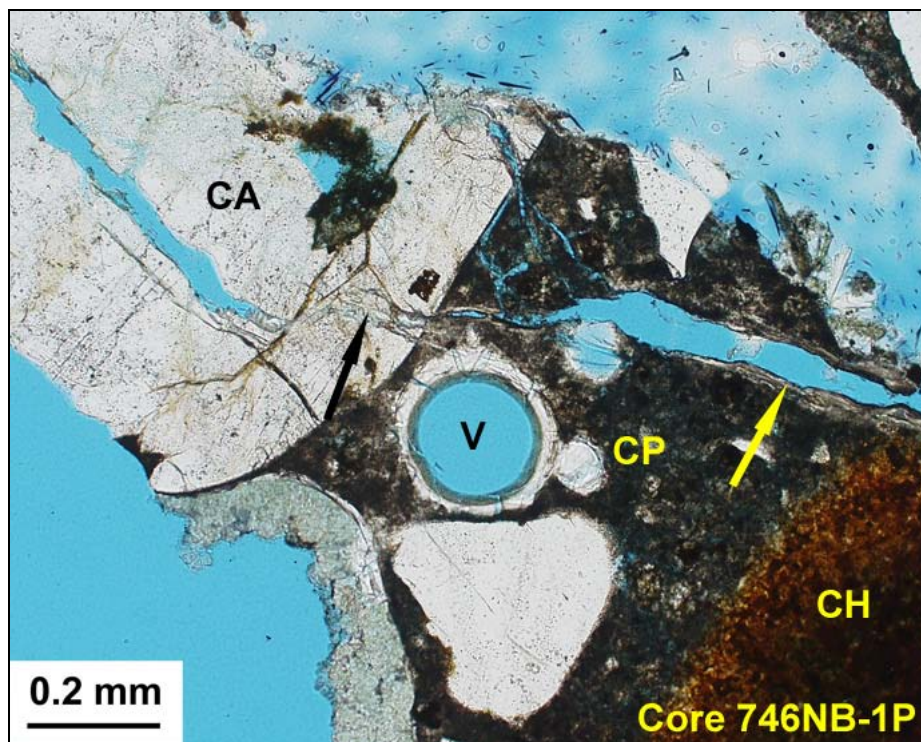
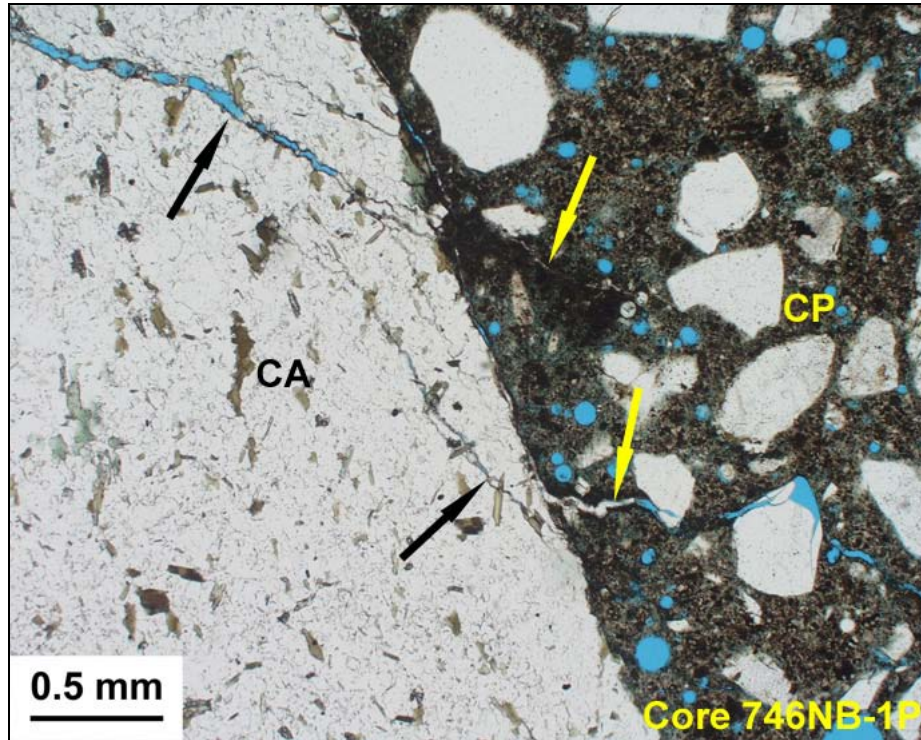


**Figure 20:** Core 746NB-1P exhibits an early stage ASR reaction almost equivalent to that observed in Core 745NB-1P. (Upper PPL image) The black arrows indicate reaction cracks within a granofels coarse aggregate grain (CA). The yellow arrows indicate where these have propagated into the adjacent cement paste (CP). ASR gel plugs are found at the periphery of the reactive stone. (Lower PPL image) A granitoid coarse aggregate (CA) and a chert sand particle (CH) are both involved in ASR reaction in this image. The arrows indicate cracks within the aggregate as well as the adjacent cement paste (CP). An adjacent air-void (V) is lined with reaction gel.

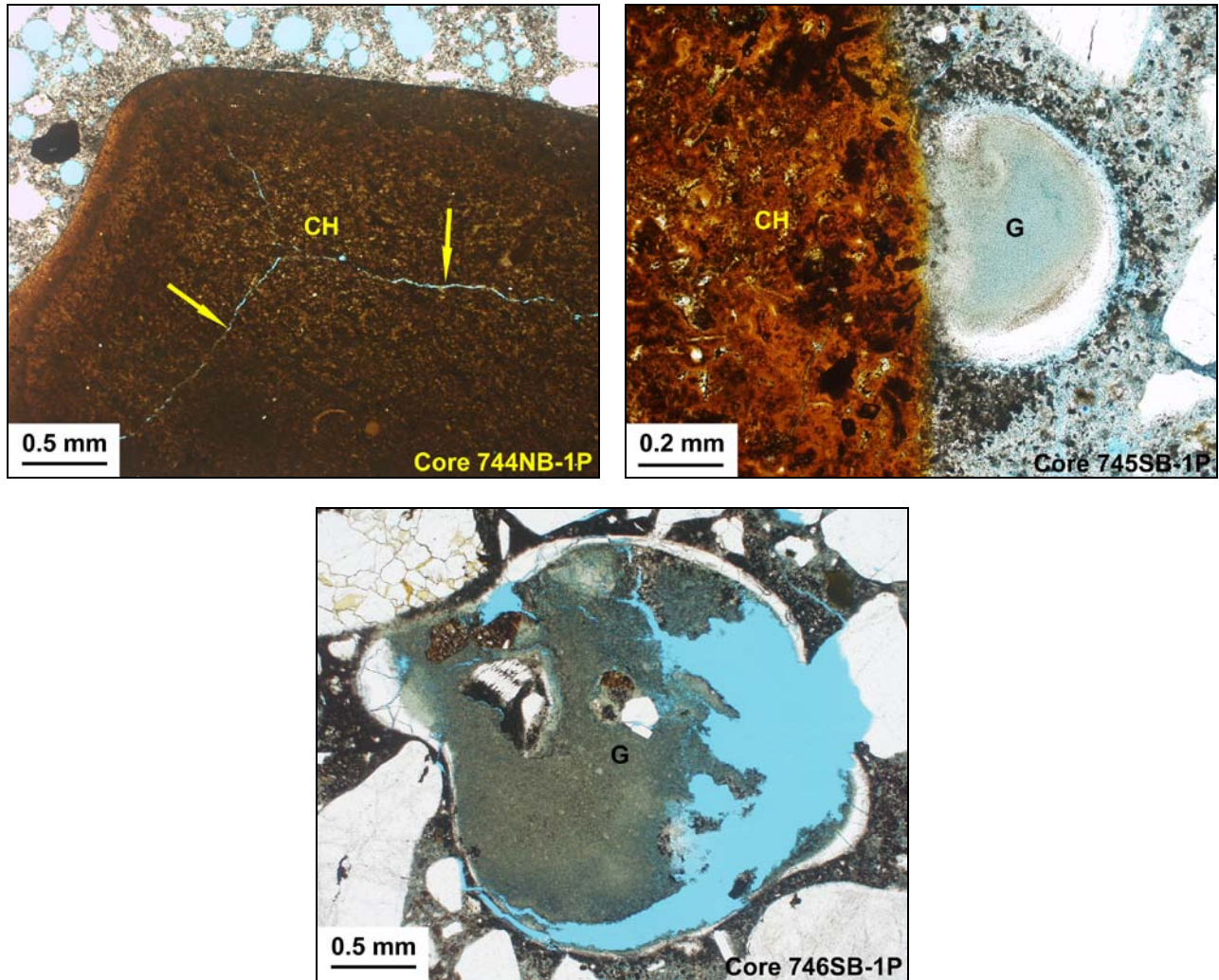


**Figure 21:** Only traces of ASR reaction are identified in the chert sand (CH) in the other core samples. (Upper left) The arrows indicate fine microcracks within a chert particle. (Upper right) A small deposit of reaction gel (G) has formed adjacent to a chert grain. (Lower image) A porous gel deposit (G) is shown in an air-void in the vicinity of a chert grain.

## PETROGRAPHIC EXAMINATION REPORT

---

<b>Client:</b>	Pennoni Associates, Inc.	<b>Client ID:</b>	PENN003
<b>Project:</b>	I-95 Viaduct Project	<b>Report #:</b>	SL0845-02
<b>Location:</b>	Delaware	<b>Dates Received:</b>	12/15/14, 01/07/15, 01/14/15
<b>Sample Type:</b>	Concrete cores	<b>Report Date:</b>	03/25/15
<b>Delivered by:</b>	Client (M. Padula)	<b>Petrographer:</b>	J. Walsh
		<b>Analyst:</b>	M. Pattie

---

**Page 1 of 64**

---

### Report Summary

- This report presents the results of petrographic examination and air-void analysis on eleven concrete core samples taken from viaduct structures along I-95 near Wilmington, DE.
- All examined concrete is similar in composition though the material represented by Core 748NB-1P exhibits sufficient differences from the other ten cores. The other ten samples could possibly represent a single mix design despite variability in the aggregate sources.
- The materials are normal weight, portland cement concretes with no supplementary cementitious materials. Original water to cement ratios are estimated to have been moderate within the mid to high 0.4's. Cores 748NB-2P, 748NB-3P, 748SB-3P, and 748SB-4P are estimated at the higher end of this range as suggested by slightly higher paste permeabilities. All of the cores exhibit air structures consistent with intentional air-entrainment and most are within a range that meets industry standards for adequate freeze-thaw protection.
- Coarse aggregates are highly varied but all include crushed stone with gradations ranging from No. 56 to No. 67. Core 748NB-1P is the only one containing all carbonate aggregate though some of this dolostone is also found in Core 748SB-3P. Quartz diorite, schistose granofels, tonalite/granodiorite, and minor to trace amphibolite constitute the remaining rock types and the other ten cores contain one or more of these lithologies. All cores have quartz-based natural fine aggregates though there are four different "batches" that are clearly identifiable within the sample set. One of these contains several percent ferruginous chert.
- All concrete materials are well mixed, cast, and consolidated and no significant workmanship deficiencies are identified in any core sample. It is assumed that the concrete was designed with the estimated moderate water to cement ratio and the mixtures were not overwatered at the job site. The only minor deficiency is the migration of bleed water and its partial entrapment around aggregate surfaces in Core 748SB-3P. Denser paste is adhered to coarse aggregate surfaces in the 758 cores but this does not appear to have been the result of inappropriate retempering.
- The concrete represents moderate quality mixtures suitable for many normal-duty, non-aggressive service environments. The only existing distress in the examined samples includes microcracking related to early stage alkali-silica reactions. The most well-developed reactions are associated with the granofels and granitoid aggregates. Reactions are also identified in the chert and strained quartzite present in some of the fine aggregate. Though relatively minor, Cores 748SB-1P and 748SB-2P exhibit the greatest degree of reaction and evidence is found throughout the full depth each core. Reactions are limited to the outermost surfaces in several of the other cores and only as trace occurrences in others. The cores with dolostone aggregate exhibit early stage alkali-carbonate reactions with no associated expansion.
- The reactions have not compromised the integrity of the concrete and no imminent threat is suggested by the existing conditions. Though no mitigating factors are identified, the concrete may remain provisionally stable over the course of a normal life cycle. However, this cannot be guaranteed and continued reaction may proceed at a relatively slow rate.
- A more detailed discussion of these findings may be found in the "Petrographic Findings and Discussion" section on page 3 of this report.

## **1. Introduction**

On December 15, 2014, and January 7 and 14, 2015, Highbridge received a total of twenty-seven (27) concrete core samples from Mr. Michael Padula of Pennoni Associates, Inc. reported to have been taken from viaduct structures along I-95 near Wilmington, DE. At the client's request, testing is performed on the structural layers of all core samples. No testing is requested for any wear courses present. For each sample, petrographic examination is requested to identify constituents, evaluate condition, and investigate the potential causes of any observed distress. No specific emphasis is requested and a general comprehensive examination is performed. Quantitative air-void analysis is also requested for the same samples.

Results for eleven of the core samples are presented in this report. The samples chosen to be included are those containing crushed stone coarse aggregate. Though 748NB-4P belongs to one of the structures included in this report, it contains a natural gravel coarse aggregate and will be described with other similar cores under separate cover. This report presents the results for the following cores:

748NB-1P	748SB-1P	758E-1P
748NB-2P	748SB-2P	758F-1P
748NB-3P	748SB-3P	758G-1P
	748SB-4P	758H-1P

## **2. Methods of Examination**

The petrographic examination is conducted in accordance with the standard practices contained in ASTM C856. Data collection is performed by a degreed geologist who by nature of his/her education is qualified to operate the analytical equipment employed. Analysis and interpretation is performed or directed by a supervising petrographer who satisfies the qualifications as specified in Section 4 of ASTM C856.

Air-void analysis is performed in accordance with the point-count method of ASTM C457. Component point counts are performed on hand-lapped concrete slabs sliced parallel to the core axis. The analysis is performed at a magnification of 75x on a Bausch and Lomb Stereozoom microscope and a dedicated cross-slide table machined to produce 0.05 inch translations per count. Air-void percentages are presented as those whose two-dimensional cross sectional diameter are less than or greater than one millimeter. The one millimeter diameter is considered a reasonable distinction between voids that are entrained and those that are entrapped in concrete that has been air-entrained. It should be understood that this threshold is somewhat arbitrary.

## **3. Standard of Care**

Highbridge has performed its services in conformance with the care and skill ordinarily exercised by reputable members of the profession practicing under similar conditions at the same time. No other warranty of any kind, expressed or implied, in fact or by law, is made or intended. Interpretations and results are based strictly on samples provided and/or examined.

## **4. Confidentiality**

This report presents the results of laboratory testing requested by the client to satisfy specific project requirements. As such, the client has the right to use this report as necessary in any commercial matters related to the referenced project. Any reproduction of this report must be done in full. In offering a more thorough analysis, it may have been necessary for Highbridge to describe proprietary laboratory methodologies or present opinions, concepts, or original research that represent the intellectual property of Highbridge Materials Consulting and its successors. These intellectual property rights are not transferred in part or in full to any other party. Presentation of any or all of the data or interpretations for purposes other than those necessary to satisfy the goals of the investigation are not permitted without the express written consent of the author. The findings may not be used for purposes outside those originally intended. Unauthorized uses include but are not limited to internet or electronic presentation for marketing purposes, presentation of findings at professional venues, or submission of scholarly articles.

**5. Petrographic Findings and Discussion**

**5.1 - General Summary**

This report presents the results of petrographic examination and air-void analysis on eleven concrete core samples taken from viaduct structures along I-95 near Wilmington, DE (Fig. 1). The study includes only the substrate concrete layers and not the 1.7” to 3.1” thick wear courses adhered to six of the samples. All examined concrete is similar in composition though the material represented by Core 748NB-1P exhibits sufficient differences from the other ten cores. This might represent a different mix design than used for the rest of the concrete. The other ten samples could possibly represent a single mix design despite variability in the aggregate sources. Important variations in the original mixture qualities are summarized in Table 5.1a below.

**Table 5.1a: Highlights of Concrete Mix Variations**

Core ID	Major stone type	Chert in sand	Air <sup>1</sup>	Relative paste permeability <sup>2</sup>	Alkali-aggregate reaction
748NB-1P	Dolostone			Lower	Early stage ACR in dolostone.
748NB-2P	Diorite	Yes	Low SS, High SF	Higher	Early stage ASR limited to top surface and only in chert sand.
748NB-3P	Diorite	Yes	Low SS, High SF	Higher	Early stage ASR limited to top surface and only in chert sand.
748SB-1P	Granofels/ Granitoid		High air		Early stage ASR throughout core with granofels and granitoid most reactive.
748SB-2P	Granitoid				Early stage ASR throughout core with granitoid most reactive.
748SB-3P	Mixed	Yes	Low SS, High SF	Higher	Trace ASR limited to top surface. Granitoid stone and chert sand both involved. Early stage ACR in dolostone.
748SB-4P	Granitoid	Yes	High air, Low SS	Higher	Early ASR limited to top surface. Granitoid stone and chert sand both involved.
758E-1P	Granitoid		High SF		Very minor ASR in granitoid.
758F-1P	Granitoid				Trace ASR in granitoid.
758G-1P	Granitoid				Trace ASR in granitoid.
758H-1P	Granitoid		High air		Trace ASR in granitoid.

Notes:

1. SS = specific surface, SF = spacing factor.
2. Paste permeabilities do not vary greatly. Reported differences are relatively subtle.

In all cases, the material is a normal weight, portland cement concrete with no supplementary cementitious materials. Original water to cement ratios are estimated to have been moderate within the mid to high 0.4’s. Cores 748NB-2P, 748NB-3P, 748SB-3P, and 748SB-4P are estimated at the higher end of this range as suggested by slightly higher paste permeabilities. All of the cores exhibit air structures consistent with intentional air-entrainment and most are within a range that meets industry standards for adequate freeze-thaw protection. Five cores have slightly lower specific surfaces and/or slightly higher spacing factors. Three samples have air contents that may be considered a bit excessive and this could have a modest impact on strength.

Coarse aggregates are highly varied but all include crushed stone with gradations ranging from No. 56 to No. 67. Core 748NB-1P is the only one containing all carbonate aggregate though some of this dolostone is also found in Core 748SB-3P. Quartz diorite, schistose granofels, tonalite/granodiorite, and minor to trace amphibolite constitute the remaining rock types and the other ten cores contain one or more of these lithologies. All cores have quartz-based natural fine aggregates though there are four different “batches” that are clearly identifiable within the sample set. One of these contains several percent ferruginous chert.

All concrete materials are well mixed, cast, and consolidated and no significant workmanship deficiencies are identified in any core sample. It is assumed that the concrete was designed with the estimated moderate water to cement ratio and the mixtures were not overwatered at the job site. The only minor deficiency is the migration of bleed water and its partial entrapment around aggregate surfaces in Core 748SB-3P. Denser paste is adhered to coarse aggregate surfaces in the 758 cores but this does not appear to have been the result of inappropriate retempering.

The concrete represents moderate quality mixtures suitable for many normal-duty, non-aggressive service environments. The only existing distress in the examined samples includes microcracking related to early stage alkali-silica reactions. The most well-developed reactions are associated with the granofels and granitoid aggregates. Reactions are also identified in the chert and strained quartzite present in some of the fine aggregate. Though relatively minor, Cores 748SB-1P and 748SB-2P exhibit the greatest degree of reaction and evidence is found throughout the full depth each core. Reactions are limited to the outermost surfaces in several of the other cores and only as trace occurrences in others. The cores with dolostone aggregate exhibit early stage alkali-carbonate reactions with no associated expansion. The reactions have not compromised the integrity of the concrete and no imminent threat is suggested by the existing conditions. Though no mitigating factors are identified, the concrete may remain provisionally stable over the course of a normal life cycle. However, this cannot be guaranteed and continued reaction may proceed at a relatively slow rate.

**5.2 - Coarse Aggregate Materials**

All cores described in this report contain a crushed stone coarse aggregate of one kind or another. Core 748NB-4P is part of one of the location groups discussed for this report. However, this sample contains a natural gravel aggregate and it was decided to group this core with other similar samples in Highbridge Report SL0845-03. Total aggregate contents are estimated to range between 30% and 40% by hardened concrete volume (see Table 5.2a below). The estimate is made visually using the hand samples and honed cross sections (Fig. 2). Almost all of the aggregate contents are considered within a normal range for conventional concrete. Only Core 748NB-1P is considered deficient in stone at about 30% by hardened volume. Admittedly, this core sample is rather small and some errors are possible. Nonetheless, if these pieces are representative of the concrete, then this mixture is certainly mortar-rich.

**Table 5.2a: Summary of Coarse Aggregate Contents**

Approximate volume	Core samples
~30%	748NB-1P <sup>1</sup>
~30-35%	748SB-1P, 758E-1P, 758F-1P
~35%	748SB-2P, 748SB-3P, 748SB-4P, 758H-1P
~35-40%	748NB-2P, 748NB-3P, 758G-1P

Notes:

1. The core sample pieces are somewhat small and the content is difficult to estimate accurately as a result.

**Table 5.2b: Distribution of Rock Types in Coarse Aggregate**

Core ID	Dolostone	Quartz Diorite	Tonalite/ Granodiorite (Granitoid)	Schistose Granofels	Amphibolite
748NB-1P	All				
748NB-2P		All			
748NB-3P		All			
748SB-1P			Major	Major	Minor
748SB-2P			Major		Minor
748SB-3P	Major	Major	Major		
748SB-4P		Trace	Major		
758E-1P			Major	Trace	
758F-1P			Major	Minor	Trace
758G-1P			Major	Lesser	Trace
758H-1P			Major	Minor	Trace

A variety of lithologies are identified in the crushed stone coarse aggregates. Table 5.2b presents a simple summary of which of these is detected in which cores. Some of the rock types may be related while others are clearly from a different source. One type of stone not previously identified in cores from this project is a carbonate crushed stone composed predominantly of dolomite (i.e. calcium-magnesium carbonate). This rock is found as the sole aggregate type in Core 748NB-1P and combined with a quartz diorite and granitoid in Core 748SB-3P (Fig. 3). Based on the visual characteristics of the stone, there is likely a certain degree of variation only some of which is represented in the petrographic sections. Nonetheless, most grains are fine to medium-grained and equigranular dolostones. Some mild to moderate shear strain is noted in a lesser proportion of the particles. One example of strained dolostone with a crackle-breccia texture and some cemented gouge is detected in the thin section for Core 748SB-3P. Quartz and strained quartz are found as inclusions along with minor white mica. Argillaceous grains are relatively rare and only traces of pyrite or other sulfides are detected.

In a previous report for this project (Highbridge Report SL0845-01), a quartz diorite lithology was detected in trace quantity in Cores 745SB-1P and 746SB-1P. In this group of samples, the quartz diorite is found as the sole aggregate in Cores 748NB-2B and 748NB-3P. The diorite is a major component in a mixture of aggregate types in Core 748SB-3P and as a trace constituent in association with a more quartz-rich granitoid in Core 748SB-4P (Fig. 4). In fact, it would be expected that the quartz diorite would be geologically associated with the granitoid. However, the granitoid is more often found grouped with a schistose granofels suggesting that the two are part of the same geological assemblage. Of course, it is possible that all are geologically associated. The quartz diorites are exceptionally fresh and appear dark-colored to slightly mottled in hand sample. The stone is mostly fine-grained and equigranular. Constituents include evenly distributed plagioclase feldspar, quartz, orthopyroxene, and clinopyroxene. Opaque phases are common and likely consist of magnetite or ilmenite. No potentially deleterious sulfides are noted. Traces of biotite are detected. In Core 748NB-3P, several particles are medium-grained and one grain contains a concentration of clinopyroxene. The trace grains in Core 748SB-4P are only identified in hand sample and are not viewed in thin section.

All of the remaining samples contain a granitoid lithology as a major phase appearing as a medium-grained, gray mottled stone in hand sample (Figs. 5 and 6). These often occur in association with varying quantities of a schistose granofels. The granitoid is similar to rocks identified in several cores of the previous study. A larger population was available for study in the cores described here and the average stone may classify as either a tonalite or a granodiorite. The common matrix in all grains is a mixture of quartz and feldspar the latter containing minor amounts of sericitic alteration. Only a minor proportion of the feldspar includes potassium varieties. Chlorite and biotite are most commonly identified as accessory phases though epidote and amphibole are also detected. There appears to be some variation in the content of the accessory mineralogies. These are relatively common in Cores 748SB-1P, 748SB-2P, and 748SB-3P. In the latter two samples, coarse aggregate grains are identified where chlorite and biotite are rather concentrated. In Cores 748SB-4P, 758E-1P, 758F-1P, 758G-1P, and 758H-1P, the rock contains a lower content of the accessory minerals. In the first report for this project, the granitoid was found to be unusually rich in interstitial material including graphic intergrowths of quartz and feldspar as well as regions of strained quartz characterized by multiple fine subgrains. These are also observed to some degree in the samples studied for this report though some variability is noted. For example, graphic intergrowths are not noted in Cores 748SB-1P, 748SB-2P, 748SB-3P, and 758G-1P. Other minor variations are noted between samples and all of these subtle differences are summarized in Table 5.2c below.

**Table 5.2c: Variations in Characteristics within Tonalite/Granodiorite Coarse Aggregate**

Core ID	Accessories	Interstitial phases
748SB-1P	Chlorite, biotite common.	Relatively few interstitial phases
748SB-2P	Chlorite, biotite common and sometimes concentrated. Epidote also detected.	Minor fine-grained interstitial strained quartz.
748SB-3P	Chlorite, biotite common and sometimes concentrated. Epidote also detected.	Minor fine-grained interstitial strained quartz.
748SB-4P	Chlorite, epidote, opaques in lesser quantity.	Fine-grained interstitial quartz and graphic intergrowths are common.
758E-1P	Chlorite, biotite, epidote, opaques in lesser quantity.	Interstitial material is relatively common. Graphic intergrowths are less abundant and quartz tends to be coarser-grained.
758F-1P <sup>1</sup>	Accessories generally in lower quantity. However, several grains rich in fine-grained chlorite, biotite, epidote, and amphibole.	Interstitial material is relatively common. Graphic intergrowths are less abundant and quartz tends to be coarser-grained.
758G-1P	Accessories generally in lower quantity. However, several grains rich in fine-grained chlorite, biotite, epidote, and amphibole.	Interstitial material is relatively common. Graphic intergrowths are not identified. Quartz tends to be coarser-grained.
758H-1P	Chlorite, biotite, epidote in lesser quantity.	Interstitial material is relatively common. Graphic intergrowths are not identified. Quartz tends to be much coarser-grained.

Notes:

1. Some grains are rich in chlorite and amphibole and appear to be a gradational lithology between the tonalite and the granofels.

A less abundant lithology usually associated with the granitoid rocks may be classified as a schistose granofels. The rock type is found in Core 748SB-1P and in the 758 samples (Fig. 7). The material is only significant in Cores 748SB-1P and 758G-1P. All are somewhat similar in texture tending to be rich in a fine-grained matrix of highly sheared quartz with or without distributed amphibole. Porphyroclasts of mildly sericitized feldspar, quartzite, and micaceous material are also included in some grains. The rocks are clearly deformed and many grains display S-C shear banding.

An amphibolite lithology was common in the core samples examined for Highbridge Report SL0845-01. In this report, the amphibolite is only a minor component of Cores 748SB-1P and 748SB-2P and as a trace component in Cores 758F-1P, 758G-1P, and 758H-1P (Figs. 8 and 9). In the previous report, the amphibolites were interpreted to represent metabasites of varying metamorphic grade. Less evidence for the provenance is detected in these samples but the metamorphic grades are low to moderate based on the inclusion of pumpellyite, chlorite, and epidote. Sulfide minerals are detected in relatively low abundance throughout the amphibolites.

From a physical perspective, the stone in all eleven cores is considered hard, inelastic, and non-porous. No significant preferential weaknesses are identified. The lithological types are not among those considered to be particularly alkali-silica reactive. Nonetheless, some evidence for reaction is noted in several of the samples. The strained quartz is likely the more reactive component within the stone. An early stage dedolomitization reaction is also detected in the dolostones though these rock types are also generally considered to be at low risk. All of these features are discussed in greater detail below.

The carbonate crushed stone in Core 748NB-1P and 748SB-3P is angular to subangular in shape. Aspect ratios are mostly equant with fewer subequant particles and no significant anisotropic grains. For the cores containing siliceous crushed stone (i.e. all except Core 748NB-1P), the aggregate shapes are mostly angular. Grains have subequant aspect ratios on average. In Cores 748NB-2P, 748NB-3, 748SB-1P, 748SB-2P, and 748SB-3P, there are a moderate proportion of plate-like particles having aspect ratios in the 3:1 to 4:1 range. In Cores 748SB-4P, 758E-1P, 758F-1P, 758G-1P, and 758H-1P these are only identified in minor proportion. In all cases, the presence of anisotropic grains is not significant and the particle shapes are suitable for aggregate to be used in portland cement concrete mixtures.

**Table 5.2d: Estimated Coarse Aggregate Gradations**

Core ID	Nominal top size	Approximate gradation type	Remarks
748NB-1P <sup>1</sup>	1"	Probably No. 56 but No. 57 is possible	The gradation appears deficient below the 1/2" sieve.
748NB-2P	3/4"	No. 57 to No. 6	All particles may pass the 3/4" sieve. Rich over the 3/8" sieve with little material passing this mesh.
748NB-3P	3/4"	No. 57 to No. 6	All particles may pass the 3/4" sieve. Rich over the 3/8" sieve with little material passing this mesh.
748SB-1P	3/4"	No. 57 to No. 6	All particles may pass the 3/4" sieve. Rich over the 3/8" sieve with little material passing this mesh.
748SB-2P	3/4"	No. 57 to No. 6	Most if not all particles pass the 3/4" sieve. Rich over the 3/8" sieve with little material passing this mesh.
748SB-3P	3/4"	Probably closer to No. 67 but a finer gradation of No. 57 is also possible	Most if not all particles pass the 3/4" sieve. Moderately broad gradation down to the No. 4 sieve.
748SB-4P	3/4"	No. 56 most likely but possibly on the cusp of No. 57	Possibly greater than 75% retained on the 1/2" sieve.
758E-1P	3/4"	No. 56 more likely but No. 57 possible	Possibly greater than 65% retained on the 1/2" sieve. A relatively low proportion is present near the 3/8" sieve.
758F-1P	3/4"	No. 57 to No. 6	Moderately broad gradation down to the No. 4 sieve.
758G-1P	3/4"	No. 57 to No. 6	Most particles pass the 3/4" sieve. Rich over the 3/8" sieve with little material passing this mesh.
758H-1P	3/4"	No. 57 to No. 6	Most particles pass the 3/4" sieve. Rich over the 3/8" sieve with little material passing this mesh.

Notes:

1. The core sample pieces are somewhat small and the gradations are difficult to estimate accurately as a result.

The gradations cannot be quantified petrographically and the particle size distributions are estimated from two-dimensional cross sections of the concrete (Fig. 2). Based on the permissible gradation limits of ASTM C33, the size distribution profiles range from a No. 56 to a No. 6 (and possibly a No. 67 in one case). A summary of the gradation estimates are presented in Table 5.2d above. The carbonate crushed stone in Core 748NB-1P is somewhat coarser than the other rock types with a nominal top size estimated at the 1" sieve. The particle size distribution is likely consistent with a No. 56 profile as specified by ASTM C33. All of the other core samples have coarse aggregate with nominal top sizes estimated at the 3/4" sieve. Six of the ten have nearly identical particle size distributions with most particles sized between the 3/4" and 3/8" sieves. These are estimated to have gradation profiles consistent with either a No. 57 or a No. 6. The other four samples exhibit some moderate differences either coarser or finer than these six samples.

### **5.3 - Fine Aggregate Materials**

All eleven samples contain a siliceous natural sand. The fine aggregate content is estimated at 35-40% by hardened mortar fraction for Cores 748NB-1P, 748SB-1P, 748SB-2P, 758E-1P, 758F-1P, and 758G-1P. The others are estimated at 40-45% by hardened mortar fraction though likely at the lower end of this range.

All sands are quartz-based aggregates consisting predominantly of monocrystalline quartz grains with lesser polycrystalline quartz particles. The latter are usually prevalent in the coarsest grain sizes. No clay coatings or friable materials are identified. From a physical perspective, all sands are considered hard, inelastic, and non-porous. Chemically, the chert in the coarser sizes of some of the sand is considered potentially alkali-reactive and this could represent a modest durability concern (Fig. 10). There are four distinctive batches identified in the eleven samples.

One sand type is identified only in Core 748NB-1P (the same core containing the carbonate stone). Alkali feldspar and mildly to moderately strained quartzite are minor constituents in this sand. Fresh and altered glauconite grains are found as minor to trace constituents. Granite and sillimanite schist are identified as traces as well and typical heavy accessory minerals are exceedingly rare. Aggregate particles are equidimensional and subrounded to subangular in shape. The nominal top size is estimated at the No. 8 sieve. Though the gradation is broad, a peak abundance at around the No. 50 sieve is somewhat strong. The fines content is moderate. Based on the qualitative petrographic observations, the particle size distribution is estimated to comply with the gradation requirements of ASTM C33 likely near the finer size limits of the current standard.

The second sand type is identical to the fine aggregate described for the cores in Highbridge Report SL0845-01. For this report, the material is found in Cores 748NB-2P, 748NB-3P, 748SB-3P, and 748SB-4P. Alkali feldspar is a lesser component and mildly to moderately strained quartzite is a minor constituent. A minor but significant amount of ferruginous chert is included in all samples at several percent of the total sand volume. Some of the ferruginous particles appear to include siltstones or argillites as well. However, their texture under reflected light suggests that all are cemented by a cryptocrystalline silicification. Both the chert and the strained quartzite are more concentrated in the grain sizes coarser than the No. 8 sieve. Heavy accessory minerals are rare. The sand consists of equidimensional particles that are subrounded to subangular in shape. Based on the qualitative petrographic observations, the particle size distributions are estimated to nearly comply with the gradation requirements of ASTM C33 though likely near the coarser size limits of the current standard. Technically, the sand in Cores 748NB-3P and 748SB-3P do not comply with permissible limits due to rare particles of cherty siltstone up to 1/2". Aside from these, nominal top sizes are estimated at the No. 4 sieve, particle size distributions are rich above the No. 30 sieve, and little material is estimated to pass the No. 50 mesh.

The third and fourth sand types have similar compositions but with different gradations. These are found in Cores 748SB-1P and 748SB-2P as well as all four 758 core samples. Both are predominantly monocrystalline quartz with lesser polycrystalline quartz. Other materials are exceedingly rare and include fine mica flakes, feldspar, heavy accessory minerals, and chert. Aggregate particles are equidimensional with grain shapes that mostly range from subrounded to subangular. Subangular particles are more dominant in the two 748 cores and subrounded grains are more common in the 758 samples.

Though not confirmed through a quantitative gradation analysis, the particle size distributions might not comply with those required by ASTM C33. For the two 748 samples, the aggregate may be a bit too fine. For the 758 cores, the gradation may be overly narrow. In Cores 748SB-1P and 2P, the nominal top sizes are estimated at the No. 4 sieve. Most grains are estimated to pass but there is still an abundance of material coarser than a No. 8 sieve. The profile is rich in the vicinity of the No. 50 sieve and possibly greater than 25% could pass this mesh. The fines below a No. 200 sieve are not estimated to be excessive. For Cores 758E-1P through 758H-1P, there is clearly material retained on the No. 4 sieve though the abundance in the coarser sizes is not as high. There is a strong peak abundance estimated between the No. 30 and No. 50 sieves. The fines content is minor in these core samples.

**5.4 - Cementitious Materials and Microstructure**

Ordinary gray portland cement is identified as the sole binder in all examined samples and no supplementary cementitious materials are present. Liquid admixtures cannot be identified petrographically though their influence on paste microstructure can often be detected. It is not clear whether or not any water-reducing admixtures had been added. The cementitious hydrate in Core 748SB-3P has a microscopically “clotted” texture. This is usually attributed to cement particle flocculation in mixtures not containing plasticizers. However, the texture is not diagnostic. In the last round of testing, it was suggested that there could be a correlation between this feature and the occurrence of early-stage alkali-silica reaction. That correlation is not present here and the fine heterogeneity is interpreted to be an original feature of the concrete. The paste in the other ten cores is more uniform at the microscopic scale though some slight mottling is detected in Core 748NB-1P. The size and distribution of spherical air-voids indicates that all concrete was intentionally air-entrained. There is some variability in the development and quality of the air system between these eleven samples.

All concrete is estimated to have been mixed at a moderate water to cement ratio (w/c). Though the ratios cannot be quantified petrographically, cement paste characteristics are consistent with w/c in the mid to high 0.4’s. Based on minor to moderate differences in the microporosity of the hardened binder, fracture behavior of the concrete, and subtle visual differences in color and luster of the hydrated paste, Cores 748NB-3P, 748SB-3P, 748SB-4P, 758H-1P and possibly 748NB-2P contain concrete estimated to have been mixed with w/c closer to the high 0.4 range. Most of the remaining samples are difficult to distinguish within the range estimated as some properties suggest higher water content while others suggest lower water content. Only Core 748NB-1P with the dolostone aggregate was clearly mixed at the lower end of the estimated w/c range.

The characteristics used to estimate original water to cement ratio include the capillary porosity of the cured cementitious hydrate (Fig. 11). The capillary pore structure is produced by the evaporable water present in the fresh mixture. As described above, Core 748SB-3P has cementitious product with a microscopically clotted texture consisting of denser clots surrounded by paste with moderately high capillary porosity. Despite the lower porosity zones, the permeability is controlled by the more porous regions. Other than this one core, capillary pore structures tend to be relatively homogeneous throughout the sample set. Core 748NB-1P exhibits the densest structure with a moderately low capillary pore structure. Cores 748NB-2P, 748SB-3P, 748SB-4P have more moderate porosities that may even be moderately high locally. Assuming the eleven cores were meant to represent concrete of the same design, the paste quality suggests some variability in mix proportioning. However, the differences are not especially major. The variations in pore structure are summarized in Table 5.4a below.

**Table 5.4a: Summary of Capillary Pore Structures**

Capillary porosity	Core samples
Moderately low capillary porosity, slightly mottled but otherwise homogeneous paste	748NB-1P
Moderate capillary porosity, homogeneous paste	748SB-1P, 748SB-2P, 758E-1P, 758F-1P, 758G-1P, 758H-1P
Microscopically clotted with moderately low to moderately high capillary porosity but averaging toward the higher porosity.	748SB-3P
Moderate capillary porosity though tending toward moderately high in some areas, otherwise homogeneous paste	748NB-2P, 748NB-3P, 748SB-4P

Calcium hydroxide is a primary phase of portland cement hydration and its size, morphology, and content can also be an indicator of original water contents when preserved (Fig. 13). There is some moderate variation in these crystallizations though these differences do not always correlate with other indicators of water content. These variations are summarized in Table 5.4b below with features arranged from those suggestive of lower water content to those indicating higher water content. Overall, hydroxide crystal masses have a non-compact texture typical of conventional concrete mixed with w/c greater than about 0.40. Tighter platelets are less common in those samples where they are observed. The density of the crystals ranges from moderate to high. Cores 748SB-2P and 758H-1P are notable in that the hydroxide is appreciably more abundant and coarser-grained. These features are more clearly indicative of w/c in the high 0.4s at least.

**Table 5.4b: Summary of Primary Calcium Hydroxide Crystallization**

Abundance	Morphology	Deposits on aggregate	Core samples
Moderate	Fine-grained masses to platelets	Discontinuous	748NB-2P, 748SB-3P
Moderately high	Fine-grained masses to platelets	Discontinuous	758E-1P
Moderately high	Fine to medium-grained masses	Discontinuous	748NB-1P
Moderately high	Fine to medium-grained masses	Discontinuous to semi-continuous	748NB-3P, 748SB-1P, 748SB-4P, 758F-1P, 758G-1P
High	Medium-grained masses	Discontinuous	748SB-2P
High	Medium-grained masses to platelets	Discontinuous to semi-continuous	758H-1P

Any differences in the presence of portland cement residuals between samples is relatively subtle with the exception of Core 748NB-1P. Though features of the cement hydration are affected by mix water contents, the estimated w/c variation may be too low to be well illustrated in the cement textures. Instead, the full range of observable textures is found to be consistent with moderate w/c. For ten of the cores, all of the cement exhibits a high degree of hydration and relatively little of the hydraulic calcium silicate remains unhydrated (Fig. 12). Residual grains include agglomerates of former calcium silicate with an interstitial matrix of residual iron-bearing ferrite. Isolated flakes of ferrite without obvious calcium silicate impressions are also observed. A notable but fairly low quantity of single fine alite crystals with moderately thick hydration rims are observed in Core 758G-1P. Similar crystals are detected in rare abundance in Core 758H-1P. Cores 748NB-3P and 748SB-3P have a moderate abundance of cement residuals while the other cores have a moderately high density of hydrated residuals. Relatively few of the hydrated grains are well-defined agglomerates. Some unhydrated calcium silicate material remains but only within the cores of the coarsest agglomerates. These are especially rare in Core 748SB-3P but more abundant in Cores 748SB-4P, 758G-1P, and 758H-1P. The cement is fine to medium-grained with most estimated to pass a No. 200 sieve and relatively few retained or approaching the No. 100 sieve. Finally, there is a minor tendency for hydrated grains to have become filled with cementitious hydrate in the portions of Cores 748SB-4P and 758H-1P.

Core 748NB-1P again exhibits clear differences from the other ten cores. The sample is only included in this report because it contains crushed stone instead of natural gravel coarse aggregate. Even here the stone is a carbonate rather than a meta-igneous lithology. In this case, there is a moderate high abundance of cement residuals but a notable abundance of these remain partially unhydrated. The assemblage of unhydrated material is very rich in residual alite with moderately thick hydration rims. Fewer calcium silicate agglomerates are present. The cement is still fine to medium-grained but there are moderate occurrences of grained near or coarser than the No. 100 sieve.

The air content and microstructure in all eleven cores is indicative of intentional air-entrainment (Fig. 11). A summary of the air contents, structural parameters, and qualitative distribution is presented in Table 5.4c. Details of the quantitative air-void analyses are presented in Section 6 below. The samples mostly have air structures that meet or nearly meet the generally accepted parameters for adequate freeze-thaw resistance. These criteria include specific surfaces greater than 600 in.<sup>-1</sup> and spacing factors less than 0.008 in. Cores 748NB-2P, 748NB-3P, 748SB-3P, and 748SB-4P do not meet this criterion but in no case is the specific surface less than 530 in.<sup>-1</sup>. Spacing factors exceed 0.008 in. in Cores 748NB-2P, 748NB-2P, 748SB-3P, and 758E-1P but not by more than 10%. It is notable that there appears to be some correlation between less ideal air structures and higher estimated mix water contents. The total air contents may be considered somewhat excessive in Cores 748SB-1P, 748SB-4P, and 758H-1P at 8.7% to 9.5%. A modest reduction in compressive strength relative to the design strength can be expected in cores that have excessive air contents.

Overall, the fine air-voids are well distributed with depth in each core sample. For the most part, the voids are well dispersed at the microscopic scale and there is little to no clustering within the paste or along aggregate interfaces. Very minor instances are found in Cores 748NB-2P and 748SB-3P.

**Table 5.4c: Summary of Air Contents and Parameters**

Core ID	Total air (%)	Specific surface (in. <sup>-1</sup> )	Spacing factor (in.)	Remarks
748NB-1P	5.2	911	0.0056	
748NB-2P	5.1	546	0.0087	Minor instances of clustering are observed locally around coarse aggregate and less commonly within the paste.
748NB-3P	5.1	588	0.0084	
748SB-1P	8.7	666	0.0048	The paste has a frothy texture due to the high air content.
748SB-2P	5.6	643	0.0075	
748SB-3P	5.6	558	0.0083	The size distribution is possibly somewhat deficient in fines. Trace instances of clustering are observed locally around coarse aggregate and within the paste.
748SB-4P	9.1	530	0.0055	The size distribution appears to be rich over 200 μm. The paste has a frothy texture due to the high air content.
758E-1P	5.2	634	0.0085	
758F-1P	6.5	697	0.0066	
758G-1P	5.9	695	0.0069	
758H-1P	9.5	771	0.0039	The paste has a frothy texture due to the high air content.

**5.5 - Original Placement and Hydration**

Based on the samples examined, the components of the structural concrete were well mixed in each core. There are no cement lumps, sand streaks, or rock pockets. It is not known whether the concrete was designed with the moderate water to cement ratios estimated for these cores. Therefore, it cannot be stated whether an inappropriate later addition was introduced on site. Nonetheless, the mix water appears to have been mostly well incorporated. There was some bleed water migration in the concrete represented by Core 748SB-3P (Fig. 14). However, this is not interpreted to have been the result of late watering. A minor proportion of the coarse aggregate in the 758 cores contain very thin and discontinuous linings of denser cement paste (Fig. 15). These are very minor in Cores 758G-1P and 758H-1P and trace in Cores 758E-1P and 758F-1P. The denser paste would have had a lower water content when the concrete was fresh. This type of feature is sometimes found when concrete is retempered on site and the new water addition does not fully incorporate with the paste adhered to stone. However, the linings are exceptionally minor and could also simply indicate a shorter mixing time. Regardless of the cause, it is clear that there are no major deficiencies related to the original mixing.

Assuming that all mixes were intended to have the same air structure, there are some inconsistencies observed in the development of the entrained air. However, these are within the range often encountered in many concrete projects. Generally, it is not possible to isolate a particular cause for variability in the development of entrained air. Certainly these can be caused by admixture dosages. However, qualities of the mixing equipment, presence of incompatible materials, or environmental conditions may all result in air content variability. It is noted that cores having air with lower specific surfaces and higher spacing factors are the same ones for which the water to cement ratio is estimated to have been highest. Certainly higher slumps can result in a lower quality air structure. Higher air contents in these samples do not appear to correlate with any particular feature.

All cores contain materials that are monolithic throughout the entire structural cross section and no cold joints are identified within the structural layers (Fig. 2). The lower forming of the concrete is not evaluated as the cores do not include lower surfaces. In all samples, the structural concrete was well compacted and consolidated. There are no large void structures or honeycombing. Coarser air-voids are generally no more than several millimeters in size. Minor exceptions are found in Cores 758F-1P and 758G-1P where entrapped voids have diameters of about one centimeter. Overall, voids greater than one millimeter constitute up to a little over 2% of the total volume in any core sample (see Section 6). There is no evidence for excessive vibration. Coarse aggregate grains are homogeneously distributed throughout each concrete section without segregation. Though some grains are plate-like in shape, there are no preferential alignments of the stone due to excessive fluidity. The size, spacing, and location and steel reinforcement are outside the scope of a petrographic examination. In any case, steel reinforcement is only included in Cores 758F-1P and 758G-1P and this only includes welded wire lower in the concrete cross sections. Lower surfaces are not included with the samples and the amount of cover to the base is not estimated. The upper finished surfaces are not always preserved or fully available for evaluation. Nevertheless, there is no obvious evidence for weakened finish layers due to laitance, incipient delamination, or other workmanship deficiencies. Any cracking identified is attributable to secondary chemical reactions.

For most of the core samples, there is no evidence for excessive bleed water development. Only Core 748SB-3P contains microporous zones adjacent to coarse aggregate grains related to original mix water concentrations (Fig. 14). These are relatively common. There are also local patches of more highly porous paste and these likely represent bleed water concentrations. However, discrete channels are not identified. The microporous zones are interpreted to have reduced the quality of the paste-aggregate bond. Though other cores do not exhibit bleed water features, the paste-aggregate bonds in most samples are only moderately well developed as well. Though not necessarily deficient, the moderate mix water contents result in a concrete that tends to fracture around rather than through aggregate grains. In addition to Core 748SB-3P, more “crumbly” fracture behavior around weaker coarse aggregate boundaries is also noted in Cores 748NB-3P and 748SB-4P. Only Core 748NB-1P exhibits a sharper fracture behavior with induced cracks transecting rather than deflecting around coarse aggregate particles.

As described above, the portland cement hydration is quite advanced in all samples (Fig. 12). The hydration characteristics are mostly consistent throughout the full depth of each sample and there is no evidence for differential drying of the slab or loss of water near exposed surfaces. However, the original screeded surface is not present in all of the samples. In particular, the top surface of Core 748NB-1P was saw-cut rather than weathered and the depth to the original surface is not known.

Six of the examined samples have wear courses installed over the structural concrete (Fig. 16). The wear courses are not part of the examination but are identified in a cursory manner. The wear course thicknesses range from 1.7” to 3.1”. In Cores 748SB-1P, 748SB-2P, 748SB-3P, and 748SB-4P, the wear courses appear to have been installed directly over fresh concrete substrate. There are no truncations of the stone and the contact face is consistent with a “wet-on-wet” placement. In fact, “fingers” of wear course material appear plastically embedded in the substrate in Cores 748SB-1P and 748SB-2P (Fig. 1). The fingers are approximately two to three millimeters wide and several millimeters deep. They are closely but irregularly spaced. No debris is identified at the contact surface but the wear course mortar often appears somewhat drier at the furthest extent of the fingers.

In Cores 748NB-2P and 748NB-3P, there are truncations of coarse aggregate at the surface below the wear course (Fig. 18). This could suggest that the wear course was either installed after some substrate erosion had occurred or after a scarification or other treatment of the substrate concrete. Given the apparently original quality of the wear courses in the other samples, it would appear that early scarification is a more likely interpretation.

No wear courses are present in Cores 758E-1P, 758F-1P, 758G-1P, and 758H-1P. The upper surfaces of these cores are eroded with coarse aggregates exposure notable in Cores 758F-1P and 758H-1P (Fig. 19). Surface grooving is present only along the top of Core 758G-1P.

### **5.6 - Condition and Durability**

The structural concrete examined for the eleven core samples represents a moderate quality mixture considered suitable for many normal-duty service applications. The only notable issue identified in this report is the inclusion of potentially alkali-reactive materials in both the fine and coarse aggregates. Moderate permeabilities are also noted but are not considered a major deficiency in their own right. However, compressive strength results provided by the client for the 748NB and 748SB structures indicate some variability. Where higher permeabilities are identified, it can be expected that these correlate with original water to cement ratios. By extension, these would correlate with variations in compressive strength. With respect to the current condition of the concrete, only limited microscopic cracking is identified in several of the samples. This is discussed at greater length below. Carbonation is limited to a thin veneer no greater than two millimeters thick at the top of the structural concrete (Fig. 2). Minor extensions of the carbonation are found ringing aggregate grains and lining surface crazing cracks in some of the 758 samples but this is quite minor with the deepest occurrence around cracks in Core 758G-1P at up to two centimeters depth (Fig. 20). There does not appear to be any risk for pH-related depassivation of embedded steel if any is actually present in the concrete. All other mineralizations identified are related to early-stage alkali-aggregate reactions (AAR) including the deposition of minor amounts of ettringite in the air-voids of Cores 748NB-1P, 748SB-1P, and 748SB-3P.

The moderate permeability of the concrete is a result of mix water contents that are perhaps a little higher than desirable for exterior applications. However, none of the concrete is considered to be excessively permeable. Nonetheless, the concrete should not be considered fully water-resistant and this can increase the susceptibility to any distress mechanisms that are associated with moisture infiltration. Of course, the possibility of denser wear courses could mitigate this susceptibility while any larger cracks going through the slab could promote increased infiltration of water. These last two are outside the scope of the examination.

Aside from the potential for chloride infiltration, the issue most closely tied to water permeability would be freeze-thaw resistance. Assuming the wear courses are equally permeable, it should be expected that the structural concrete is capable of at least partial saturation if regularly exposed to moisture. However, most cores have entrained air structures that would be considered by most industry professionals to be sufficient for adequate freeze-thaw protection. Admittedly, Cores 748BNB-2P, 748NB-3P, 748SB-3P, 748SB-4P, and 758E-1P have spacing factors somewhat greater than 0.008 in. and specific surfaces somewhat lower than 600 in.<sup>-1</sup>. However, the deviations are not excessive. No evidence for freeze-thaw related distress is identified in the structural concrete of any core sample.

Trace to early stage alkali-silica reactions (ASR) are identified in all of the core samples and details of these are described in Table 5.6a below. ASR is a reaction in which chemically unstable forms of silica react with alkalis normally found in the cement paste to produce a hygroscopic gel. Absorption of water into the gel causes the material to expand and this can often lead to significant expansive cracking. In the coarse aggregate for these samples, the reaction is greatest in the granofels and a little bit less aggressive in the granitoids. No reaction is detected in diorites. A trace reaction is detected in the dolostone but this material is considered more prone to alkali-carbonate reaction. The variable reactivity is caused by the presence of fine subgrains of strained quartz in the granofels and granitoids. Deformation in the quartz crystal matrix is responsible for the higher reactivity. Strained quartz exhibiting this level of deformation is usually considered only slowly reactive. In the fine aggregate, limited reactions are also detected in the strained quartzite present in the coarsest fractions of the fine aggregate of some of the samples. Reactions are noted in the chert grains for three of the four cores for which this type of sand is present. Chert is generally considered a more aggressively reactive species due to the cryptocrystalline nature of the constituent quartz.

In the eleven core samples examined for this report, none of the reactions are at more than an early stage of advancement and none of the concrete is currently compromised by any resulting microcracks. The greatest degree of reaction is observed in Cores 748SB-1P and 748SB-2P (Figs. 21 and 22). The former is the only sample in which the schistose granofels constitutes a major proportion of the stone. In the latter, much of the reaction is present in the granitoid and no granofels is present. In both samples, evidence for reaction is found throughout the core sample. Internal aggregate cracking is common though crack widths rarely exceed 100  $\mu\text{m}$ . Paste cracks lined with ASR gel extend short distances from the reactive stone in Core 748SB-1P. The aggregate cracks tend to terminate against ASR gel deposits in the adjacent paste in Core 748SB-2P. ASR gel plugs are found at the intersection between reacted aggregate and adjacent cement paste in both samples. The reaction in the two cores has not become sufficiently organized to produce a preferential alignment of cracking. Any microcracks identified appear more or less random in orientation and distribution.

Trace to early-stage ASR reactions are also identified in Cores 748NB-2P, 748NB-3P, 748SB-3P, and 748SB-4P (Figs. 23 through 26). In these cases, any notable reaction is limited to the uppermost few millimeters of the substrate concrete. At depth, nothing more than a few trace gel deposits or exudates on freshly cut sections are observed. It is interesting to note that these four cores are also the samples exhibiting the highest capillary porosity and are considered to be the most permeable of the group (albeit only slightly so). The higher porosity could explain the presence of reaction in samples that do not contain the more reactive granofels. In the upper sections, it is difficult to tell which materials have reacted as only a limited area is available for examination. Nevertheless, examples of granitoid, strained quartzite, and chert reaction are all identified. In Cores 748NB-2P and 748NB-3P, it is assumed that all reactions have occurred in the strained quartzite and chert in the fine aggregate. The quartz diorite does not appear to be reactive. In Cores 748SB-3P and 748SB-4P, reactions may have occurred in the sand but there are granitoids in the coarse aggregate also available for ASR reaction. Microcracks in this upper horizon are exceptionally fine with opening widths generally no more than 50  $\mu\text{m}$ . It should be noted that the “disbond” in Core 748NB-2P is actually a cohesive failure within the substrate concrete along a pre-existing ASR crack. An incipient fracture just below the top of the substrate in Core 748SB-3P is also coincident with an ASR crack.

The 758 cores exhibit very minor examples of ASR reaction with only localized incipient microcracking observed within reactive aggregate (Fig. 27). The granitoid appears to be the reactive stone in these cases. For these samples, the reactions are distributed throughout the core sections rather than isolated along the top surfaces of the substrate. However, the degree of reaction is even less than observed in the cores for which the ASR is restricted to the top surfaces. Of the four samples, Core 758E-1P exhibits the most notable reaction. Even here, the reaction is at a very early stage with no imminent threat to the stability of the concrete.

Two of the core samples contain a dolostone crushed stone. Core 748NB-1P contains only this rock type as a coarse aggregate while Core 748SB-3P has the dolostone intermixed with the other siliceous rocks. Nevertheless, evidence for early-stage alkali-carbonate reaction is detected in these samples and this is distinguished from the ASR (Figs. 30 and 31). Alkali-carbonate reactions (ACR) are not fully understood but most examples appear to be related to a dedolomitization reaction that can cause expansive cracking. The reaction involves the conversion of dolomite to calcium carbonate and brucite. The critical observations include a “corrosion” of the constituent dolomite grains indicating chemical decomposition and usually a “bloom” of carbonate reaction product adjacent to the corrosion site. The brucite is generally too fine to observe petrographically. Most of the most damaging ACR reactions reported in the literature include specific types of dolomitic limestone that are relatively rich in clay. There are few reports of pure sedimentary dolostone causing expansion. There is still significant debate as to whether the dedolomitization alone can result in cracking failure or if there must be an associated alkali-silica reaction responsible for the damage.

In this particular case, most dolostone particles in both samples exhibit some evidence for reaction including near surface “corrosions” and discontinuous blooms of carbonate in the adjacent cement paste. However, no expansion is positively identified in association. The only cracking identified in connection with the dolostone is found in Core 748SB-3P and this particular reaction is attributed to ASR. Some of the dolostone contains strained quartz as well as fine argillaceous zones. Either of these types of features could also be alkali-silica reactive to some degree. Overall, the potential for any significant damage due to ACR appears to be quite limited. Any occurrences identified in the two core samples are at an incipient stage and do not pose an immediate threat to the continued serviceability of the substrate concrete.

**Table 5.6a: Summary of Alkali-Aggregate Reactions**

Photographic documentation of these features are presented in Figures 21 through 31 in Appendix II below.

Core ID	Stage	Details
748NB-1P	Early	Dolostone exhibits mild dedolomitization “corrosion”. Trace internal microcracks are noted as are discontinuous, minor carbonate blooms adjacent to reacted stone. No expansion is found in association. Trace random polygonal microcracking in paste is not related.
748NB-2P	Early but limited	Several ASR cracks including the wear course disbond are localized within the uppermost few mm of the substrate. Fairly continuous microcracks are parallel to the surface all less than 50 µm in width. Some ASR “flames”. One example of ASR in a strained quartz fine aggregate in this horizon. Otherwise, the rock association is not viewed in thin section. Minor sulfate mineralizations are also observed in these cracks. In hand sample, there are a few local instances of gel deposits and exudates adjacent to chert grains but no clear evidence in coarse aggregate.
748NB-3P	Early but limited	ASR microcracking only in the uppermost 2-3 mm of the substrate. In thin section, parallel cracks are less than 50 µm in width and contain clear gel linings. There is no obvious association with coarse aggregate though one crack deflects around a diorite particle. In hand sample, trace gel deposits and minor exudates are detected adjacent to reactive chert fine aggregate. Otherwise, there is no evidence for ASR in coarse aggregate deeper in the section.
748SB-1P	Early	Early-stage ASR reactions are found throughout the core section. Most granofels aggregate contains internal microcracks and these extend short to moderate distances into the adjacent cement paste. Cracks are usually filled with ASR gel. Crack widths are generally less than 100 µm. Crack orientations are more or less random and any axial arrangements appear coincidental. In hand sample, very few reaction rims are noted but internal microcracks are very common. Note that the concrete remains cohesive. Granitoids and strained quartzite also exhibit internal cracking but no reaction gels are positively identified in association with these cracks in thin section.
748SB-2P	Early	This core exhibits the same degree of ASR reaction as observed in Core 748SB-1P except that all cracking is clearly associated with the granitoid aggregate and to some extent the coarsest grains of strained quartzite in the sand. Larger “blobs” of reaction gel are more commonly associated with the granitoid reaction instead of the consistently lined paste cracks.
748SB-3P	Trace and limited	Only traces of ASR are detected most of which are directly below the wear course. In thin section, there is some local microcracking and a clear association only with some chert fine aggregate and a dolostone coarse aggregate that contains an internal fill of hydrous silica reaction product and a gel plug at the grain boundary. Below the surface, only minor internal cracking is detected in aggregate most of which is found in the granitoid. No ASR is found in association with chert in hand sample. All dolostone exhibits mild dedolomitization “corrosion” with minor carbonate blooms adjacent to reacted stone. No expansion is found in association.
748SB-4P	Early but limited	ASR reactions are only detected within the uppermost 1 cm of the substrate concrete though exudates are noted throughout the honed cross section. Most cracking is associated with chert fine aggregate and lesser with granitoid coarse aggregate in this horizon. Internal aggregate cracks are less than 50 µm in width. Gel “blobs” are more significant.
758E-1P	Very early	Very minor reactions are detected throughout the core. Very thin reaction rims are common on granitoid aggregate. Internal cracks are moderately common but not pervasive. Crack widths are generally less than 25 µm. Fine gel plugs are rare at the termination of aggregate cracks. However, adjacent gel “blobs” with no associated cracking is moderately common and relatively large where present. A few are also noted adjacent to strained quartzite in the sand.
758F-1P	Trace	Trace internal microcracks are noted in granitoid aggregate. Almost no other evidence for reaction is observed though faint exudates on the honed cross section are noted.
758G-1P	Trace	Only very local occurrences of ASR are detected in thin section. In honed section, evidence for reaction is limited to faint exudates throughout the honed cross section. These are relatively common. In thin section, one fine crack (less than 50 µm) in granofels is associated with a large adjacent gel deposit. Another very fine crack (less than 25 µm) is observed in a granitoid grain.
758H-1P	Trace	Exceedingly trace and exceptionally fine microcracks are noted in granitoid with one or two minor gel deposits identified.

With respect to future durability, there is no evidence to suggest that continued ASR development is mitigated by any particular feature of the concrete. ASR is sometimes controlled by the addition of supplementary cementitious materials or (more recently) lithium-based admixtures. The former are clearly not part of the mix design and the latter is unlikely though this can only be demonstrated chemically. Alkaline cement paste is one precondition for the initiation of aggregate dissolution. The lack of carbonation has allowed all concrete to maintain a high alkalinity throughout the full cross section of each core. Continued aggregate reactions can be expected even if somewhat slowly. Availability of moisture is also an important factor in the rate of ASR development and distress. Again, the concrete is not especially water-resistant even if the permeabilities are not excessive. Cores 748NB-2P, 748NB-3P, 748SB-3P, and 748SB-4P are estimated to have the higher permeabilities of the group and may be slightly more susceptible to water infiltration. Of course, exposure and drainage will also have an impact on the amount of water available and this cannot be evaluated in the laboratory.

Despite the lack of mitigating factors, the coarse aggregate is not considered to be among the most aggressively reactive rock types. Any reactions identified in this study are at an early stage and have not compromised the integrity of the represented concrete. It is quite possible that the concrete may remain provisionally stable over the course of a normal life cycle. The chert in the fine aggregate is considered to be significantly more reactive than the granofels and granitoids. However, the reactivity might be overshadowed by that of the coarse aggregate in most cases. To be sure, the chert is present at several percent of the fine aggregate volume and this might be expected to produce unacceptable levels of expansion if the raw material were subjected to accelerated durability tests in the laboratory. Nonetheless, there is clearly no imminent durability threat produced by the chert alone. Of course, it must be stressed that while petrographic examination can identify potential durability threats, it cannot be fully predictive. Monitoring of concrete containing such components may be prudent. It is also possible that the concrete studied for this examination is not fully representative of all material on site. If other areas of the construction exhibit visible cracking not captured in the provided samples, these should be considered to have a potential association with the types of reactions described herein. Patterned cracking with a polygonal shape or “map-cracking” would be one possible indication of more advanced alkali-aggregate reaction as would the presence of white mineral exudates.

**6. Air-Void Analysis**

**Table 6.1: Point-Count Data**

<b>Core ID</b>	<b>748NB-1P</b>	<b>748NB-2P</b>	<b>748NB-3P</b>	<b>748SB-1P</b>	<b>748SB-2P</b>	<b>748SB-3P</b>	<b>748SB-4P</b>
Aggregate nominal top size (in.)	1	0.5	0.75	0.75	0.5	0.5	0.75
Total traverse length (in.)	74.5	76	76.2	76.05	76	77.05	76.75
Total area (in. <sup>2</sup> )	15.5	13.0	13.0	13.0	13.0	13.0	12.8
Aggregate points	939	1027	1000	963	971	1028	990
Paste points	474	414	446	425	464	427	405
Air points (less than 1 mm)	71	52	46	125	68	77	109
Air points (greater than 1 mm)	6	26	32	8	17	9	31
Crack points <sup>1</sup>	0	1	0	0	0	0	0
Total points	1490	1520	1524	1521	1520	1541	1535
Air intercept	877	532	573	1108	683	600	928

<b>Core ID</b>	<b>758E-1P</b>	<b>758F-1P</b>	<b>758G-1P</b>	<b>758H-1P</b>
Aggregate nominal top size (in.)	0.75	0.75	0.75	0.5
Total traverse length (in.)	76	75.75	76.05	77.75
Total area (in. <sup>2</sup> )	13.0	12.8	13	12.5
Aggregate points	890	932	950	962
Paste points	551	485	482	445
Air points (less than 1 mm)	66	73	72	126
Air points (greater than 1 mm)	13	25	17	22
Crack points <sup>1</sup>	0	0	0	0
Total points	1520	1515	1521	1555
Air intercept	626	854	773	1426

Notes:

1. Cracks are non-totaling and do not influence the air-void parameter calculation.

**Table 6.2: Calculated Volumes and Air-Void Parameters**

<b>Core ID</b>	<b>748NB-1P</b>	<b>748NB-2P</b>	<b>748NB-3P</b>	<b>748SB-1P</b>	<b>748SB-2P</b>	<b>748SB-3P</b>	<b>748SB-4P</b>
Aggregate (volume %)	63.0	67.6	65.6	63.3	63.9	66.7	64.5
Paste (volume %)	31.8	27.3	29.3	27.9	30.5	27.7	26.4
Air less than 1 mm (volume %)	4.8	3.4	3.0	8.2	4.5	5.0	7.1
Air greater than 1 mm (volume %)	0.4	1.7	2.1	0.5	1.1	0.6	2.0
<b>Total air (volume %)</b>	<b>5.2</b>	<b>5.1</b>	<b>5.1</b>	<b>8.7</b>	<b>5.6</b>	<b>5.6</b>	<b>9.1</b>
Paste/air ratio	6.16	5.31	5.72	3.20	5.46	4.97	2.89
Voids/inch	11.77	7.00	7.52	14.57	8.99	7.79	12.09
Average chord length (in.)	0.004	0.007	0.007	0.006	0.006	0.007	0.008
Specific surface (in. <sup>-1</sup> )	911.17	545.64	587.69	666.47	642.82	558.14	530.29
<b>Spacing factor (in.)</b>	<b>0.0056</b>	<b>0.0087</b>	<b>0.0084</b>	<b>0.0048</b>	<b>0.0075</b>	<b>0.0083</b>	<b>0.0055</b>

<b>Core ID</b>	<b>758E-1P</b>	<b>758F-2P</b>	<b>758G-1P</b>	<b>758H-1P</b>
Aggregate (volume %)	58.6	61.5	62.5	61.9
Paste (volume %)	36.3	32.0	31.7	28.6
Air less than 1 mm (volume %)	4.3	4.8	4.7	8.1
Air greater than 1 mm (volume %)	0.9	1.7	1.1	1.4
<b>Total air (volume %)</b>	<b>5.2</b>	<b>6.5</b>	<b>5.9</b>	<b>9.5</b>
Paste/air ratio	6.97	4.95	5.42	3.01
Voids/inch	8.24	11.27	10.16	18.34
Average chord length (in.)	0.006	0.006	0.006	0.005
Specific surface (in. <sup>-1</sup> )	633.92	697.14	694.83	770.81
<b>Spacing factor (in.)</b>	<b>0.0085</b>	<b>0.0066</b>	<b>0.0069</b>	<b>0.0039</b>

Respectfully submitted,

John J. Walsh  
 President/ Senior Petrographer  
**Highbridge Materials Consulting, Inc.**

**Appendix I: Visual Description of Petrographic Samples**

<b>Sample ID</b>	<b>748NB-1P</b>
Dimensions and Details	The sample consists of a 3.25” diameter core. The core is received as two non-contiguous pieces of similarly appearing concrete. No wear course material is identified. The top piece is approximately 2.5” in length and saw-cut on both sides. The bottom piece is approximately 2.0” in length and irregularly fractured on both sides.
Top/Outer Surface	The top surface is saw-cut
Bottom/Inner Surface	The bottom surface is a clean, artificial drilling break.
Core Circumference	Smooth with no differential erosion from coring.
Embedded Items	No reinforcement is included in the sample.
Visible Cracks	The core break is the only crack in the visible hand sample. This may represent a pre-existing structure. Some white mineralizations noted around a few coarse aggregate grains.

<b>Sample ID</b>	<b>748NB-2P</b>
Dimensions and Details	The sample consists of a 3.25” diameter core approximately 7.75” in length. A wear course of approximately 2.8” thickness overlies a layer of structural concrete. The wear course is bound to the substrate along a roughly planar surface in most areas. The core is received in two contiguous pieces with a core break running through the structural concrete at approximately 2.9” depth just below the wear course in most locations. However, the break refracts into the boundary between the wear course and the substrate along one edge of the core.
Top/Outer Surface	The top surface is roughly planar with low relief coarse aggregate exposure. Moderate soiling of the paste is also apparent.
Bottom/Inner Surface	The bottom surface is a clean, artificial drilling break.
Core Circumference	Smooth with no differential erosion from coring.
Embedded Items	No reinforcement is included in the sample.
Visible Cracks	The core break is the only crack visible in hand sample. This is interpreted to represent a pre-existing structure. Some white mineralizations are noted around a few coarse aggregate grains.

<b>Sample ID</b>	<b>748NB-3P</b>
Dimensions and Details	The sample consists of a 3.25” diameter core approximately 8” in length. The core is received as one intact piece. A wear course of approximately 2.1” thickness overlies the structural concrete. The wear course is tightly bound to the substrate along a roughly planar surface.
Top/Outer Surface	The top surface is roughly planar with low relief coarse aggregate exposure. Moderate soiling of the paste is also apparent.
Bottom/Inner Surface	The bottom surface is a clean, artificial drilling break.
Core Circumference	Smooth with no differential erosion from coring.
Embedded Items	No reinforcement is included in the sample.
Visible Cracks	No macroscopic cracking is visible in hand sample.

**HIGHBRIDGE MATERIALS CONSULTING, INC.**

Pennoni Associates, Inc.; I-95 Viaduct Project

Report #: SL0845-02

Page 20 of 64

<b>Sample ID</b>	<b>748SB-1P</b>
Dimensions and Details	The sample consists of a 3.25" diameter core approximately 6" in length. The core is received as one intact piece. A wear course of approximately 1.6" thickness overlies the structural concrete. The wear course is tightly bound to the substrate along a roughly planar surface.
Top/Outer Surface	The top surface is roughly planar with low relief coarse aggregate exposure. Marking paint is covering the majority of the top surface. Moderate soiling of the paste is apparent in the portion of the surface not covered by marking paint.
Bottom/Inner Surface	The bottom surface is a clean, artificial drilling break.
Core Circumference	Smooth with no differential erosion from coring.
Embedded Items	No reinforcement is included in the sample.
Visible Cracks	A longitudinal crack is identified that intersects the top surface near the edge of the core. The crack penetrates the core to no greater than 1" depth.

<b>Sample ID</b>	<b>748SB-2P</b>
Dimensions and Details	The sample consists of a 3.25" diameter core approximately 7.5" in length. The core is received as one intact piece. A wear course of approximately 1.7" thickness overlies the structural concrete. The wear course is tightly bound to the substrate along a roughly planar surface.
Top/Outer Surface	The top surface is roughly planar with low relief coarse aggregate exposure. Moderate soiling of the paste is also apparent.
Bottom/Inner Surface	The bottom surface is a clean, artificial drilling break. Aggregate is visible but coated with dried drilling slurry.
Core Circumference	Smooth with no differential erosion from coring.
Embedded Items	No reinforcement is included in the sample.
Visible Cracks	No macroscopic cracking is visible in hand sample.

<b>Sample ID</b>	<b>748SB-3P</b>
Dimensions and Details	The sample consists of a 3.25" diameter core approximately 7.5" in length. The core is received as one intact piece. A wear course of approximately 3.1" thickness overlies the structural concrete. The wear course is tightly bound to the substrate along roughly planar surface.
Top/Outer Surface	The top surface is roughly planar with low relief coarse aggregate exposure. Moderate soiling of the paste is also apparent.
Bottom/Inner Surface	The bottom surface is a clean, artificial drilling break.
Core Circumference	Smooth with no differential erosion from coring.
Embedded Items	No reinforcement is included in the sample.
Visible Cracks	An sharp, hairline axial crack is identified in the structural concrete just below the wear course. The crack both transects and deflects around aggregate particles. The crack spans approximately two thirds of the circumference of the core.

<b>Sample ID</b>	<b>748SB-4P</b>
Dimensions and Details	The sample consists of a 3.25" diameter core approximately 8" in length. The core is received as one intact piece. A wear course of approximately 2.1" thickness overlies the structural concrete. The wear course is tightly bound to the substrate along a roughly planar surface.
Top/Outer Surface	The top surface is roughly planar with low relief coarse aggregate exposure. Marking paint is covering the majority of the top surface. Moderate soiling of the paste is also apparent.
Bottom/Inner Surface	The bottom surface is a clean, artificial drilling break.
Core Circumference	Smooth with no differential erosion from coring.
Embedded Items	No reinforcement is included in the sample.
Visible Cracks	No macroscopic cracking is visible in hand sample.

**HIGHBRIDGE MATERIALS CONSULTING, INC.**

Pennoni Associates, Inc.; I-95 Viaduct Project

Report #: SL0845-02

Page 21 of 64

<b>Sample ID</b>	<b>758E-1P</b>
Dimensions and Details	The sample consists of a 3.25" diameter core approximately 7.25" in length. The core is received as one intact piece. Only a single material is included with the sample.
Top/Outer Surface	The top surface is roughly planar with very low relief coarse aggregate exposure. Moderate soiling of the paste is also apparent.
Bottom/Inner Surface	Half of the bottom surface is a clean, artificial drilling break. The other half is a smooth surface formed against corrugated decking.
Core Circumference	Smooth with no differential erosion from coring.
Embedded Items	No reinforcement is included in the sample.
Visible Cracks	No macroscopic cracking is visible in hand sample.

<b>Sample ID</b>	<b>758F-1P</b>
Dimensions and Details	The sample consists of a 3.25" diameter core approximately 5.75" in length. The core is received as one intact piece. Only a single material is included with the sample.
Top/Outer Surface	The top surface is roughly planar with low relief coarse aggregate exposure. Light soiling of the paste is also apparent.
Bottom/Inner Surface	The bottom surface is a clean, artificial drilling break.
Core Circumference	Smooth with no differential erosion from coring.
Embedded Items	The sample contains three pieces of steel wire with a 3/16" diameter. There are two wires running parallel to each other and one running perpendicular to the others. The lower concrete surface is not included and the wire depth is referenced to the top of the concrete. The perpendicular piece of wire has 3.7" concrete cover from the top. The parallel wires have 3.8" and 4.8" concrete cover from the top surface. The deeper wire is mostly exposed at the bottom of the core break. However, this wire is well encased otherwise. The other two wires are also well encased. No significant corrosion of the steel wire reinforcement is visible.
Visible Cracks	No macroscopic cracking is visible in hand sample.

<b>Sample ID</b>	<b>758G-1P</b>
Dimensions and Details	The sample consists of a 3.25" diameter core approximately 7.25" in length. The core is received as one intact piece. Only a single material is included with the sample.
Top/Outer Surface	The top surface is roughly planar with low relief coarse aggregate exposure. Moderate soiling of the paste is also apparent. A linear scoring is cut into the concrete with approximately 0.5" spacing.
Bottom/Inner Surface	The bottom surface is a clean, artificial drilling break.
Core Circumference	Smooth with no differential erosion from coring.
Embedded Items	The sample contains two pieces of steel wire each with a 3/16" diameter. One wire is located approximately 4.4" from the top surface and is running obliquely, almost vertically, through the core. The second wire has 5.8" concrete cover from the top of the core. Both wires are well encased in concrete. No significant corrosion of the steel wire reinforcement is visible.
Visible Cracks	No macroscopic cracking is visible in hand sample.

<b>Sample ID</b>	<b>758H-1P</b>
Dimensions and Details	The sample consists of a 3.25" diameter core approximately 3.75" in length. The core is received as one intact piece. Only a single material is included with the sample.
Top/Outer Surface	The top surface is roughly planar with low relief coarse aggregate exposure. Light soiling of the paste is also apparent.
Bottom/Inner Surface	The bottom surface is a clean, artificial drilling break that intersects few aggregate particles.
Core Circumference	Smooth with no differential erosion from coring.
Embedded Items	No reinforcement is included in the sample.
Visible Cracks	No macroscopic cracking is visible in hand sample.

**Appendix II: Photographs and Photomicrographs**

Microscopic examination is performed on an Olympus BX-51 polarized/reflected light microscope and a Bausch and Lomb Stereozoom 7 stereoscopic reflected light microscope. Both microscopes are fitted with an Olympus DP-11 digital camera. The overlays presented in the photomicrographs (e.g., text, scale bars, and arrows) are prepared as layers in Adobe Photoshop and converted to the jpeg format. Digital processing is limited to those functions normally performed during standard print photography processing. Photographs intended to be visually compared are taken under the same exposure conditions whenever possible.

The following abbreviations may be found in the figure captions and overlays and these are defined as follows:

cm	centimeters	PPL	Plane polarized light
mm	millimeters	XPL	Crossed polarized light
µm	microns (1 micron = 1/1000 millimeter)		
mil	1/1000 inch		

Microscopical images are often confusing and non-intuitive to those not accustomed to the techniques employed. The following is offered as a brief explanation of the various views encountered in order that the reader may gain a better appreciation of what is being described.

**Reflected light images:** These are simply magnified images of the surface as would be observed by the human eye. A variety of surface preparations may be employed including polished and fractured surfaces. The reader should note the included scale bars as minor deficiencies may seem much more significant when magnified.

**Plane polarized light images (PPL):** This imaging technique is most often employed in order to discern textural relationships and microstructure. To employ this technique, samples are milled (anywhere from 20 to 30 microns depending on the purpose) so as to allow light to be transmitted through the material. In many cases, Highbridge also employs a technique whereby the material is impregnated with a low viscosity, blue-dyed epoxy. Anything appearing blue therefore represents some type of void space (e.g.; air voids, capillary pores, open cracks, etc.) Hydrated cement paste typically appears a light shade of brown in this view (with a blue hue when impregnated with the epoxy). With some exceptions, most aggregate materials are very light colored if not altogether white. Some particles will appear to stand out in higher relief than others. This is a function of the refractive power of different materials with respect to the mounting epoxy.

**Crossed polarized light images (XPL):** This imaging technique is most often employed to distinguish components or highlight textural relationships between certain components not easily distinguished in plane polarized light. Using the same thin sections, this technique places the sample between two pieces of polarizing film in order to determine the crystal structure of the materials under consideration. Isotropic materials (e.g.; hydrated cement paste, pozzolans and other glasses, many oxides, etc.) will not transmit light under crossed polars and therefore appear black. Non-isotropic crystals (e.g.; residual cement, calcium hydroxide, calcium carbonate, and most aggregate minerals) will appear colored. The colors are a function of the thickness, crystal structure, and orientation of the mineral. Many minerals will exhibit a range of colors due to their orientation in the section. For example, quartz sand in the aggregate will appear black to white and every shade of gray in between. Color difference does not necessarily indicate a material difference. When no other prompt is given in the figure caption, the reader should appeal to general shapes and morphological characteristics when considering the components being illustrated.

**Chemical treatments:** Many chemical techniques (etches and stains typically) are used to isolate and enhance a variety of materials and structures. These techniques will often produce strongly colored images that distinguish components or chemical conditions.

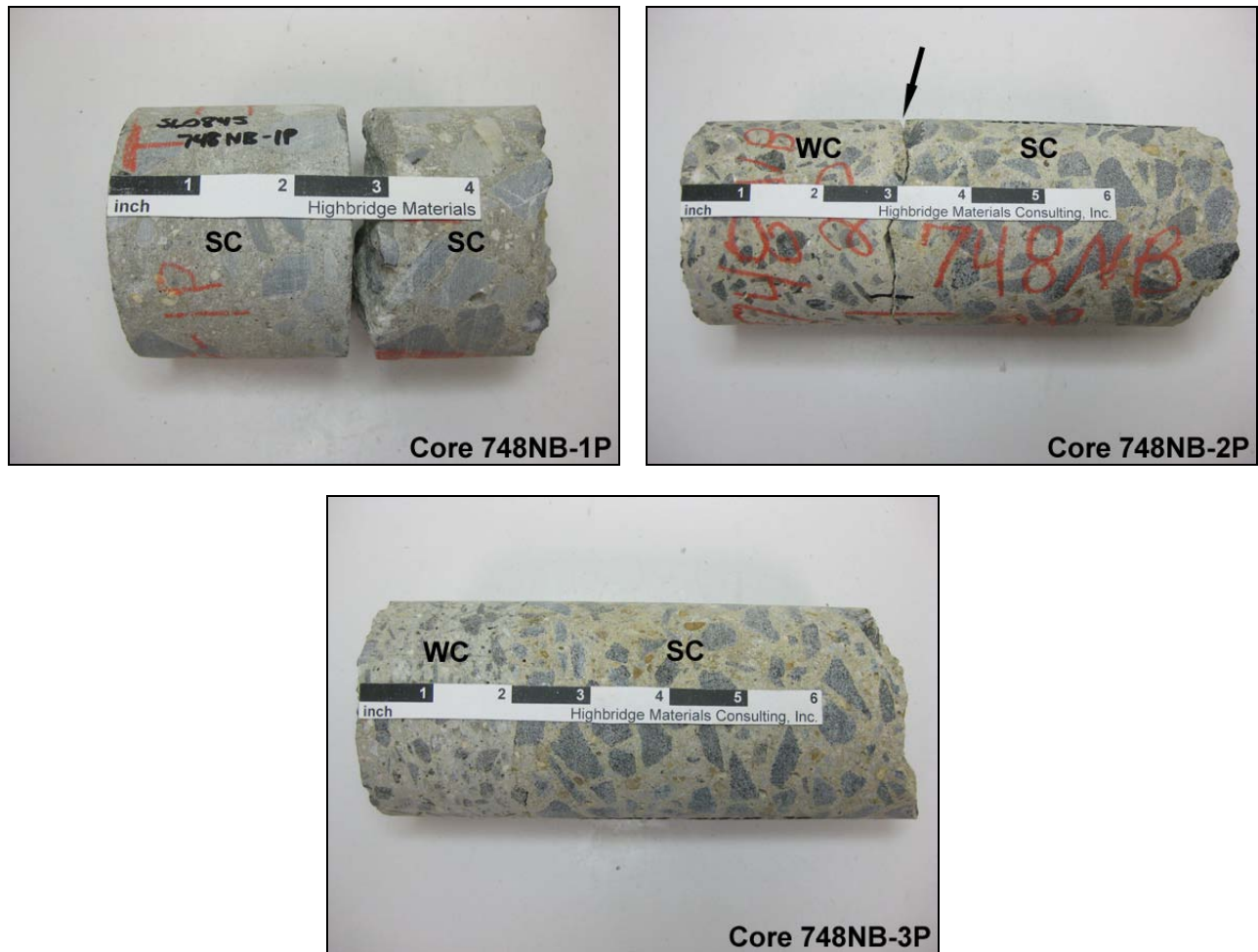


**Figure 1:** Photographs of the eleven concrete core samples used for petrographic examination and air-void analysis of the structural concrete layers. All are shown with their upper surfaces toward the left of each image. Core 748NB-1P was saw-cut and does not contain any original finished surfaces. Some of the cores contain wear course layers (WC) overlying normal weight structural concrete (SC). Wear courses are not present in the 758 Cores. The black arrow in the image for Core 748NB-2P illustrates a core break present in the sample as delivered. This is actually a cohesive failure in the substrate material. The blue arrow indicates a sharp, partial crack just below the wear course in Core 748SB-3P. Finally, steel wire reinforcement is included in Cores 758F-1P and 758G-1P. These are shown by the red arrows.



**Figure 1 (cont'd.):** Photographs of the eleven concrete core samples used for petrographic examination and air-void analysis of the structural concrete layers.



**Figure 1 (cont'd.):** Photographs of the eleven concrete core samples used for petrographic examination and air-void analysis of the structural concrete layers.

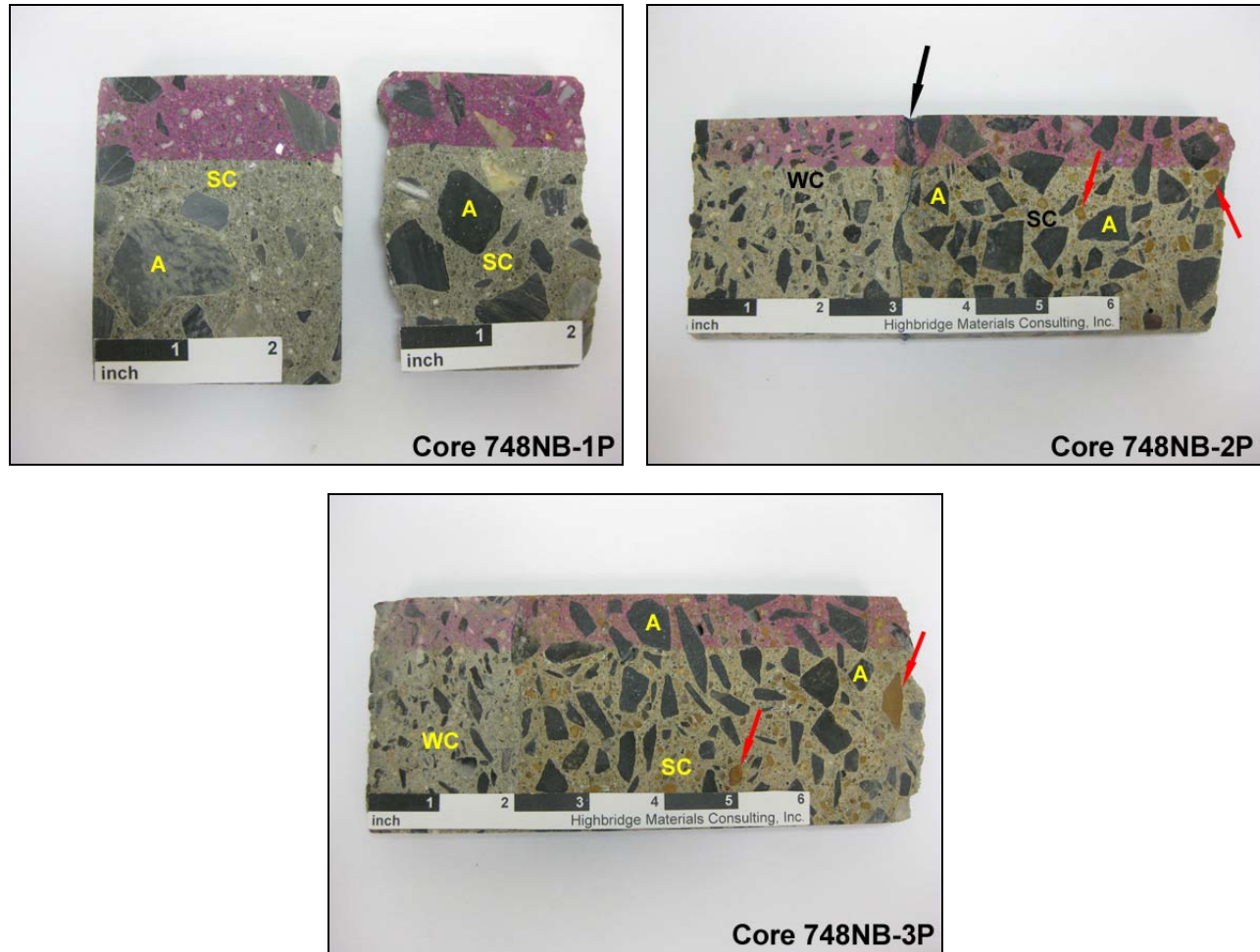


**Figure 2:** Photographs of honed concrete cross sections prepared for the full depth of each provided sample. The upper surfaces are shown to the left in each example. The black arrows indicate where core breaks were epoxied together prior to honing. Wear courses (WC) overlie structural concrete (SC). The size and gradation of the crushed stone aggregate (A) can be observed in the structural layers. Most cores have aggregate with a 3/4" nominal top size except for Core 748NB-1P where aggregate as coarse as 1" is observed. The aggregate is well distributed and no segregations are identified. Four of the cores contain a small but significant proportion of ferruginous chert in the fine aggregate. These orange-colored grains are highlighted by the red arrows. Finally, a portion of each core is treated with phenolphthalein indicator solution. The pink color indicates that the structural concrete is alkaline throughout all but a thin veneer along the upper surfaces. The high pH is indicative of the relative lack of carbonation within the structural layers. Steel embedded within the substrate concrete would not be at risk for depassivation at least within the upper portions represented here.

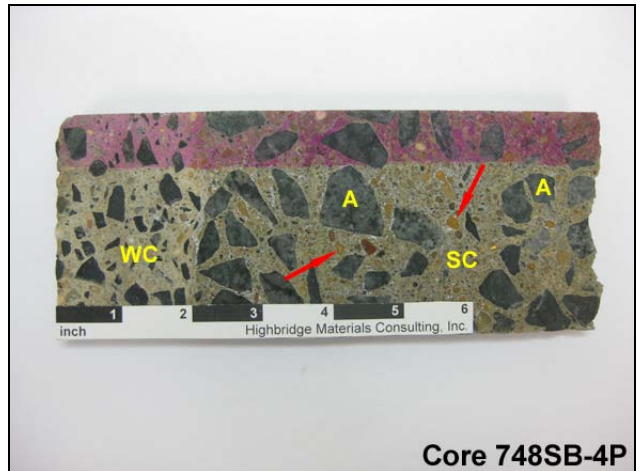
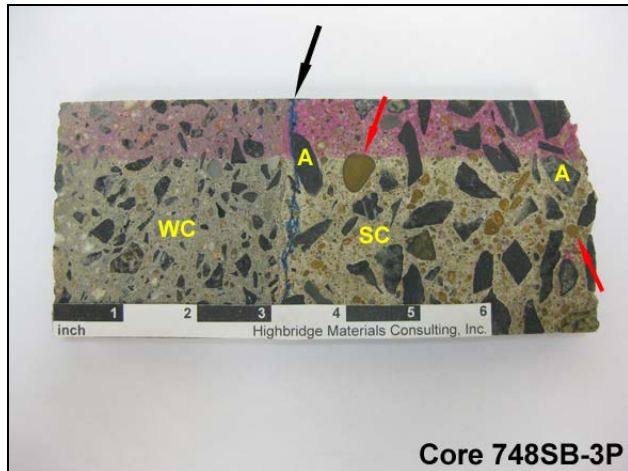
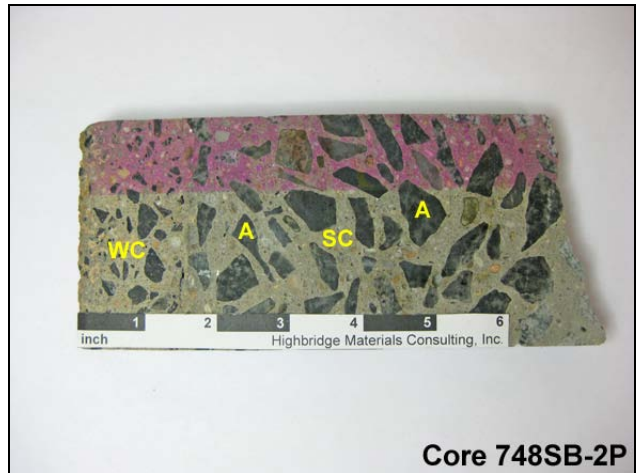
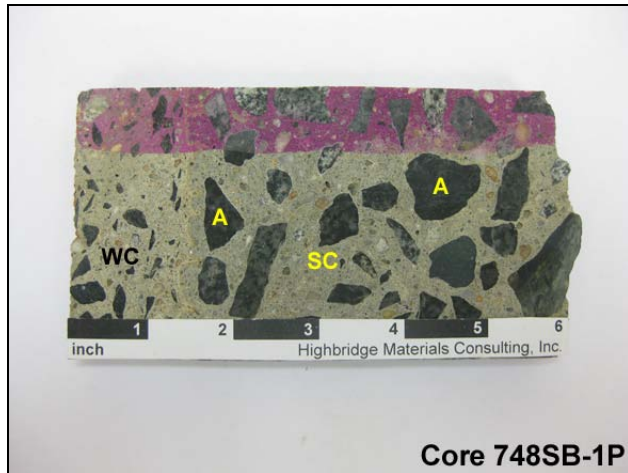
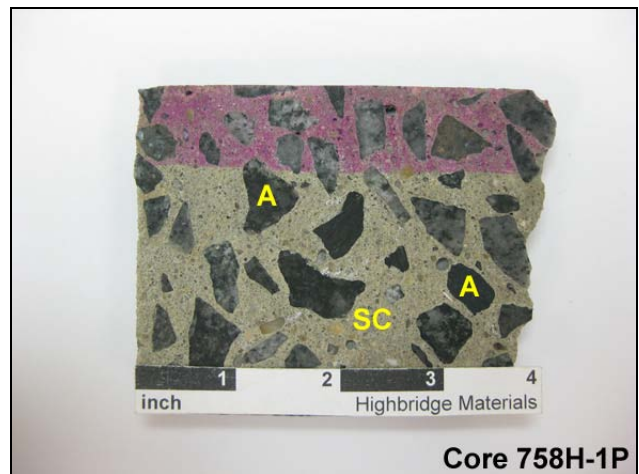
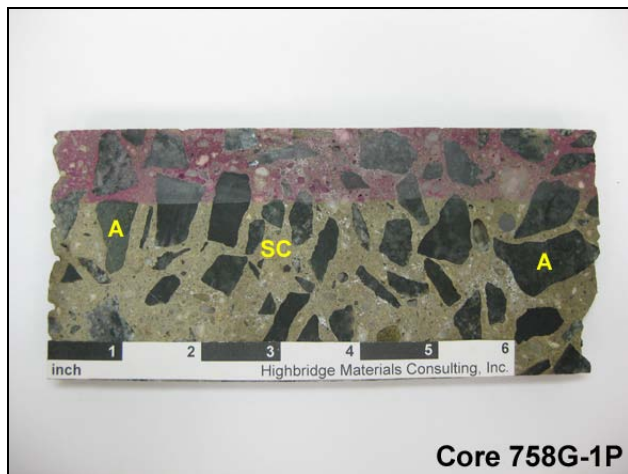
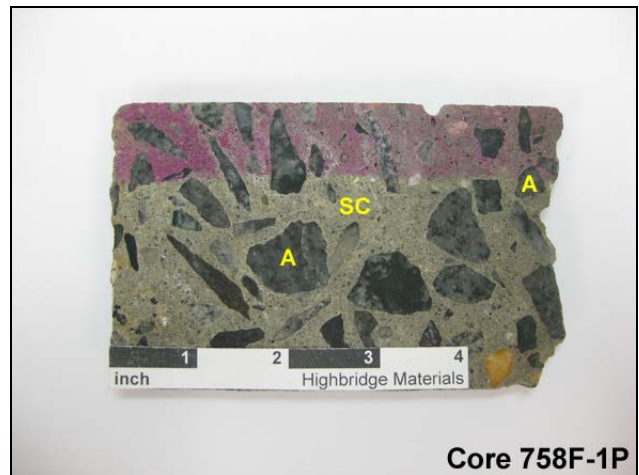
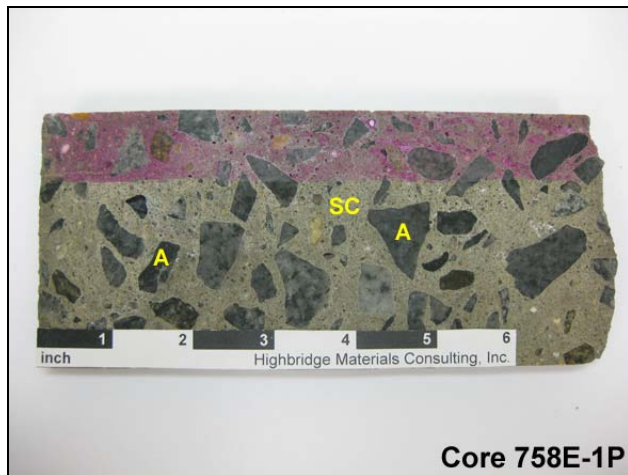
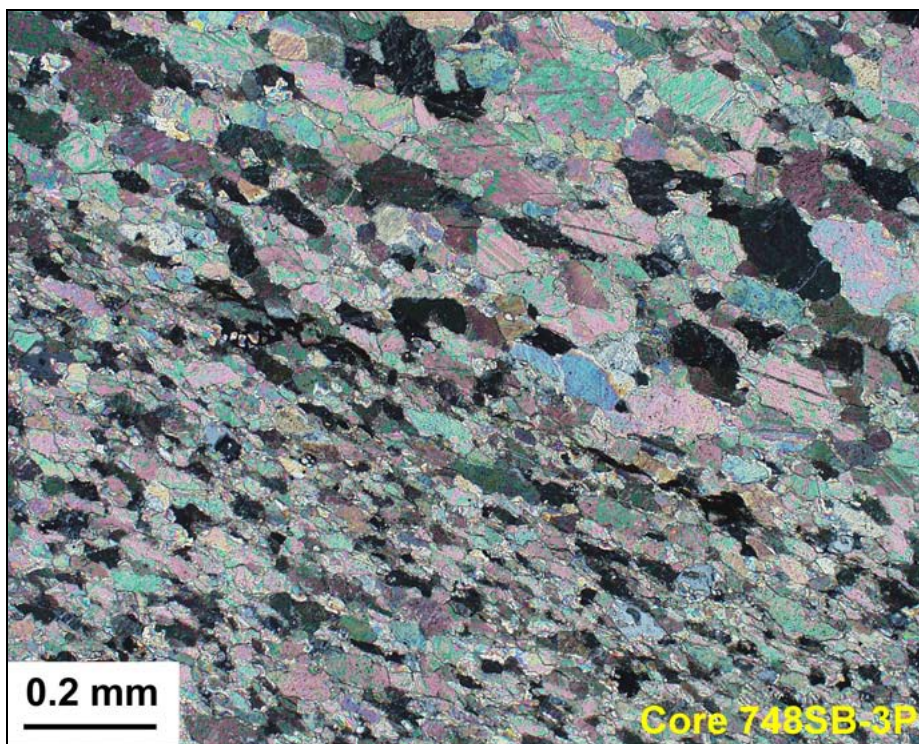
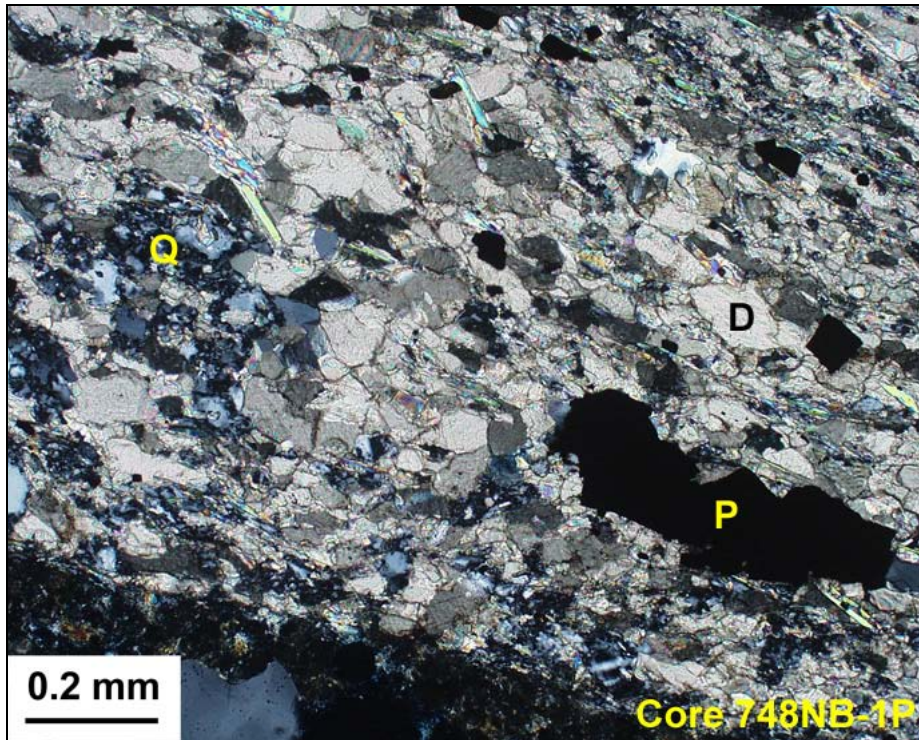


Figure 2 (cont'd.): Photographs of honed concrete cross sections prepared for the full depth of each provided sample.



**Figure 2 (cont'd.):** Photographs of honed concrete cross sections prepared for the full depth of each provided sample.



**Figure 3:** XPL photomicrographs illustrating examples of the dolostone coarse aggregate identified in Cores 748NB-1P and 748SB-3P. In the upper image, most of the stone comprises fine, rhombic dolomite crystals (D). Traces of pyrite (P) are too few to represent a durability issue. Strained quartzite inclusions (Q) are also detected. The mosaic of dolomite crystals occupying the entirety of the lower image are mildly strained as indicated by the preferred elongation. Two different grain sizes are juxtaposed here.

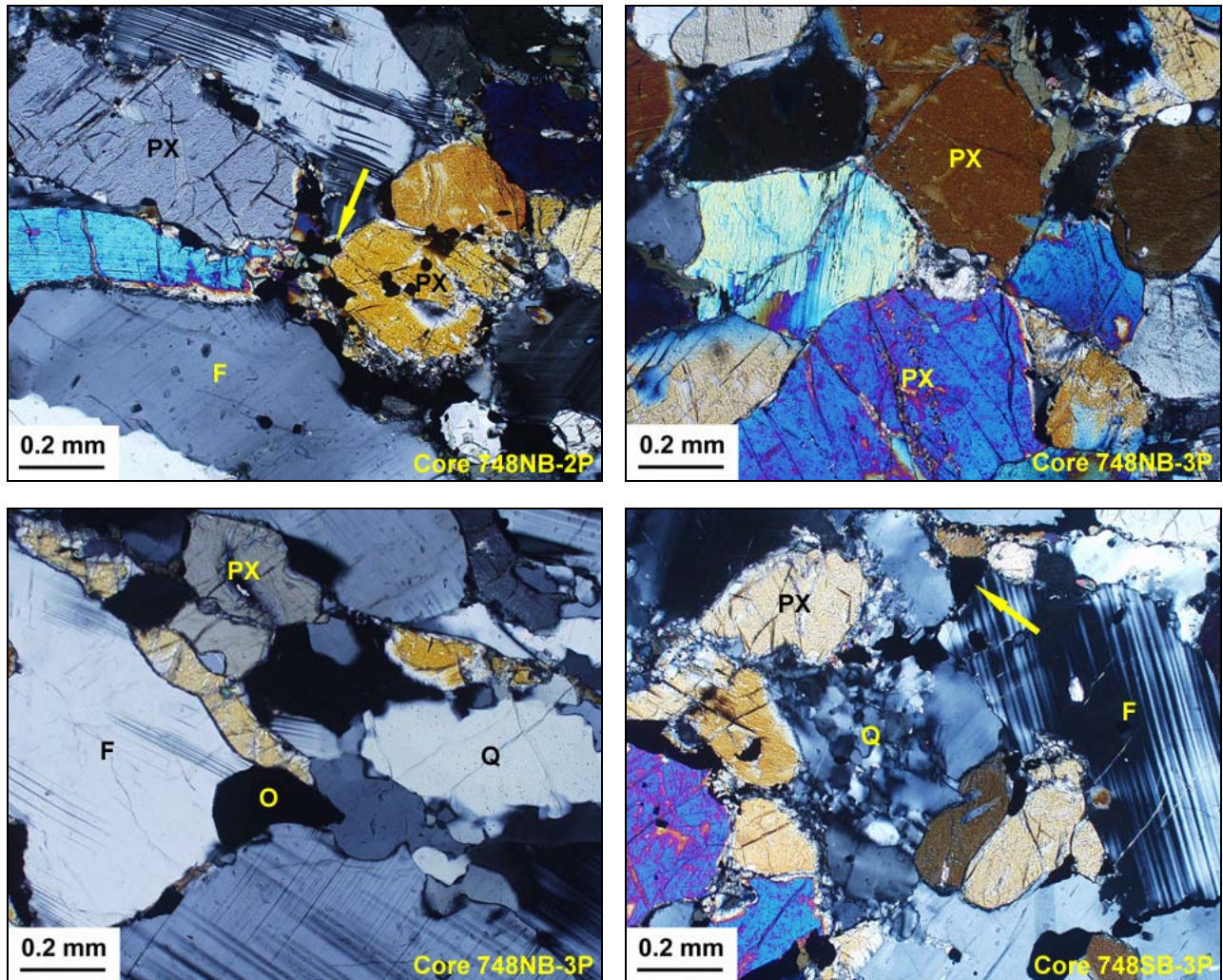


**Figure 4:** XPL photomicrographs. Quartz diorite is the sole coarse aggregate in Cores 748NB-2P and 748NB-3P and a major component of Core 748SB-3P. The diorite has a medium-grained, granoblastic texture. Minerals include plagioclase feldspar (F), pyroxene (PX), quartz (Q), and opaque phases (O or arrows). The particle at upper right contains a concentration of equigranular pyroxene crystals with no interstitial plagioclase. The quartz diorite appears to have remained stable in service.

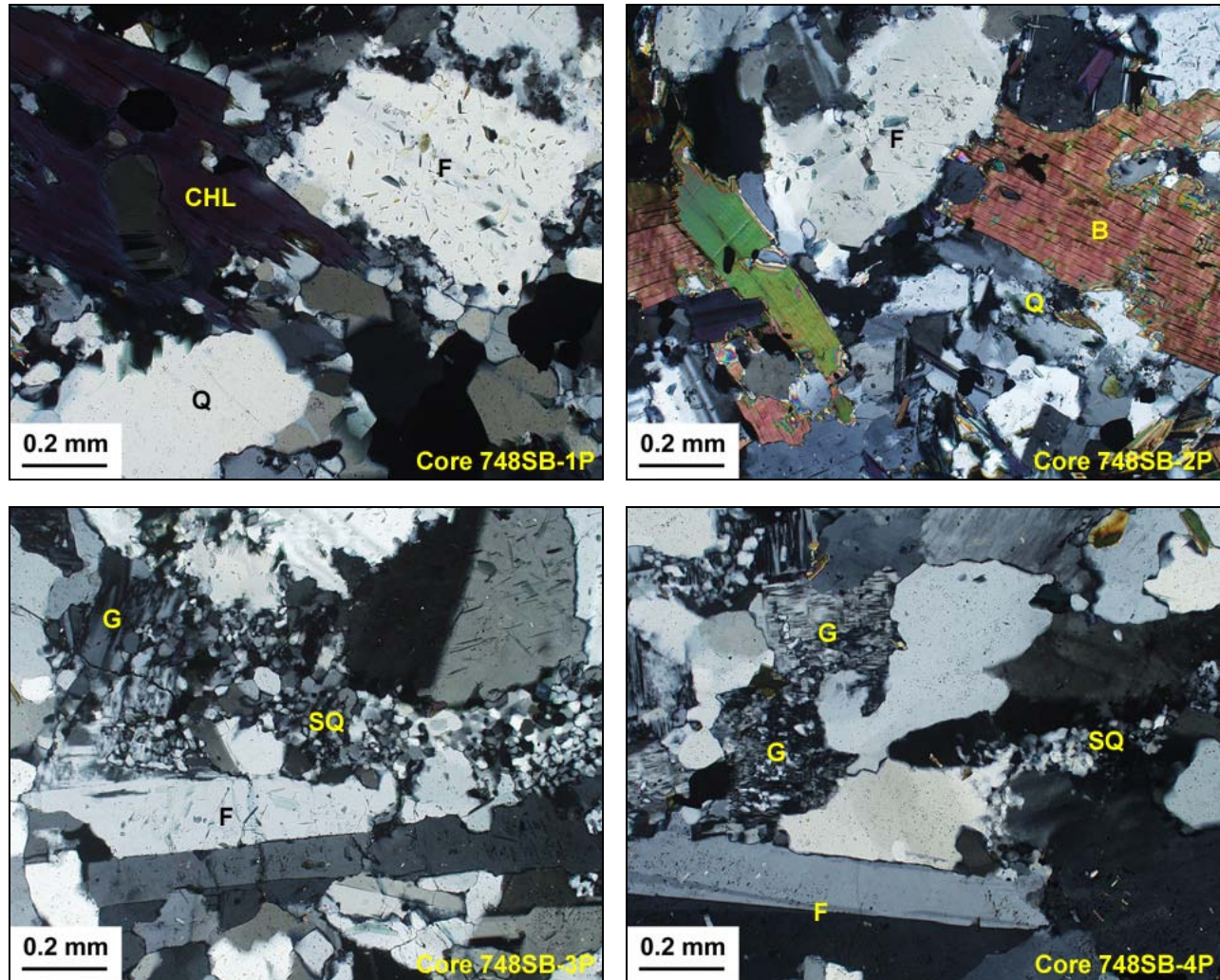


**Figure 5:** Granitoid rock types are a major component of the coarse aggregate in the 748SB samples as shown in these XPL photomicrographs. These include tonalites and possibly granodiorites. Feldspar is dominant (F) and these crystals usually exhibit a mild alteration to fine white mica and clay. Quartz (Q) is also present as a primary crystallization though it is more common as interstitial late-stage material. Accessory minerals are more common in three of the 748SB samples and may include biotite (B) or chlorite (CHL) along with other minor phases. More importantly, there is an abundance of fine interstitial matrix in all of the granitoid rocks. This contains both graphic intergrowths (G) of quartz and feldspar as well as patches of strained quartz (SQ). These are shown in the lower two images. The fine, deformed quartz is considered to be alkali-silica reactive and some of the early stage reactions observed in this study are found in these rocks.

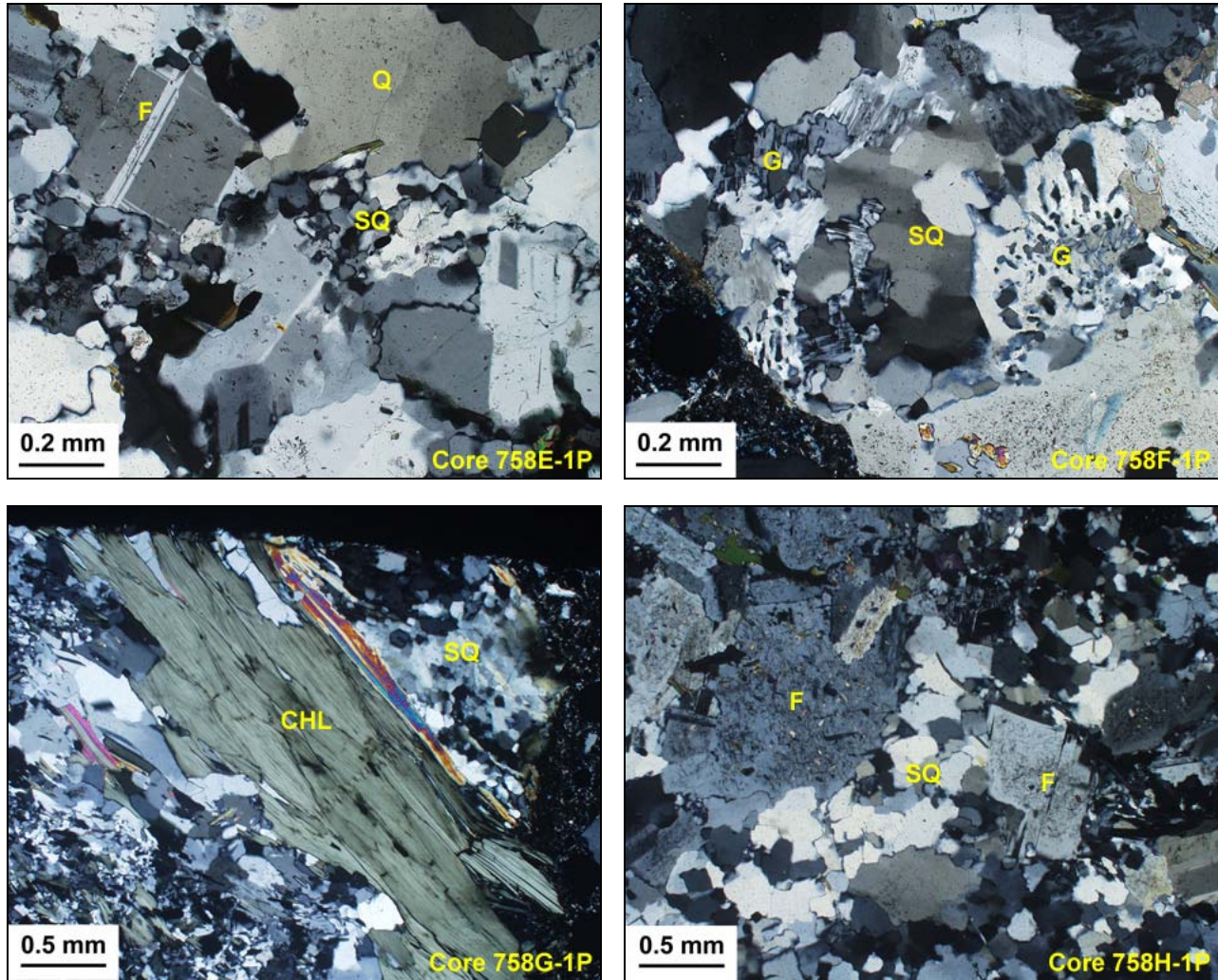


**Figure 6:** XPL photomicrographs. The tonalites and granodiorites are also a major component of the coarse aggregate in the 758 core samples. Feldspar and quartz (F and Q respectively) are again major components but are not highlighted in this set of images. Instead, the interstitial material is emphasized as this tends to be more concentrated in the coarse aggregate from the 758 group of cores. Note that the strained quartzite (SQ) is much coarser-grained in these samples. Graphic intergrowths (G) are also present but similar to those of the 748SB samples. Accessory mineral phases tend to be less abundant in these samples. However, grains rich in chlorite (CHL) are present in Cores 758F-1P and 758G-1P. An example is shown for the latter.

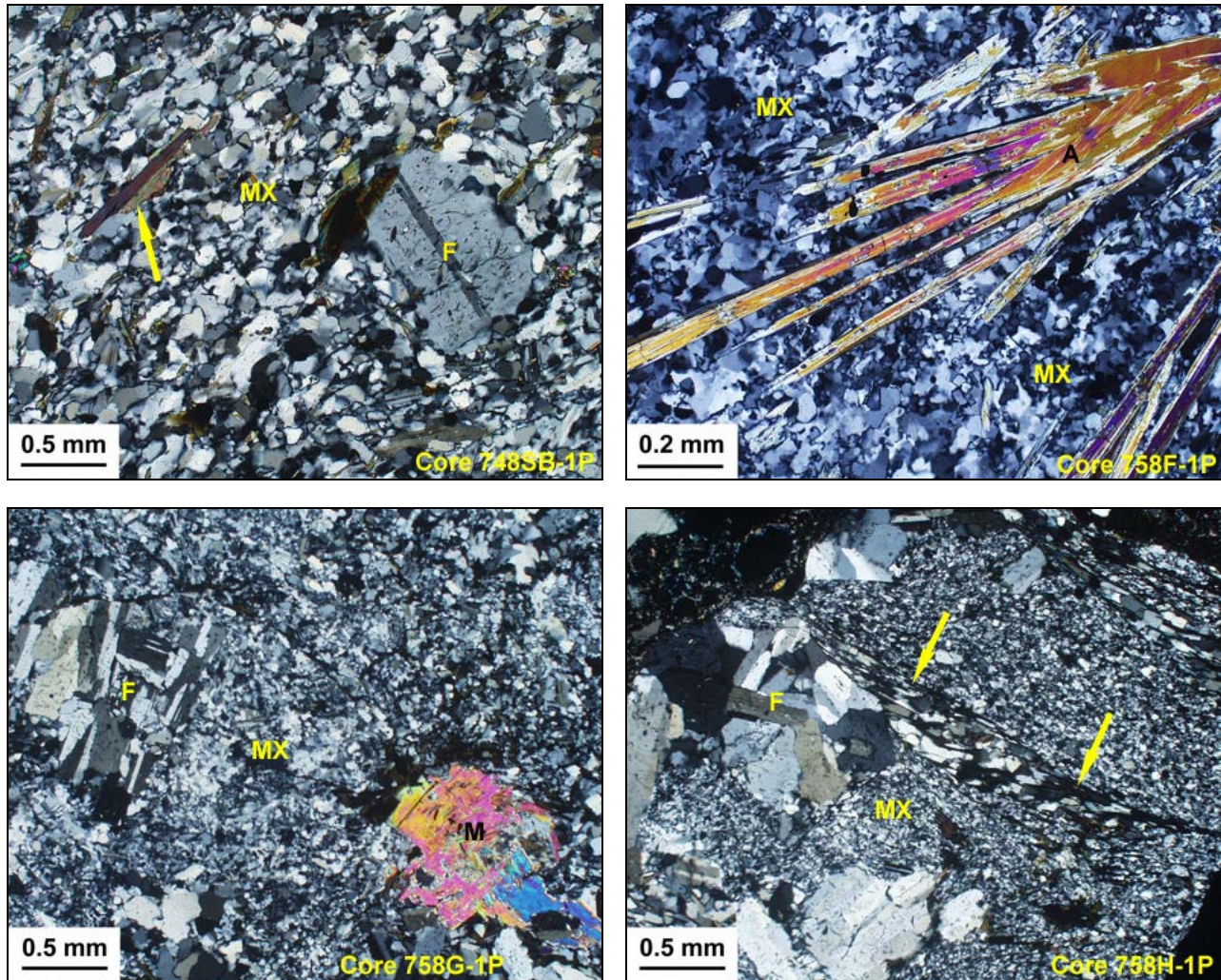


**Figure 7:** Examples of schistose granofels are shown in these XPL photomicrographs. This rock type present in some of the coarse aggregate exhibits the greatest degree of alkali-aggregate reactivity out of all the lithologies identified in the twenty-seven core samples. However, the granofels are only abundant in Cores 748SB-1P and 758G-1P of the eleven cores studied for this report. Minor to trace quantities are found in the other 758 cores. In all cases, the stone is dominated by a matrix (MX) of fine-grained quartz subgrains. The matrix is essentially a strained quartzite and the deformation causes the stone to be alkali-silica reactive. Coarser porphyroclasts are entrained within the sheared matrix including but not limited to feldspar (F), muscovite (M), and amphibole (A). A mild schistosity is caused by the preferred alignment of sparsely distributed micas such as the biotite shown by the arrow in the upper left image. The arrows in the lower right image indicate a sheared tail of chlorite and feldspar rotated off the main feldspar clast. This texture clearly indicates the shear deformation embodied by the granofels.

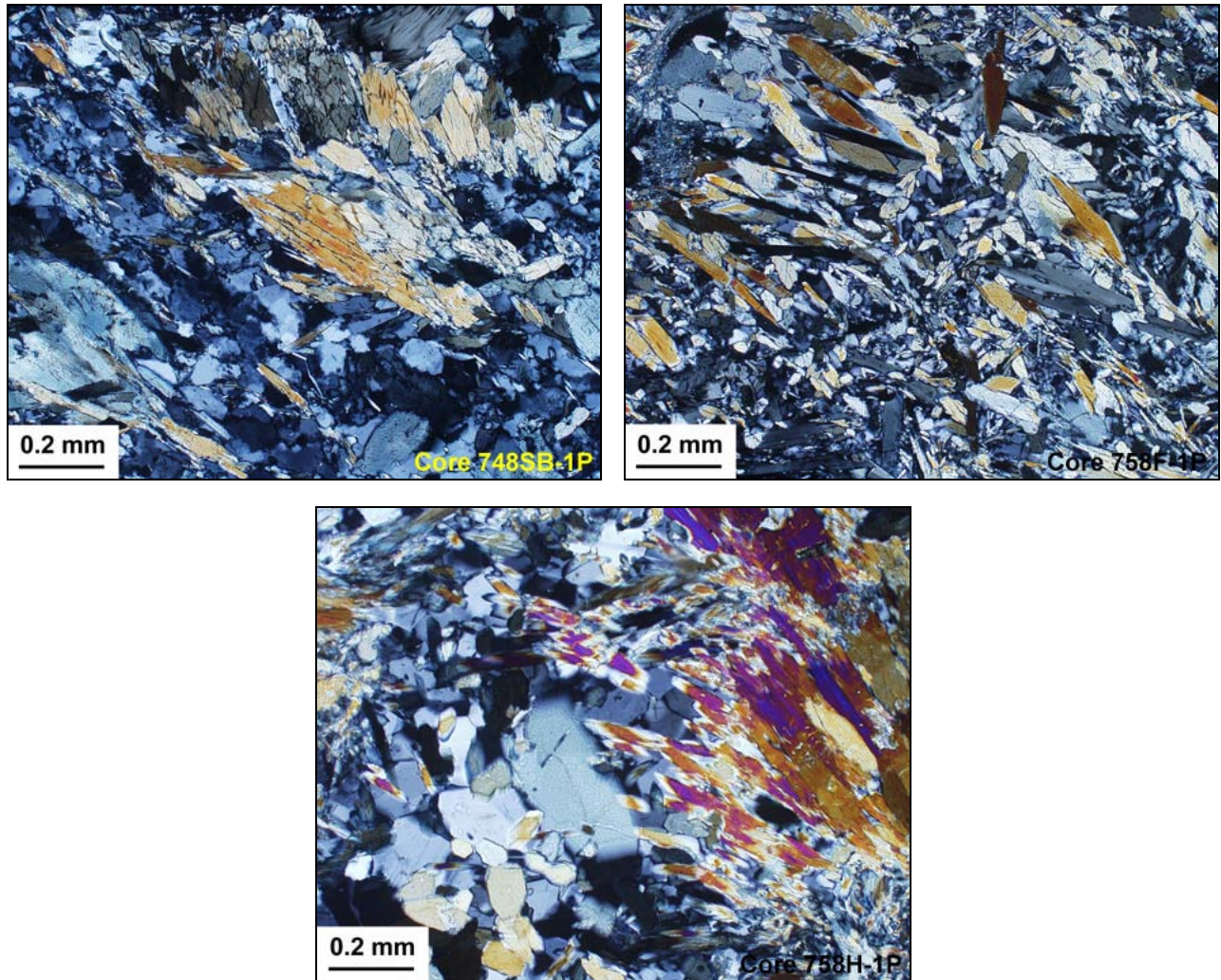


**Figure 8:** Amphibolites are only present in minor to trace quantity in the coarse aggregate of several of the core samples. Examples are shown in these XPL photomicrographs. The bright colored minerals are euhedral to subhedral amphiboles as well as some lower-grade alteration products. The white and gray phases are mostly composed of plagioclase feldspar though quartz is also present.

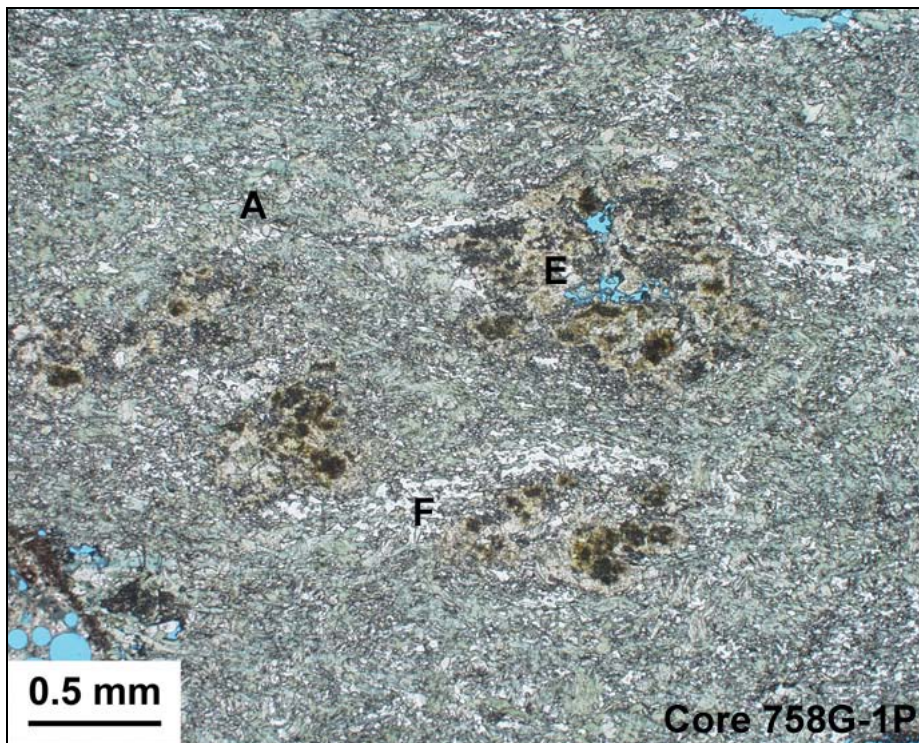
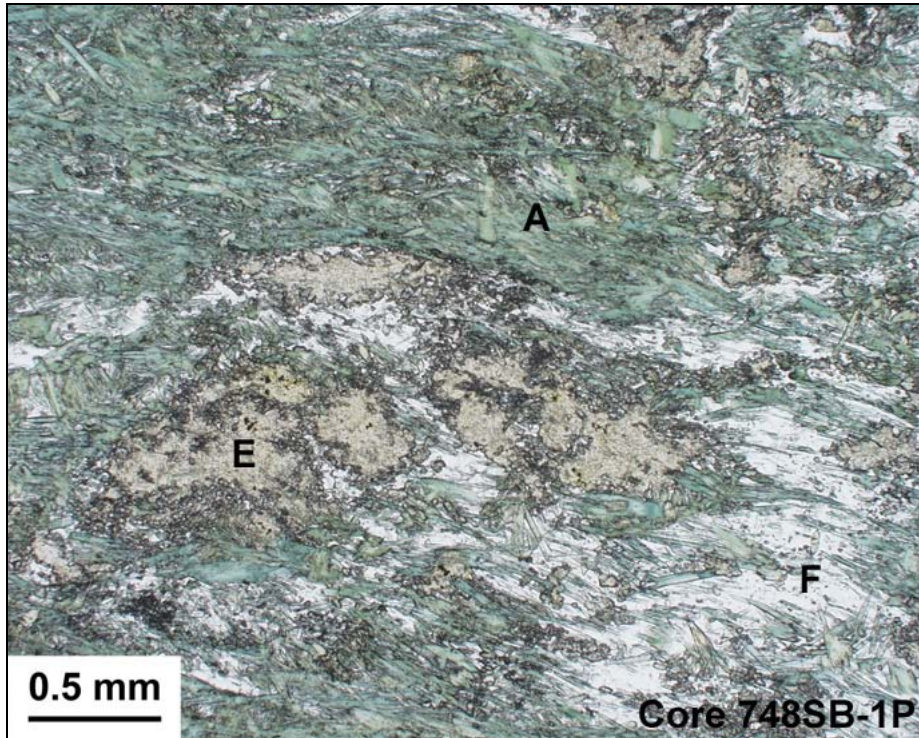


**Figure 9:** Additional examples of amphibolite are shown in these PPL photomicrographs. Here, the yellowish pods of epidote (E) appear to represent low-grade alterations of mafic minerals. This would indicate an igneous rather than a sedimentary origin for the amphibolite. Green amphibole (A) and white plagioclase feldspar (F) are also shown.

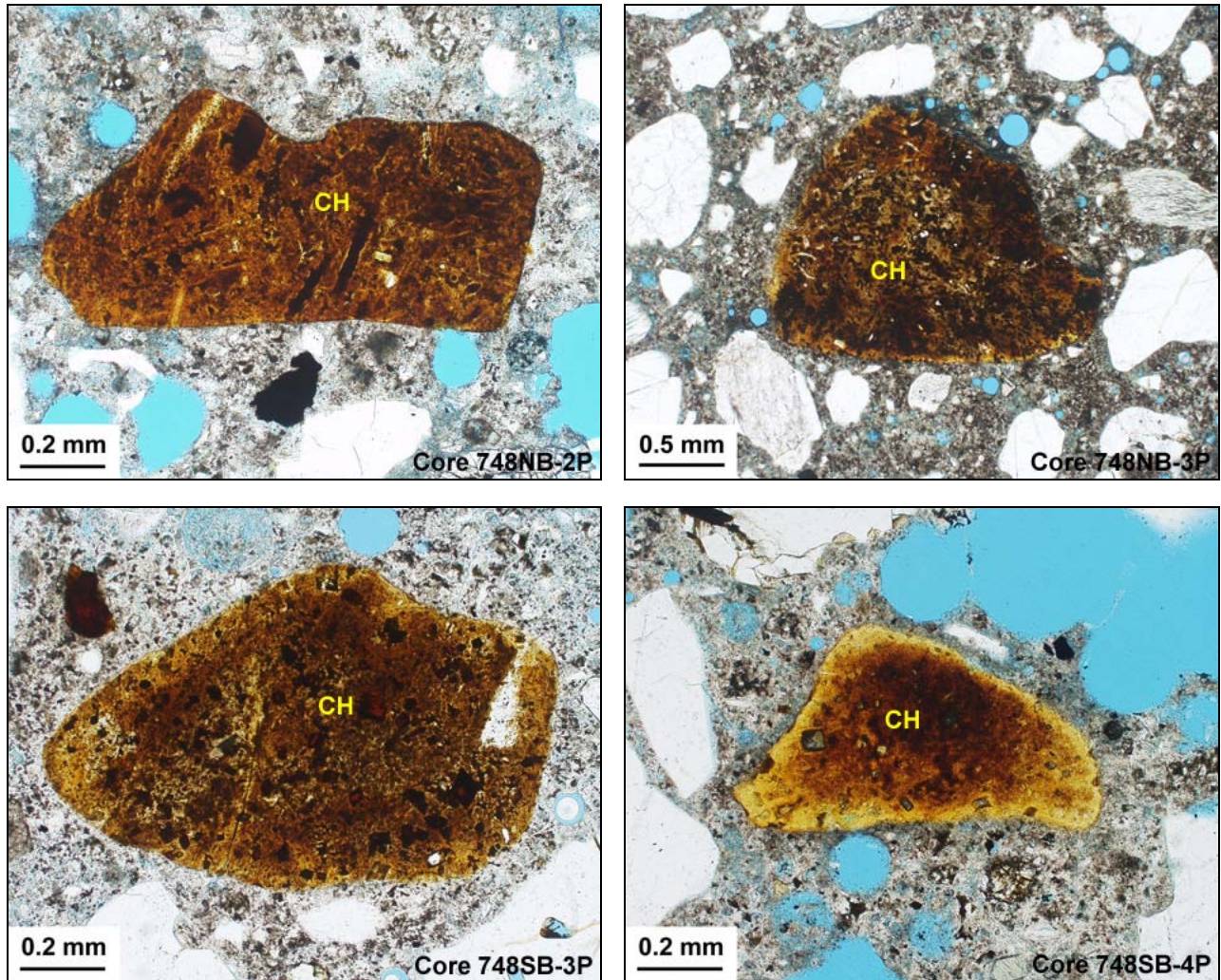


**Figure 10:** PPL photomicrographs. Four of the ten cores contain ferruginous chert (CH) in the fine aggregate at about several percent by volume. Chert is considered to be one of the most highly alkali-reactive rock types. Traces of reaction are observed in this material in all cores containing the phase.

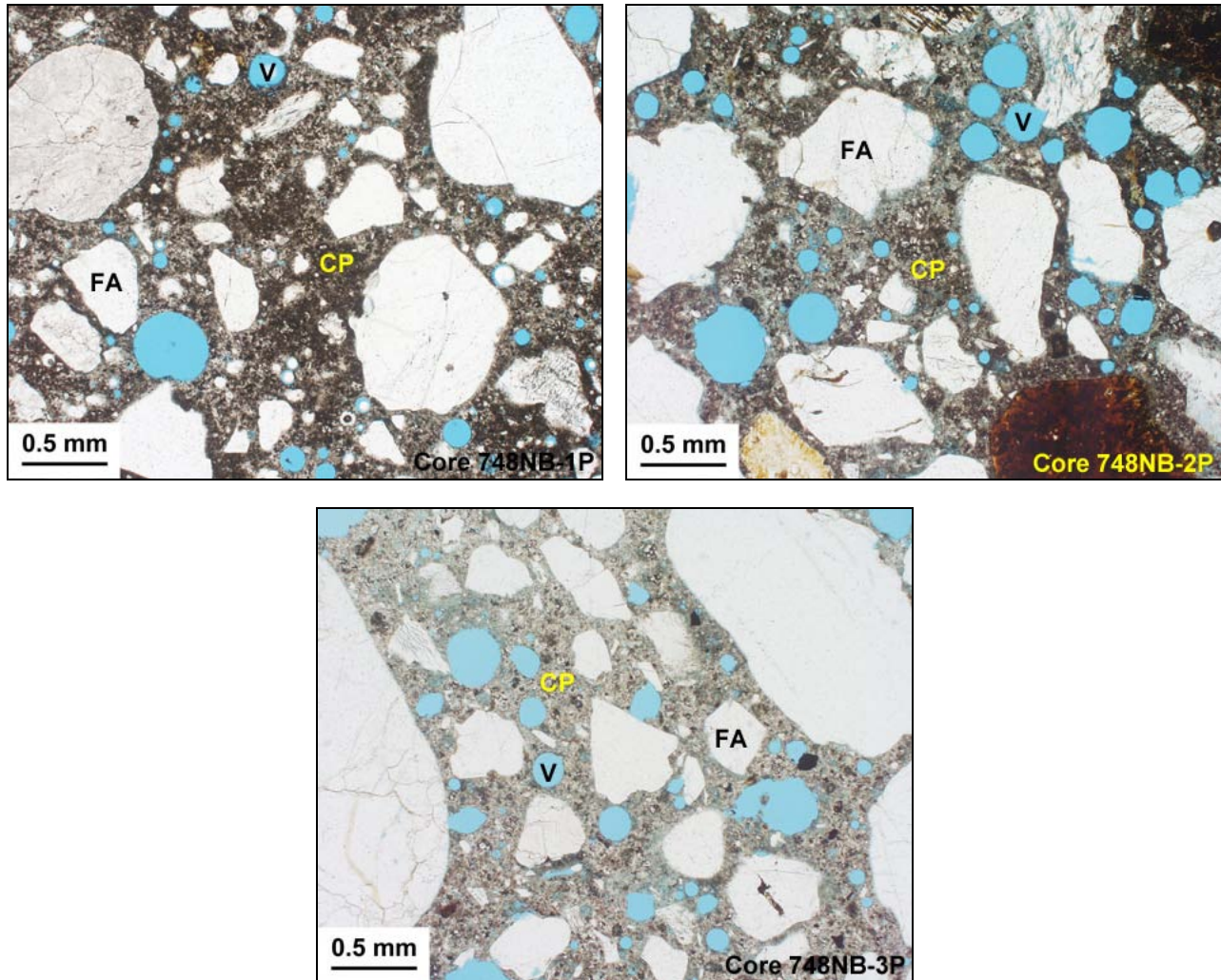


**Figure 11:** PPL photomicrographs illustrating the overall microstructure of the structural concrete. There is some variability in water contents and entrained-air development that result in some quality differences. In all of the examined samples, the cement paste (CP) is well-developed and relatively dense as indicated by the even brown coloration under plane light. Some microscopic clotting is detected in Core 748SB-3P and some mottling in Core 748NB-1P though this is not particularly obvious in the images. The features may represent a primary cement flocculation. The samples are impregnated with a low-viscosity, blue-dyed epoxy in order to highlight cracks, pores, and voids. There is a moderate absorption of the epoxy consistent with moderate mix water contents. Note the notably lower absorption in Core 748NB-1P. The fine aggregate (FA) is well distributed throughout the matrix though there are some subtle differences in the gradations between samples. Fine, spherical voids (V) indicate intentional air-entrainment in all cores. Air contents might be considered somewhat excessive in Cores 748SB-1P, 748SB-4P, and 758H-1P.

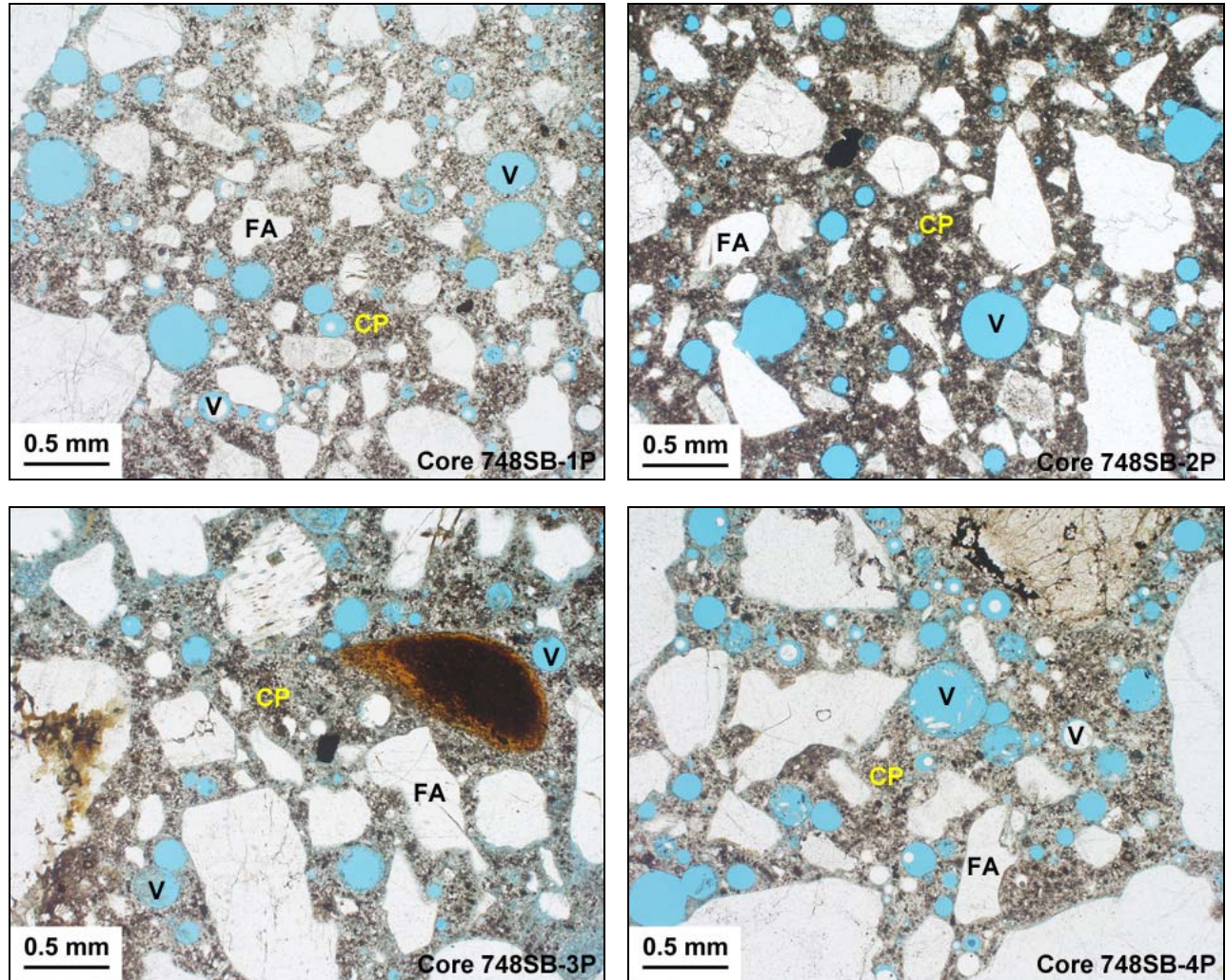


Figure 11 (cont'd.): PPL photomicrographs illustrating the overall microstructure of the structural concrete.

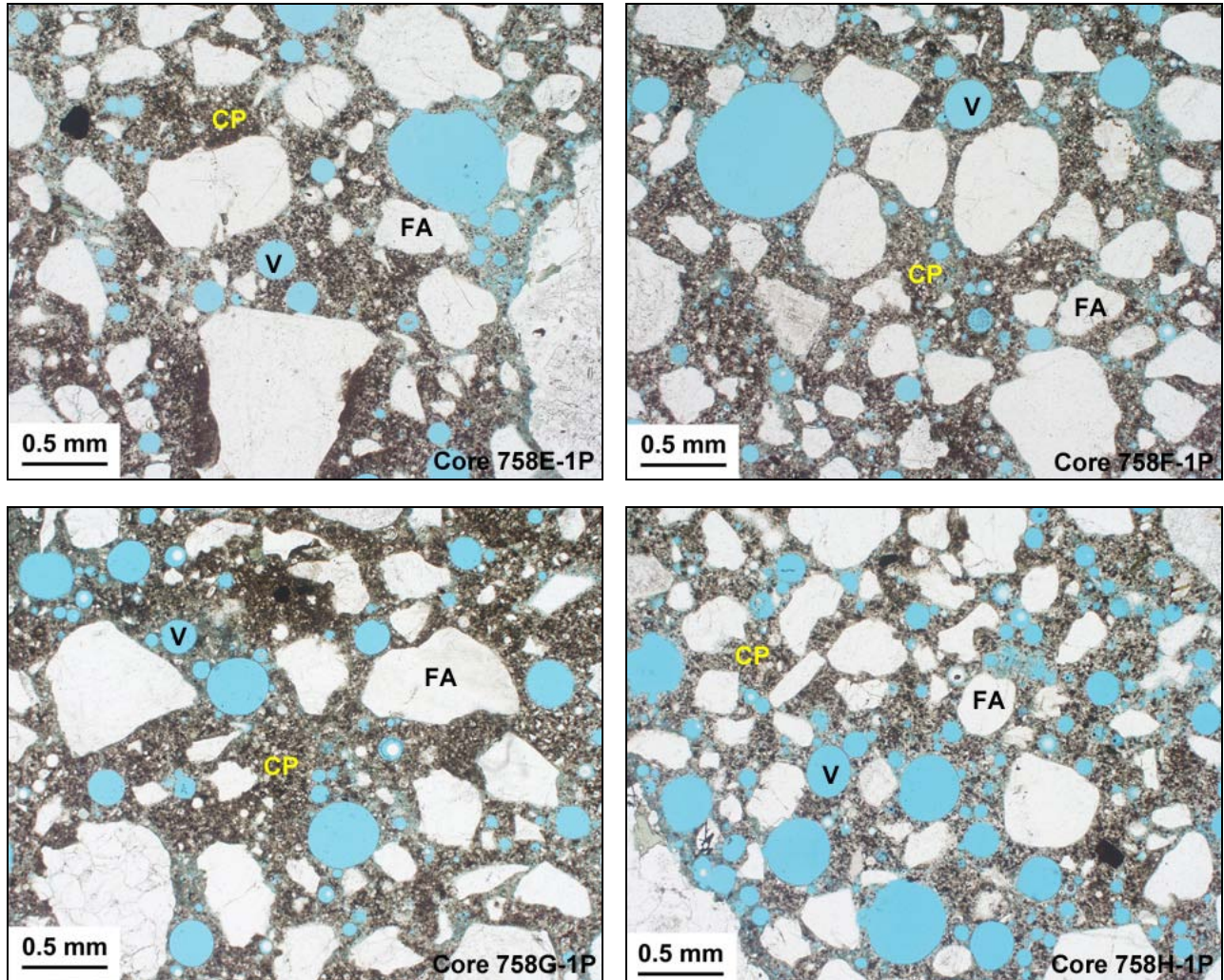
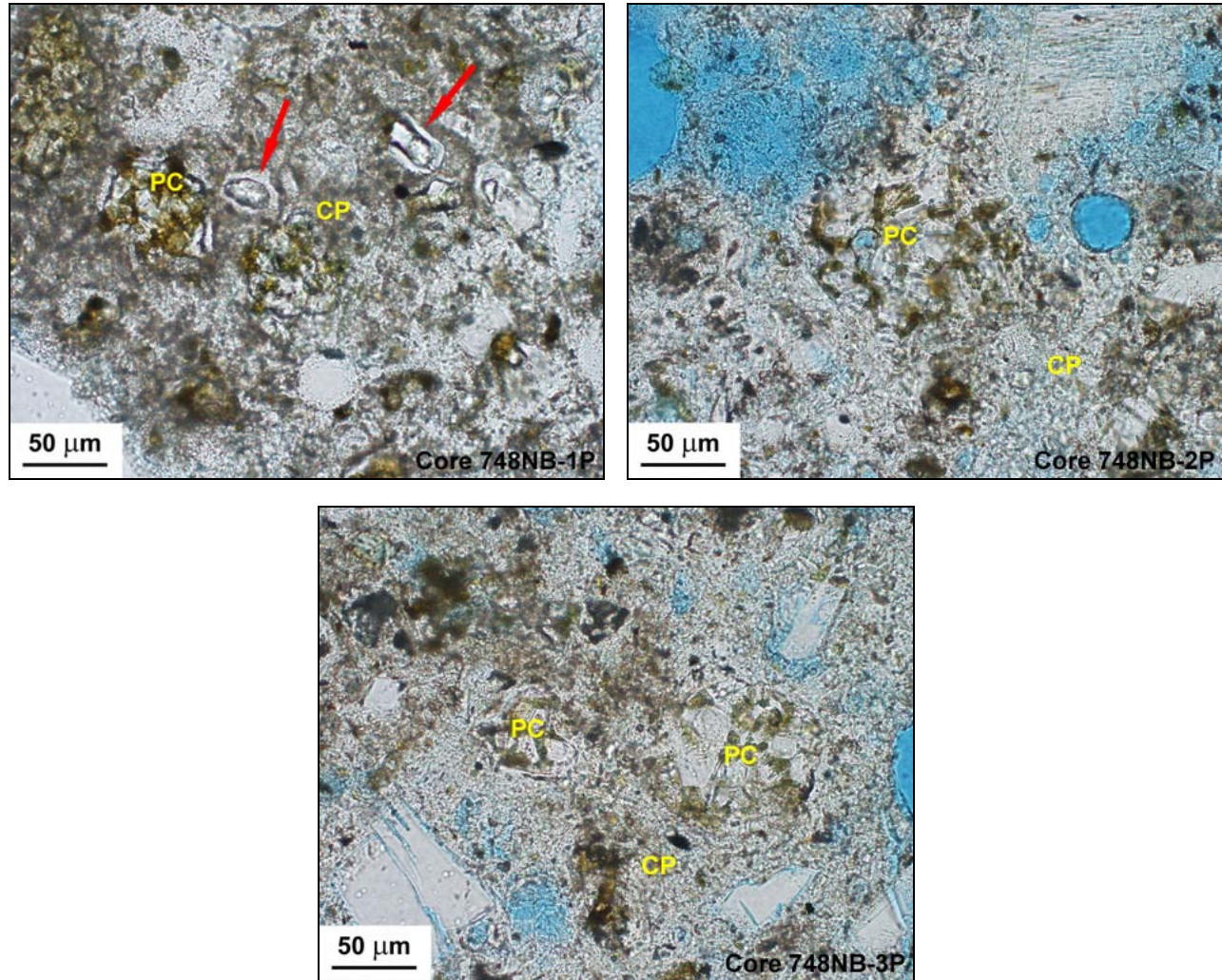


Figure 11 (cont'd.): PPL photomicrographs illustrating the overall microstructure of the structural concrete.



**Figure 12:** PPL photomicrographs illustrating the occurrence of residual portland cement (PC) in the examined concrete. The cement hydration is advanced and most calcium silicate is fully consumed. These appear as light-colored areas within the cement agglomerates. Exceptions are shown for Cores 748NB-1P, 748SB-1P, 748SB-4P where belite remains unhydrated. Unhydrated alite is also detected in Cores 748NB-1P and 758G-1P and these crystals are indicated by the red arrows. Traces are also detected in Core 758H-1P but not illustrated here. Moderately thick hydration rims surround these alite crystals where they are identified. For Core 758H-1P, an area is shown where the empty pores are now filled with an amorphous cementitious hydrate. All of the cement residuals are fine to medium-grained agglomerates with brown-colored interstitial ferrite. The adjacent cement paste (CP) is well-formed in all samples.

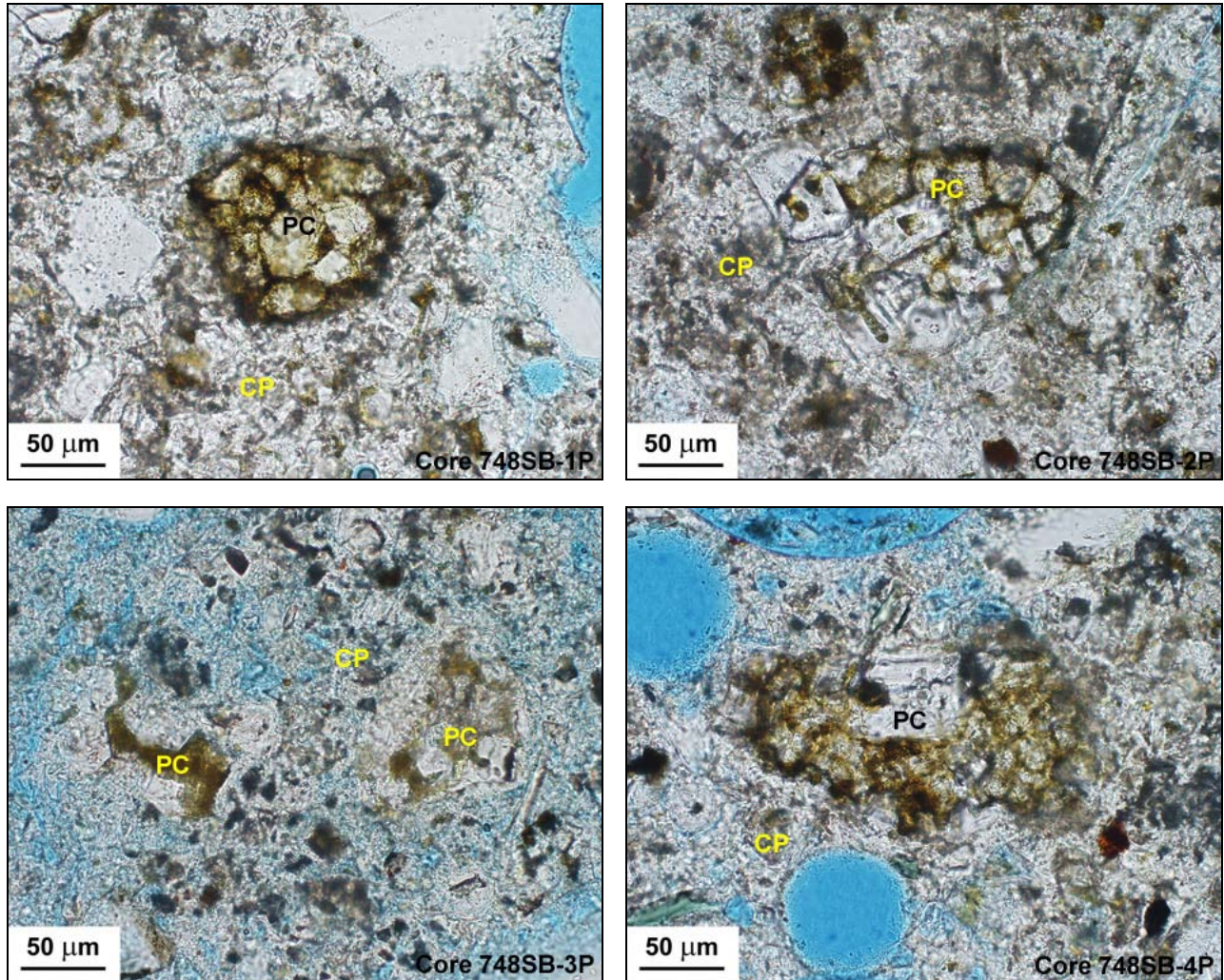


Figure 12 (cont'd.): PPL photomicrographs illustrating the occurrence of residual portland cement (PC) in the examined concrete.

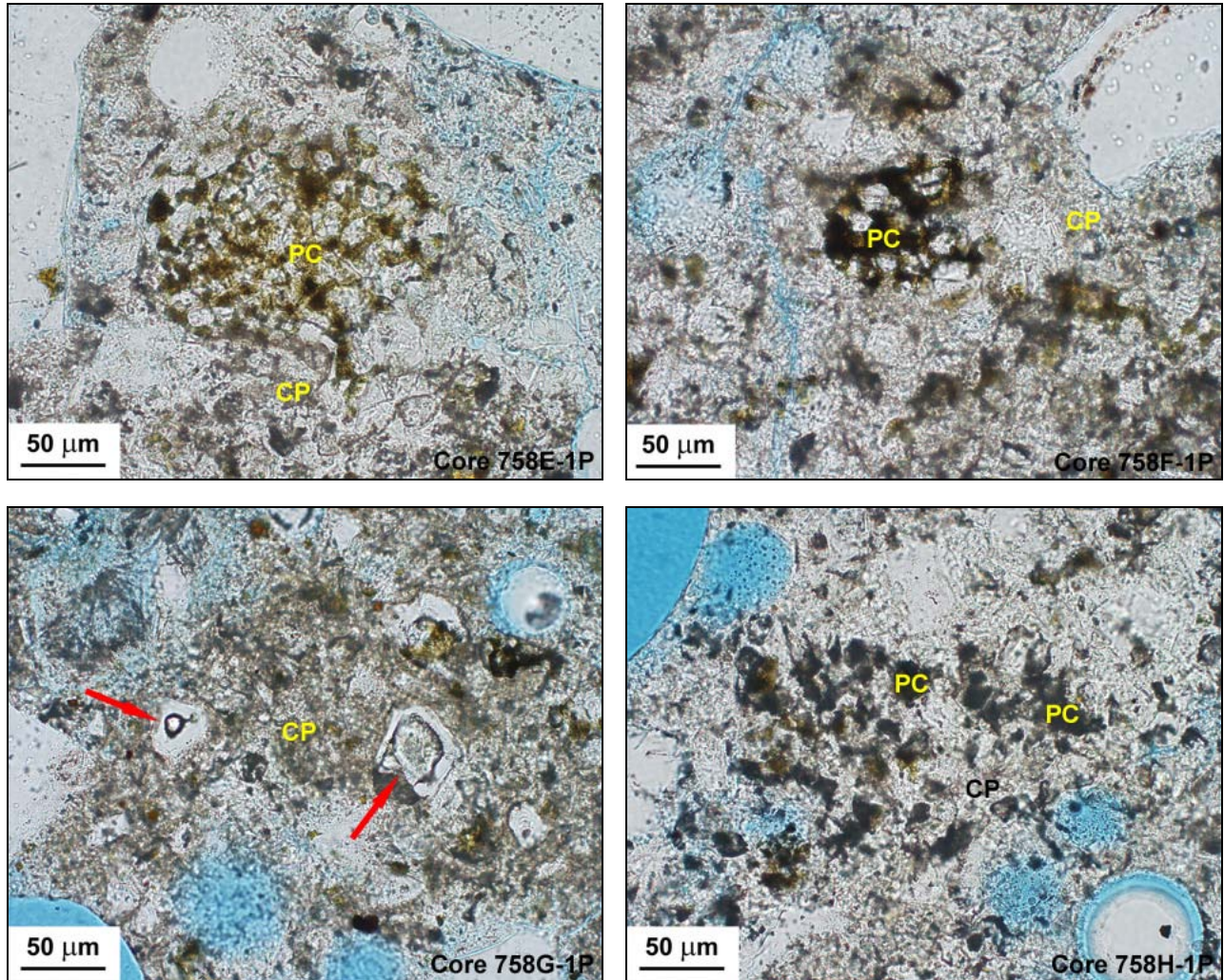
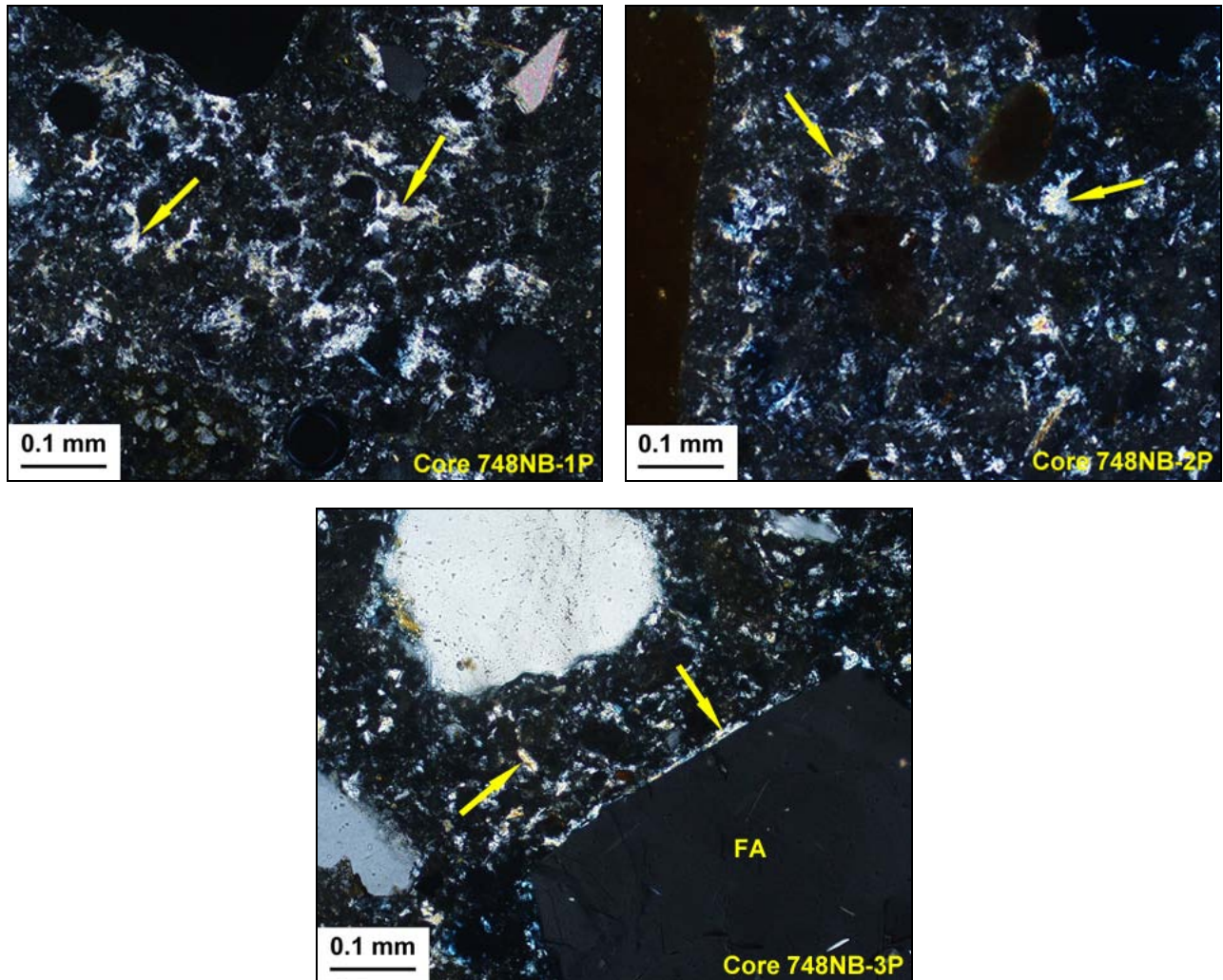


Figure 12 (cont'd.): PPL photomicrographs illustrating the occurrence of residual portland cement (PC) in the examined concrete.



**Figure 13:** XPL photomicrographs illustrating the occurrence of primary calcium hydroxide produced during the cement hydration. The hydroxide (arrows) is evenly distributed throughout the paste. Crystal size and morphology varies somewhat between samples but the non-compact morphologies are generally indicative of moderate mix water contents. Note that in some cases, semi-continuous deposits of the hydroxide line fine aggregate surfaces (FA).

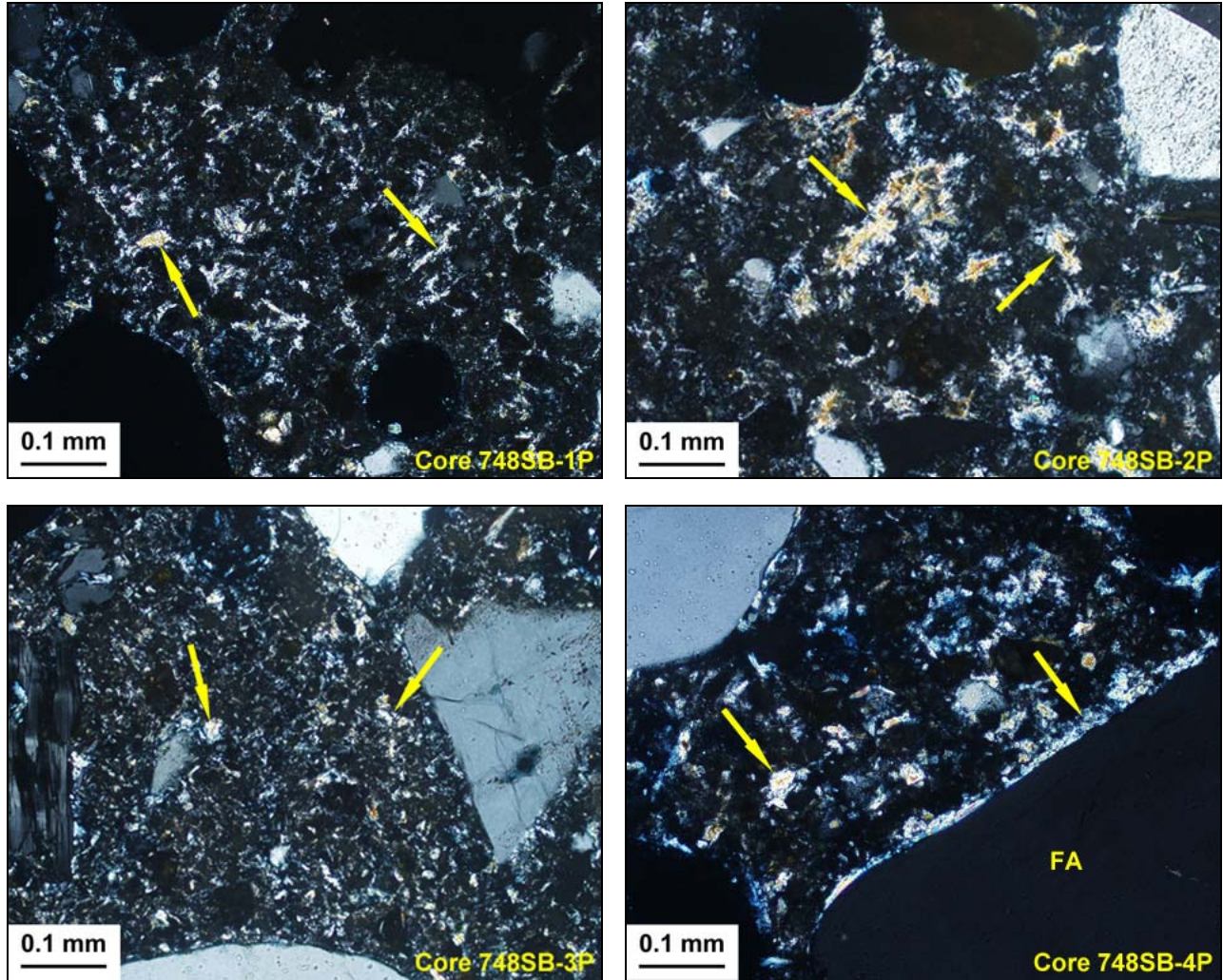


Figure 13 (cont'd.): XPL photomicrographs illustrating the occurrence of primary calcium hydroxide produced during the cement hydration.

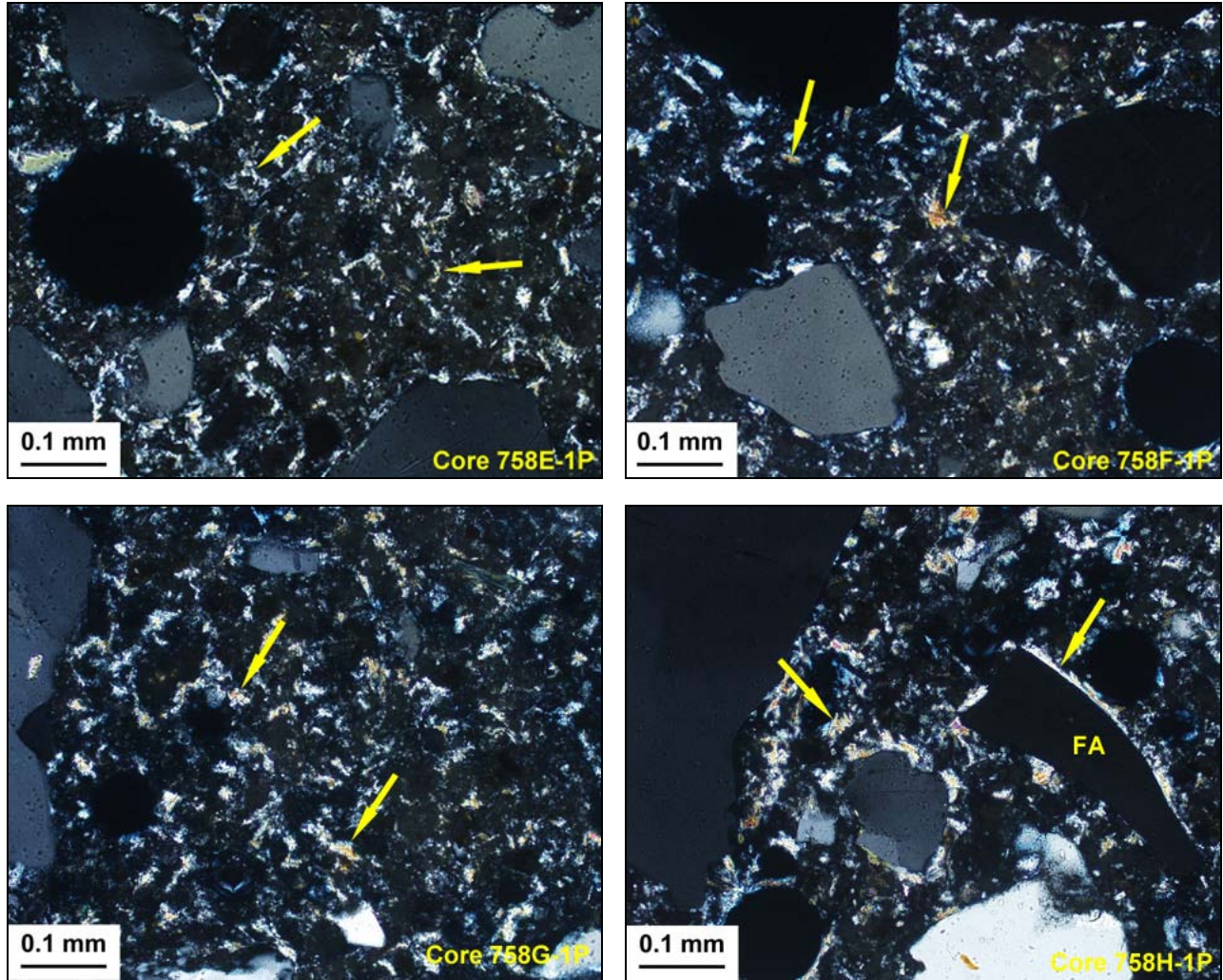
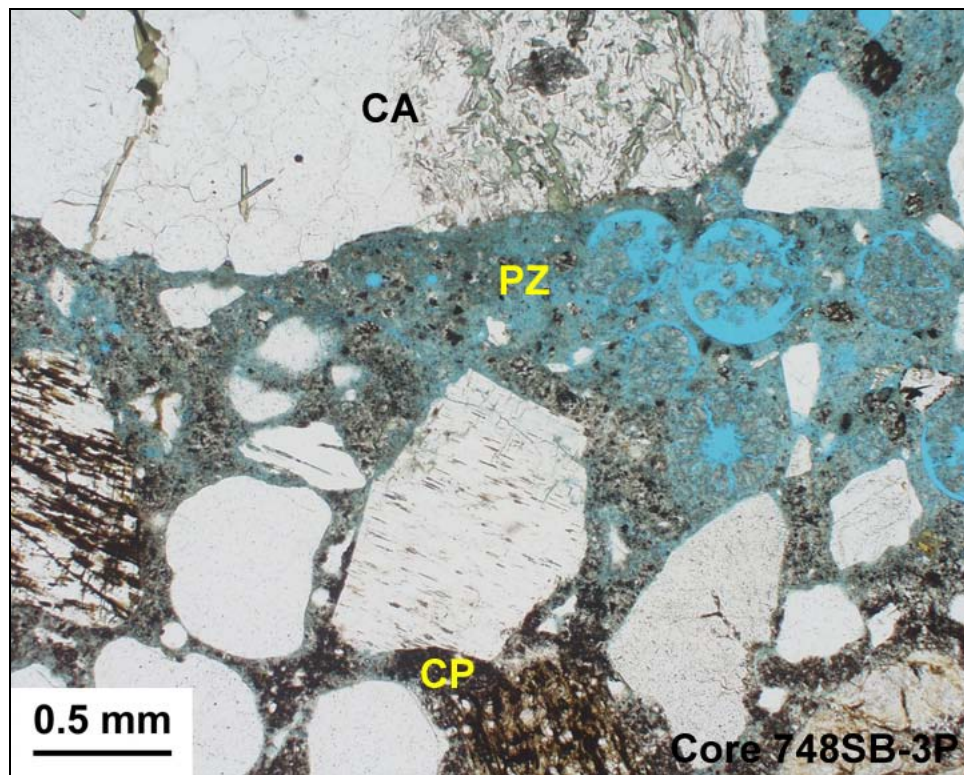
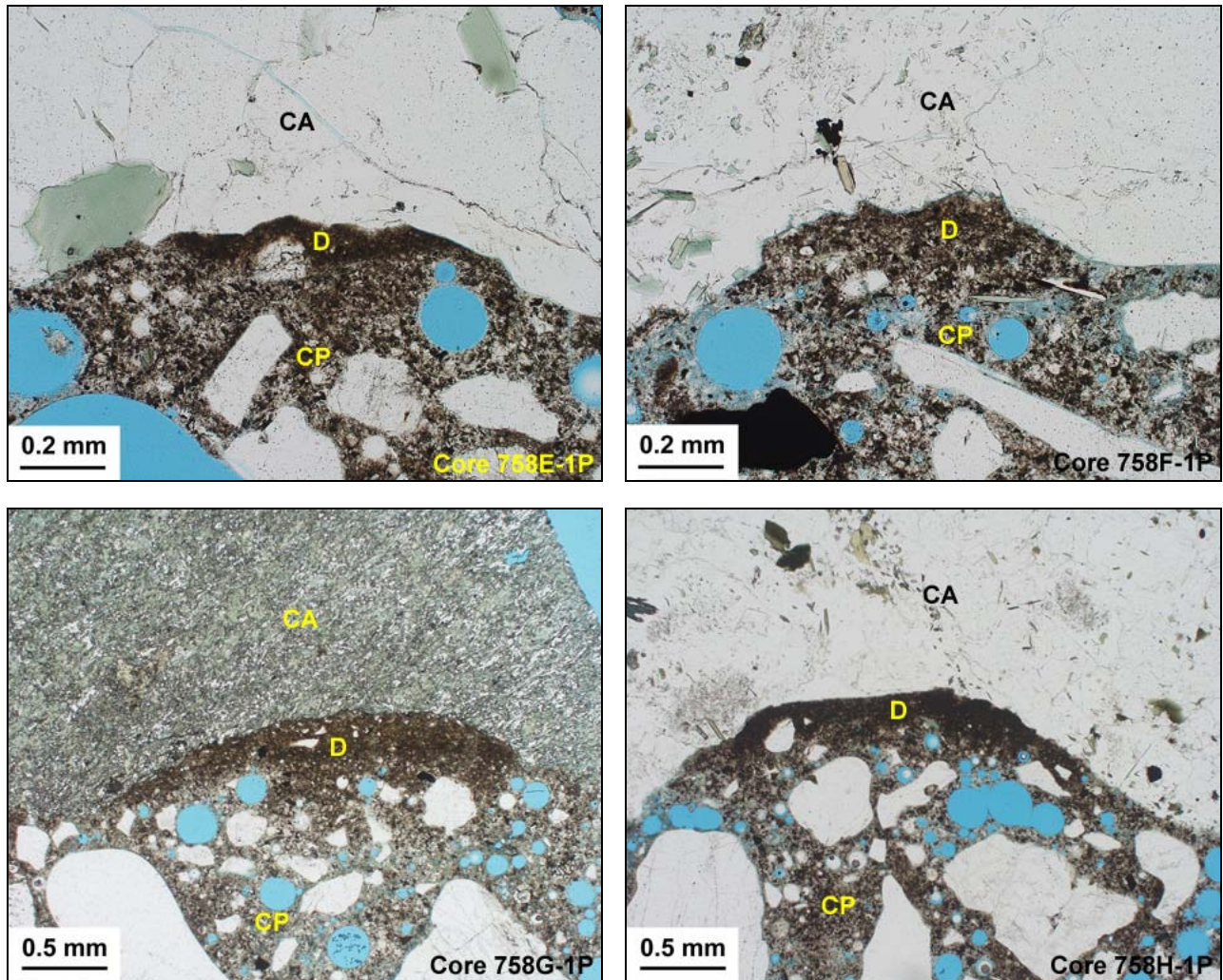


Figure 13 (cont'd.): XPL photomicrographs illustrating the occurrence of primary calcium hydroxide produced during the cement hydration.



**Figure 14:** Evidence for bleed water migration and entrapment is found in Core 748SB-3P as shown in this PPL photomicrograph. A porous zone (PZ) is shown between the cement paste (CP) and coarse aggregate (CA). This is caused by the local entrapment of mix water under the aggregate grain. The paste-aggregate bond is weakened as a result.



**Figure 15:** PPL photomicrographs. Thin discontinuous linings of dense cement paste (D) are also found between the “normal” cement paste (CP) and coarse aggregate (CA) in several of the core samples. These represent small bits of cement that did not fully incorporate with the mix water. However, they are more likely the result of microscopic embayments along aggregate surfaces and not indicative of inappropriate retempering.

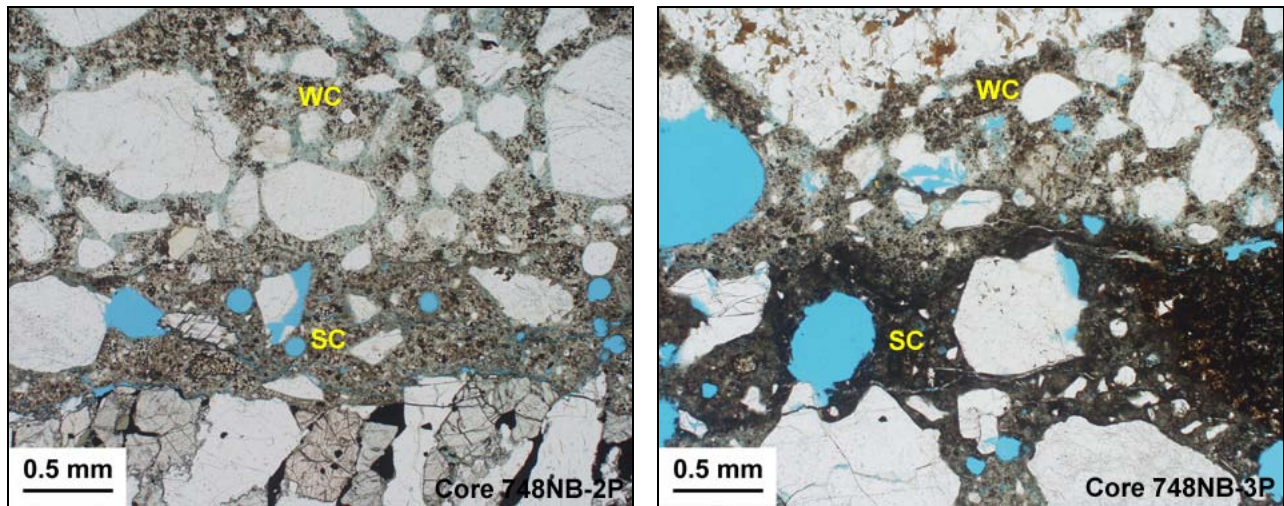


**Figure 16:** PPL photomicrographs illustrating the tight contacts between wear course (WC) and structural concrete (SC) in six of the eleven core samples. Note the rounded bead of wear course that actually penetrates the substrate in the image for Core 748SB-2P. This type of texture is best explained by a “wet-on-wet” placement.

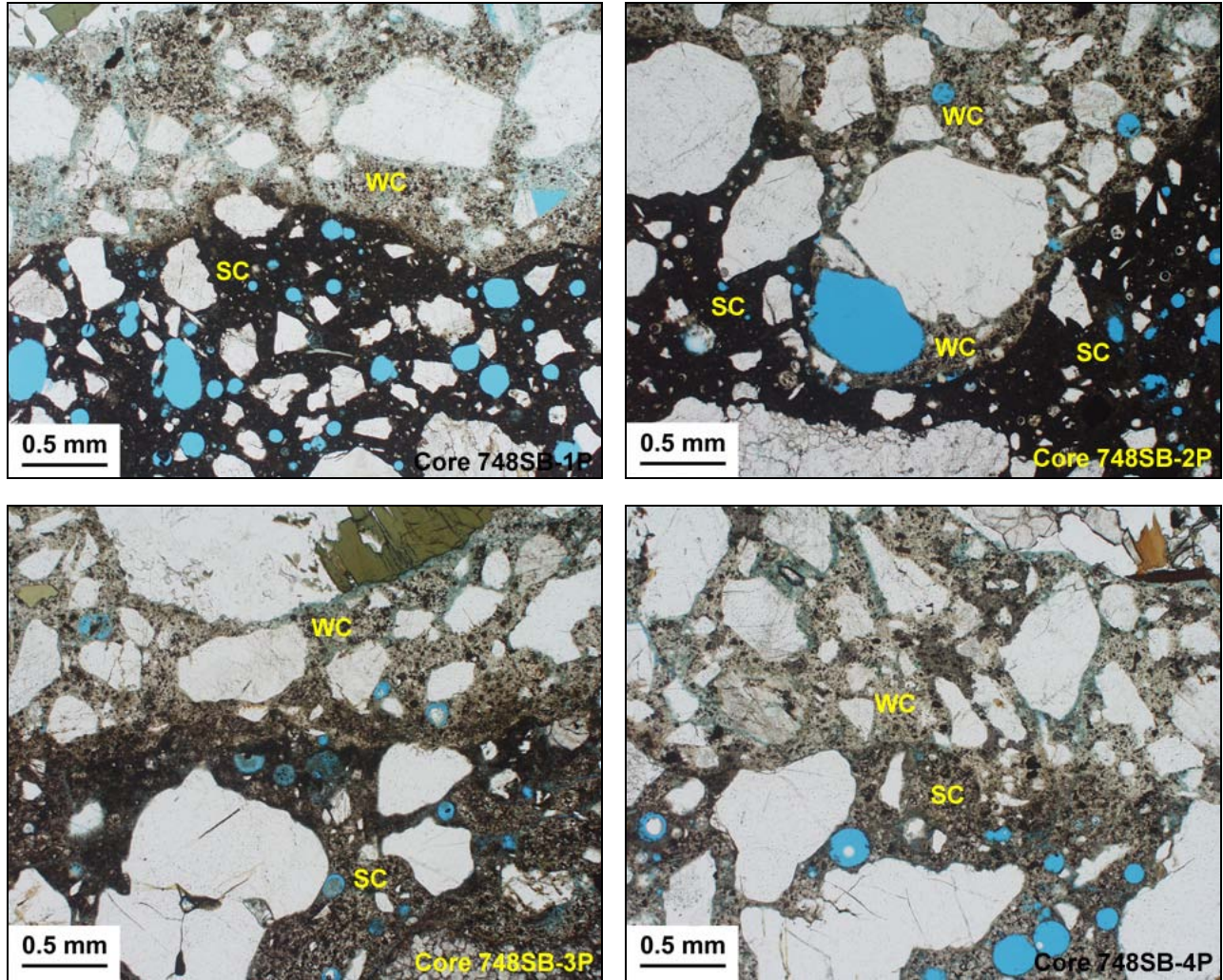
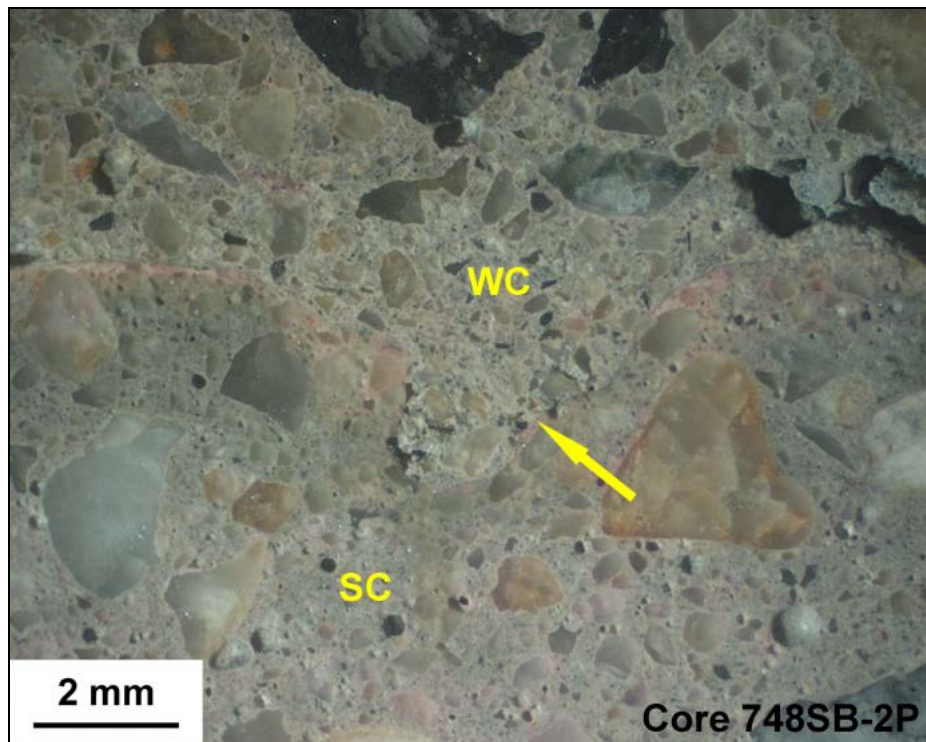
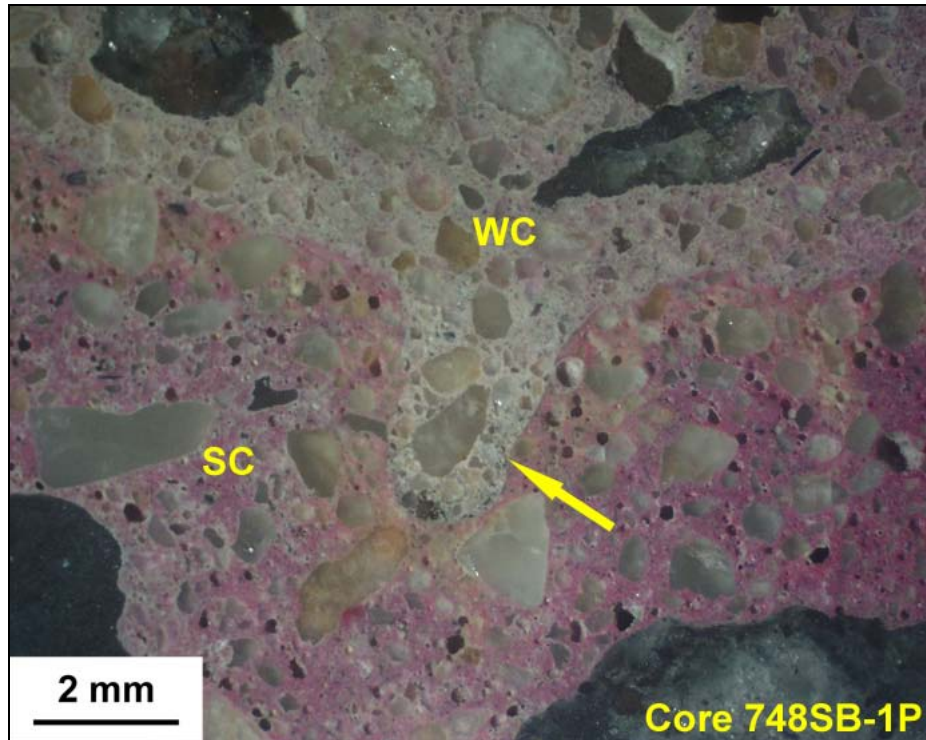
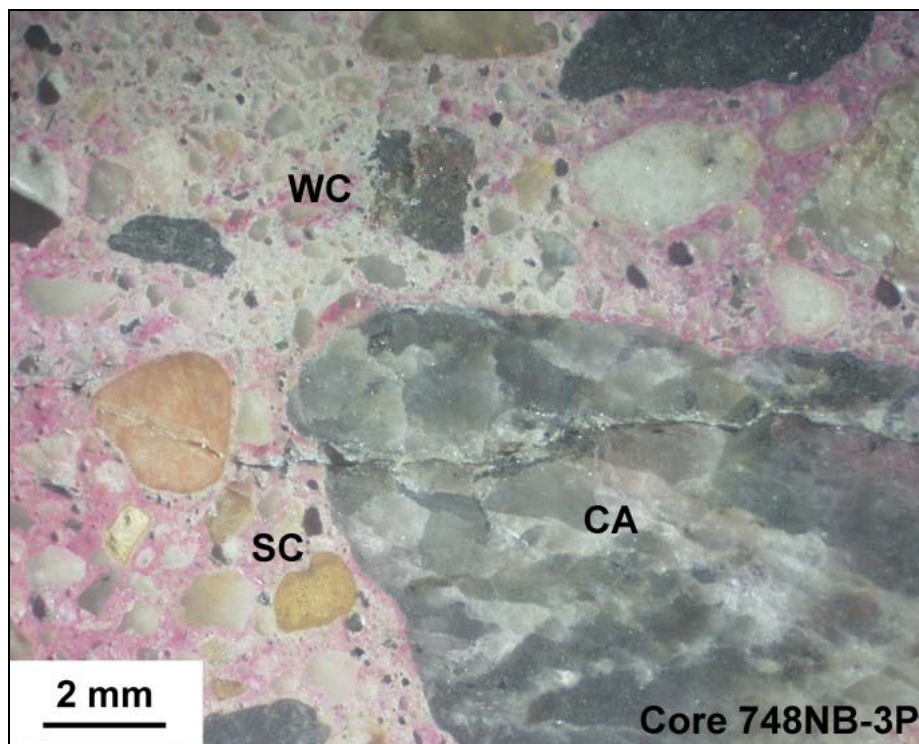
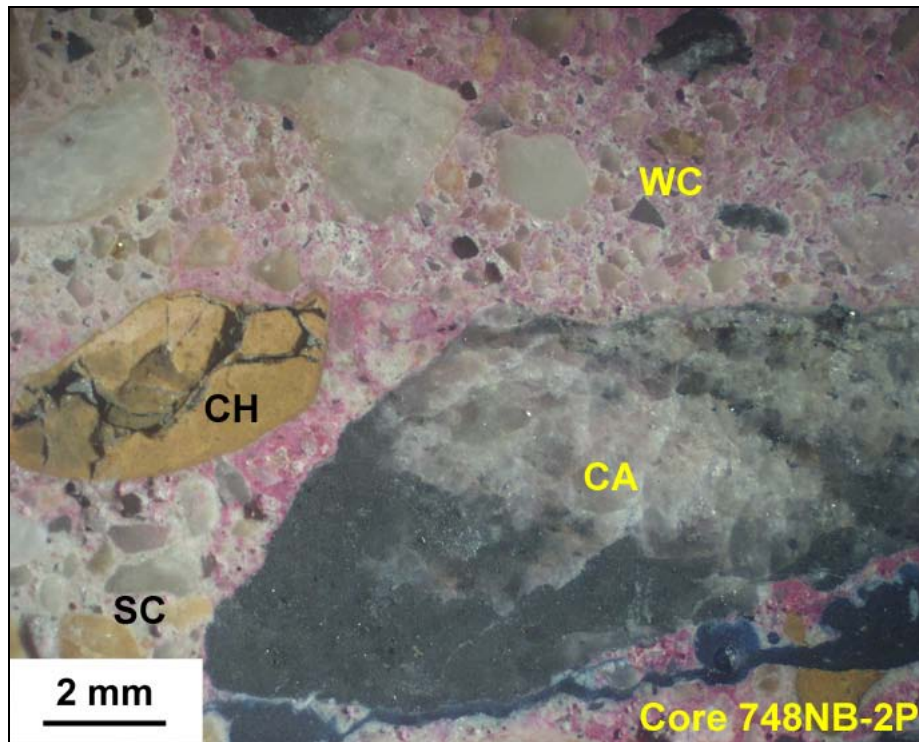


Figure 16 (cont'd.): PPL photomicrographs illustrating the tight contacts between wear course (WC) and structural concrete (SC) in six of the eleven core samples.



**Figure 17:** Reflected light photomicrographs. In two of the cores, thin “fingers” of wear course (WC) appear plastically embedded in the structural concrete (SC). These features are similar to those shown in plane polarized light for Core 748SB-2P in Figure 16.



**Figure 18:** Reflected light photomicrographs of Cores 748NB-2P and 748NB-3P. In these two samples, coarse aggregate grains (CA) are truncated at the top of the structural concrete (SC). Wear course material (WC) is placed directly over the broken aggregate surface. This type of texture is suggestive of some type of scarification process. A chert grain (CH) appears broken as well in one of the samples. However in this case, the grain is actually below the surface and the cracking is due to alkali-silica reaction.



**Figure 19:** The 758 cores do not contain wear course material and the upper surfaces of the structural concrete are apparently exposed to the environment. Grooving is only applied to the surface of the concrete represented by Core 758G-1P. Weathering and erosion has resulted in the low to moderate relief exposure of coarse aggregate along the surface (CA). However, this is minimal in Core 758E-1P.

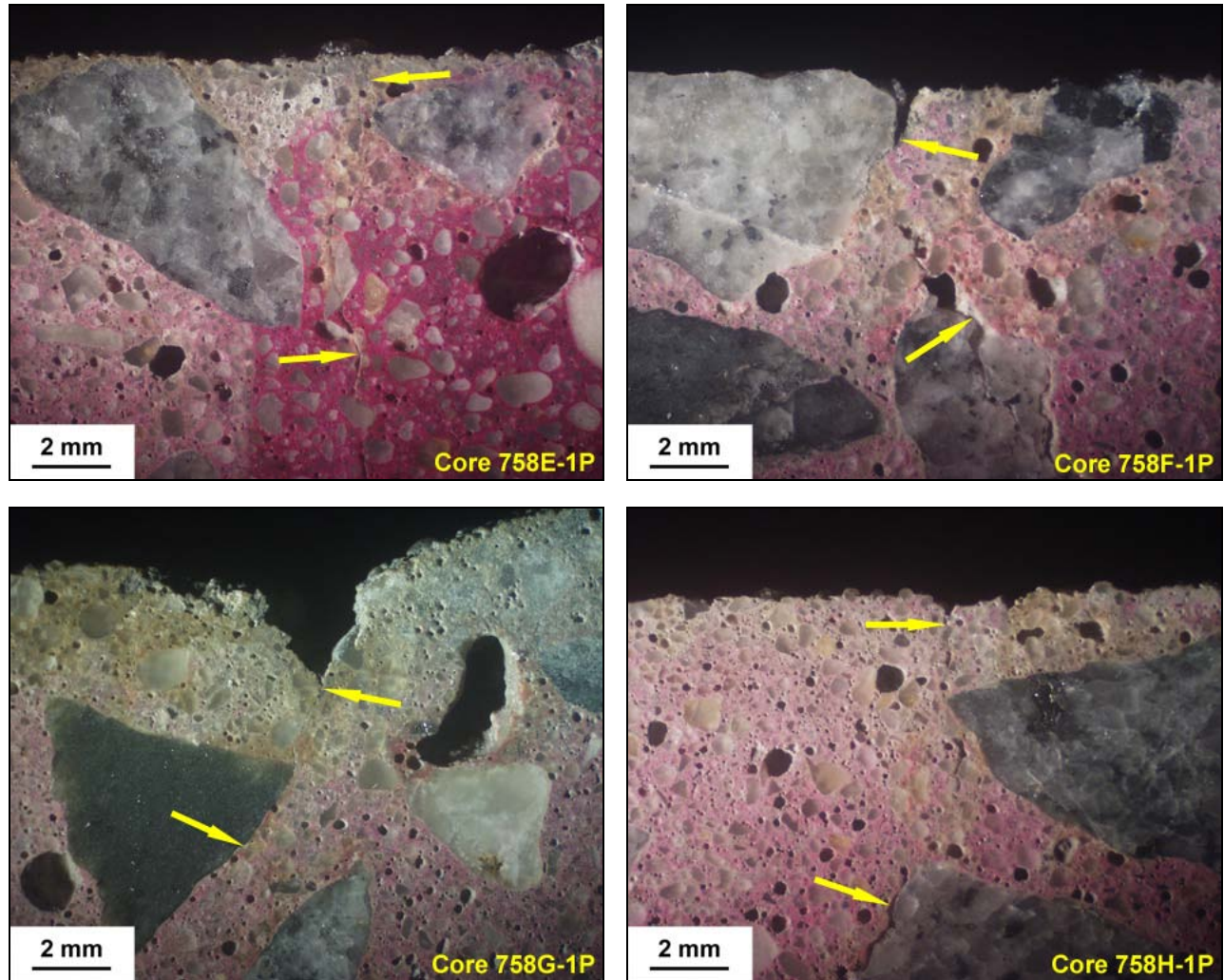


**Figure 20:** Reflected light photomicrographs of the 758 cores. Minor vertical crazing cracks (arrows) extend downward from the upper surfaces to relatively short depths. These hairline cracks are considered innocuous.

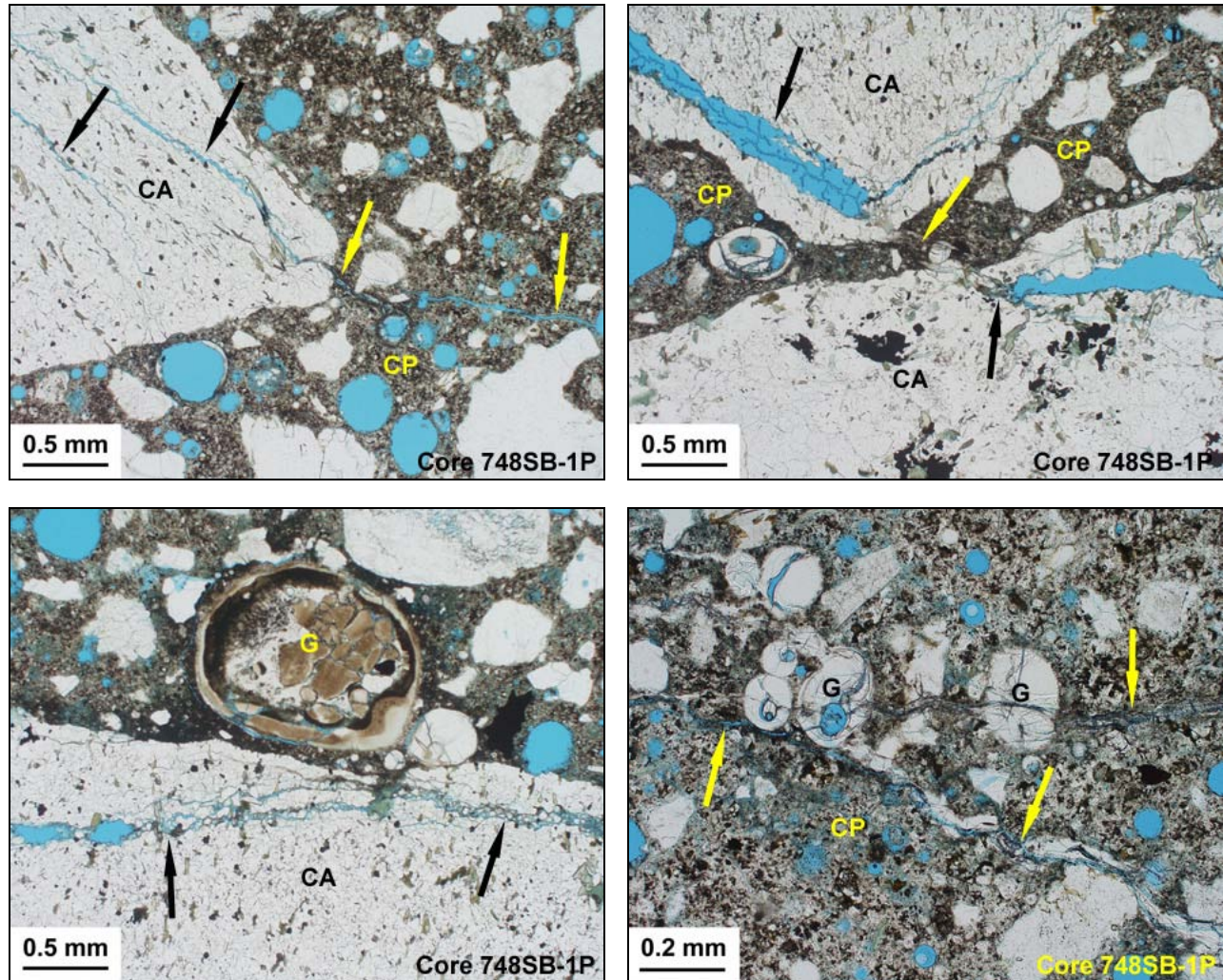


**Figure 21:** Cores 748SB-1P and 748SB-2P exhibit the most well-developed alkali-silica reaction even if the reaction is only in its early stages. Examples illustrating the microstructure of the reaction are shown for Core 748SB-1P in these PPL photomicrographs. In the upper two images, the black arrows indicate reaction cracks within coarse aggregate grains (CA). The yellow arrows indicate where these have propagated into the adjacent cement paste (CP). ASR gel plugs are found at the periphery of the reactive stone. The reactive grain in the left image is a granofels. The cracks span a granofels (upper) and a granitoid particle (lower) in the right image. Another granofels coarse aggregate grain (CA) is shown in the lower left PPL image. In this case, the reaction cracking parallels the aggregate surface (arrows). A deposit of ASR gel (G) is present adjacent to the stone. In the lower right image, the arrows indicate reaction cracks transecting the cement paste. These are lined with ASR gel and some of this gel (G) has also deposited in the air-voids transected by the cracks.

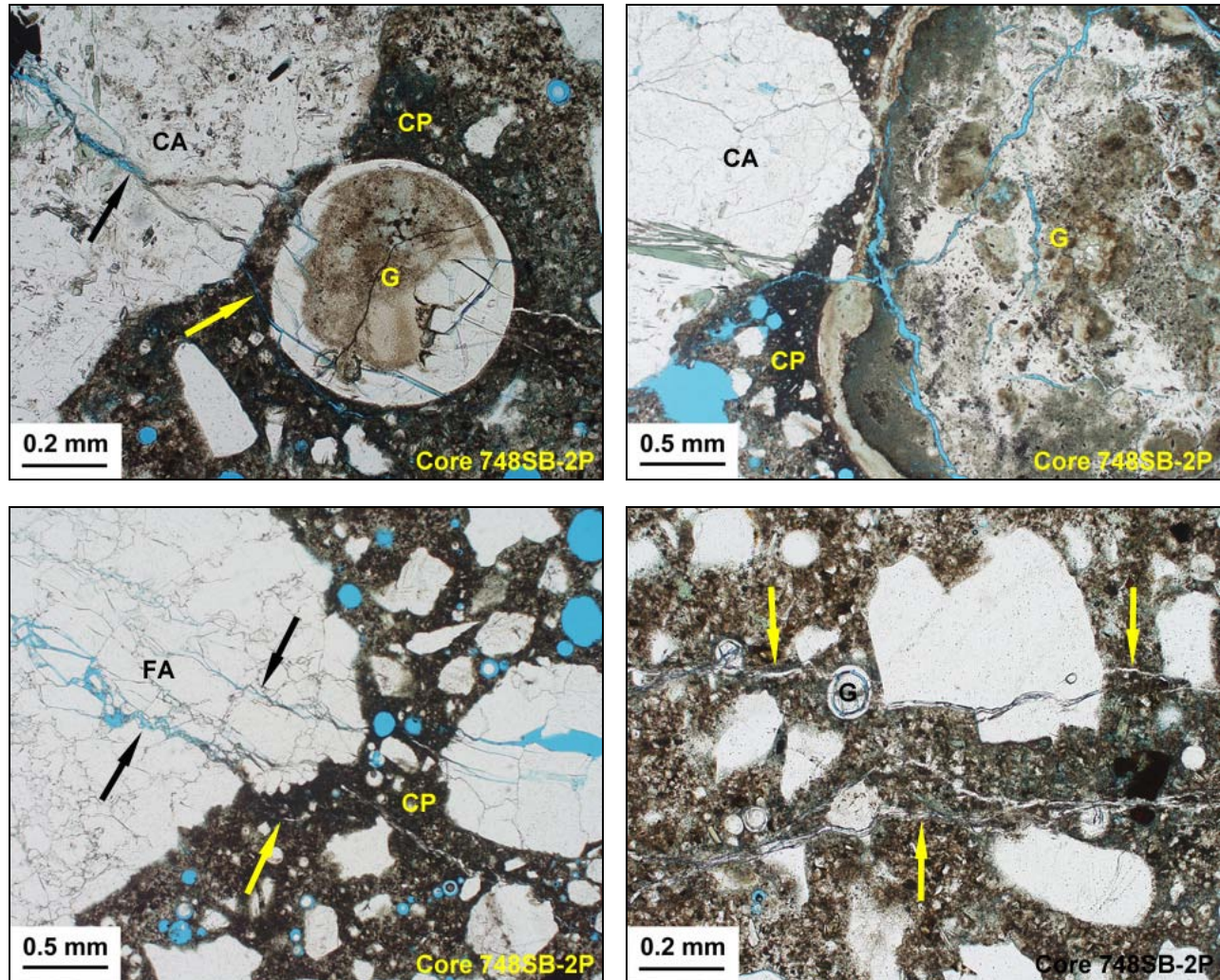


**Figure 22:** These PPL photomicrographs illustrate examples of the ASR microstructure in Core 748SB-2P. As described in the last figure, this core is one of the two exhibiting the most well-developed, even if early-stage alkali-silica reaction. In the upper two images, the black arrows (where present) indicate reaction cracks within coarse aggregate grains (CA). The yellow arrows indicate where these have propagated into the adjacent cement paste (CP). Most of the reaction has occurred within the granitoid lithologies for this sample. It is also more common in this sample for larger “blobs” of reaction gel (G) to be found at the site of reactive stone. (Lower left) In this image, the black arrows indicate reaction cracks within a strained quartzite fine aggregate grain (FA). The yellow arrow indicates where one of these has propagated into the adjacent cement paste (CP). (Lower right) The arrows indicate ASR reaction cracks transecting the paste some short distance from a reaction site. A small gel deposit (G) is found in an air-void transected by one of the reaction cracks.

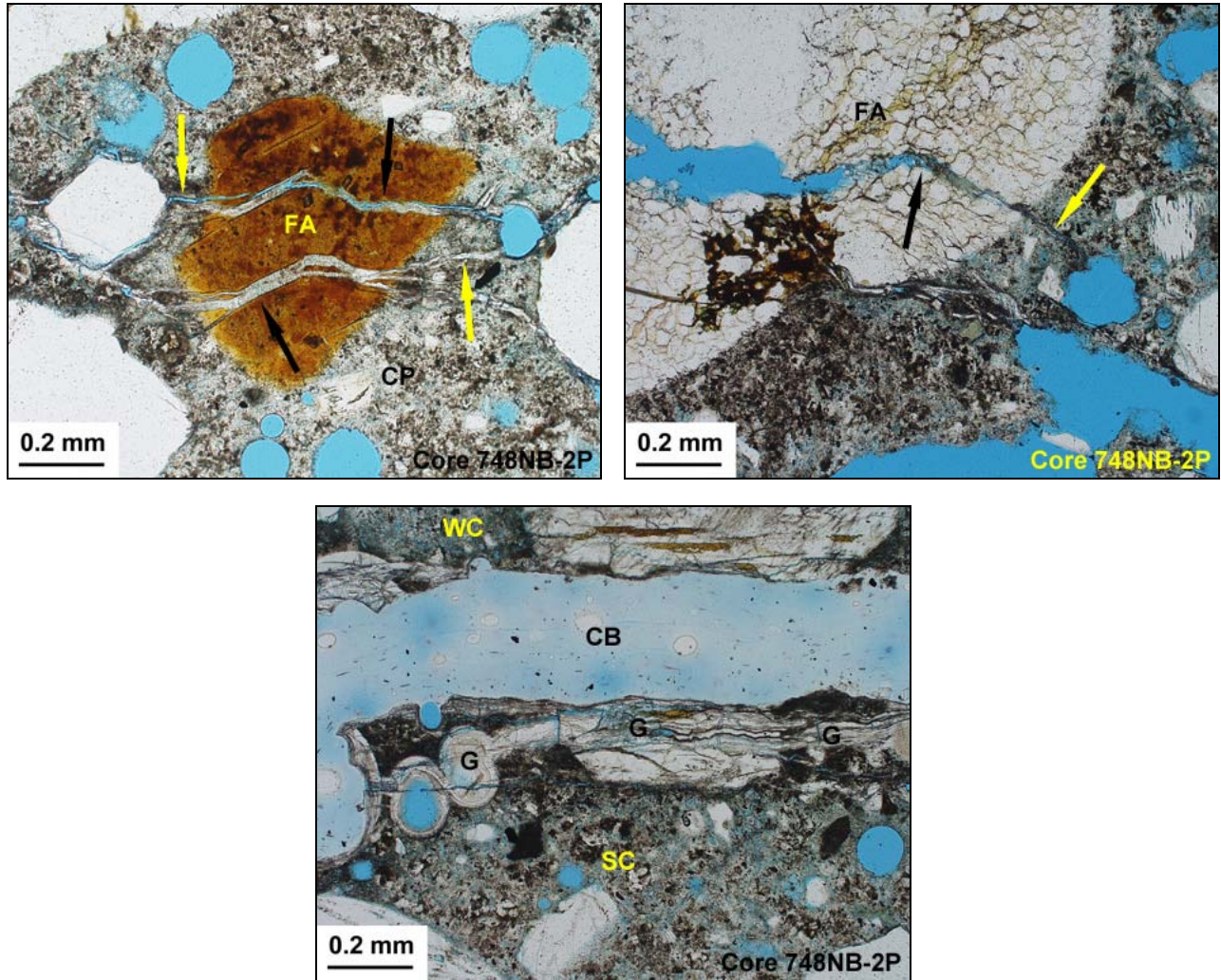


**Figure 23:** Early stage alkali-silica reactions are detected in Core 748NB-2P but these are limited to a narrow horizon at the top of the structural concrete. These PPL photomicrographs illustrate some of the microstructures identified. In the upper two images, the black arrows indicate reaction cracks within fine aggregate grains (FA). The yellow arrows indicate where these have propagated into the adjacent cement paste (CP). The reactive grain at left consists of chert and the particle at right is a strained quartzite. (Lower image) A higher magnification image illustrates a gel-lined microcrack (G) that is found just below the core break (CB) between the wear course (WC) and the structural concrete (SC).

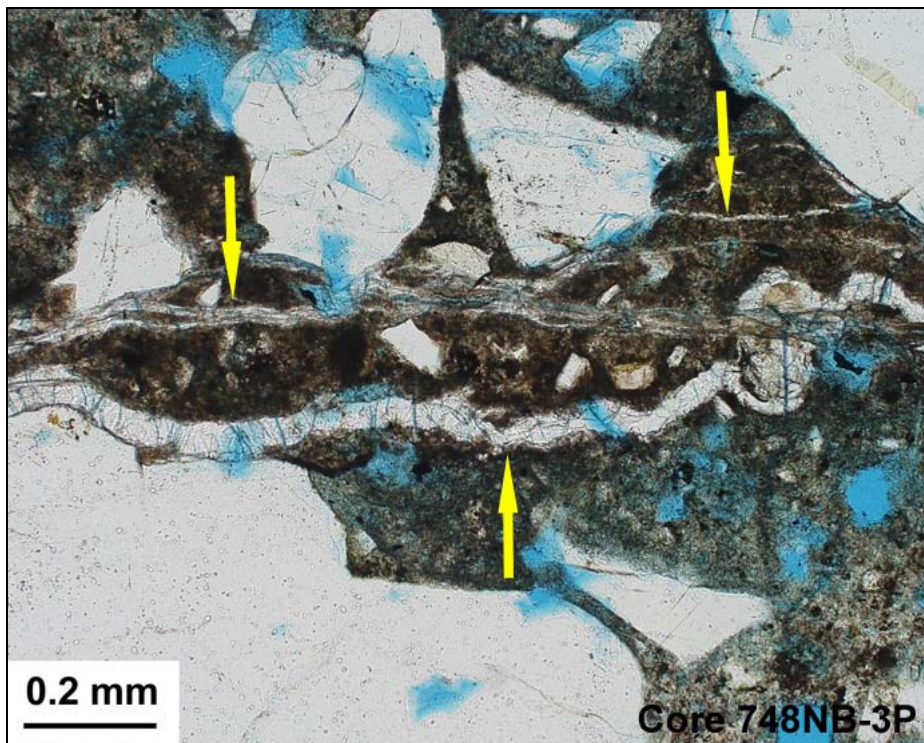
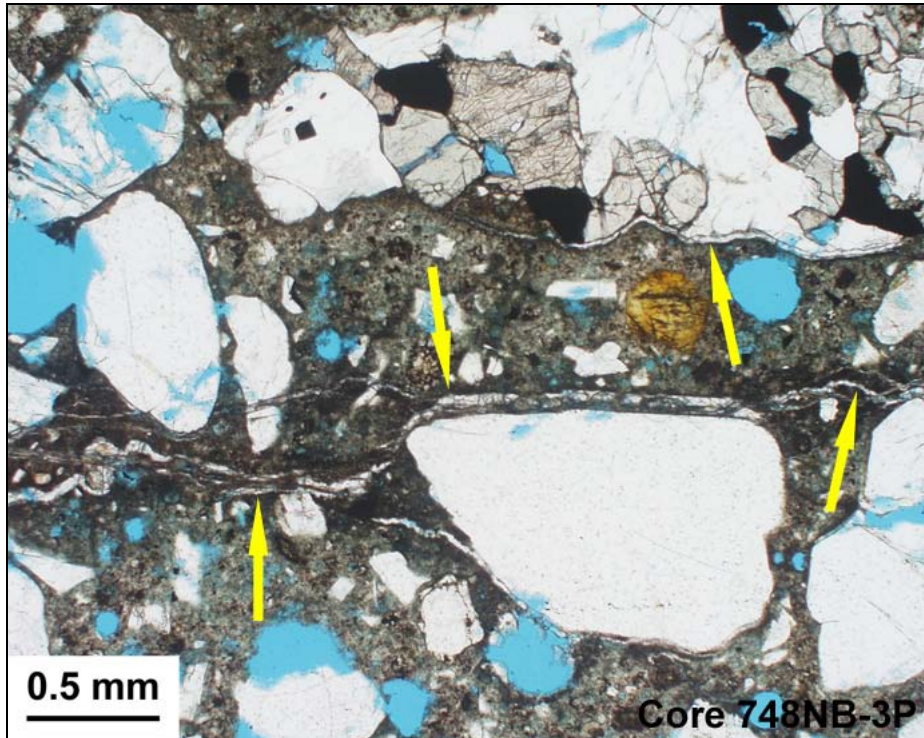


**Figure 24:** Early stage alkali-silica reactions are detected in Core 748NB-3P but these are only found within millimeters of the upper structural concrete surface. In these two PPL images, the arrows indicate microcracks lined with ASR gel that are found within this thin horizon. No positive association is identified with any particular aggregate type.

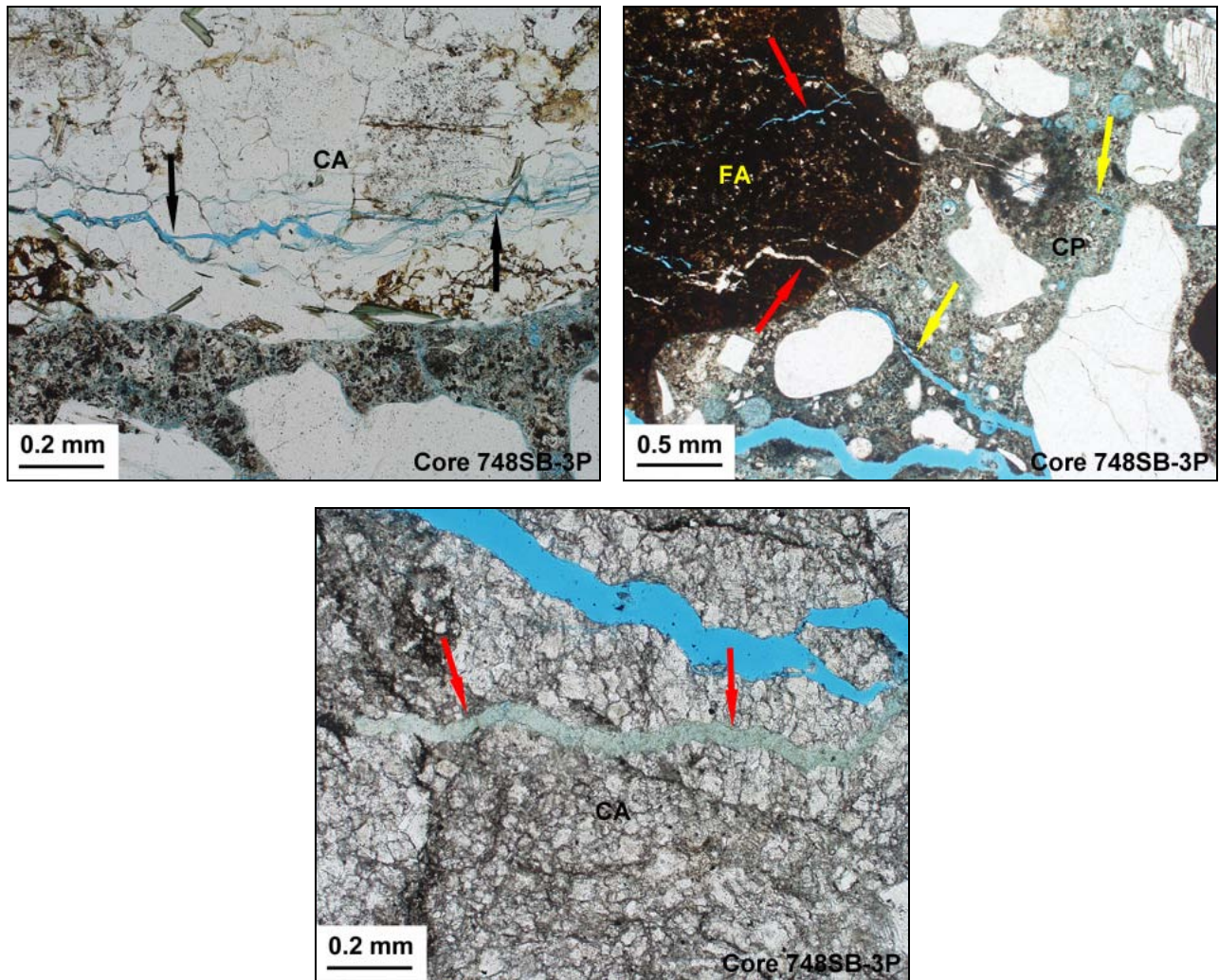


**Figure 25:** Only traces of alkali-silica reaction are detected in Core 748SB-3P and examples are shown in these PPL photomicrographs. (Upper left) The arrows indicate a microcrack that parallels a coarse aggregate surface (CA). The grain is a granitoid. (Upper right) The red arrows indicate reaction cracks within a chert fine aggregate (FA). The yellow arrows indicate where these have propagated into the adjacent cement paste (CP). (Lower) The arrows indicate a microcrack lined with a hydrous silica gel. This is a precursor to the ASR reaction. Surprisingly, this is found within a dolostone particle.

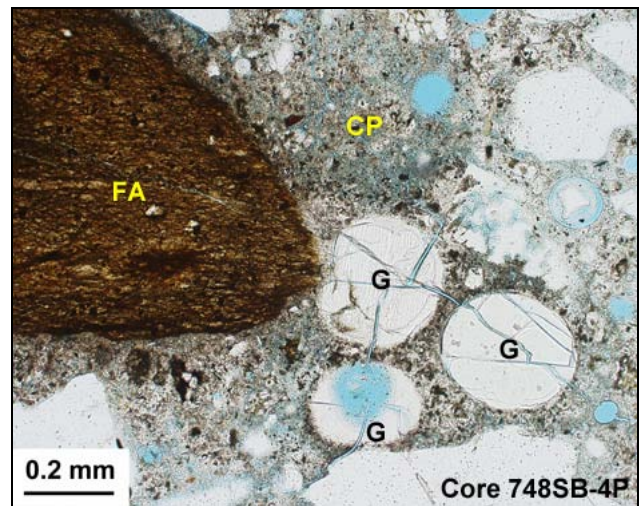
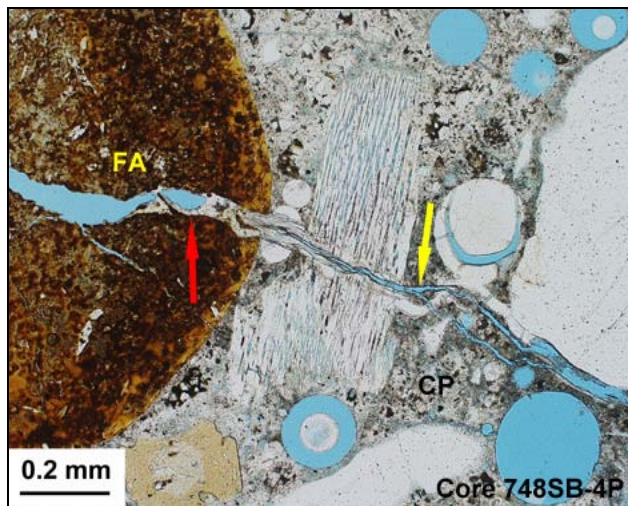
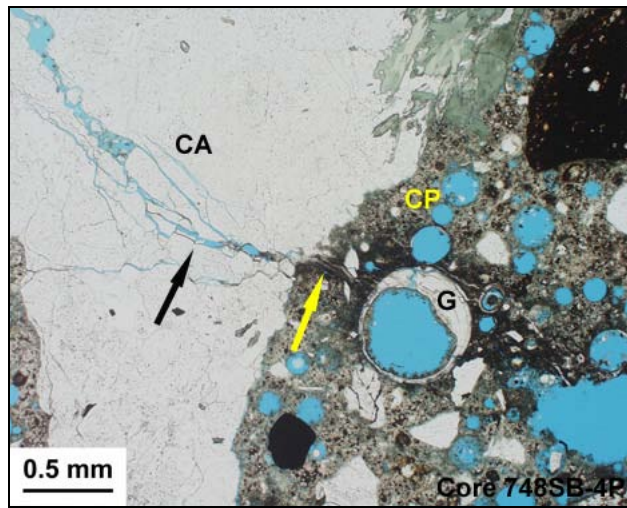


**Figure 26:** Early stage alkali-silica reactions are detected in Core 748SB-4P but these are limited to a narrow horizon at the top of the structural concrete. In the upper image, the black arrow indicates a reaction crack within a granitoid coarse aggregate grain (CA). The yellow arrow indicates where this has propagated into the adjacent cement paste (CP). In the lower two images, the reactive materials are chert fine aggregate particles. At lower left, a gel plug is present at the periphery of the grain. At lower right reaction gel (G) has deposited within adjacent entrained air-voids.

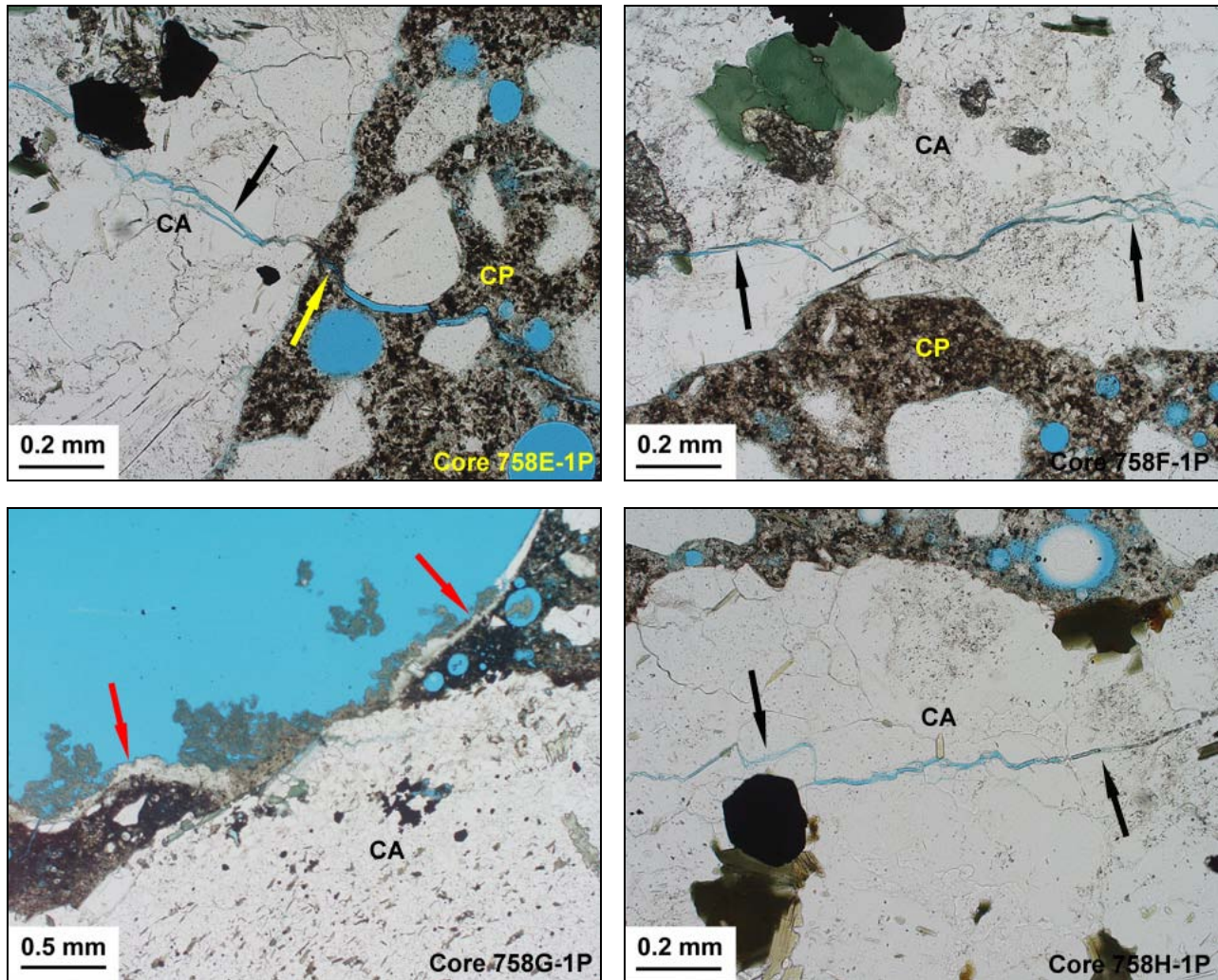


**Figure 27:** Evidence for ASR reaction is negligible in the 758 cores. Some of this minimal evidence is highlighted in these PPL photomicrographs. (Upper left) A granitoid coarse aggregate (CA) has a thin reaction crack (black arrow) that has propagated a short distance into the adjacent cement paste (CP and yellow arrow). (Upper right and lower right) The arrows indicate minor reaction cracks within coarse aggregate particles (CA). Granitoid is again the reactive stone. (Lower left) The arrows indicate the lining of a soft ASR gel deposit that was present adjacent to a granofels coarse aggregate particle (CA). The softer portion of the gel was likely eroded away during initial saw-cutting.

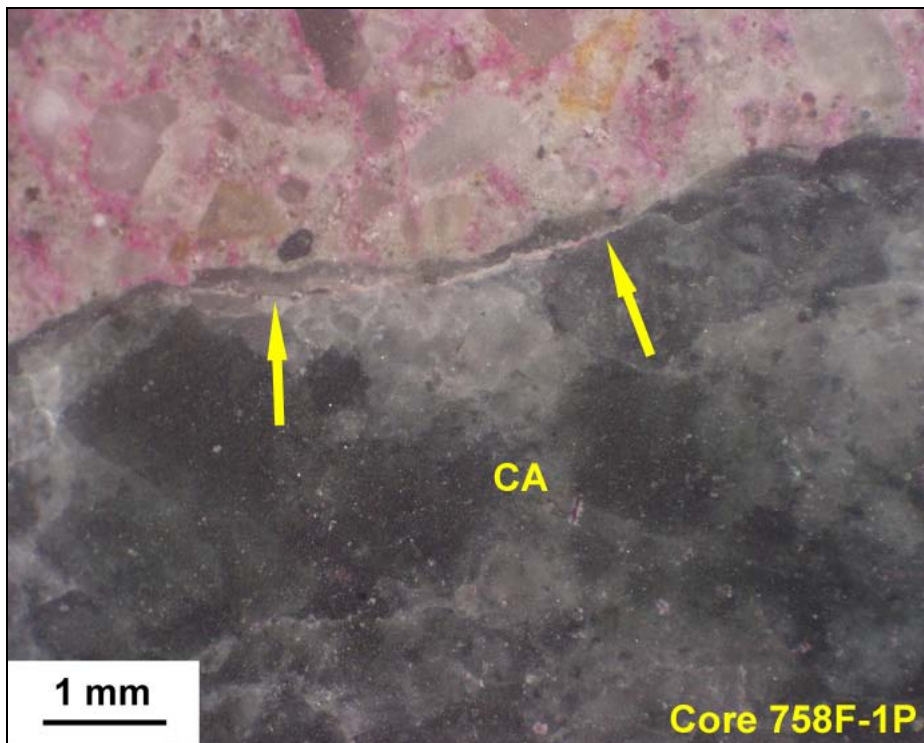
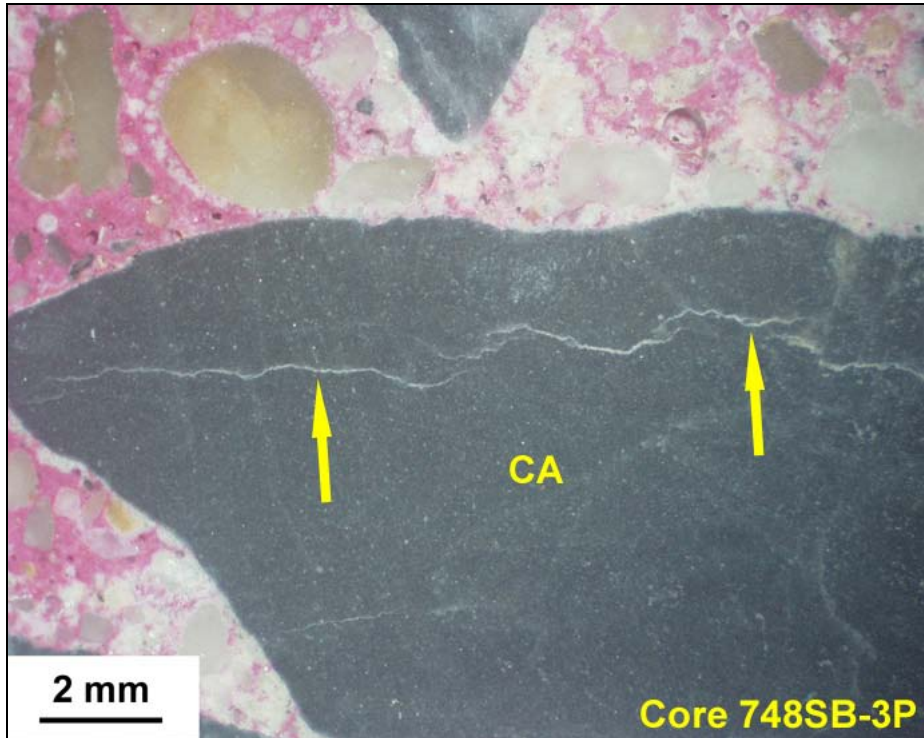


**Figure 28:** Reflected light photomicrographs taken of honed concrete core sections. The arrows indicate very fine internal microcracks within granitoid stone. While no ASR gel is found in association with these trace cracks, there are interpreted to represent a very early stage reaction.

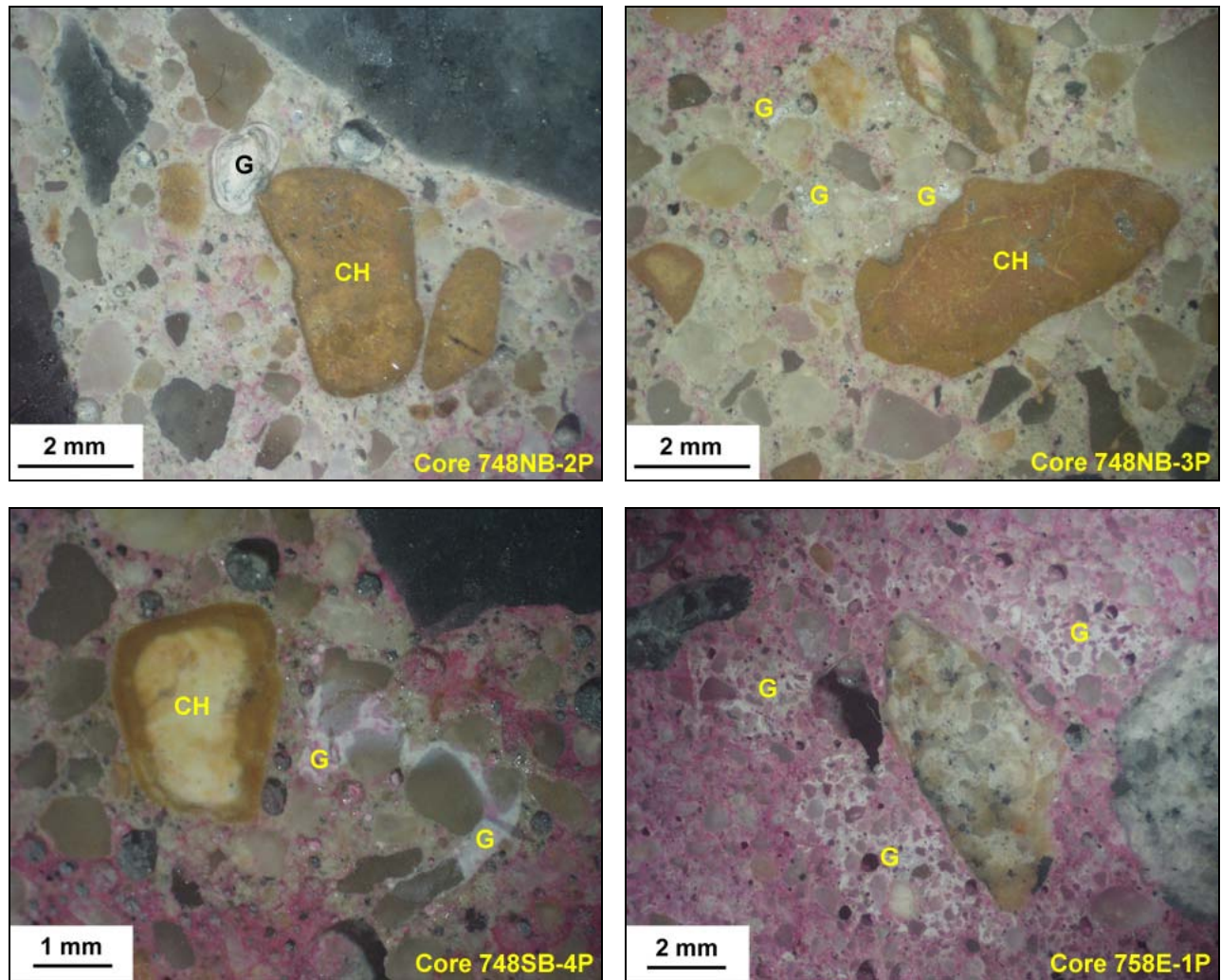


**Figure 29:** Reflected light photomicrographs taken of honed concrete core sections. A deposit of ASR gel (G) is shown adjacent to a reactive chert particle (CH) for Core 748NB-2P. In some cases, discrete gel deposits had not formed previously but rather exuded from the paste near reactive sand and stone after cutting and polishing the core section. Examples of this are shown in the other three images. This is not uncommon where the fine aggregate contains ferruginous chert (CH). In the image for Core 758E-1P, the source of the gel deposit appears to be outside the plane of the thin section.

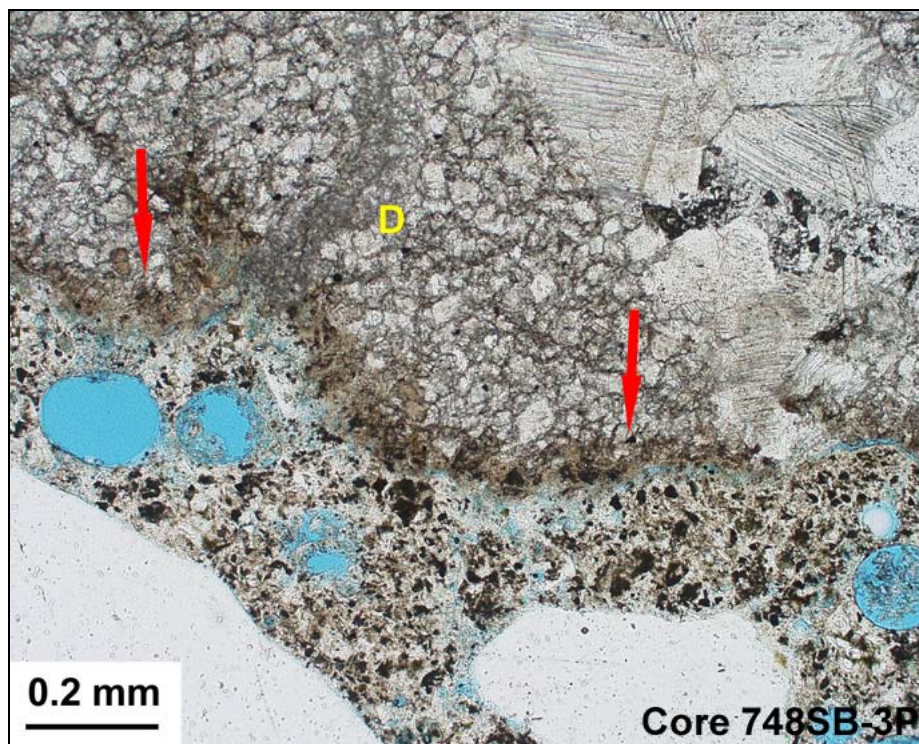
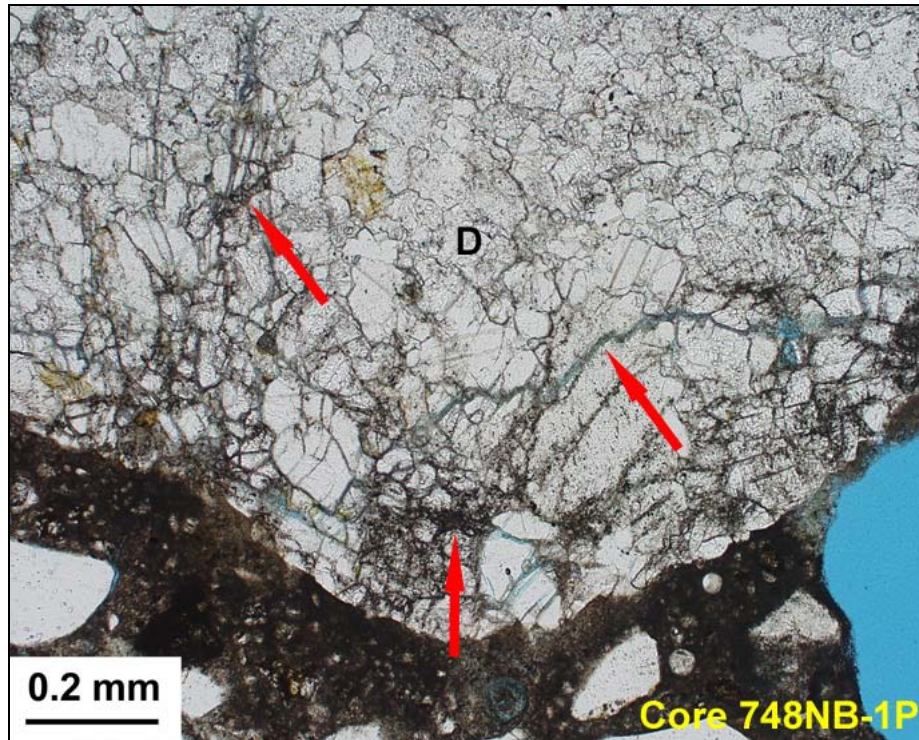


**Figure 30:** Evidence for alkali-carbonate reaction is detected in the dolomite aggregate (D) present in Cores 748NB-1P and 748SB-3P. In these PPL images, the arrows indicate corroded zone representing a dedolomitization reaction at the grain periphery. Microcracking along individual dolomite grain boundaries is shown for Core 748NB-1P. A continuous reaction rim of affected dolomite is shown for Core 748SB-3P.

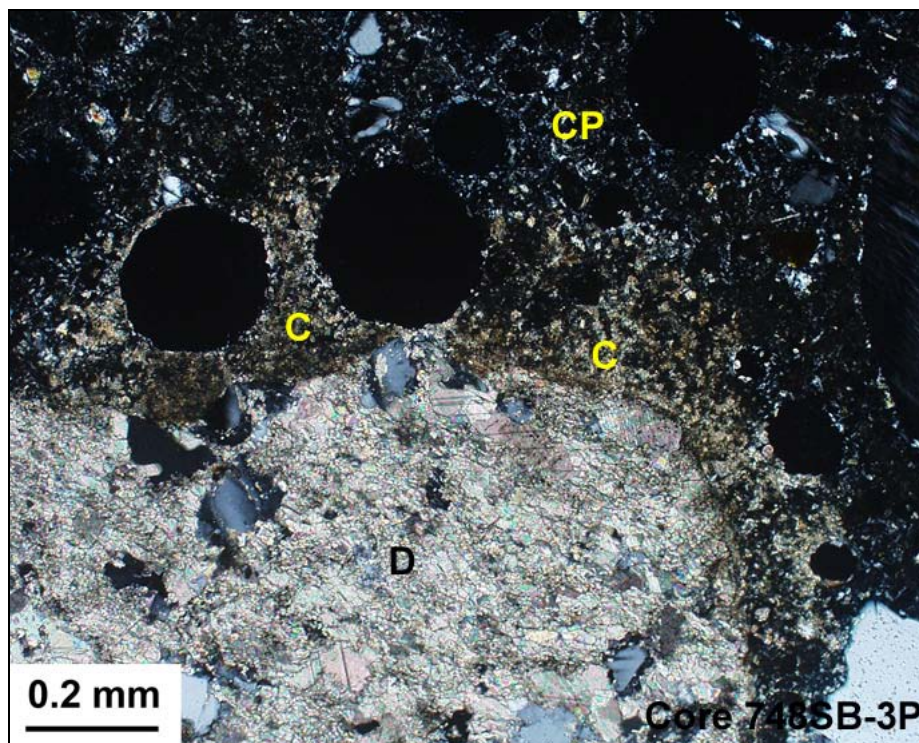
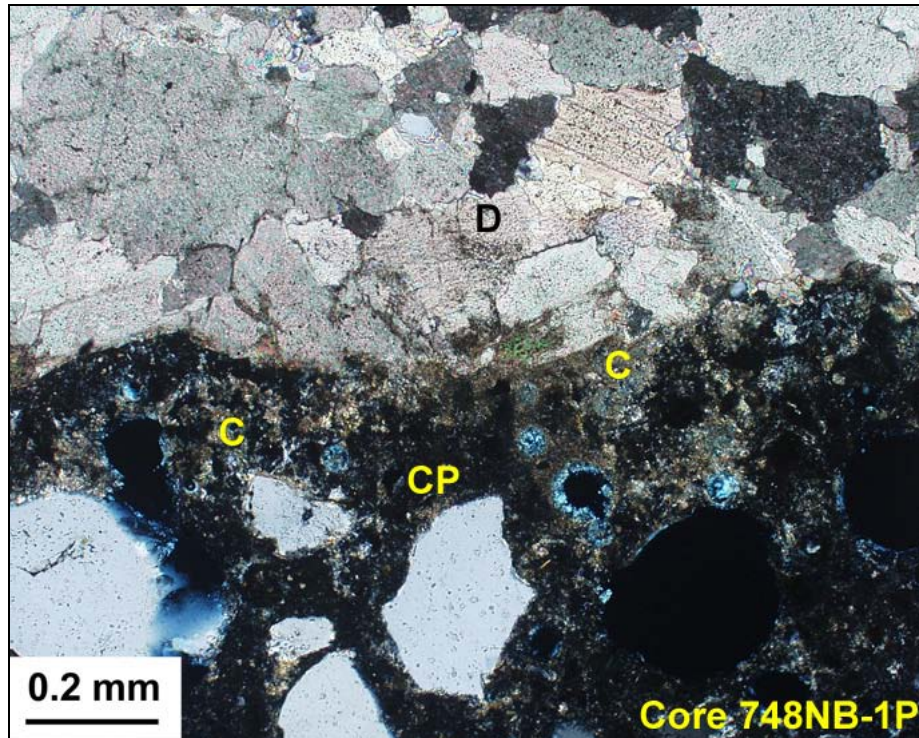


**Figure 31:** The dedolomitization reaction is also evidenced by a “bloom” of carbonation that emanates from the dolostone aggregate (D). Note the golden-color of the carbonated paste juxtaposed against the normal dark color of the cement paste (CP) in these XPL photomicrographs.

## PETROGRAPHIC EXAMINATION REPORT

---

<b>Client:</b>	Pennoni Associates, Inc.	<b>Client ID:</b>	PENN003
<b>Project:</b>	I-95 Viaduct Project	<b>Report #:</b>	SL0845-03
<b>Location:</b>	Delaware	<b>Dates Received:</b>	12/15/14, 01/07/15, 01/14/15
<b>Sample Type:</b>	Concrete cores	<b>Report Date:</b>	03/26/15
<b>Delivered by:</b>	Client (M. Padula)	<b>Petrographer:</b>	J. Walsh
		<b>Analyst:</b>	M. Pattie

---

**Page 1 of 60**

### Report Summary

- This report presents the results of petrographic examination and air-void analysis on ten concrete core samples taken from viaduct structures along I-95 near Wilmington, DE.
- All examined concrete is similar in composition and appears to represent a single mix design. In all cases, the material is a normal weight, portland cement concrete with no supplementary cementitious materials. Original water to cement ratios are estimated to have been moderate within the mid to high 0.4's. Cores 748N2-1P, 748N3-1P, and 749-1P are estimated at the higher end of this range as suggested by slightly higher paste permeabilities. Cores 748NB-4P, 750-1P, and 758-1P are estimated at the lower end of this range. All of the cores exhibit air structures consistent with intentional air-entrainment and most are within a range that meets industry standards for adequate freeze-thaw protection. One core is deficient in fine air. Four cores have lower specific surfaces and/or slightly higher spacing factors. Three samples have air contents that may be considered a bit excessive and this could have a modest impact on strength.
- The coarse aggregate in all samples is a natural gravel with gradations ranging from No. 57 to No. 67. The material includes a variety of sedimentary clastic rock types, cherts, and minor granites. The fine aggregates appear identical and are identified as coarse-grained natural quartz sands with several percent ferruginous chert.
- All concrete materials are well mixed, cast, and consolidated and no significant workmanship deficiencies are identified in any core sample. There is a tendency for there to be a higher content of fine entrapped air-voids but these are relatively fine and evenly distributed throughout any core in which they are detected. Cores containing higher entrapped air include 748N2-1P, 748N2-2P, 748S-3P, and 758-1P. It is assumed that the concrete was designed with the estimated moderate water to cement ratio and the mixtures were not overwatered at the job site. A minor deficiency is the migration of bleed water and its partial concentration within the paste in Core 748S-1P. Denser paste is adhered to coarse aggregate surfaces in Cores 748NB-4P and 750-1P but this does not appear to have been the result of inappropriate retempering.
- The concrete represents moderate quality mixtures suitable for many normal-duty, non-aggressive service environments. Some of the coarse aggregate is somewhat porous and might be subject to expansion and cracking during saturated freezing events. However, only minor microcracking is detected in some of the stone with no extension into the surrounding cement paste. The chert present in significant quantity should be considered more susceptible to alkali-silica reaction than other coarse aggregate types identified in this study. Nonetheless, only trace level reactions are detected in this group of cores. The only cracking related to alkali-silica reaction is found within the uppermost 2" of Core 749-1P.
- The reactions have not compromised the integrity of the concrete and no imminent threat is suggested by the existing conditions. Though no mitigating factors are identified, the concrete may remain provisionally stable over the course of a normal life cycle. However, this cannot be guaranteed and continued reaction may proceed at a relatively slow rate.
- A more detailed discussion of these findings may be found in the "Petrographic Findings and Discussion" section on page 3 of this report.

**1. Introduction**

On December 15, 2014, and January 7 and 14, 2015, Highbridge received a total of twenty-seven (27) concrete core samples from Mr. Michael Padula of Pennoni Associates, Inc. reported to have been taken from viaduct structures along I-95 near Wilmington, DE. At the client’s request, testing is performed on the structural layers of all core samples. No testing is requested for any wear courses present. For each sample, petrographic examination is requested to identify constituents, evaluate condition, and investigate the potential causes of any observed distress. No specific emphasis is requested and a general comprehensive examination is performed. Quantitative air-void analysis is also requested for the same samples.

Results for ten of the core samples are presented in this report. The samples chosen to be included are those containing natural gravel coarse aggregate. Results for other sample batches are presented under separate cover. This report presents the results for the following cores:

748NB-4P	748S-1P	749-1P
748N2-1P	748S-2P	750-1P
748N2-2P	748S-3P	758-1P
748N3-1P		

**2. Methods of Examination**

The petrographic examination is conducted in accordance with the standard practices contained in ASTM C856. Data collection is performed by a degreed geologist who by nature of his/her education is qualified to operate the analytical equipment employed. Analysis and interpretation is performed or directed by a supervising petrographer who satisfies the qualifications as specified in Section 4 of ASTM C856.

Air-void analysis is performed in accordance with the point-count method of ASTM C457. Component point counts are performed on hand-lapped concrete slabs sliced parallel to the core axis. The analysis is performed at a magnification of 75x on a Bausch and Lomb Stereozoom microscope and a dedicated cross-slide table machined to produce 0.05 inch translations per count. Air-void percentages are presented as those whose two-dimensional cross sectional diameter are less than or greater than one millimeter. The one millimeter diameter is considered a reasonable distinction between voids that are entrained and those that are entrapped in concrete that has been air-entrained. It should be understood that this threshold is somewhat arbitrary.

**3. Standard of Care**

Highbridge has performed its services in conformance with the care and skill ordinarily exercised by reputable members of the profession practicing under similar conditions at the same time. No other warranty of any kind, expressed or implied, in fact or by law, is made or intended. Interpretations and results are based strictly on samples provided and/or examined.

**4. Confidentiality**

This report presents the results of laboratory testing requested by the client to satisfy specific project requirements. As such, the client has the right to use this report as necessary in any commercial matters related to the referenced project. Any reproduction of this report must be done in full. In offering a more thorough analysis, it may have been necessary for Highbridge to describe proprietary laboratory methodologies or present opinions, concepts, or original research that represent the intellectual property of Highbridge Materials Consulting and its successors. These intellectual property rights are not transferred in part or in full to any other party. Presentation of any or all of the data or interpretations for purposes other than those necessary to satisfy the goals of the investigation are not permitted without the express written consent of the author. The findings may not be used for purposes outside those originally intended. Unauthorized uses include but are not limited to internet or electronic presentation for marketing purposes, presentation of findings at professional venues, or submission of scholarly articles.

**5. Petrographic Findings and Discussion**

**5.1 - General Summary**

This report presents the results of petrographic examination and air-void analysis on ten concrete core samples taken from viaduct structures along I-95 near Wilmington, DE (Fig. 1). The study includes only the substrate concrete layers and not the 1.2” to 3.1” thick wear courses adhered to all of the samples. All examined concrete is similar in composition and appears to represent a single mix design. Minor variations in the original mixture qualities and secondary reactions are summarized in Table 5.1a below.

**Table 5.1a: Highlights of Concrete Mix Variations**

Core ID	Air <sup>1</sup>	Relative paste permeability <sup>2</sup>	Alkali-aggregate reaction
748NB-4P		Lower	Trace ACR in dolostone. Trace ASR.
748N2-1P	Low SS	Higher	Trace ASR.
748N2-2P	Low SS		
748N3-1P		Higher	Trace ASR.
748S-1P	Low air, Low SS, High SF		Trace ASR.
748S-2P			Trace ASR.
748S-3P	High air, Low SS		Trace ASR.
749-1P		Higher	Early-stage ASR limited to the uppermost 2”
750-1P	High air	Lower	
758-1P	High air	Lower	Trace ASR.

Notes:

1. SS = specific surface, SF = spacing factor.
2. Paste permeabilities do not vary greatly. Reported differences are relatively subtle.

In all cases, the material is a normal weight, portland cement concrete with no supplementary cementitious materials. Original water to cement ratios are estimated to have been moderate within the mid to high 0.4’s. Cores 748N2-1P, 748N3-1P, and 749-1P are estimated at the higher end of this range as suggested by slightly higher paste permeabilities. Cores 748NB-4P, 750-1P, and 758-1P are estimated at the lower end of this range. All of the cores exhibit air structures consistent with intentional air-entrainment and most are within a range that meets industry standards for adequate freeze-thaw protection. One core is deficient in fine air. Four cores have lower specific surfaces and/or slightly higher spacing factors. Three samples have air contents that may be considered a bit excessive and this could have a modest impact on strength. The coarse aggregate in all samples is a natural gravel with gradations ranging from No. 57 to No. 67. The material includes a variety of sedimentary clastic rock types, cherts, and minor granites. The fine aggregates appear identical and are identified as coarse-grained natural quartz sands with several percent ferruginous chert.

All concrete materials are well mixed, cast, and consolidated and no significant workmanship deficiencies are identified in any core sample. There is a tendency for there to be a higher content of fine entrapped air-voids but these are relatively fine and evenly distributed throughout any core in which they are detected. Cores containing higher entrapped air include 748N2-1P, 748N2-2P, 748S-3P, and 758-1P. It is assumed that the concrete was designed with the estimated moderate water to cement ratio and the mixtures were not overwatered at the job site. A minor deficiency is the migration of bleed water and its partial concentration within the paste in Core 748S-1P. Denser paste is adhered to coarse aggregate surfaces in Cores 748NB-4P and 750-1P but this does not appear to have been the result of inappropriate retempering.

The concrete represents moderate quality mixtures suitable for many normal-duty, non-aggressive service environments. Some of the coarse aggregate is somewhat porous and might be subject to expansion and cracking during saturated freezing events. However, only minor microcracking is detected in some of the stone with no extension into the surrounding cement paste. The chert present in significant quantity should be considered more susceptible to alkali-silica reaction than other coarse aggregate types identified in this study. Nonetheless, only trace level reactions are detected in this group of cores. The only cracking related to alkali-silica reaction is found within the uppermost 2” of Core 749-1P. The reactions have not compromised the integrity of the concrete and no imminent threat is suggested by the existing conditions. Though no mitigating factors are identified, the concrete may remain provisionally stable over the course of a normal life cycle. However, this cannot be guaranteed and continued reaction may proceed at a relatively slow rate.

## 5.2 - Coarse Aggregate Materials

All cores contain a siliceous natural gravel interpreted to have been sourced from a common location. Nine of the cores have aggregate contents estimated at 35-40% by hardened concrete volume. Core 748S-2P has aggregate estimated at 30-35%. The natural gravel contains a rather wide assemblage of rock types including mostly sedimentary clastic grains with minor igneous or meta-igneous components. Since the assemblage is so varied, each grain type is not necessarily captured in the thin sections for each sample. However, visual assessment and low-powered stereomicroscopy suggests that the stone types are similar throughout all ten cores (Fig. 2). The assemblage is discussed based on observations taken from the full group of samples rather than listed separately (and arbitrarily) for each core sample.

Sedimentary clastic grains predominate and include quartz arenite, subarkosic arenite, quartz wacke, and arkosic wacke (if altered feldspar is counted as feldspar rather than matrix). "Redbed" sedimentary grains are also found as a lesser component. Slate and argillite are minor. Relatively few of the quartz arenites are exceptionally pure quartzites with originally rounded sand grains and a fully cemented texture composed of crystallographically continuous quartz overgrowths (Fig. 3). More commonly, the arenites are fine to medium-grained sandstones with compacted, seriate grain boundaries and evidence for mild to moderate crystal plastic strain (Fig. 4). Minor feldspar and clay or micaceous matrix are also included. At higher feldspar contents, the grains grade into subarkosic arenites. The wackes contain micaceous matrix and range from equigranular, medium-grained sandstones to fine quartz sandstones rich in heavily sericitized feldspar and elongate, compacted matrix (Figs. 5 and 6). In some cases, wackes are found interlayered with argillite and siltstone (Fig. 9). Few of this group of clastics exhibits open porosity detectable at the scale of the light microscope. However, many grains are clearly somewhat water absorptive when tested simply by applying water droplets. The porosity in these grains is clearly submicroscopic and either occurs within the more clay-rich matrix or at grain boundaries.

"Redbeds" or iron-rich clastics are much less abundant. These include fine-grained sandstones or siltstones with interstitial iron oxide (Fig. 7). Ironstone grains are also detected some of which include sparsely distributed sand or silt. Some are also chert or chalcedonic (Fig. 8). The iron-rich clastics tend to exhibit more open porosity at the interstices between sand grains particularly in the finer-grained varieties. All also exhibit a notable absorptivity when tested with the application of water droplets on exposed grain surfaces.

Associated with the clastic sediments but worthy of separate discussion is the presence of chert grains (i.e. cryptocrystalline quartz) (Fig. 10). These rock types are found in lesser but significant proportion. Many of the chert grains contain fine, rhombic pores representing former sites of dolomite crystals. These increase porosity without increasing permeability. Grains that have an interconnected microporosity (and hence permeability) are much less common. A minor proportion of the chert particles include cherty argillites with or without quartz silt and fine sand.

Minor components include fine to medium-grained granites (Fig. 11). Many of these are moderately altered including sericitization of feldspar and large-scale epidote replacement. Mildly to moderately strained quartzites are also identified as a minor constituent. Finally, dolostone and amphibolite are detected as trace constituents in Cores 748NB-4P and 748S-3P respectively (Fig. 12).

Most of the stone is generally hard and nonfriable. However, sandstones are usually less stiff than igneous or carbonate rocks and can result in hardened concrete mixtures with lower elastic modulus. Perhaps more importantly, the sandstones exhibit a microporosity that results in some notable absorptivity. Grains such as these can dilate when saturated and subjected to freezing events. This dilation can result in freeze-thaw damage to the concrete matrix. However, very little evidence of this is identified in any sample. Finally, many of the rock types are considered alkali-silica reactive. The less pure sandstones (i.e. wackes) are known to have the potential for expansive reactions at moderate to longer time scales. The trace argillites may be similarly reactive. In contrast, chert is considered one of the most aggressively reactive rock types and all core samples contain chert-based lithologies in lesser but significant abundance. Nonetheless, little if any evidence for anything more than a trace reaction is identified in most of the core samples. Potential durability issues related to the aggregates are discussed at greater length below.

The coarse aggregate shapes are rounded with much fewer subrounded particles. Most grains are equidimensional with fewer subequant shapes. All samples contain a relatively low proportion of anisotropic particles that have plate-like shapes with aspect ratios up to approximately 5 : 1. The presence of anisotropic grains is not significant and the particle shapes are suitable for aggregate to be used in portland cement concrete mixtures.

The gradations cannot be quantified petrographically and the particle size distributions are estimated from two-dimensional cross sections of the concrete (Fig. 2). Based on the permissible gradation limits of ASTM C33, the size distribution profiles range from a No. 57 to a No. 67 with a No. 6 being the most common profile. A summary of the gradation estimates are presented in Table 5.2a below. At least five of the samples have similar particle size distributions (Cores 748N2-1P, 748N2-2P, 748N3-1P, 749-1P, and 750-1P). These have nominal top sizes at the 3/4" sieve with most if not all particles passing this mesh and a broad distribution down to the No. 4 sieve. Core 748S-3P is similar with a nominal top size at the 1" sieve. These are all likely compliant with a No. 6 gradation profile. A No. 67 would also be possible but only if greater than 20% passes the 3/8" sieve. Core 758-1P has a similar profile but definitely less than 20% passing this mesh. All seven could possibly satisfy a No. 57 gradation as well though the size ranges are not within the "heart" of this gradation. Core 748S-1P and 748S-2P have a different profile consistent with a No. 57 or a No. 6. The gradation is narrower with a nominal top size at the 3/4" sieve and a major proportion retained on the 1/2" sieve. Core 748NB-4P is different still with a 1/2" nominal top size and a particle size distribution closer to a No. 67 gradation. It is doubtful that intentionally separate gradations were specified for these different samples. It is clear from the lithology that all aggregate derives from a common source. It is more likely that some variation existed in the natural deposit and not a lot of effort was made to adjust the stone after extraction. It is not unusual to see this type of variability in natural gravel deposits.

**Table 5.2a: Estimated Coarse Aggregate Gradations**

Core ID	Nominal top size	Approximate gradation type	Remarks
748NB-4P	1/2"	No. 67	Well graded down to the No. 4 sieve.
748N2-1P	3/4"	No. 6 but possibly on the cusp of No. 67. No. 57 is also possible.	Most if not all particles pass the 3/4" sieve. Broadly graded down to the No. 4 sieve.
748N2-2P <sup>1</sup>	3/4"	No. 6 but possibly on the cusp of No. 67. No. 57 is also possible.	Most if not all particles pass the 3/4" sieve. Broadly graded down to the No. 4 sieve.
748N3-1P	3/4"	No. 6 but possibly on the cusp of No. 67. No. 57 is also possible.	Most if not all particles pass the 3/4" sieve. Broadly graded down to the No. 4 sieve.
748S-1P	3/4"	No. 57 to No. 6	Most particles pass the 3/4" sieve. Rich over the 1/2" sieve and little if any passing the 3/8" mesh.
748S-2P	3/4"	No. 57 to No. 6	Most particles pass the 3/4" sieve. Rich over the 1/2" sieve and little if any passing the 3/8" mesh.
748S-3P	1"	No. 6 but possibly on the cusp of No. 67. No. 57 is also possible.	All particles pass the 1" sieve. Broadly graded down to the No. 4 sieve.
749-1P	3/4"	No. 6 but possibly on the cusp of No. 67. No. 57 is also possible.	Most if not all particles pass the 3/4" sieve. Broadly graded down to the No. 4 sieve.
750-1P	3/4"	No. 6 but possibly on the cusp of No. 67. No. 57 is also possible.	Most if not all particles pass the 3/4" sieve. Broadly graded down to the No. 4 sieve.
758-1P	3/4"	No. 6 but No. 57 is also possible.	Most if not all particles pass the 3/4" sieve. Broadly graded down to the No. 4 sieve but likely less than 20% passing the 3/8" sieve.

Notes:

1. The core sample piece is somewhat small and the gradation is difficult to estimate accurately as a result.

### **5.3 - Fine Aggregate Materials**

All ten samples contain a siliceous natural sand that is nearly identical in composition and quality and also identical to that described for the cores in Highbridge Report SL0845-01. The fine aggregate content is estimated at 35-40% by hardened mortar fraction for all samples with the exception of Core 750-1P. This sample has a sand content estimated at 40-45% by hardened mortar fraction though likely at the lower end of this range. The material is a natural quartz sand consisting predominantly of monocrystalline quartz with lesser polycrystalline quartz and alkali feldspar. Mildly to moderately strained quartzite is a minor constituent. A minor but significant amount of ferruginous chert is included in all samples at several percent of the total sand volume (Fig. 13). Some of the ferruginous particles appear to include siltstones or argillites as well. However, their texture under reflected light suggests that all are cemented by a cryptocrystalline silicification. Both the chert and the strained quartzite are more concentrated in the grain sizes coarser than the No. 8 sieve. Heavy accessory minerals are rare in the sand. Trace glauconite is detected in Cores 749-1P and 750-1P. No clay coatings or friable materials are identified. From a physical perspective, the sand is considered hard, inelastic, and non-porous. Chemically, the chert in the coarser sizes is considered potentially alkali-reactive and this could represent a modest durability concern.

The sand consists of equidimensional particles that are subangular to subrounded in shape. Based on the qualitative petrographic observations, the particle size distributions are estimated to comply with the gradation requirements of ASTM C33. However, these are likely near the coarser size limits of the current standard (Fig. 14). The nominal top sizes are estimated at the No. 4 sieve for the most part. Possibly all grains pass this mesh for the aggregate in Cores 748NB-4P, 748N3-1P, and 749-1P. Several coarser grains of chert up to 3/8" in size are detected in Core 750-1P. In all cases, the particle size distributions are rich above the No. 30 sieve with little estimated to pass the No. 50 mesh.

### **5.4 - Cementitious Materials and Microstructure**

Ordinary gray portland cement is identified as the sole binder in all examined samples and no supplementary cementitious materials are present. Liquid admixtures cannot be identified petrographically though their influence on paste microstructure can often be detected. It is not clear whether or not any water-reducing admixtures had been added. The cement paste in all samples is uniform at the microscopic scale as might be expected with the use of water-reducers. Nonetheless, the texture is not diagnostic. The size and distribution of spherical air-voids indicates that all concrete was intentionally air-entrained though the development of fine voids was inhibited in the concrete represented by Core 748S-1P. Overall, there is some variability in the development and quality of the air system between all ten samples.

All concrete is estimated to have been mixed at a moderate water to cement ratio (w/c). Though the ratios cannot be quantified petrographically, cement paste characteristics are consistent with w/c in the mid to high 0.4's. Based on minor to moderate differences in the microporosity of the hardened binder, fracture behavior of the concrete, and subtle visual differences in color and luster of the hydrated paste, Cores 748NB-4P, 750-1P, and 758-1P contain concrete estimated to have been mixed with w/c closer to the mid 0.4 range. In contrast, Cores 749-1P, 748N2-1P and 748N3-1P are estimated to have been proportioned at the higher end of the range. Most of the remaining samples are difficult to distinguish within the range estimated as some properties suggest higher water content while others suggest lower water content. It should be stressed that the differences in most microstructural characteristics appear relatively minor.

The characteristics used to estimate original water to cement ratio include the capillary porosity of the cured cementitious hydrate (Fig. 14). The capillary pore structure is produced by the evaporable water present in the fresh mixture. Capillary pore structures tend to be relatively homogeneous throughout the sample set. The only exception is Core 748S-1P where some bleed water migration has left localized zones with moderately high microporosity. Other than this, most cores exhibit a uniform structure with a moderate permeability. Assuming the ten cores were meant to represent concrete of the same design, the paste quality suggests some variability in mix proportioning. However, the differences are not especially major. The variations in pore structure are summarized in Table 5.4a below.

**Table 5.4a: Summary of Capillary Pore Structures**

Capillary porosity	Core samples
Moderately to moderately low capillary porosity, homogeneous paste	748NB-4P
Moderate capillary porosity, homogeneous paste	748S-3P, 750-1P, 758-1P
Moderate capillary porosity, mostly homogeneous paste with some localized areas of moderately high capillarity	748S-1P
Moderate capillary porosity though tending toward moderately high in some areas, otherwise homogeneous paste	748N2-1P, 748N2-2P, 748N3-1P, 748S-2P, 749-1P

Calcium hydroxide is a primary phase of portland cement hydration and its size, morphology, and content can also be an indicator of original water contents when preserved (Fig. 16). There is some moderate variation in these crystallizations though these differences do not always correlate with other indicators of water content. These variations are summarized in Table 5.4b below with features arranged from those suggestive of lower water content to those indicating higher water content. Overall, hydroxide crystal masses have a non-compact texture typical of conventional concrete mixed with w/c greater than about 0.40. Tighter platelets are less common in those samples where they are observed. The density of the crystals ranges from moderate to moderately high.

**Table 5.4b: Summary of Primary Calcium Hydroxide Crystallization**

Abundance	Morphology	Deposits on aggregate	Core samples
Moderate	Fine-grained masses	Discontinuous	748S-1P, 749-1P
Moderately high	Fine-grained masses to platelets	Discontinuous to semi-continuous	748NB-4P
Moderately high	Fine-grained masses	Discontinuous	748N2-2P
Moderately high	Fine to medium-grained masses	Discontinuous	748S-2P, 748S-3P, 750-1P, 758-1P
Moderately high	Fine to medium-grained masses	Discontinuous to semi-continuous	748N2-1P, 748N3-1P

Any differences in the presence of portland cement residuals between samples is relatively subtle. Though features of the cement hydration are affected by mix water contents, the estimated w/c variation may be too low to be well illustrated in the cement textures. Instead, the full range of observable textures is found to be consistent with moderate w/c. For the ten cores, all of the cement exhibits a high degree of hydration and relatively little of the hydraulic calcium silicate remains unhydrated (Fig. 15). Residual grains include agglomerates of former calcium silicate with an interstitial matrix of residual iron-bearing ferrite. Isolated flakes of ferrite without obvious calcium silicate impressions are also observed. Single alite crystals or sites of former such crystals are relatively scarce in all samples. Cores 748N2-1P, 748S-2P, and 748S-3P have a moderate abundance of cement residuals while the other cores have a moderately high density of hydrated residuals. Relatively few of the hydrated grains are well-defined agglomerates. Some unhydrated calcium silicate material remains but only within the cores of the coarsest agglomerates. These are found in low proportion in Cores 748NB-4P, 748N2-2P, 748S-1P, 750-1P, and 758-1P and rare quantity in the other five cores. The cement is fine to medium-grained with most estimated to pass a No. 200 sieve and relatively few retained or approaching the No. 100 sieve. Finally, there is a minor tendency for hydrated grains to have become filled with cementitious hydrate in portions of Cores 748N3-1P, 748S-1P, 750-1P, and 758-1P.

The air content and microstructure in all ten cores is indicative of intentional air-entrainment (Fig. 14). A summary of the air contents, structural parameters, and qualitative distribution is presented in Table 5.4c. Details of the quantitative air-void analyses are presented in Section 6 below. Nine of the ten samples have air structures that meet at least some of the generally accepted parameters for adequate freeze-thaw resistance. These criteria include specific surfaces greater than 600 in.<sup>-1</sup> and spacing factors less than 0.008 in. Cores 748N2-1P, 748N2-2P, 748S-1P, and 748S-3P do not meet the specific surface benchmark but this is mostly due to the presence of coarse entrapped air-voids. These contribute negatively to the mathematical calculation of specific surface even when fine air contents are sufficiently high. Only Core 748S-1P has a deficiency of fine air-voids and this is reflected in the spacing factor of 0.0091 in. In fact, this is the only sample with a spacing factor greater than 0.008 in. Total air contents may be considered excessive in Cores 748S-3P, 750-1P, and 758-1P all of which equal to or greater than 8.5%. A modest reduction in compressive strength relative to the design strength can be expected in cores that have excessive air contents.

Overall, the fine air-voids are well distributed with depth in each core sample. For the most part, the voids are well dispersed at the microscopic scale and there is little to no clustering within the paste or along aggregate interfaces. Minor instances are found in Cores 750-1P and 758-1P.

**Table 5.4c: Summary of Air Contents and Parameters**

Core ID	Total air	Specific surface	Spacing factor	Remarks
	(%)	(in. <sup>-1</sup> )	(in.)	
748NB-4P	6.8	681	0.0049	Coarser voids over one millimeter contribute 2.1% to the total air volume.
748N2-1P	8.1	477	0.0059	Coarser voids over one millimeter contribute 2.7% to the total air volume.
748N2-2P	7.5	558	0.0053	Coarser voids over one millimeter contribute 2.5% to the total air volume.
748N3-1P	5.2	823	0.0057	
748S-1P	5.0	490	0.0091	Fine voids only constitute 2.7% and the air-entrainment is sparsely developed. Coarser voids over one millimeter contribute 2.3% to the total air volume.
748S-2P	7.8	685	0.0055	
748S-3P	9.6	434	0.0055	The size distribution appears to be somewhat rich over 200 μm. Coarser voids over one millimeter contribute 4.1% to the total air volume.
749-1P	5.8	669	0.0070	
750-1P	8.5	665	0.0044	The size distribution may be deficient in the finest sizes below 100 μm in diameter. Minor instances of clustering are observed locally around coarse aggregate.
758-1P	9.0	647	0.0044	Coarser voids over one millimeter contribute 2.7% to the total air volume. Minor instances of clustering are observed locally around coarse aggregate.

**5.5 - Original Placement and Hydration**

Based on the samples examined, the components of the structural concrete were well mixed in each core. There are no cement lumps, sand streaks, or rock pockets. It is not known whether the concrete was designed with the moderate water to cement ratios estimated for these cores. Therefore, it cannot be stated whether an inappropriate later addition was introduced on site. Nonetheless, the mix water appears to have been mostly well incorporated. There was some bleed water migration in the concrete represented by Core 748S-1P (Fig. 17). However, this is not interpreted to have been the result of late watering. A minor to moderate proportion of the coarse aggregate in Cores 748NB-4P and 750-1P respectively, contain very thin and discontinuous linings of denser cement paste. The denser paste would have had a lower water content when the concrete was fresh. This type of feature is sometimes found when concrete is retempered on site and the new water addition does not fully incorporate with the paste adhered to stone. However, the linings are minor and could also simply indicate a shorter mixing time. Regardless of the cause, it is clear that there are no major deficiencies related to the original mixing.

Assuming that all mixes were intended to have the same air structure, there are some inconsistencies observed in the development of the entrained air. However, these are within the range often encountered in many concrete projects. The most significant is the deficiency in fine air in Core 748S-1P. Generally, it is not possible to isolate a particular cause for variability in the development of entrained air. Certainly these can be caused by admixture dosages. However, qualities of the mixing equipment, presence of incompatible materials, or environmental conditions may all result in air content variability.

All cores contain materials that are monolithic throughout the entire structural cross section and no cold joints are identified within the structural layers (Fig. 2). The lower forming of the concrete is not evaluated as the cores do not include lower surfaces. In all samples, the structural concrete was mostly well compacted and consolidated with no large void structures or honeycombing. However, coarser air-voids generally no more than several millimeters in size are notably abundant in Cores 748N2-1P, 748N2-2P, 748S-3P, and 758-1P. Still, these are evenly distributed throughout each concrete section and do not compromise the integrity of the hardened mixtures. Other than these, voids greater than one millimeter constitute up to a little over 2% of the total volume in any core sample (see Section 6).

There is no evidence for excessive vibration. Coarse aggregate grains are homogeneously distributed throughout each concrete section without segregation. Though some grains are plate-like in shape, there are no preferential alignments of the stone due to excessive fluidity. The size, spacing, and location and steel reinforcement is outside the scope of a petrographic examination. Nevertheless, no reinforcement is included with the examined samples. It is not certain whether the original concrete surfaces are present below the wear courses. If they are, then there is no evidence for a weakened finish layer or other deficiencies that might be related to workmanship.

For most of the core samples, there is no evidence for excessive bleed water development. Only Core 748S-S1 contains microporous zones within the paste related to local bleed water concentrations (Fig. 17). These are not particularly common and discrete bleed water channels are not identified. Some of the microporous zones coincide with aggregate locations and these are interpreted to have reduced the quality of the paste-aggregate bond locally. Though other cores do not exhibit bleed water features, the paste-aggregate bonds in most samples are only moderately well developed as well. Though not necessarily deficient, the moderate mix water contents result in a concrete that tends to fracture around rather than through aggregate grains. A more “crumbly” fracture is particularly notable in Core 749-1P which is estimated to have been mixed at the highest water content of the ten examined cores. Some “crumbliness” is also noted in Core 748S-1P with the bleed water features. However, the property is also noticed in Cores 750-1P and 758-1P. In these cases, the original mix water contents are interpreted to have been lower. Perhaps higher air contents have contributed to a weaker paste-aggregate bond in these samples. Only Core 748NB-4P exhibits a sharper fracture behavior with induced cracks transecting rather than deflecting around coarse aggregate particles.

As described above, the portland cement hydration is quite advanced in all samples (Fig. 15). The hydration characteristics are mostly consistent throughout the full depth of each sample and there is no evidence for differential drying of the slab or loss of water near exposed surfaces. However, it is not certain that the original screeded surface is present in all of the samples. In particular, the top surface of Core 748N2-2P was saw-cut rather than weathered and the depth to the original surface is not known.

All ten samples have wear courses installed above the structural concrete (Fig. 18). The wear courses are not part of the examination but are identified in a cursory manner. The total thickness of wear course ranges from 1.2” to 3.1”. Microscopically, there is no debris identified at the contact between wear course and structural concrete. With the exception of Core 748N2-2P where the contact has been saw-cut, coarse aggregate particles are found to be truncated at the upper surface of the substrate concrete in each core. In Cores 748N3-1P, 748S-1P, and 748S-2P, there are examples of truncated aggregate that exhibit shattering consistent with some type of scarification process (Fig. 19). It is clear that some type of surface preparation had been performed in advance of the wear course application. However, all nine cores also exhibit areas that appear to represent “wet-on-wet” placements. In Core 758-1P, “fingers” of wear course material appear plastically embedded in the substrate (Fig. 20). The wear course mortar appears somewhat drier at the furthest extent of these fingers. These other features are more typical of contemporaneous placement. It is possible that scarification was performed shortly after the substrate installation but not in such a way as to completely remove the original surface of the substrate. However, the apparent plastic embedment of the wear course into the substrate is inconsistent with this interpretation.

## **5.6 - Condition and Durability**

The structural concrete examined for the ten core samples represents a moderate quality mixture considered suitable for many normal-duty service applications. The only notable issues identified in this report are potential durability issues in the aggregate. These include the potential for dilation during freezing events for the more porous types of sedimentary rocks and the inclusion of potentially alkali-reactive materials in both the fine and coarse aggregates. Moderate permeabilities are also noted but are not considered a major deficiency in their own right. However, compressive strength results provided by the client indicate some variability. Where higher permeabilities are identified, it can be expected that these correlate with original water to cement ratios. By extension, these would correlate with variations in compressive strength. With respect to the current condition of the concrete, only limited axial cracking is identified near the upper sections of the substrate concrete in Core 749-1P. This is discussed at greater length below. No other significant physical distress is identified. Carbonation is limited to a thin veneer no greater than 2.5 millimeters thick at the top of the structural concrete (Fig. 2). In these particular cores, most of the carbonation is only partial, patchy, and sometimes discontinuous. A minor extension of the carbonation is

found ringing aggregate grains and lining a single vertical hairline crack in Core 748S-3P to a maximum depth of one inch (Fig. 21). There does not appear to be any risk for pH-related depassivation of embedded steel if any is actually present in the concrete. All other mineralizations identified are related to trace or early-stage alkali-aggregate reactions (AAR) including the deposition of minor amounts of ettringite in the air-voids of Cores 748NB-4P and 749-1P.

The moderate permeability of the concrete is a result of mix water contents that are perhaps a little higher than desirable for exterior applications. However, none of the concrete is considered to be excessively permeable. Nonetheless, the concrete should not be considered fully water-resistant and this can increase the susceptibility to any distress mechanisms that are associated with moisture infiltration. Of course, the possibility of denser wear courses could mitigate this susceptibility while any larger cracks going through the slab could promote increased infiltration of water. These last two are outside the scope of the examination.

Aside from the potential for chloride infiltration, the issue most closely tied to water permeability would be freeze-thaw resistance. Assuming the wear courses are equally permeable, it should be expected that the structural concrete is capable of at least partial saturation if regularly exposed to moisture. Many of the coarse aggregate rock type contain a minor to moderate microporosity and are not as dense as a higher quality granitic or carbonate stone. This type of rock is capable of dilation when saturated and subjected to freezing conditions. This dilation may be capable of producing damaging expansion. With the exception of the 748S cores, internal microcracks are sometimes observed in the finer-grained sedimentary rocks (e.g. siltstone and argillite) and particularly within the redbed sediments and ironstones (Fig. 22). These are only trace in Cores 749-1P and 750-1P. It is possible that this cracking is related to some small degree of saturated freezing damage. However, none of the internal aggregate microcracking has propagated into the adjacent cement paste and there is no real damage associated with the fine features. In fact, it cannot be demonstrated conclusively that the cracking was not already present in the stone prior to inclusion in the concrete mixtures.

Air-entrainment is also an important feature contributing to the freeze-thaw resistance of the concrete. Most cores have entrained air structures that would be considered by most industry professionals to be sufficient for adequate freeze-thaw protection. Admittedly, several of the samples have low specific surfaces. But in most cases, spacing factors are still well within acceptable limits. The only core where a sparse entrained air structure might not be adequate is Core 748S-1P. Despite these deficiencies, there is no significant evidence for freeze-thaw related distress in the structural concrete of any sample. The only possible feature is a trace level of incipient scaling within the uppermost millimeter of structural concrete in Cores 748N3-1P, 748S-1P, and 750-1P (Fig. 23). Even here, these may be related to scarification damage rather than service distress.

Alkali-silica reactions (ASR) are identified in some of the core samples and details of these are described in Table 5.6a below. ASR is a reaction in which chemically unstable forms of silica react with alkalis normally found in the cement paste to produce a hygroscopic gel. Absorption of water into the gel causes the material to expand and this can often lead to significant expansive cracking. Of the rock types identified, the chert representing a small but significant proportion of both the coarse and fine aggregates in all cores is considered to be among the more aggressively reactive species due to the cryptocrystalline nature of the constituent quartz. Chert and similarly reactive chalcedony are also observed in association with the ironstone rock types. The sedimentary clastic rocks also have a known potential for ASR though less universally and more likely at slower rates if reactive at all.

In the ten core samples examined for this report, none of the reactions are at more than an early stage of advancement. In fact, only trace occurrences of ASR are generally found in nine of the examined core samples despite the higher potential for reaction. Core 749-1P is the only sample with any notable degree of reaction. Even here, the ASR is at an early stage and the concrete is not seriously compromised by the resulting microcracks. Based strictly on the aggregate types, the natural gravels should exhibit a greater degree of reaction than the crushed stone aggregates examined for Highbridge Reports SL0845-01 and SL0845-02 all else being equal. However, lithology alone is not always predictive of performance. There does not appear to be much difference between the various mixtures aside from the coarse aggregate types. This suggests that environmental factors may have played some role in the variable occurrence of the ASR reactions. Of course, this cannot be effectively evaluated through a laboratory examination alone. Nonetheless, it is notable that the only core where any appreciable reaction has occurred is the same one for which the original water to cement ratio is estimated to have been highest. This may indicate that availability of moisture has contributed to the reactivity.

In these ten samples, the greatest degree of reaction is observed in Core 749-1P (Fig. 24). Even here, the reaction is limited to the uppermost two inches of the substrate concrete. Axial reaction cracks are localized just below the wear course and approximately 1.5” below the wear course. The latter is coincident with the core break observed in the sample as provided. Typical ASR gel plugs and gel-linings are found in association with these two cracks and features have a maximum thickness of 250 µm. Other ASR reactions within this zone are limited to exceedingly fine microcracks within reactive stone that extend only short distances into the adjacent cement paste. Quartz arenite and silty argillite are positively identified as two of the reactive species petrographically in this sample.

Only some localized reaction is found in Core 748NB-4P including an axial microcrack originating in a chert particle just below the wear course contact (Fig. 25). Another minor reaction is identified in chert at depth. Aside from this, only minor exudates of reaction gel are detected in the honed cross sections of several of the other cores. These white mineralizations typically border chert in the fine aggregate and sometimes emanate from ironstone (Fig. 26). No cracking is detected in association with these minor exudates. These minor mineralizations are detected in Cores 748N2-1P, 748N3-1P, 748S-1P, and 748S-2P.

In the cores examined for Highbridge Report SL0845-02, two of the samples contained a dolostone crushed stone that exhibited a type of early-stage alkali-carbonate reaction (ACR). In the ten cores examined for this report, only a single dolostone gravel particle is identified petrographically for Core 748NB-4P. Nonetheless, an early stage ACR reaction is identified in this grain (Fig. 27). The periphery of the particle exhibits “corrosion” due to dedolomitization along with surface-parallel microcracks. The cement paste adjacent to the grain contains “blooms” of calcium carbonate as a product of the dedolomitization reaction and a few minor microcracks radiating from the reacted grain. Despite this clear reaction, it is obvious that there is no potential for any significant damage due to ACR given the limited occurrence of the aggregate.

**Table 5.6a: Summary of Alkali-Aggregate Reactions**

Photographic documentation of these features are presented in Figures 24 through 27 in Appendix II below.

Core ID	Stage	Details
748NB-4P	Trace	A single, approximately 25 µm wide microcrack is found just below the wear course. A gel plug is found in association with a chert coarse aggregate. Another chert grain is found at depth with extremely fine microcracking and gel filling (much less than 25 µm wide). A single dolostone grain in thin section exhibits mild dedolomitization “corrosion” and a minor carbonate bloom in the adjacent cement paste. Extremely fine peripheral microcracks are found within the grain and extremely fine radial microcracks are found in the adjacent paste.
748N2-1P	Trace	Trace local ASR gel exudations are found around chert fine aggregate or sometimes ironstone in hand sample. No ASR evidence is detected in thin section.
748N2-2P	None	No evidence for ASR is found in thin section or hand sample.
748N3-1P	Trace	In hand sample, trace local ASR gel exudations are found around chert fine aggregate or some ironstone or clastic coarse aggregate. No ASR evidence is detected in thin section.
748S-1P	Trace	Trace local ASR gel exudations are found around chert fine aggregate in hand sample. Some more diffuse exudates are also observed without an obvious source. No ASR evidence is detected in thin section.
748S-2P	Trace	In hand sample, very local ASR gel exudations are found around chert fine aggregate only but these are relatively common. In thin section, only one instance of very local microcracking and gel plugs are detected in the same grain type.
748S-3P	Trace	In hand sample, only one chert coarse aggregate grain near the base of the core exhibits some internal microcracking with no local gel deposition. No evidence for ASR is found in thin section.
749-1P	Early but limited	Early stage ASR reactions are limited to the upper 2” of the substrate concrete. The crack orientations are roughly axial though random orientations are also observed in finer local microcracks. The distribution is somewhat gradational with most of the reactions found in the upper 0.75”. Except for throughgoing cracks just below the wear course and 1.5” below the wear course, most other cracking is limited to fine discontinuous cracks in the paste just adjacent to reaction sites. Internal aggregate cracks have a maximum width of 250 µm. Gel plugs and linings are observed in association. In thin section, only a silty argillite and a quartz arenite with minor clay matrix are positively identified as reactive.
750-1P	None	No evidence for ASR is found in thin section or hand sample.
758-1P	Trace	One chert fine aggregate grain is detected in thin section just below the wear course with internal microcracking and adjacent gel deposits in air-voids. A silty ironstone fractured at the lower core break exhibits a thin rim of ASR reaction product. Otherwise, there is no evidence for ASR in thin section or hand sample.

With respect to future durability, there is no evidence to suggest that continued ASR development is mitigated by any particular feature of the concrete. ASR is sometimes controlled by the addition of supplementary cementitious materials or (more recently) lithium-based admixtures. The former are clearly not part of the mix design and the latter is unlikely though this can only be demonstrated chemically. Alkaline cement paste is one precondition for the initiation of aggregate dissolution. The lack of carbonation has allowed all concrete to maintain a high alkalinity throughout the full cross section of each core. Continued aggregate reactions can be expected even if somewhat slowly. Availability of moisture is also an important factor in the rate of ASR development and distress. Again, the concrete is not especially water-resistant even if the permeabilities are not excessive. Cores 748N2-1P, 748N3-1P, and 749-1P are estimated to have the higher permeabilities of the group and may be slightly more susceptible to water infiltration. Of course, exposure and drainage will also have an impact on the amount of water available and this cannot be evaluated in the laboratory.

Any reactions identified in this study are at an early stage and have not compromised the integrity of the represented concrete. It is quite possible that the concrete may remain provisionally stable over the course of a normal life cycle. Nonetheless, the chert present in both the coarse and fine aggregates is considered to be among the more aggressively reactive species and should be considered to be a long-term durability threat. Of course, it must be stressed that while petrographic examination can identify potential durability threats, it cannot be fully predictive. Monitoring of concrete containing such components may be prudent. It is also possible that the concrete studied for this examination is not fully representative of all material on site. If other areas of the construction exhibit visible cracking not captured in the provided samples, these should be considered to have a potential association with the types of reactions described herein. Patterned cracking with a polygonal shape or “map-cracking” would be one possible indication of more advanced alkali-aggregate reaction as would the presence of white mineral exudates.

**6. Air-Void Analysis**

**Table 6.1: Point-Count Data**

<b>Core ID</b>	<b>748NB-4P</b>	<b>748N2-1P</b>	<b>748N2-2P</b>	<b>748N3-1P</b>	<b>748S-1P</b>	<b>748S-2P</b>	<b>748S-3P</b>
Aggregate nominal top size (in.)	0.5	0.75	0.75	0.75	0.75	0.75	1.0
Total traverse length (in.)	78.2	75.65	74.6	75.4	76	76	76.15
Total area (in. <sup>2</sup> )	12.7	13.0	8.8	13.0	12.8	13.0	13.0
Aggregate points	1102	1045	1048	1026	1090	956	1030
Paste points	356	346	332	403	344	445	347
Air points (less than 1 mm)	73	81	74	62	40	92	83
Air points (greater than 1 mm)	33	41	38	17	35	27	63
Crack points <sup>1</sup>	0	0	0	0	11	0	0
Total points	1564	1513	1492	1508	1520	1520	1523
Air intercept	902	728	781	813	459	1019	792

<b>Core ID</b>	<b>749-1P</b>	<b>750-1P</b>	<b>758-1P</b>
Aggregate nominal top size (in.)	0.75	0.75	0.75
Total traverse length (in.)	76	76	74.9
Total area (in. <sup>2</sup> )	13.0	13.0	12.4
Aggregate points	967	1010	977
Paste points	446	381	386
Air points (less than 1 mm)	68	101	95
Air points (greater than 1 mm)	19	28	40
Crack points <sup>1</sup>	20	0	0
Total points	1520	1520	1498
Air intercept	727	1073	1091

Notes:

1. Cracks are non-totaling and do not influence the air-void parameter calculation.

**Table 6.2: Calculated Volumes and Air-Void Parameters**

<b>Core ID</b>	<b>748NB-4P</b>	<b>748N2-1P</b>	<b>748N2-2P</b>	<b>748N3-1P</b>	<b>748S-1P</b>	<b>748S-2P</b>	<b>748S-3P</b>
Aggregate (volume %)	70.5	69.1	70.2	68.0	72.2	62.9	67.6
Paste (volume %)	22.8	22.9	22.3	26.7	22.8	29.3	22.8
Air less than 1 mm (volume %)	4.7	5.4	5.0	4.1	2.7	6.1	5.4
Air greater than 1 mm (volume %)	2.1	2.7	2.5	1.1	2.3	1.8	4.1
<b>Total air (volume %)</b>	<b>6.8</b>	<b>8.1</b>	<b>7.5</b>	<b>5.2</b>	<b>5.0</b>	<b>7.8</b>	<b>9.6</b>
Paste/air ratio	3.36	2.84	2.96	5.10	4.59	3.74	2.38
Voids/inch	11.53	9.62	10.47	10.78	6.04	13.41	10.40
Average chord length (in.)	0.006	0.008	0.007	0.005	0.008	0.006	0.009
Specific surface (in. <sup>-1</sup> )	680.75	477.38	557.86	823.29	489.60	685.04	433.97
<b>Spacing factor (in.)</b>	<b>0.0049</b>	<b>0.0059</b>	<b>0.0053</b>	<b>0.0057</b>	<b>0.0091</b>	<b>0.0055</b>	<b>0.0055</b>

<b>Core ID</b>	<b>749-1P</b>	<b>750-1P</b>	<b>758-1P</b>
Aggregate (volume %)	64.5	66.4	65.2
Paste (volume %)	29.7	25.1	25.8
Air less than 1 mm (volume %)	4.5	6.6	6.3
Air greater than 1 mm (volume %)	1.3	1.8	2.7
<b>Total air (volume %)</b>	<b>5.8</b>	<b>8.5</b>	<b>9.0</b>
Paste/air ratio	5.13	2.95	2.86
Voids/inch	9.57	14.12	14.57
Average chord length (in.)	0.006	0.006	0.006
Specific surface (in. <sup>-1</sup> )	668.51	665.43	646.52
<b>Spacing factor (in.)</b>	<b>0.0070</b>	<b>0.0044</b>	<b>0.0044</b>

Respectfully submitted,

John J. Walsh  
 President/ Senior Petrographer  
**Highbridge Materials Consulting, Inc.**

**Appendix I: Visual Description of Petrographic Samples**

<b>Sample ID</b>	<b>748NB-4P</b>
Dimensions and Details	The sample consists of a 3.25" diameter approximately 7" in length. The core is received as one intact piece. A wear course of approximately 3.0" thickness overlies the structural concrete. The wear course is tightly bound to the substrate along a roughly planar surface.
Top/Outer Surface	The top surface is roughly planar with low relief coarse aggregate exposure. Marking paint is covering a portion of the top surface. Moderate soiling of the paste is also apparent.
Bottom/Inner Surface	The bottom surface is a clean, artificial drilling break.
Core Circumference	Smooth with no differential erosion from coring.
Embedded Items	No reinforcement is included in the sample.
Visible Cracks	No macroscopic cracking is visible in hand sample.

<b>Sample ID</b>	<b>748N2-1P</b>
Dimensions and Details	The sample consists of a 3.25" diameter approximately 7.5" in length. The core is received as one intact piece. A wear course of approximately 2.0" thickness overlies the structural concrete. The wear course is tightly bound to the substrate along a roughly planar surface.
Top/Outer Surface	The top surface is roughly planar with low to moderate relief coarse aggregate exposure. Moderate soiling of the paste is also apparent.
Bottom/Inner Surface	The bottom surface is a clean, artificial drilling.
Core Circumference	Smooth with no differential erosion from coring.
Embedded Items	No reinforcement is included in the sample.
Visible Cracks	No macroscopic cracking is visible in hand sample.

<b>Sample ID</b>	<b>748N2-2P</b>
Dimensions and Details	The sample consists of a 3.25" diameter core. The core is received as two non-contiguous pieces. The top piece consists of wear course material and is approximately 2.6" in length. The top piece is saw-cut on the bottom and may include a very minor portion of structural concrete. The bottom piece is approximately 2.7" in length and contains only structural concrete. This piece is saw-cut on both top and bottom surfaces.
Top/Outer Surface	The top surface is roughly planar with low to moderate relief coarse aggregate exposure. Moderate soiling of the paste is also apparent.
Bottom/Inner Surface	The bottom surface is saw-cut.
Core Circumference	Smooth with no differential erosion from coring.
Embedded Items	No reinforcement is included in the sample.
Visible Cracks	No macroscopic cracking is visible in hand sample.

<b>Sample ID</b>	<b>748N3-1P</b>
Dimensions and Details	The sample consists of a 3.25" diameter core approximately 7.75" in length. The core is received as one intact piece. A wear course of approximately 2.7" thickness overlies the structural concrete. The wear course is tightly bound to the substrate along a roughly planar surface.
Top/Outer Surface	The top surface is roughly planar with low to moderate relief coarse aggregate exposure. Moderate soiling of the paste is also apparent.
Bottom/Inner Surface	The bottom surface is a clean, artificial drilling break.
Core Circumference	Smooth with no differential erosion from coring.
Embedded Items	No reinforcement is included in the sample.
Visible Cracks	No macroscopic cracking is visible in hand sample.

**HIGHBRIDGE MATERIALS CONSULTING, INC.**

Pennoni Associates, Inc.; I-95 Viaduct Project

Report #: SL0845-03

Page 16 of 60

<b>Sample ID</b>	<b>748S-1P</b>
Dimensions and Details	The sample consists of a 3.25" diameter core approximately 8" in length. The core is received in two contiguous pieces with a core break running through the structural concrete at approximately 5.7" depth. A wear course of approximately 2.5" thickness overlies the structural concrete. The wear course is tightly bound to the substrate along a roughly planar surface.
Top/Outer Surface	The top surface is roughly planar with low to moderate relief coarse aggregate exposure. Moderate soiling of the paste is also apparent.
Bottom/Inner Surface	The bottom surface is a clean, artificial drilling break.
Core Circumference	Smooth with no differential erosion from coring.
Embedded Items	No reinforcement is included in the sample.
Visible Cracks	The core break is the only crack visible in hand sample. This may represent a pre-existing structure. However, dried coring slurry is covering original features.

<b>Sample ID</b>	<b>748S-2P</b>
Dimensions and Details	The sample consists of a 3.25" diameter core approximately 8" in length. The core is received as one intact piece. A wear course of approximately 2.0" thickness overlies the structural concrete. The wear course is tightly bound to the substrate along a roughly planar surface.
Top/Outer Surface	The top surface is roughly planar with low relief coarse aggregate exposure. Moderate soiling of the paste is also apparent.
Bottom/Inner Surface	The bottom surface is a clean, artificial drilling break.
Core Circumference	Smooth with no differential erosion from coring.
Embedded Items	No reinforcement is included in the sample.
Visible Cracks	No macroscopic cracking is visible in hand sample.

<b>Sample ID</b>	<b>748S-3P</b>
Dimensions and Details	The sample consists of a 3.25" diameter core approximately 8" in length. The core is received as one intact piece. A wear course of approximately 1.2" thickness overlies the structural concrete. The wear course is tightly bound to the substrate along a roughly planar surface.
Top/Outer Surface	The top surface is roughly planar with low to moderate relief coarse aggregate exposure. Marking paint is covering a small portion of the top surface. Moderate soiling of the paste is also apparent.
Bottom/Inner Surface	The bottom surface is a clean, artificial drilling break.
Core Circumference	Smooth with no differential erosion from coring.
Embedded Items	No reinforcement is included in the sample.
Visible Cracks	No macroscopic cracking is visible in hand sample.

**HIGHBRIDGE MATERIALS CONSULTING, INC.**

Pennoni Associates, Inc.; I-95 Viaduct Project

Report #: SL0845-03

Page 17 of 60

<b>Sample ID</b>	<b>749-1P</b>
Dimensions and Details	The sample consists of a 3.25" diameter core approximately 8" in length. The core is received as two contiguous pieces with a core break running through the structural concrete at approximately 3.6" depth. A wear course of approximately 1.8" thickness overlies the structural concrete. There is also an incipient crack that appears to be a cohesive failure within the substrate concrete rather than an adhesive failure at the interface with the wearing course.
Top/Outer Surface	The top surface is roughly planar with low relief coarse aggregate exposure. Moderate soiling of the paste is also apparent.
Bottom/Inner Surface	The bottom surface is a clean, artificial drilling break.
Core Circumference	Smooth with no differential erosion from coring.
Embedded Items	No reinforcement is included in the sample.
Visible Cracks	The core break is the only failed crack visible in hand sample. This may represent a pre-existing structure. The break both intersects and deflects coarse aggregate particles. Minor mineralization is visible in the paste surrounding one coarse aggregate grain. The crack just below the wear course does not exhibit any mineralizations at least along the core circumference.

<b>Sample ID</b>	<b>750-1P</b>
Dimensions and Details	The sample consists of a 3.25" diameter core approximately 7.5" in length. The core is received as one intact piece. A wear course of approximately 1.7" thickness overlies the structural concrete. The wear course is tightly bound to the substrate along a roughly planar surface.
Top/Outer Surface	The top surface is roughly planar with low to moderate relief coarse aggregate exposure. Moderate soiling of the paste is also apparent.
Bottom/Inner Surface	The bottom surface is a clean, artificial drilling break.
Core Circumference	Smooth with no differential erosion from coring.
Embedded Items	No reinforcement is included in the sample.
Visible Cracks	No macroscopic cracking is visible in hand sample.

<b>Sample ID</b>	<b>758-1P</b>
Dimensions and Details	The sample consists of a 3.25" diameter core approximately 7.5" in length. The core is received as one piece. However, there are 2 pieces of approximately 1" length that were cleanly broken off the bottom of the core. A wear course of approximately 3.1" thickness overlies the structural concrete. The wear course is tightly bound to the substrate along a roughly planar surface.
Top/Outer Surface	The top surface is roughly planar with low to moderate relief coarse aggregate exposure. There is marking paint covering the original features along approximately 1/3 of the top surface. Moderate soiling of the paste is apparent in the visible portion of the top surface.
Bottom/Inner Surface	The bottom surface is a clean, artificial drilling break. A fine reaction rim is found within an ironstone particle fractured through at the core base.
Core Circumference	Smooth with no differential erosion from coring.
Embedded Items	No reinforcement is included in the sample.
Visible Cracks	No macroscopic cracking is visible in hand sample except for the small pieces that are broken off of the bottom of the core. It does not appear that these represent pre-existing features.

## Appendix II: Photographs and Photomicrographs

Microscopic examination is performed on an Olympus BX-51 polarized/reflected light microscope and a Bausch and Lomb Stereozoom 7 stereoscopic reflected light microscope. Both microscopes are fitted with an Olympus DP-11 digital camera. The overlays presented in the photomicrographs (e.g., text, scale bars, and arrows) are prepared as layers in Adobe Photoshop and converted to the jpeg format. Digital processing is limited to those functions normally performed during standard print photography processing. Photographs intended to be visually compared are taken under the same exposure conditions whenever possible.

The following abbreviations may be found in the figure captions and overlays and these are defined as follows:

cm	centimeters	PPL	Plane polarized light
mm	millimeters	XPL	Crossed polarized light
µm	microns (1 micron = 1/1000 millimeter)		
mil	1/1000 inch		

Microscopical images are often confusing and non-intuitive to those not accustomed to the techniques employed. The following is offered as a brief explanation of the various views encountered in order that the reader may gain a better appreciation of what is being described.

**Reflected light images:** These are simply magnified images of the surface as would be observed by the human eye. A variety of surface preparations may be employed including polished and fractured surfaces. The reader should note the included scale bars as minor deficiencies may seem much more significant when magnified.

**Plane polarized light images (PPL):** This imaging technique is most often employed in order to discern textural relationships and microstructure. To employ this technique, samples are milled (anywhere from 20 to 30 microns depending on the purpose) so as to allow light to be transmitted through the material. In many cases, Highbridge also employs a technique whereby the material is impregnated with a low viscosity, blue-dyed epoxy. Anything appearing blue therefore represents some type of void space (e.g.; air voids, capillary pores, open cracks, etc.) Hydrated cement paste typically appears a light shade of brown in this view (with a blue hue when impregnated with the epoxy). With some exceptions, most aggregate materials are very light colored if not altogether white. Some particles will appear to stand out in higher relief than others. This is a function of the refractive power of different materials with respect to the mounting epoxy.

**Crossed polarized light images (XPL):** This imaging technique is most often employed to distinguish components or highlight textural relationships between certain components not easily distinguished in plane polarized light. Using the same thin sections, this technique places the sample between two pieces of polarizing film in order to determine the crystal structure of the materials under consideration. Isotropic materials (e.g.; hydrated cement paste, pozzolans and other glasses, many oxides, etc.) will not transmit light under crossed polars and therefore appear black. Non-isotropic crystals (e.g.; residual cement, calcium hydroxide, calcium carbonate, and most aggregate minerals) will appear colored. The colors are a function of the thickness, crystal structure, and orientation of the mineral. Many minerals will exhibit a range of colors due to their orientation in the section. For example, quartz sand in the aggregate will appear black to white and every shade of gray in between. Color difference does not necessarily indicate a material difference. When no other prompt is given in the figure caption, the reader should appeal to general shapes and morphological characteristics when considering the components being illustrated.

**Chemical treatments:** Many chemical techniques (etches and stains typically) are used to isolate and enhance a variety of materials and structures. These techniques will often produce strongly colored images that distinguish components or chemical conditions.

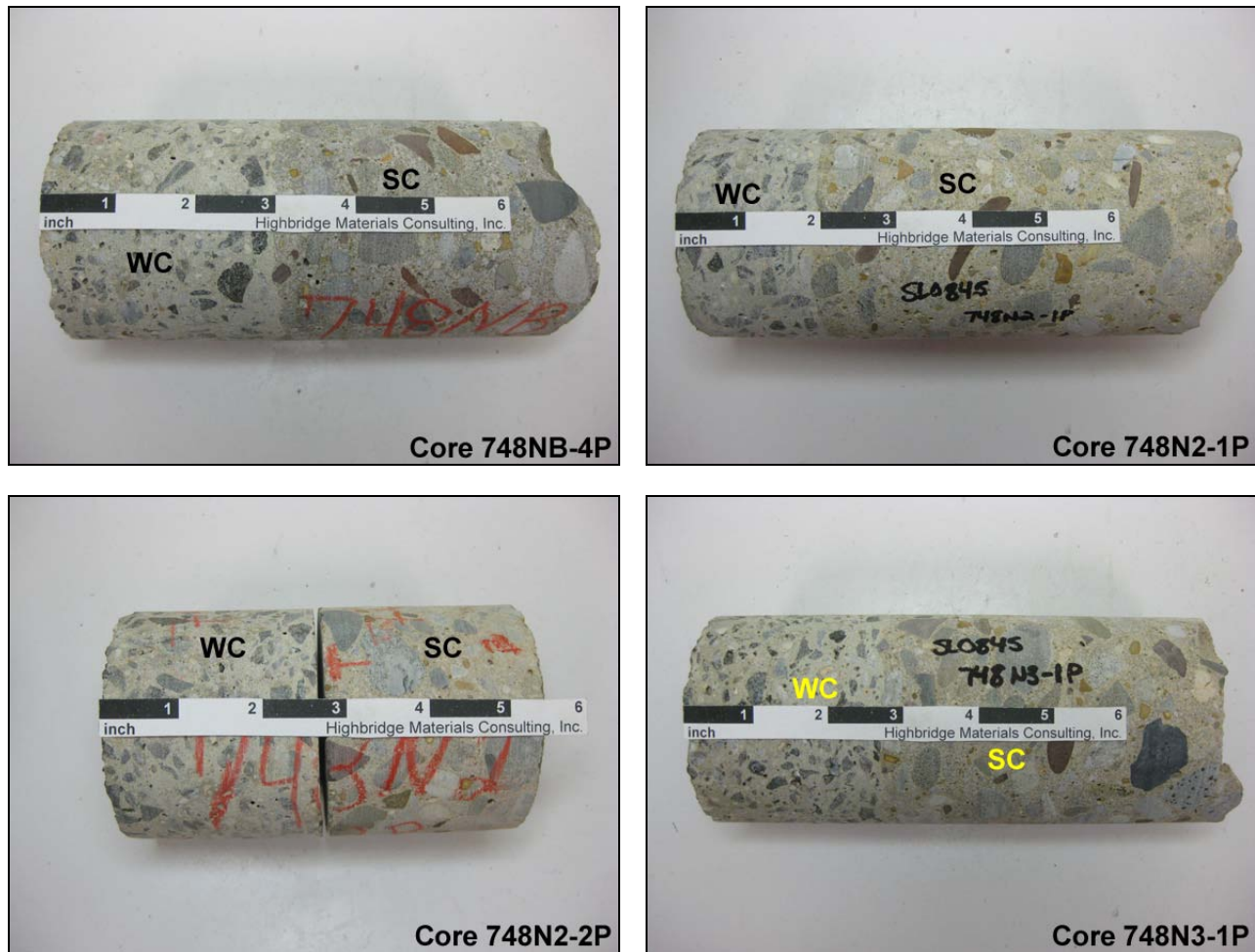


**Figure 1:** Photographs of the ten concrete core samples used for petrographic examination and air-void analysis of the structural concrete layers. All are shown with their upper surfaces toward the left of each image. All of the cores contain wear course layers (WC) overlying normal weight structural concrete (SC). Core 748N2-2P was saw-cut and does not contain any original finished surfaces and the wear course is not attached to the substrate in this sample. The black arrows in the images for Cores 748S-1P and 749-1P illustrate core breaks present in the samples as delivered. Only the one in Core 749-1P is attributed to alkali-silica reaction. The other one is likely an artifact of sample retrieval. The blue arrows in the images for Cores 749-1P and 758-1P illustrate cracks that did not fail through. Again, the one for Core 749-1P is attributed to aggregate reactivity. The basal cracks in Core 758-1P appear to be artifacts.



**Figure 1 (cont'd.):** Photographs of the ten concrete core samples used for petrographic examination and air-void analysis of the structural concrete layers.

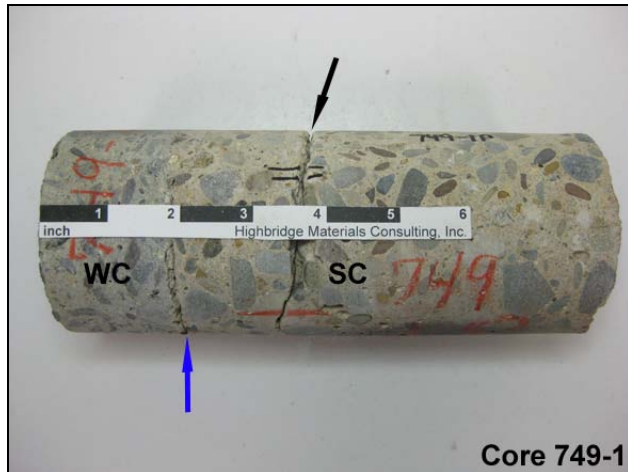


**Figure 1 (cont'd.):** Photographs of the ten concrete core samples used for petrographic examination and air-void analysis of the structural concrete layers.

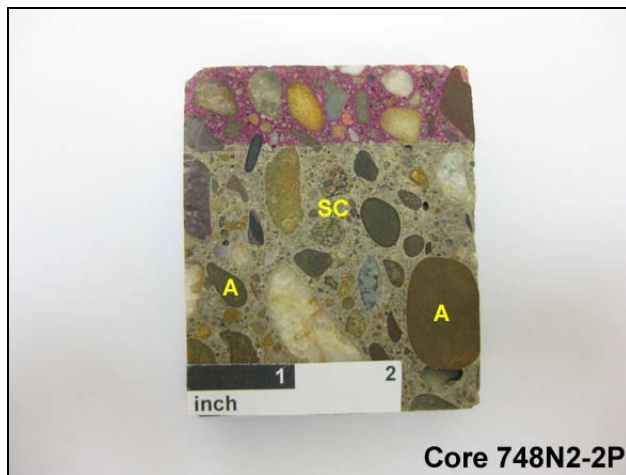
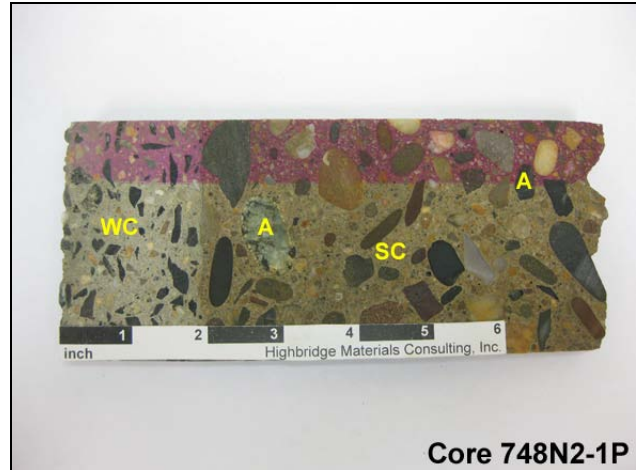
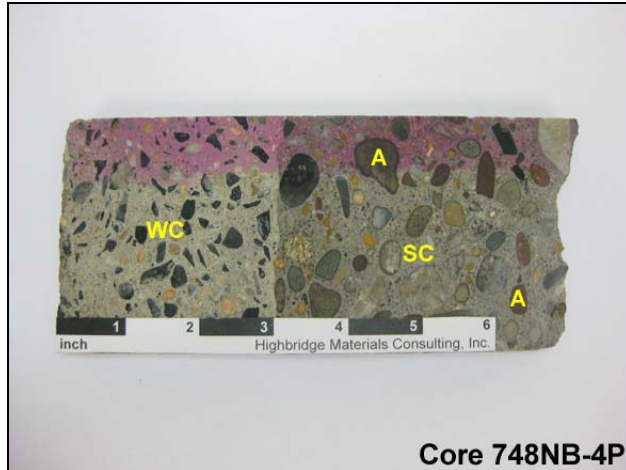


**Figure 2:** Photographs of honed concrete cross sections prepared for the full depth of each provided sample. The upper surfaces are shown to the left in each example. The black arrows indicate where core breaks were epoxied together prior to honing. Wear courses (WC) overlie structural concrete (SC). The size and gradation of the natural gravel aggregate (A) can be observed in the structural layers. Most cores have aggregate with a 3/4" nominal top size. Exceptions include Core 748NB-1P with a 1/2" top size and Core 748S-3P with a 1" top size. Variations in the particle size distributions are likely intrinsic to the original source and not necessarily intentional. The aggregate is well distributed and no segregations are identified. A portion of each core is treated with phenolphthalein indicator solution. The pink color indicates that the structural concrete is alkaline throughout all but a thin veneer along the upper surfaces. The high pH is indicative of the relative lack of carbonation within the structural layers. Steel embedded within the substrate concrete would not be at risk for depassivation at least within the upper portions represented here.

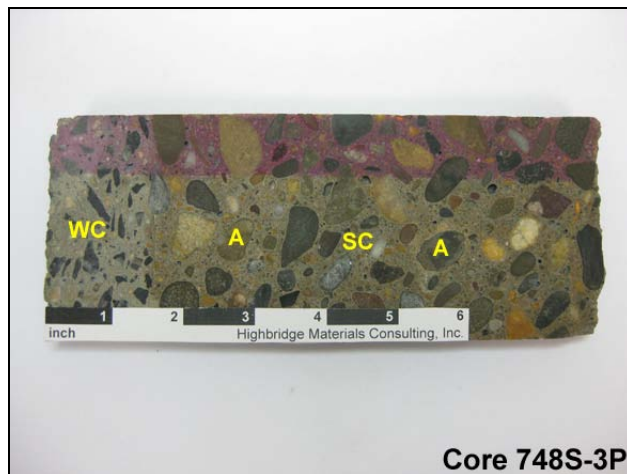
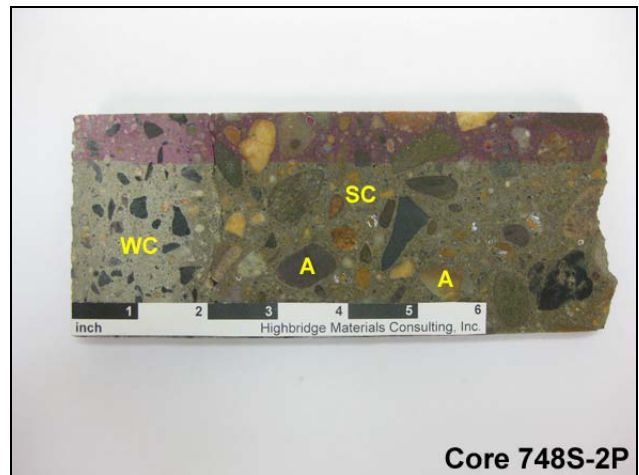
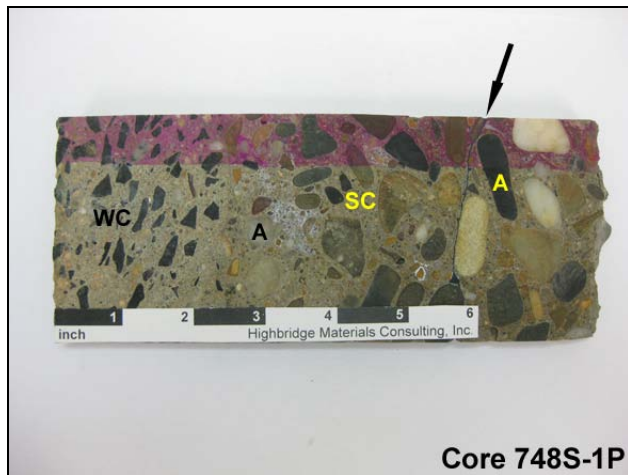
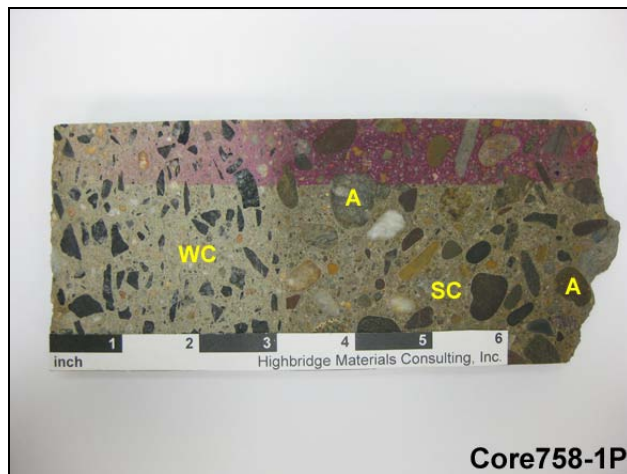
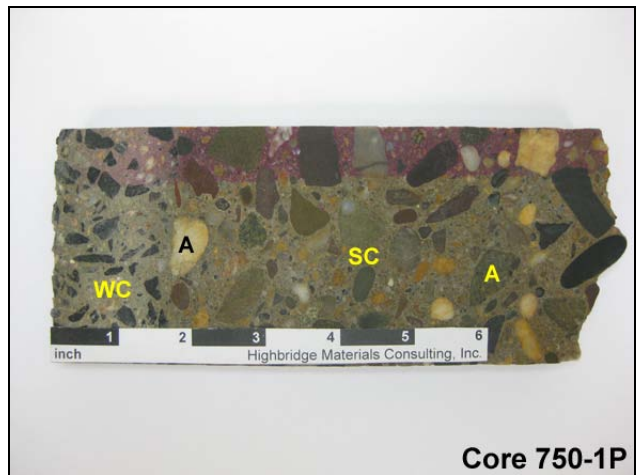
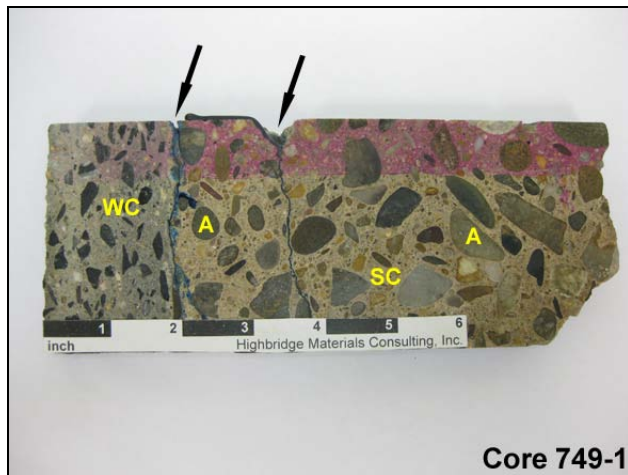
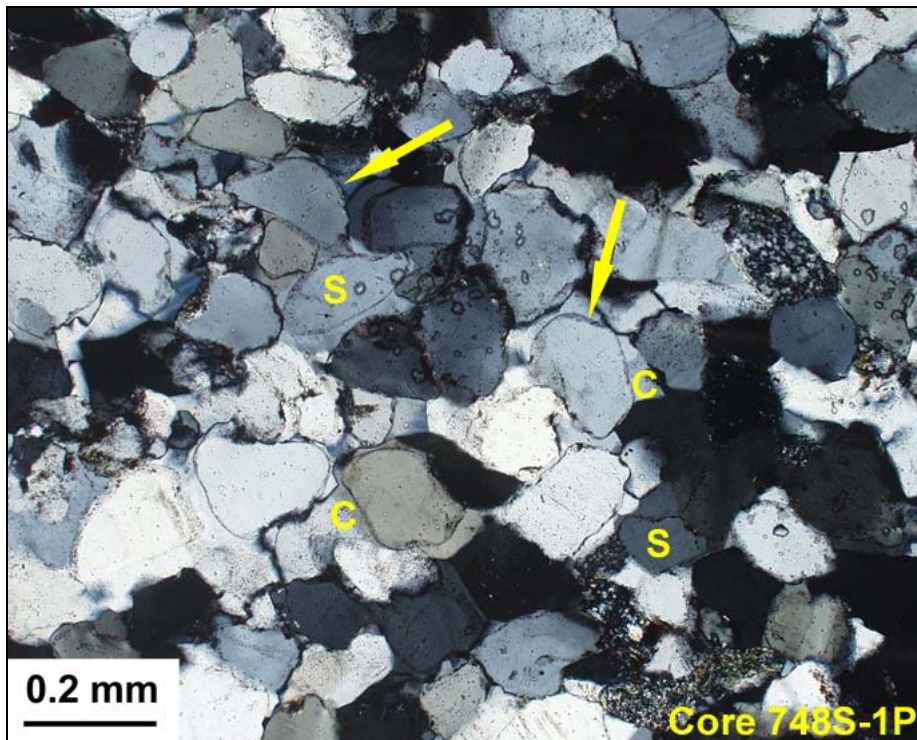
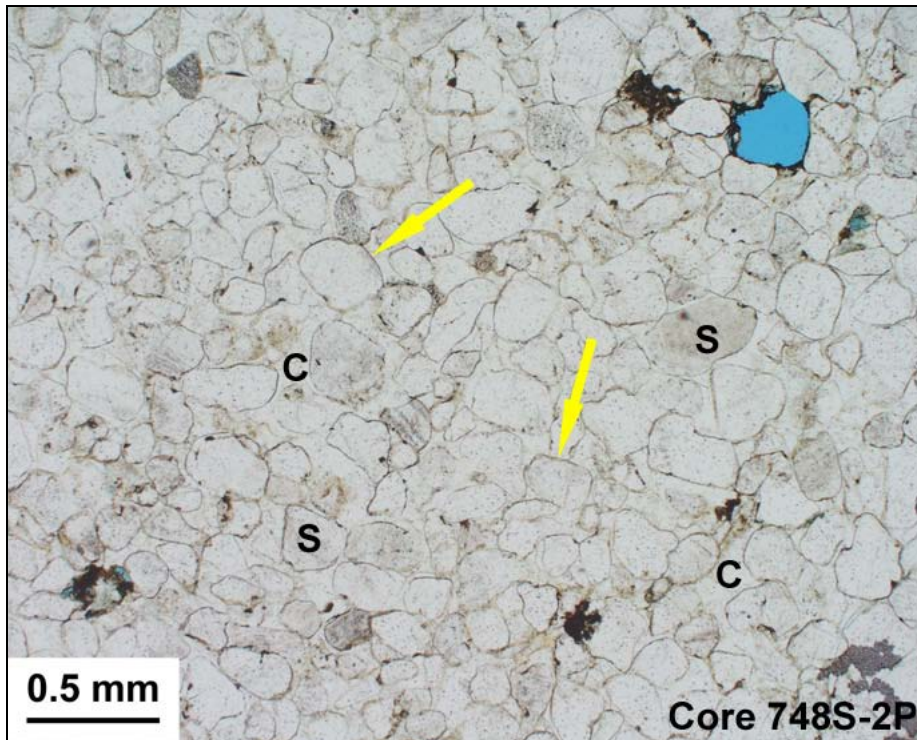


Figure 2 (cont'd.): Photographs of honed concrete cross sections prepared for the full depth of each provided sample.



**Figure 2 (cont'd.):** Photographs of honed concrete cross sections prepared for the full depth of each provided sample.



**Figure 3:** Photomicrographs illustrating examples of quartz arenite present in the natural gravel coarse aggregate. The upper image is taken in PPL and the lower image in XPL. These two examples illustrate a rock type that is less common in the sand assemblage. This type of arenite is quite pure in composition and is tightly lithified with a natural quartz cement. In both cases, the arrows indicate the original boundaries of quartz sand grains (S). The sandy microtexture is better evident in the upper PPL image. A geologic cement (C) has overgrown the original particles and nearly fills the original interstitial pore space. The cement consists of quartz that has grown in crystallographic continuity with the host particles. This is best observed in the lower XPL image where the sand particles exhibit the same interference colors as the adjacent cements.

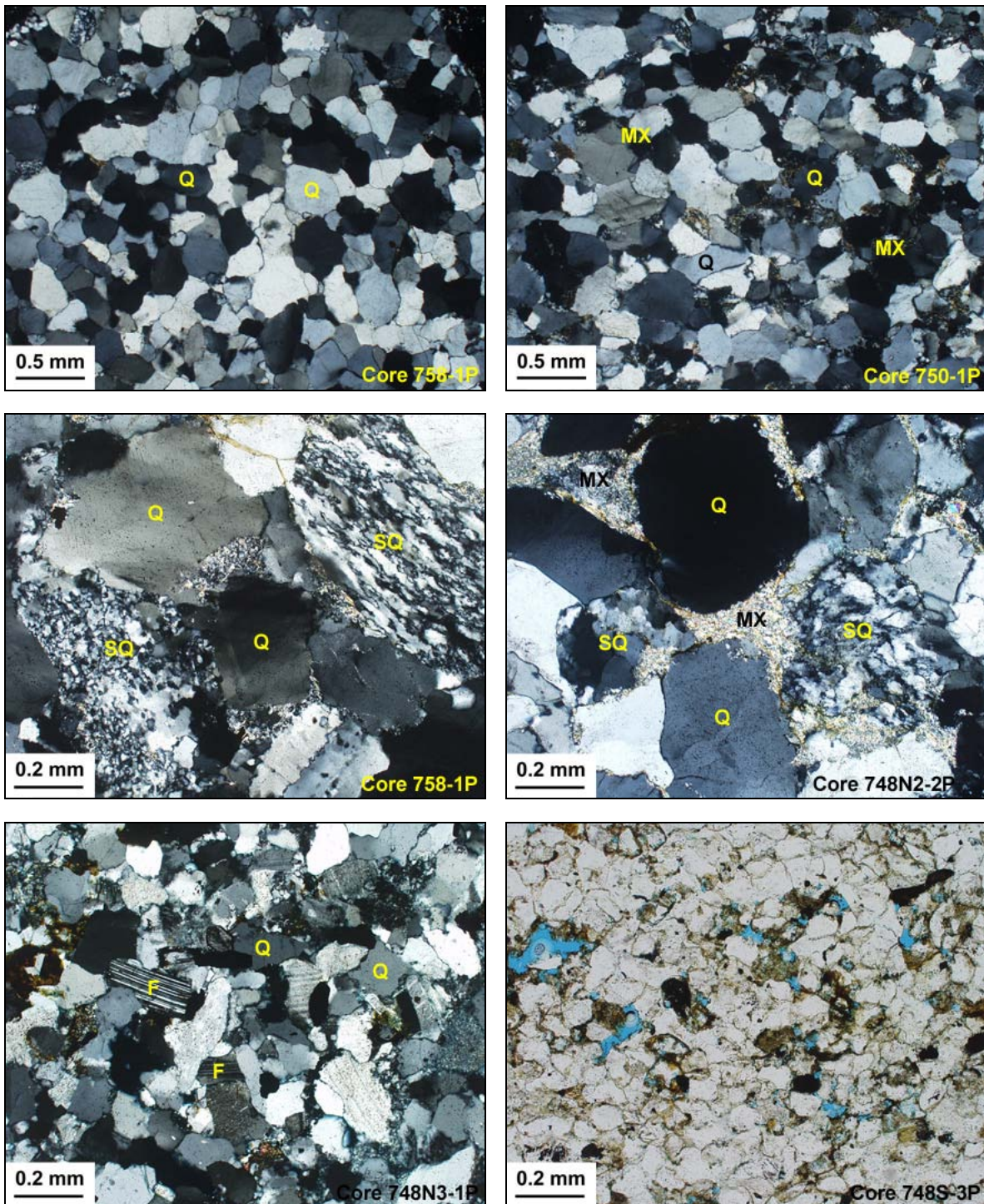


**Figure 4:** XPL photomicrographs except for the lower right image in PPL. Other quartz arenites are shown exemplifying the range of particles from nearly pure quartzites to quartz arenites with minor inclusions of other rock types or matrix. (Upper left) A mosaic of white and gray quartz crystals (Q) represents the vast majority of this pure quartzite. The rock is lithified by grain compaction. (Upper right) A similar grain contains a minor amount of matrix (MX). This includes clay and white mica. (Center left) In this grain, particles of strained quartzite (SQ) are intermixed with the quartz. This geologically deformed quartz is relatively common in the quartz arenites and this type of material is generally considered moderately alkali-silica reactive. (Center right) Some grains grade into quartz wackes and include greater amounts of strained quartzite (SQ) and fine-grained matrix (MX). (Lower left) A subarkosic arenite is only different in that it contains minor amounts of feldspar (F). (Lower right) The samples are all impregnated with a blue-dyed epoxy. The blue colors represent pore spaces. In the case of the arenites, porous grains are not particularly abundant and are more common in the finer-grained varieties.

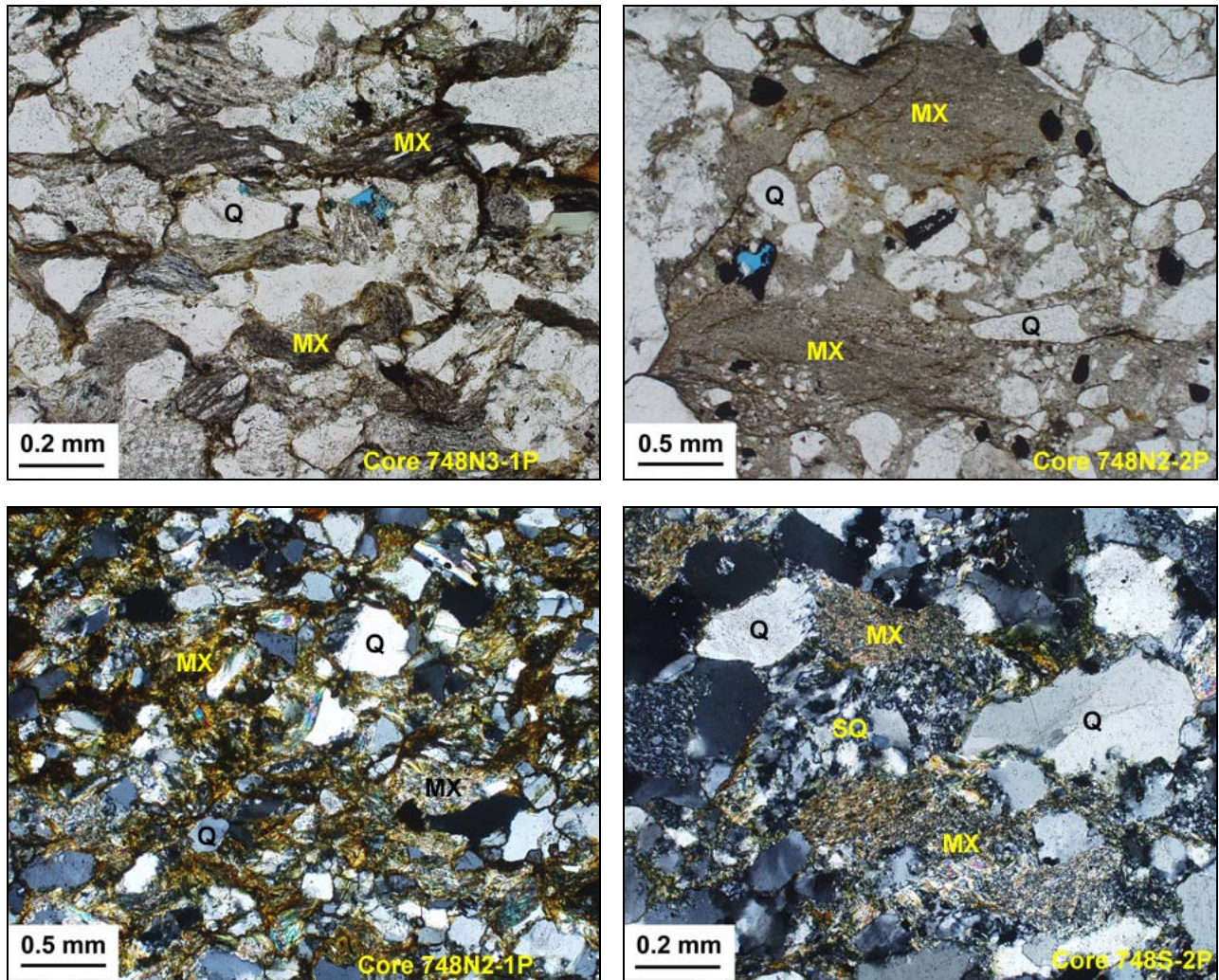


**Figure 5:** Quartz wackes are also a significant component of the sedimentary rock types in the aggregate assemblage. Examples are shown in the upper PPL images and lower XPL images. The wackes are distinguished by higher amounts of fine clay matrix (MX). The matrix tends to result in softer and more elastic particles and is also expected to increase the microporosity of the aggregate. Quartz sand (Q) is more or less abundant and strained quartzite (SQ) is also found as individual sand particles. The matrix is observed to be compacted and elongate in many of the grains as shown in the upper left image. Some particles are particularly rich in matrix as shown in the upper right image.

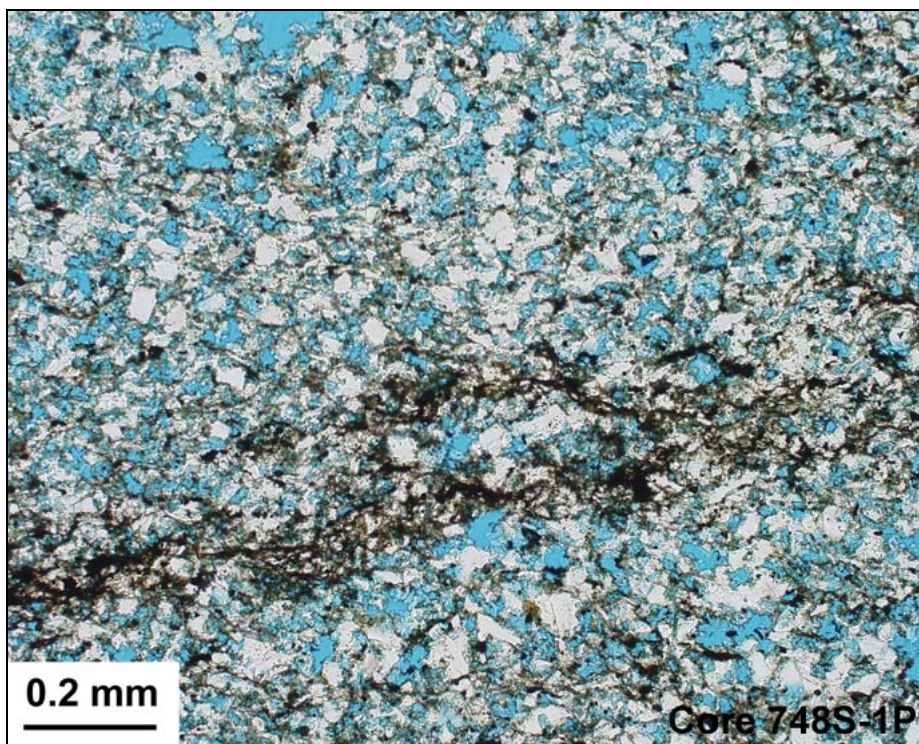
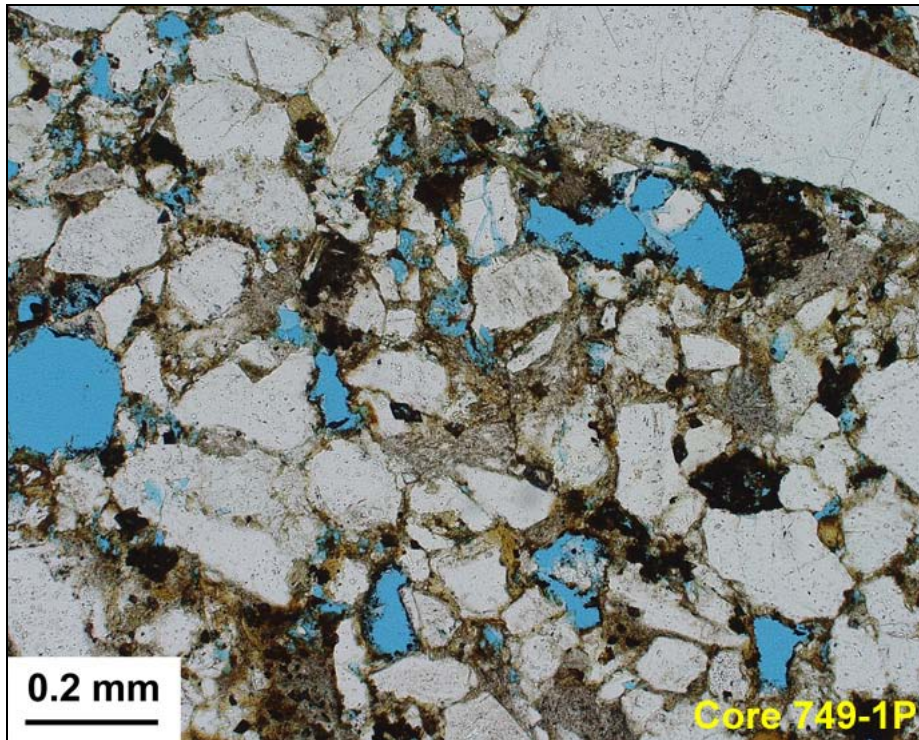


**Figure 6:** PPL photomicrographs. The quartz wackes tend to have a higher internal porosity than the quartz arenites. Again, the samples are impregnated with a blue-dyed epoxy to highlight the presence of pore spaces. Note the distributed porosity in these two examples. The larger pores in the upper image are likely connected by a submicroscopic porosity in the constituent clay matrix. In contrast, the fine interstitial pores in the lower image are fully interconnected on their own.

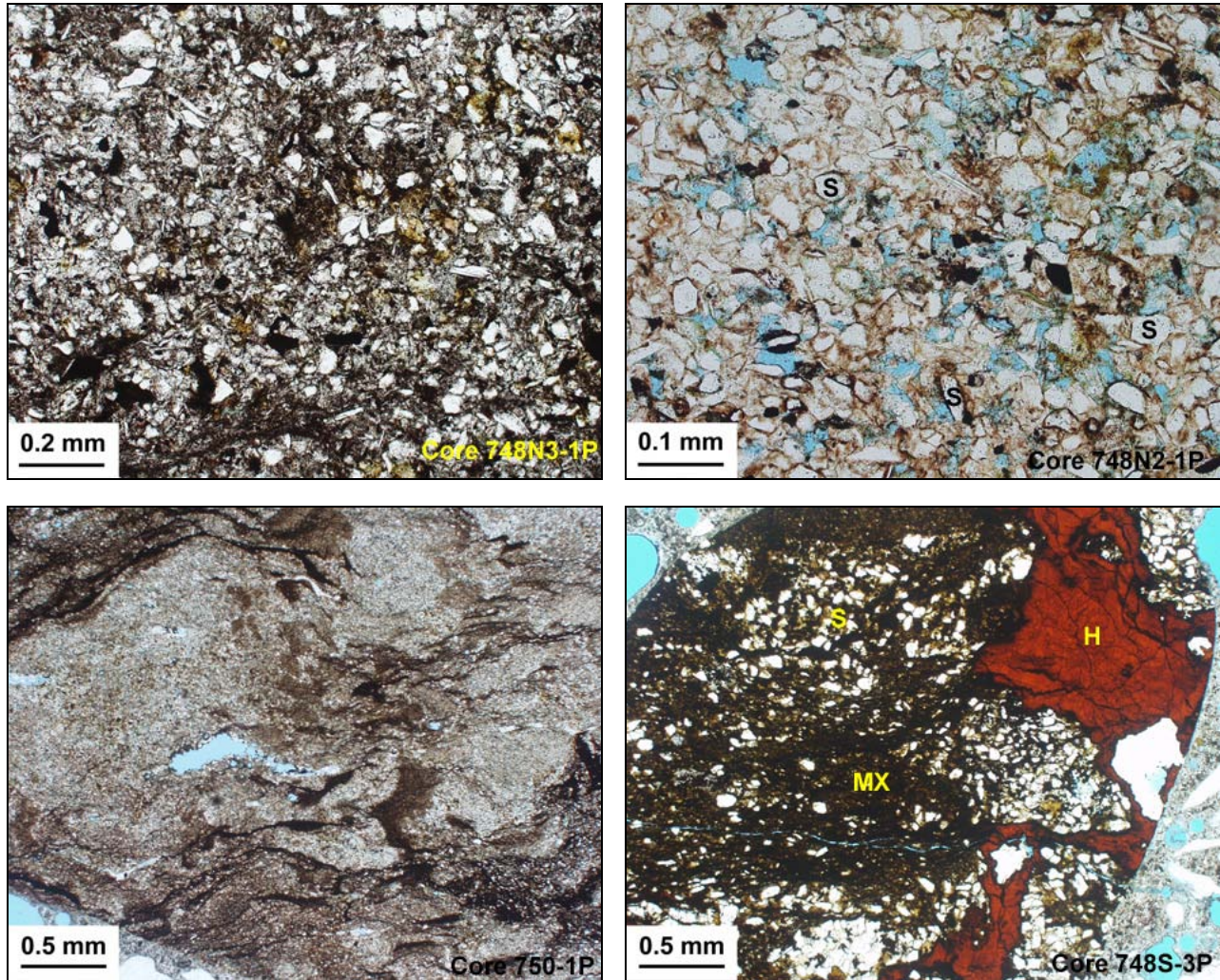


**Figure 7:** PPL photomicrographs illustrating examples of redbed sedimentary rocks in the coarse aggregate assemblage. (Upper left) A typical grain has a framework of sand and silt particles (appearing white in this image) cemented by a thick matrix of iron oxide or hematite (appearing dark in this image). (Upper right) The redbeds are also porous in many cases. Here, fine quartz sand is lined by a dark red iron oxide. However, the interstitial space is open and filled with the blue-dyed epoxy used in the sample preparation. (Lower left) A siltstone is shown with bands of dark-colored iron oxide plastically entrained within a framework of very fine silt grains. (Lower right) A complex grain is shown with locally varying amounts of sand (S) and clayey iron oxide matrix (MX). Patches of crystalline hematite (H) are also present.

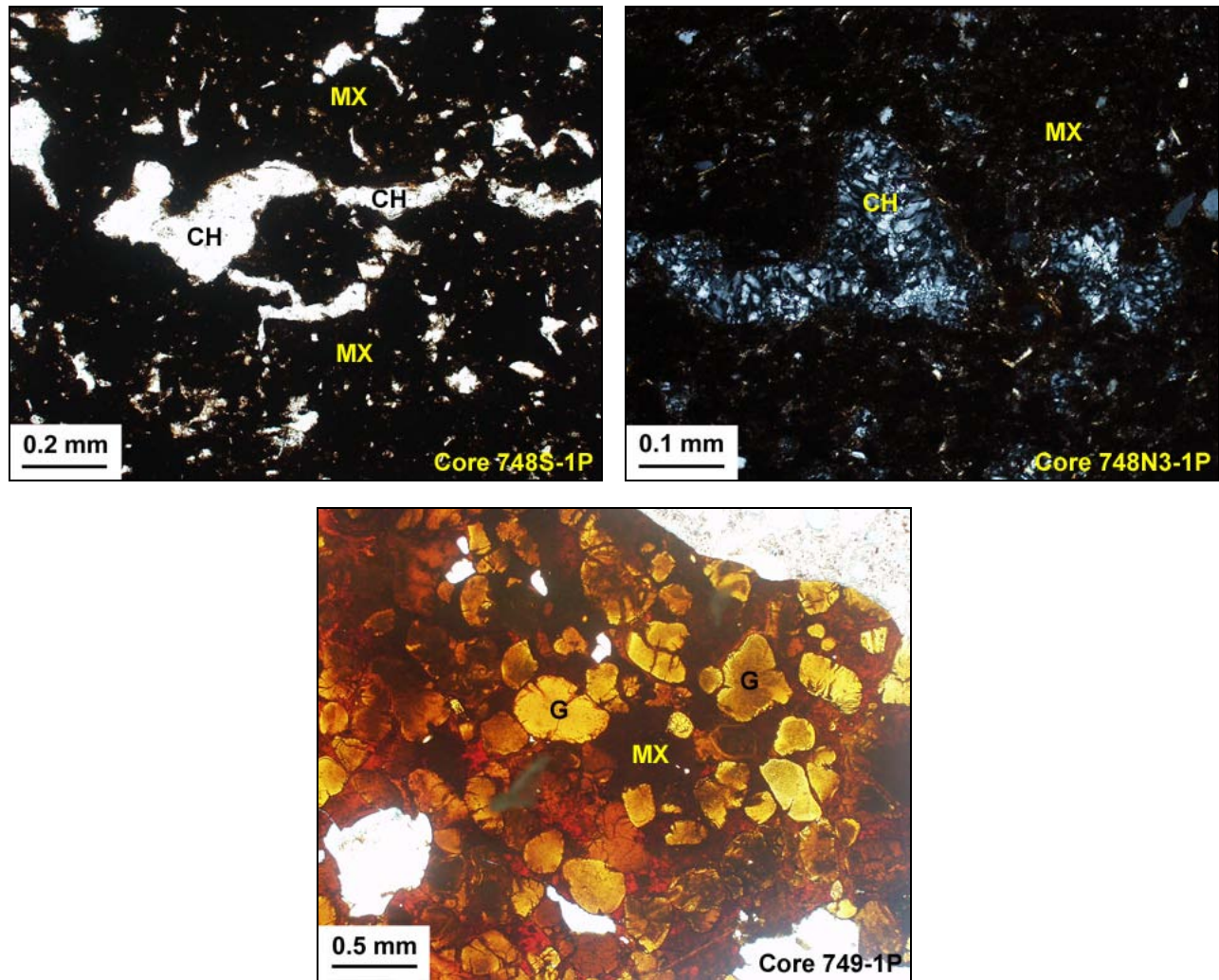


**Figure 8:** Other iron oxide rich aggregates are better classified as ironstones and some examples are shown here. In the upper images, pods of chalcidony (CH) are embedded in a matrix of iron oxide (MX). The left image is in PPL and the right image in XPL. Chalcedony is a cryptocrystalline variety of quartz that is susceptible to alkali-silica reaction. Another ironstone is shown in the lower PPL image. In this grain, altered glauconite pellets (G) are embedded in an iron oxide matrix (MX). Glauconite is an iron-rich clay commonly found in marine sediments.

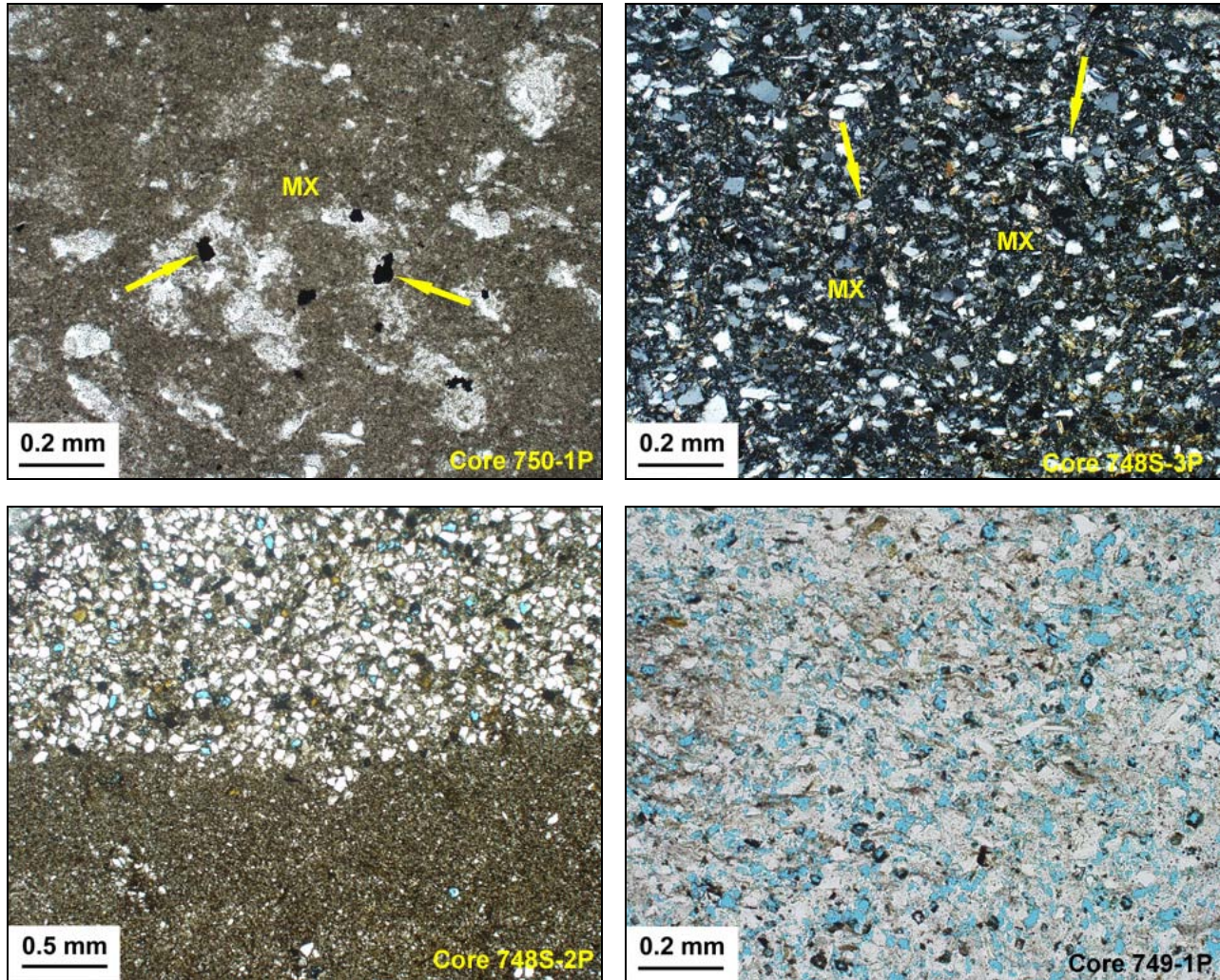


**Figure 9:** Some of the sedimentary rocks in the coarse aggregate are finer-grained than the arenites and wackes. These include rocks that range from siltstone to argillite with examples shown here. (Upper left PPL image) An argillite has a fine clayey matrix (MX). The arrows indicate sulfide phases detected in the argillite but these are too few to represent a durability or aesthetic issue. (Upper right XPL image) An argillaceous siltstone contains fine quartz silt (arrows) embedded in a fine argillaceous matrix (MX). (Lower left PPL image) The lower portion of this grain is a pure argillite. However, the upper portion contains quartz silt (appearing as white particulates). Note also that some porosity is indicated in this layer by the blue epoxy showing through the matrix. (Lower right PPL image) This cherty and silty argillite is even more porous. Blue pores are distributed evenly throughout the whole of the sample.

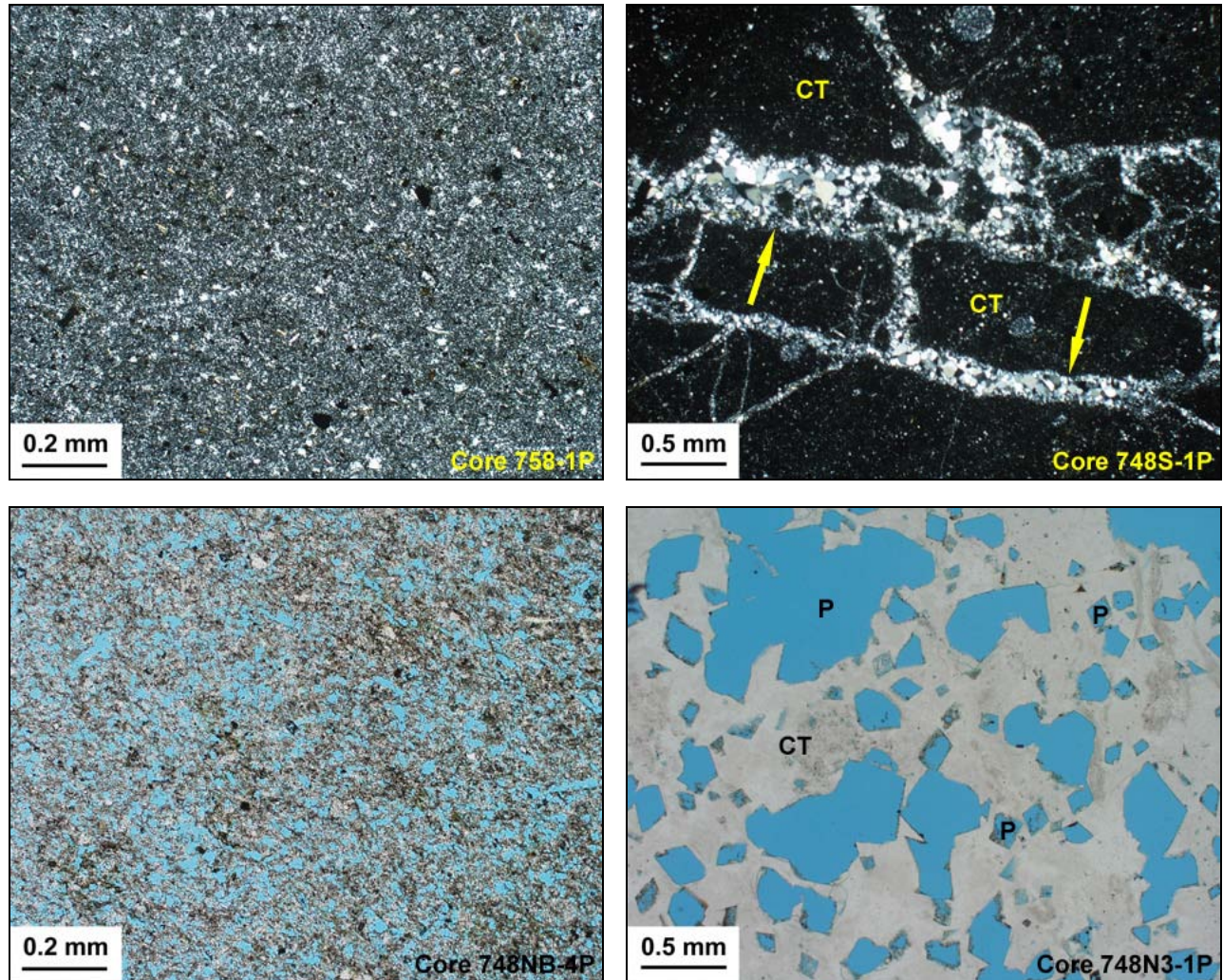


**Figure 10:** Chert is part of the coarse aggregate assemblage. Though not especially abundant, the phase is present in significant proportion given its potential reactivity. Examples of the chert are shown for several samples. (Upper left XPL image) Most grains are similar to the one shown here which includes a homogeneous and not especially porous matrix of cryptocrystalline quartz. (Upper right XPL image) This grain contains a similar type of uniform chert (CT). However, the body of the stone is dissected by chalcidony veins (arrows). (Lower left PPL image) Some of the chert exhibits a distributed and interconnected porosity as found in this grain. Again, the pores are highlighted by the blue-dyed epoxy used in the sample preparation. (Lower right PPL image) Some of the chert is porous but not permeable. In this case, rhombic-shaped pores (P) represent dolomite crystals that have dissolved away secondarily. The chert matrix (CT) is otherwise solid.

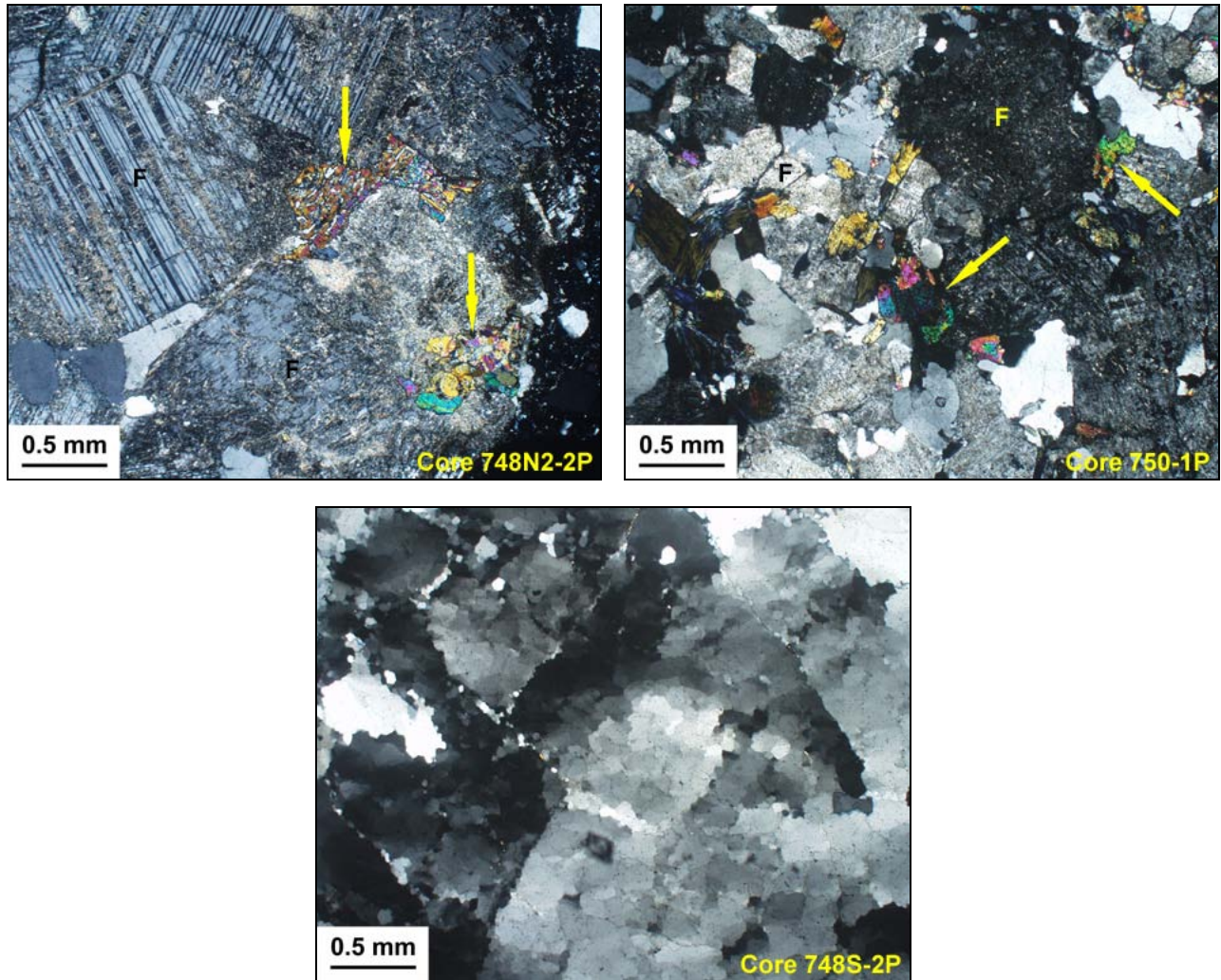


**Figure 11:** XPL photomicrographs illustrating examples of some of the minor rock types observed in the natural gravel coarse aggregate assemblage. The upper images display granites that contain mildly altered feldspar (F) along with some epidote (arrows). The mosaic of white and gray crystals in the lower XPL image consists of quartz grains that have undergone crystal plastic strain.

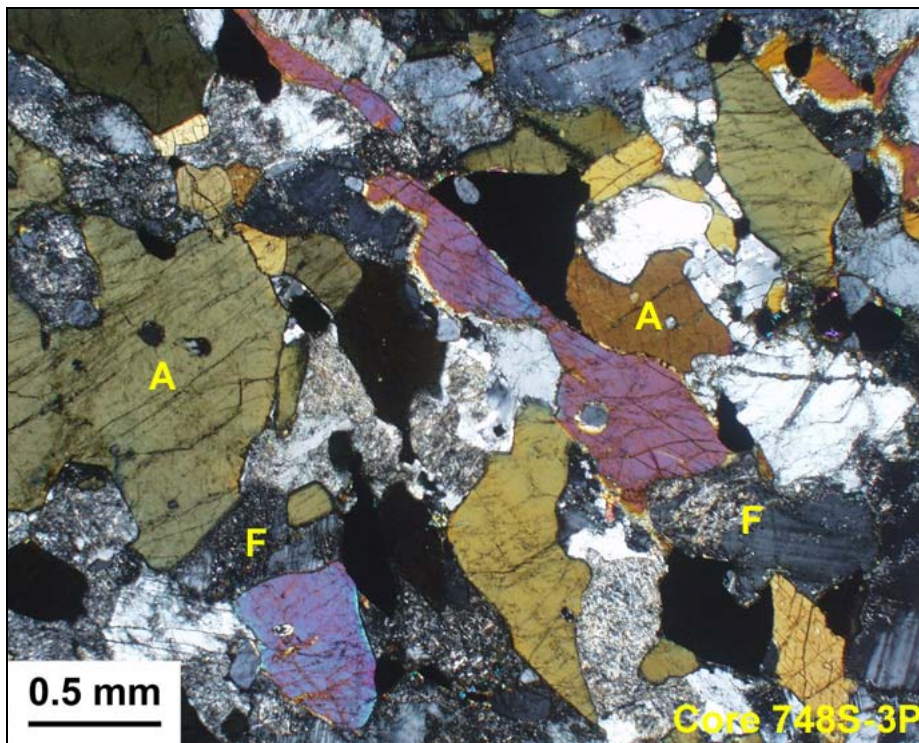
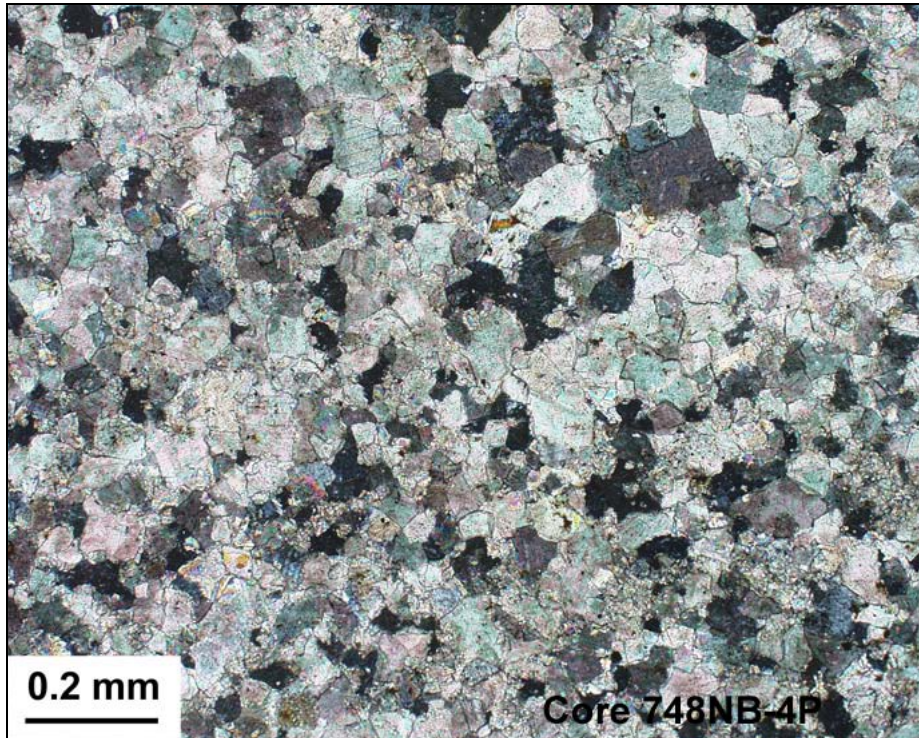


**Figure 12:** XPL photomicrographs illustrating trace grains of the coarse aggregate identified in two of the samples. (Upper image) A single grain of dolostone is detected in Core 748NB-4P. (Lower image) Amphibolite in Core 748S-3P consists of amphibole (A) and feldspar (F).

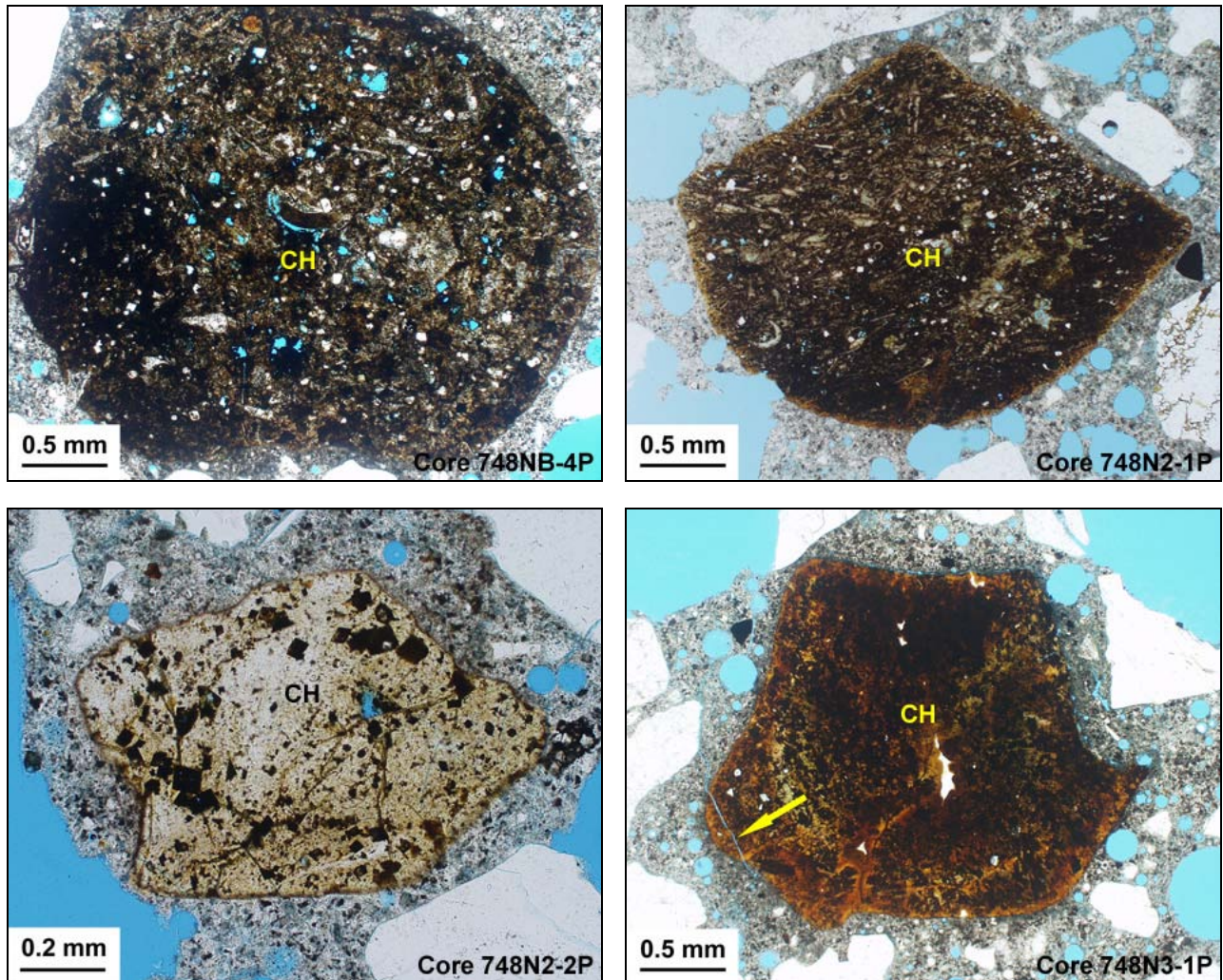


**Figure 13:** PPL photomicrographs illustrating examples of the chert identified in the fine aggregate. All cores contain ferruginous chert (CH) at about several percent by volume. Chert is considered to be one of the most highly alkali-reactive rock types. Nevertheless, only trace reaction is identified in this component if at all. The arrow in one of the images indicates an internal microcrack that may represent such reaction.

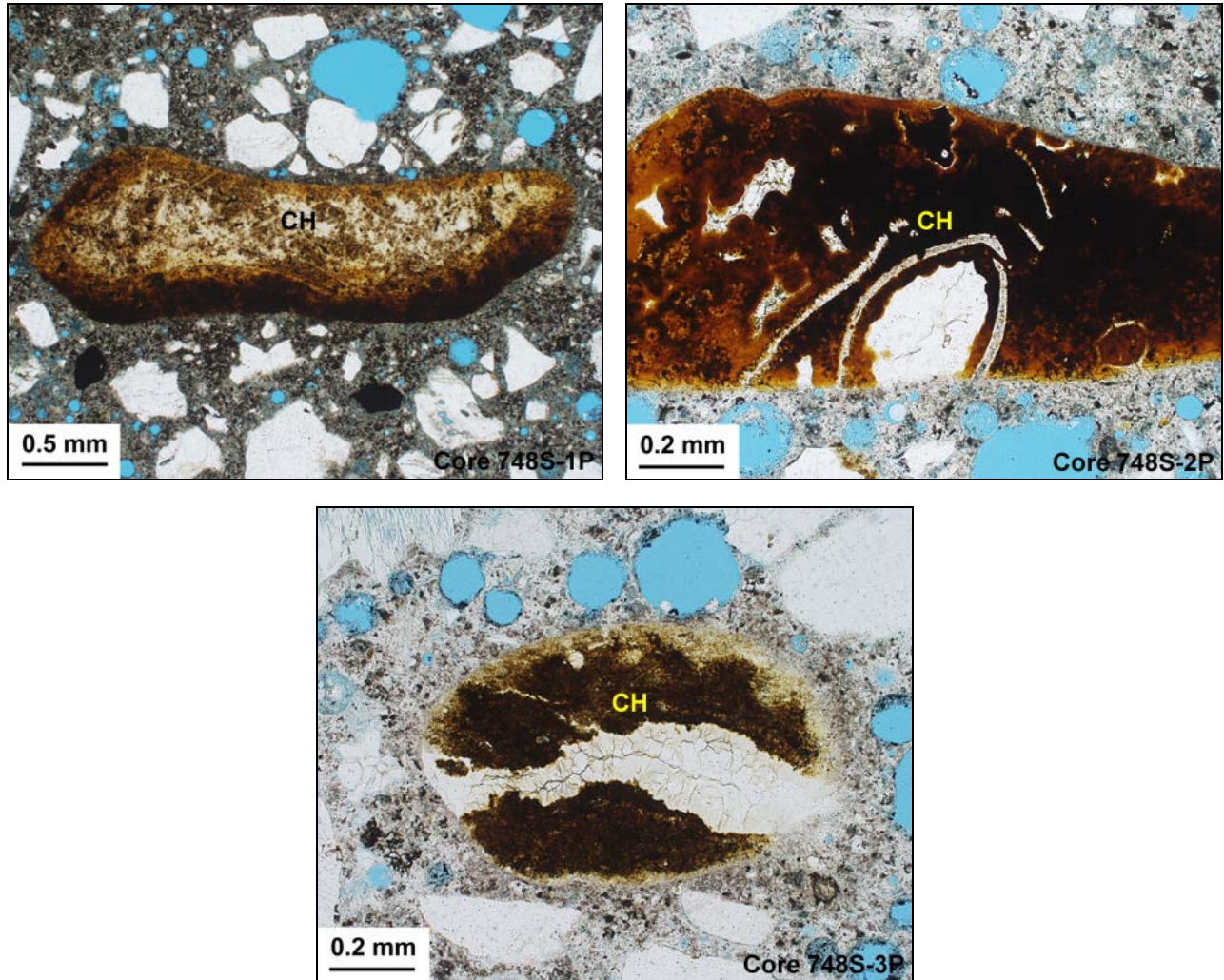


Figure 13 (cont'd.): PPL photomicrographs illustrating examples of the chert identified in the fine aggregate.

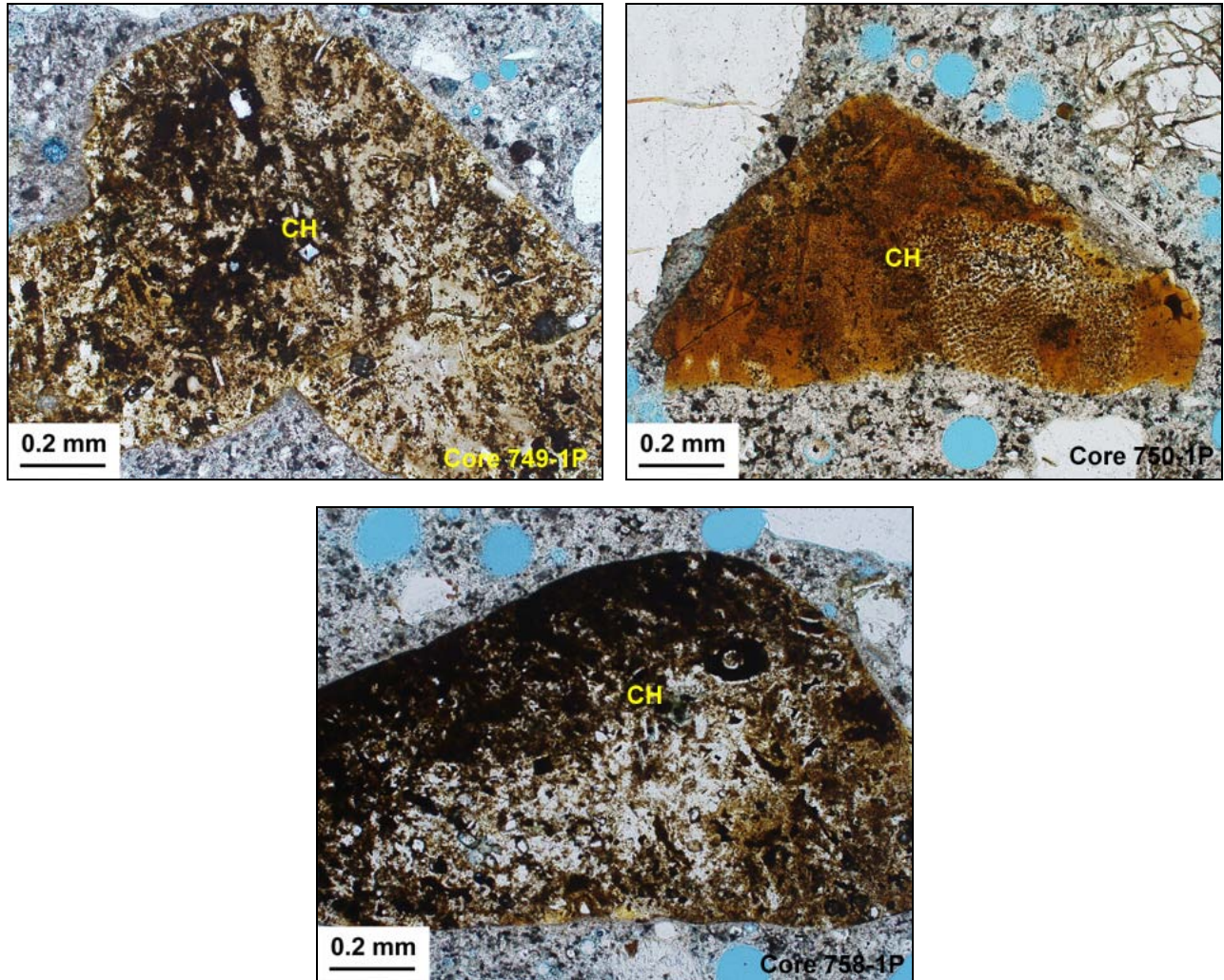
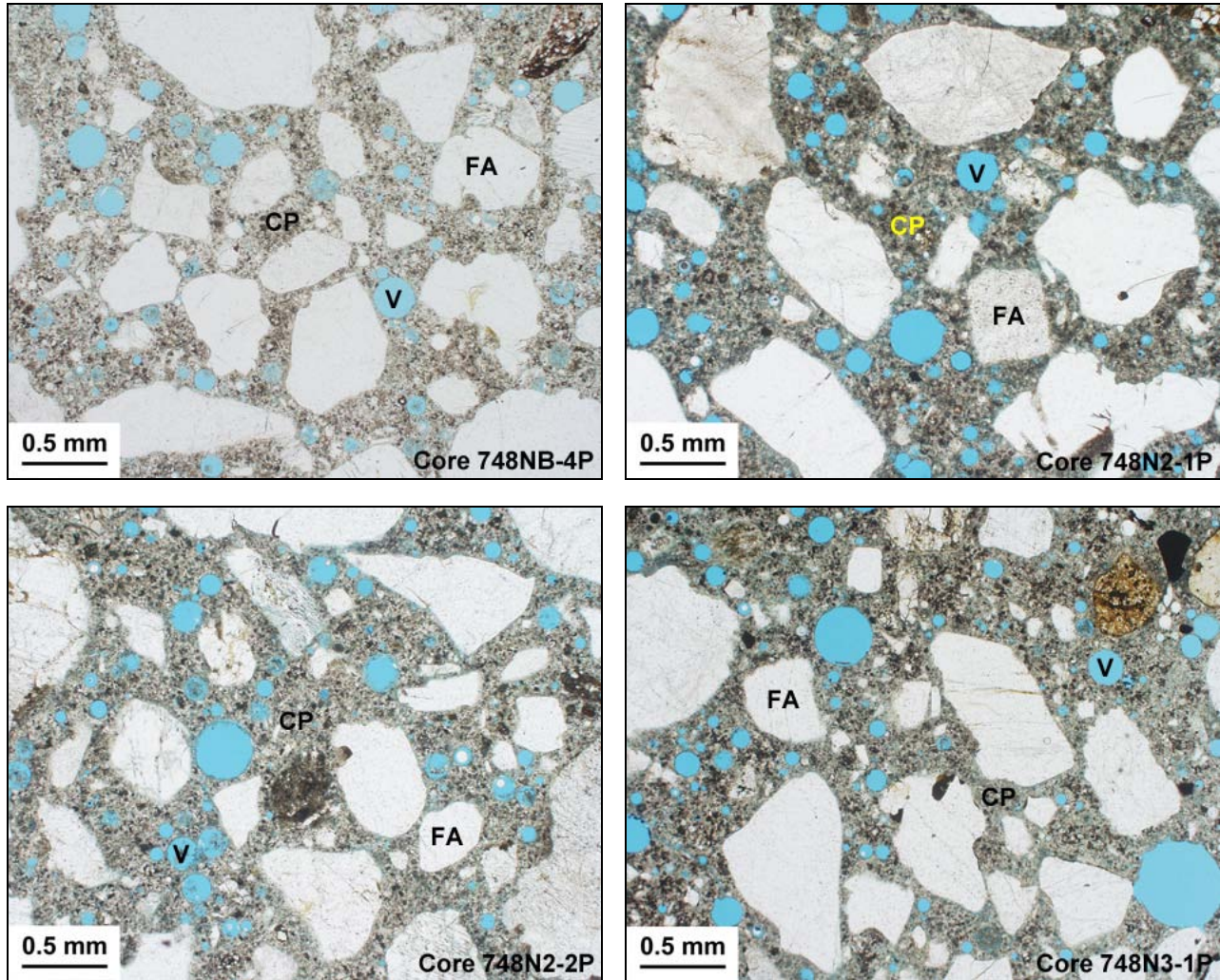


Figure 13 (cont'd.): PPL photomicrographs illustrating examples of the chert identified in the fine aggregate.



**Figure 14:** PPL photomicrographs illustrating the overall microstructure of the structural concrete. There is some variability in water contents and entrained-air development that result in some quality differences. In all of the examined samples, the cement paste (CP) is well-developed and relatively dense as indicated by the even brown coloration under plane light. The samples are impregnated with a low-viscosity, blue-dyed epoxy in order to highlight cracks, pores, and voids. There is a moderate absorption of the epoxy consistent with moderate mix water contents. The fine aggregate (FA) is well distributed throughout the matrix. The sand is somewhat coarse-grained but otherwise well-graded. Fine, spherical voids (V) indicate intentional air-entrainment in all cores though the air content is sparse in Core 748S-1P. In contrast, air volumes may be considered somewhat excessive in Cores 748S-3P, 750-1P and 758-1P.

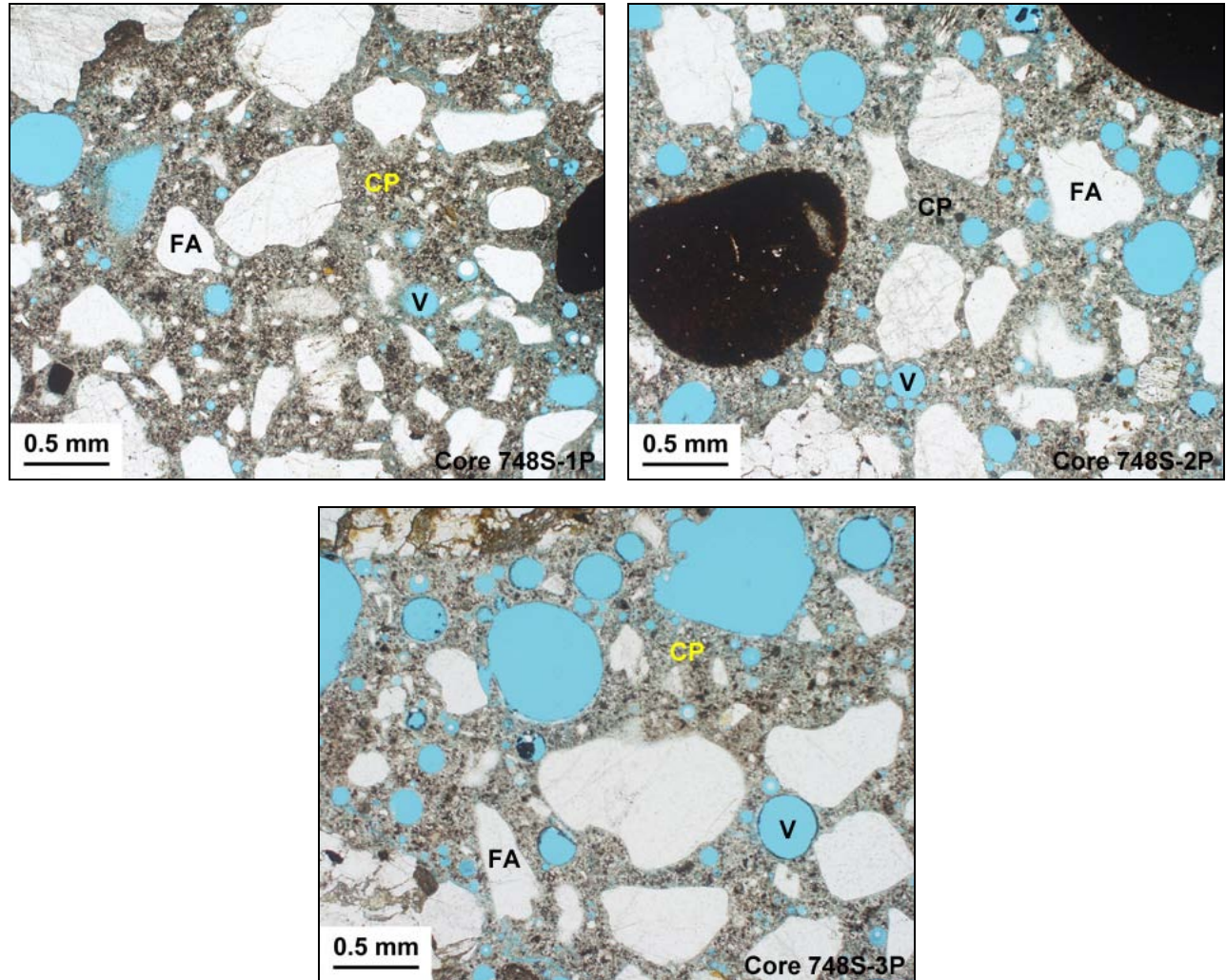


Figure 14 (cont'd.): PPL photomicrographs illustrating the overall microstructure of the structural concrete.

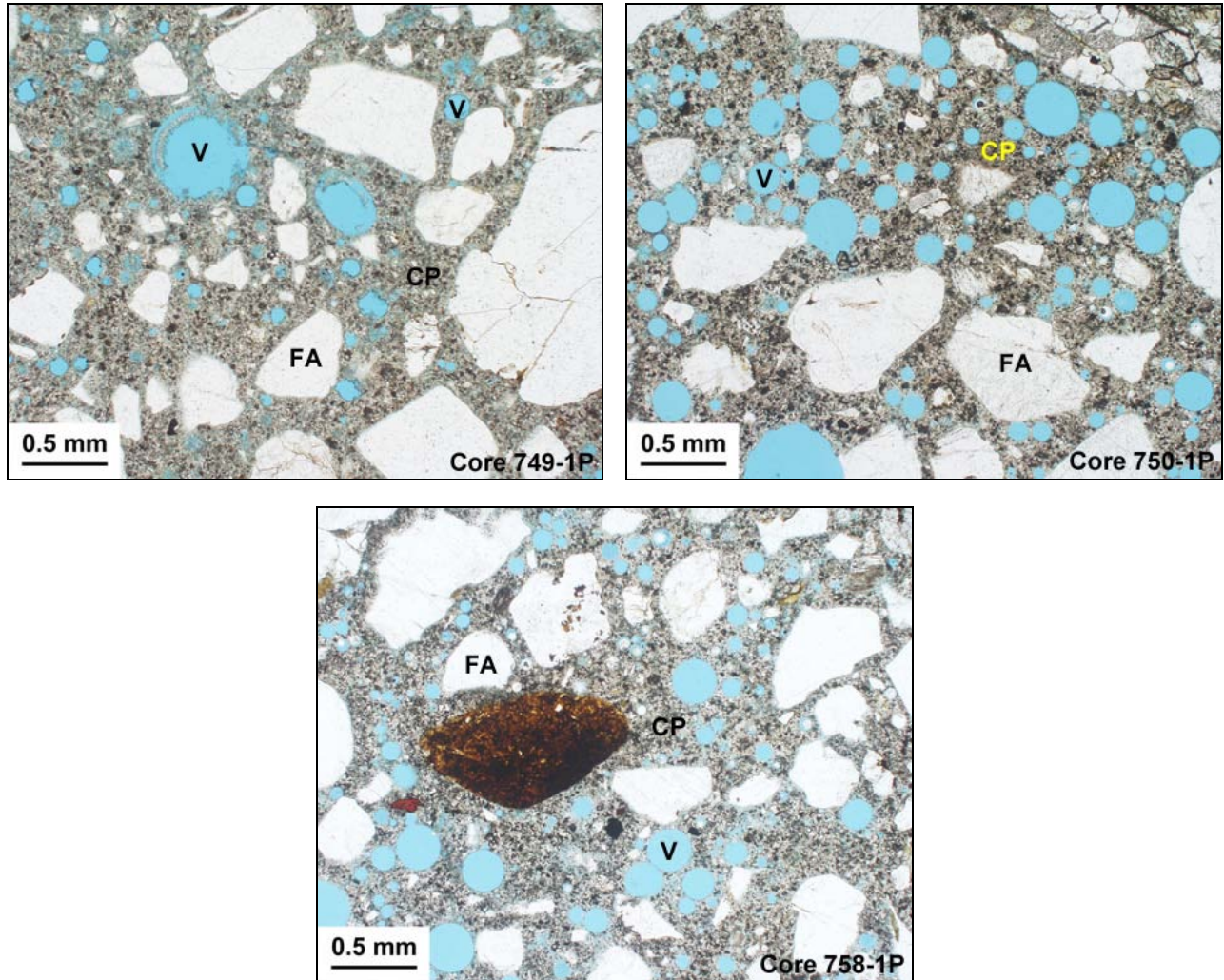
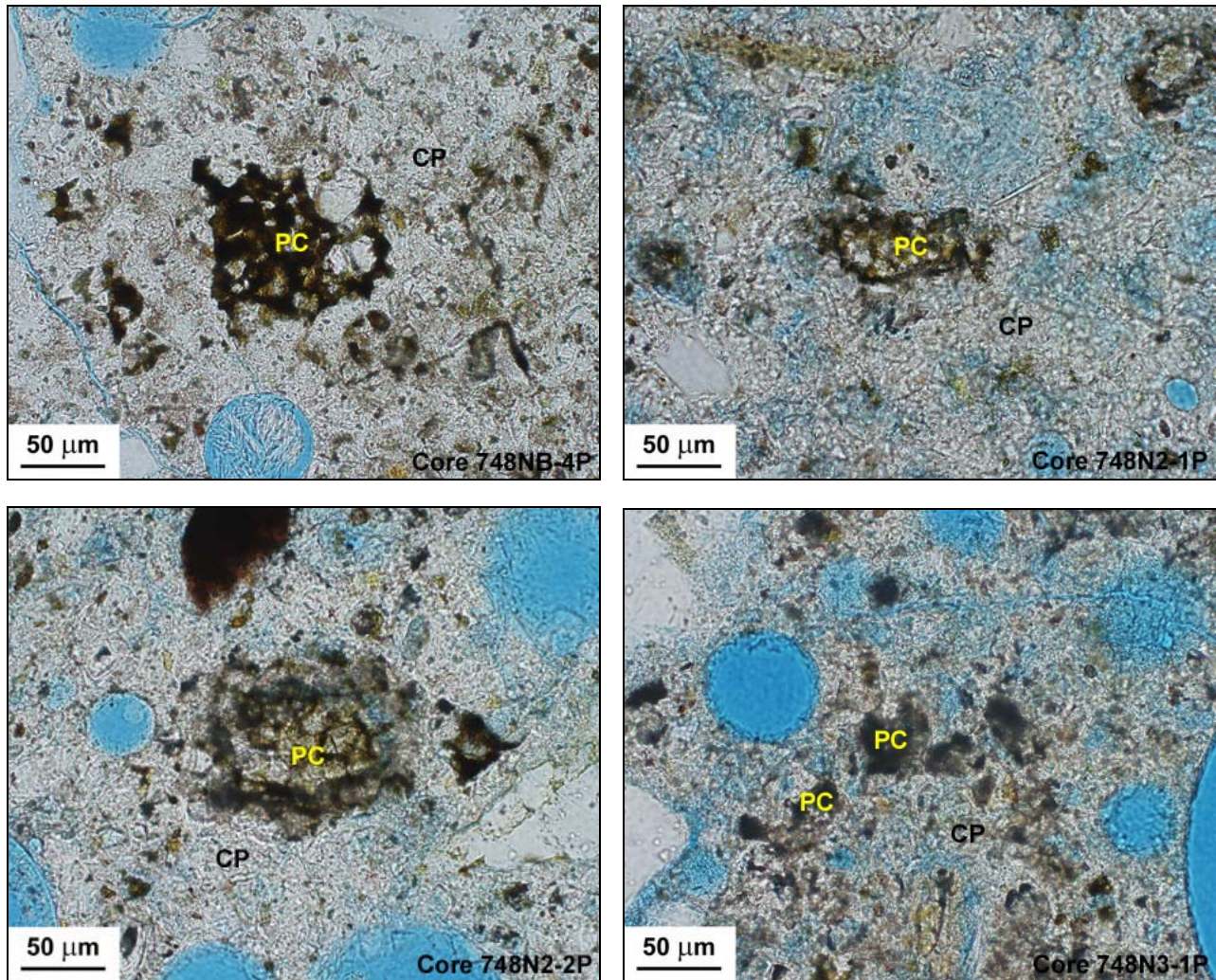


Figure 14 (cont'd.): PPL photomicrographs illustrating the overall microstructure of the structural concrete.



**Figure 15:** PPL photomicrographs illustrating the occurrence of residual portland cement (PC) in the examined concrete. The cement hydration is advanced and most calcium silicate is fully consumed. These appear as light-colored areas within the cement agglomerates. Exceptions are shown for Cores 748N2-2P, 748S-1P, 750-1P, and 758-1P where belite remains unhydrated. For Core 748S-1P, an area is shown where some of the empty pores are now filled with an amorphous cementitious hydrate. All of the cement residuals are fine to medium-grained agglomerates with brown-colored interstitial ferrite. The adjacent cement paste (CP) is well-formed in all samples.

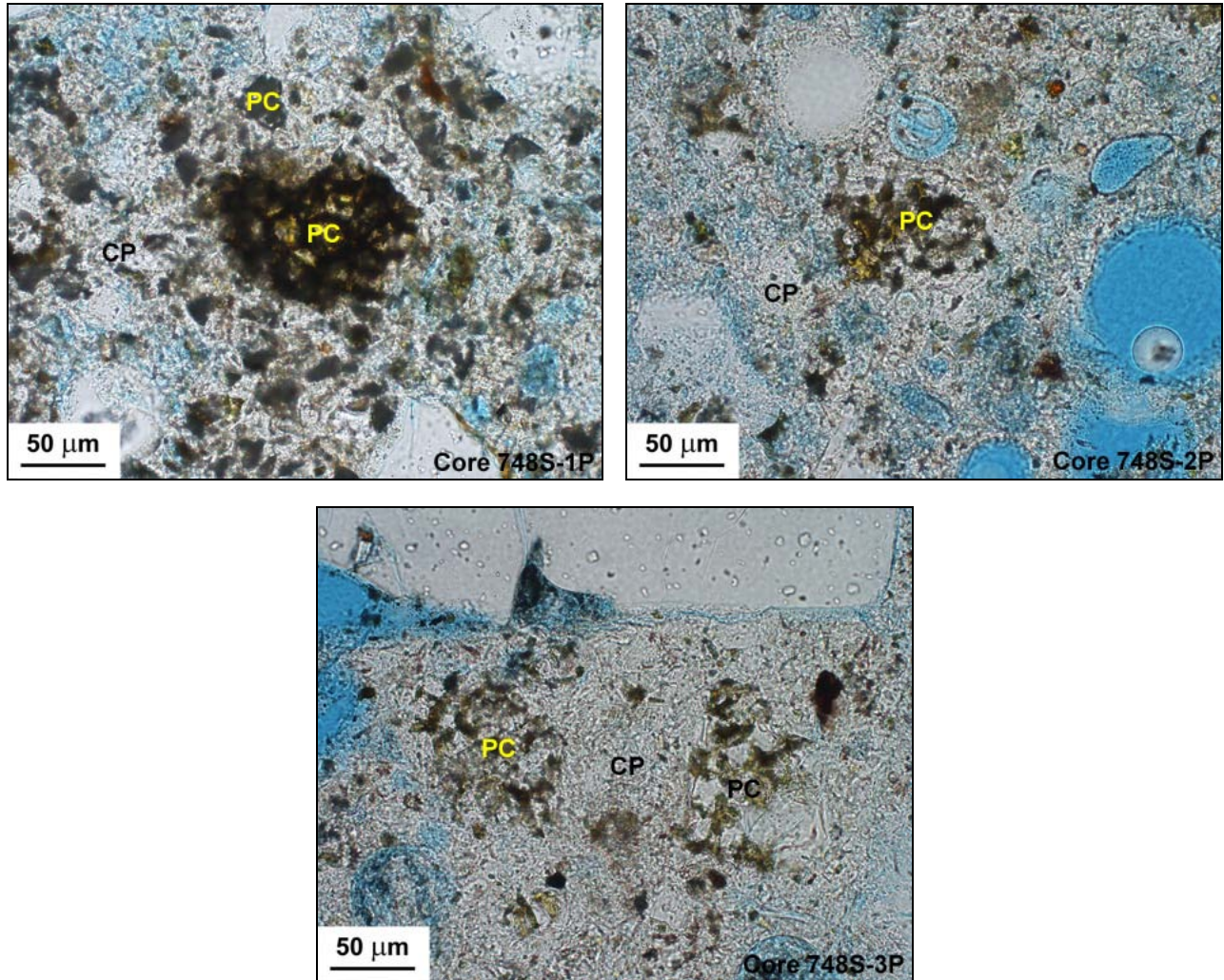


Figure 15 (cont'd.): PPL photomicrographs illustrating the occurrence of residual portland cement (PC) in the examined concrete.

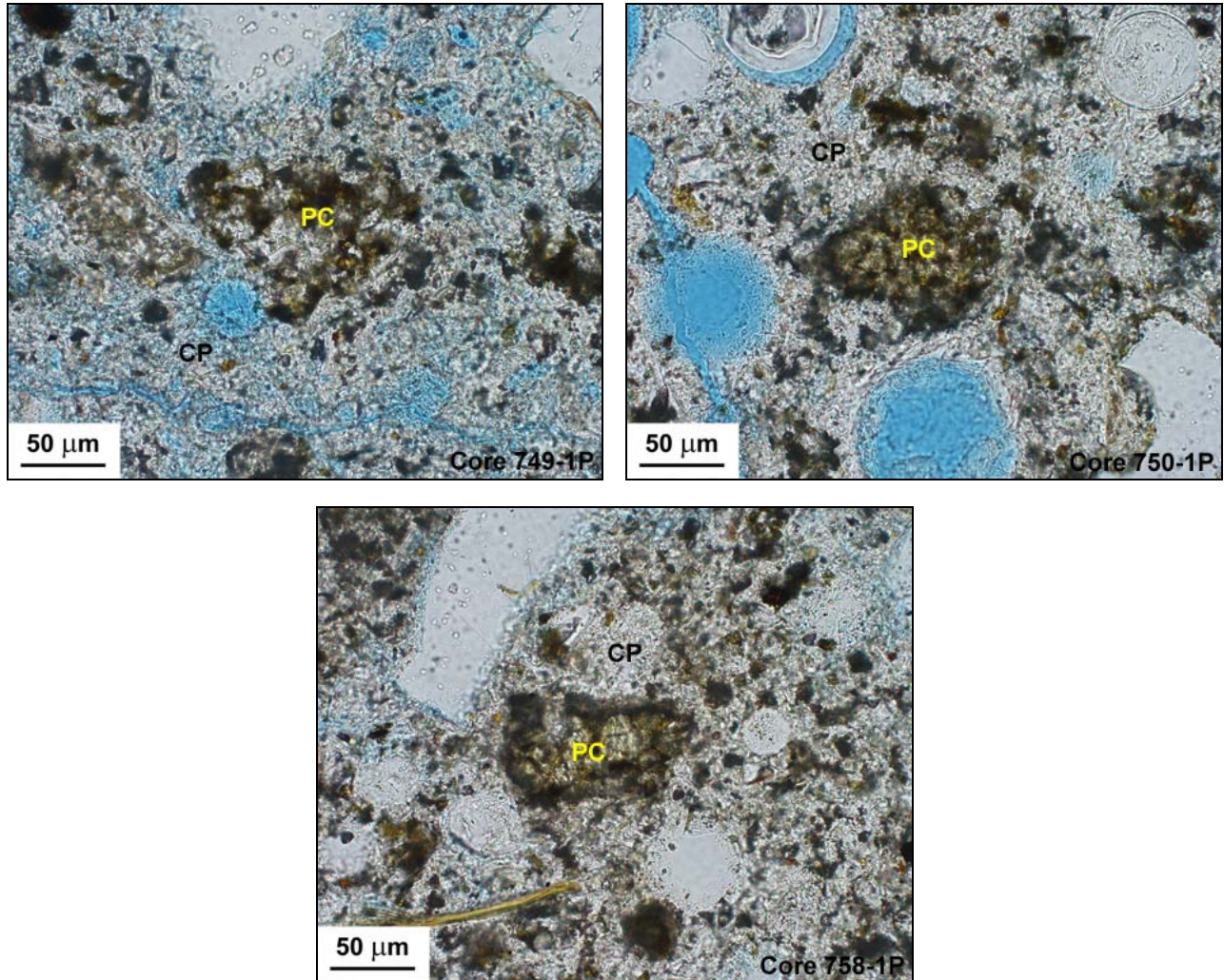
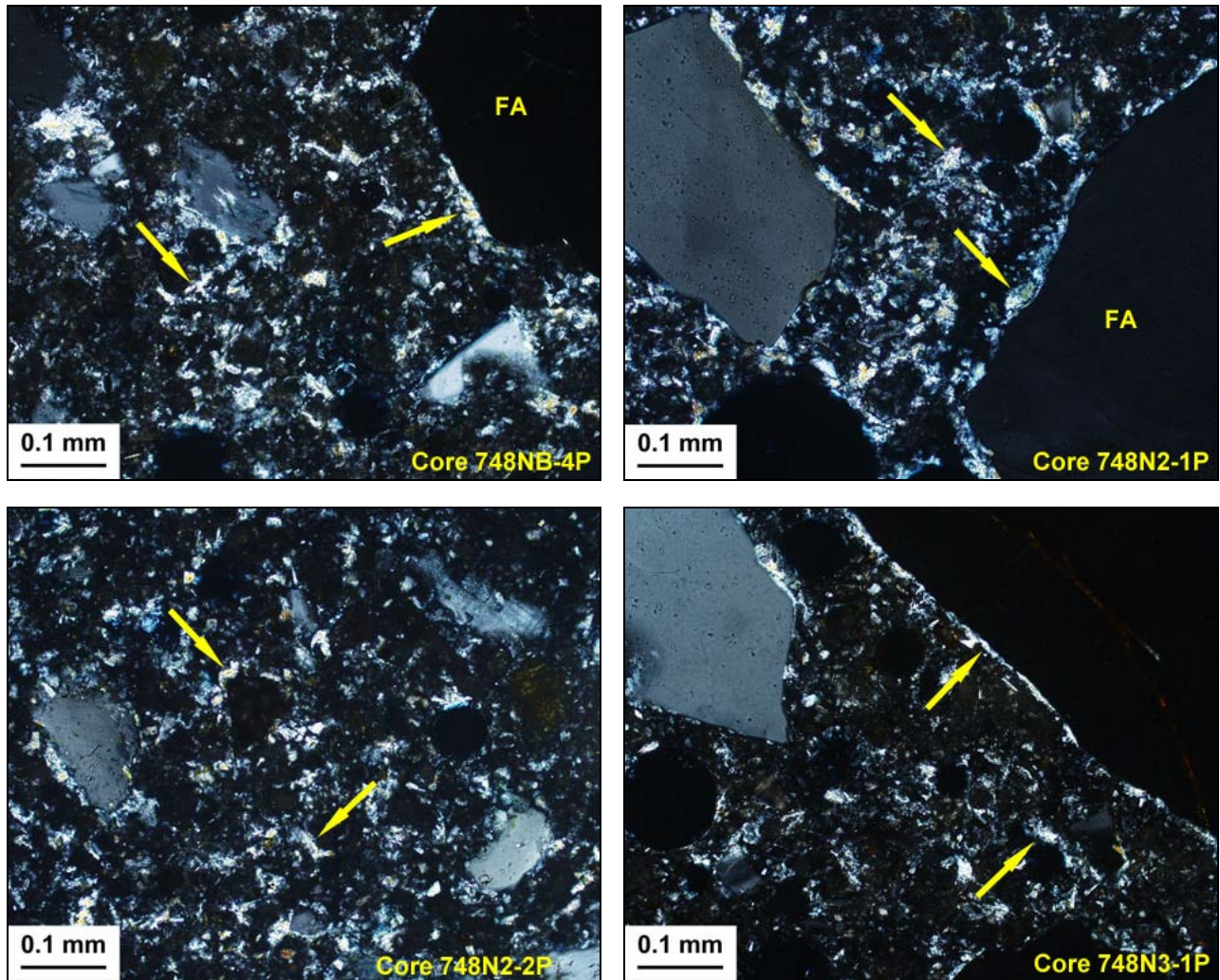
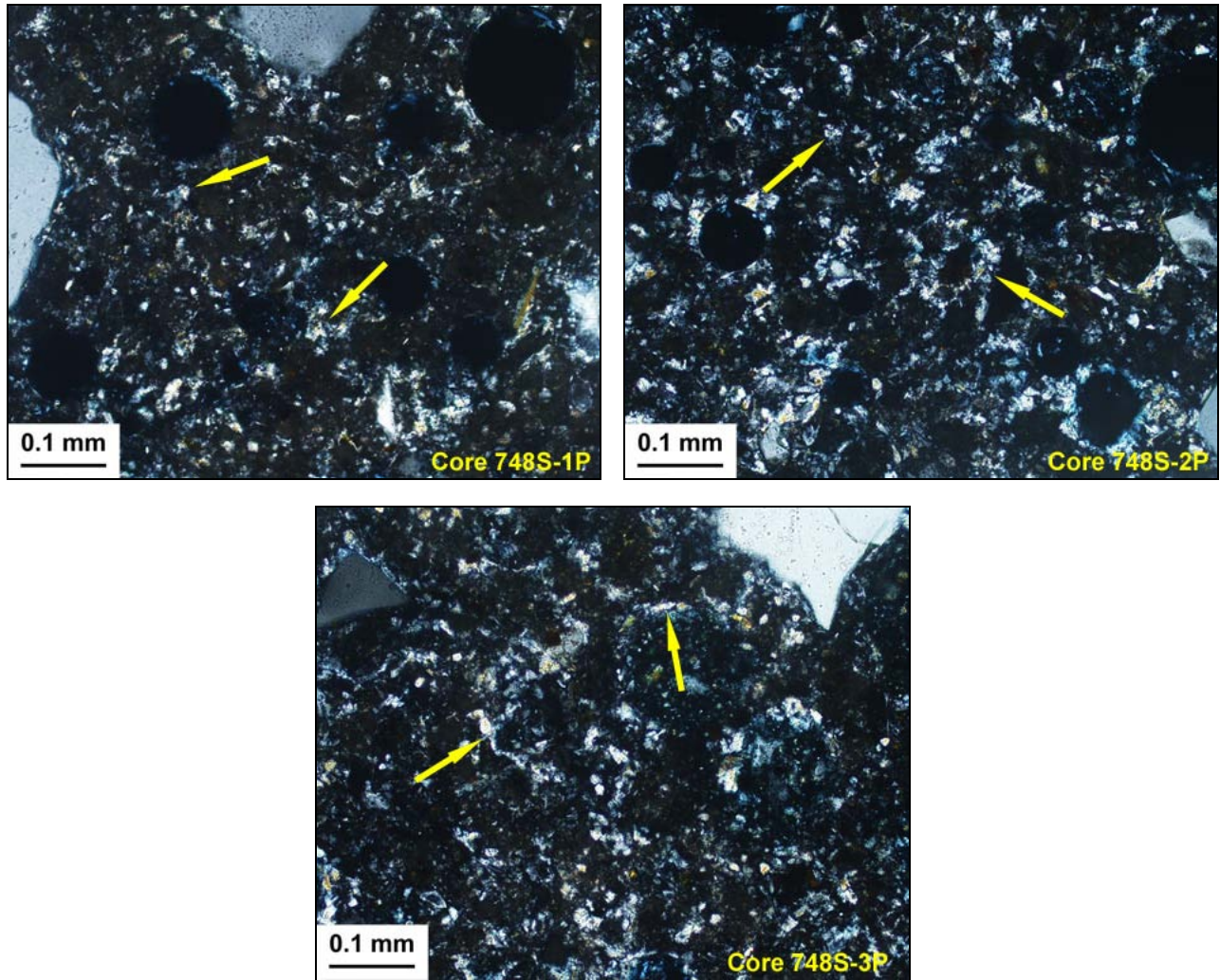


Figure 15 (cont'd.): PPL photomicrographs illustrating the occurrence of residual portland cement (PC) in the examined concrete.



**Figure 16:** XPL photomicrographs illustrating the occurrence of primary calcium hydroxide produced during the cement hydration. The hydroxide (arrows) is evenly distributed throughout the paste. Crystal size and morphology varies somewhat between samples but the non-compact morphologies are generally indicative of moderate mix water contents. Note that in some cases, semi-continuous deposits of the hydroxide line fine aggregate surfaces (FA).



**Figure 16 (cont'd.):** XPL photomicrographs illustrating the occurrence of primary calcium hydroxide produced during the cement hydration.

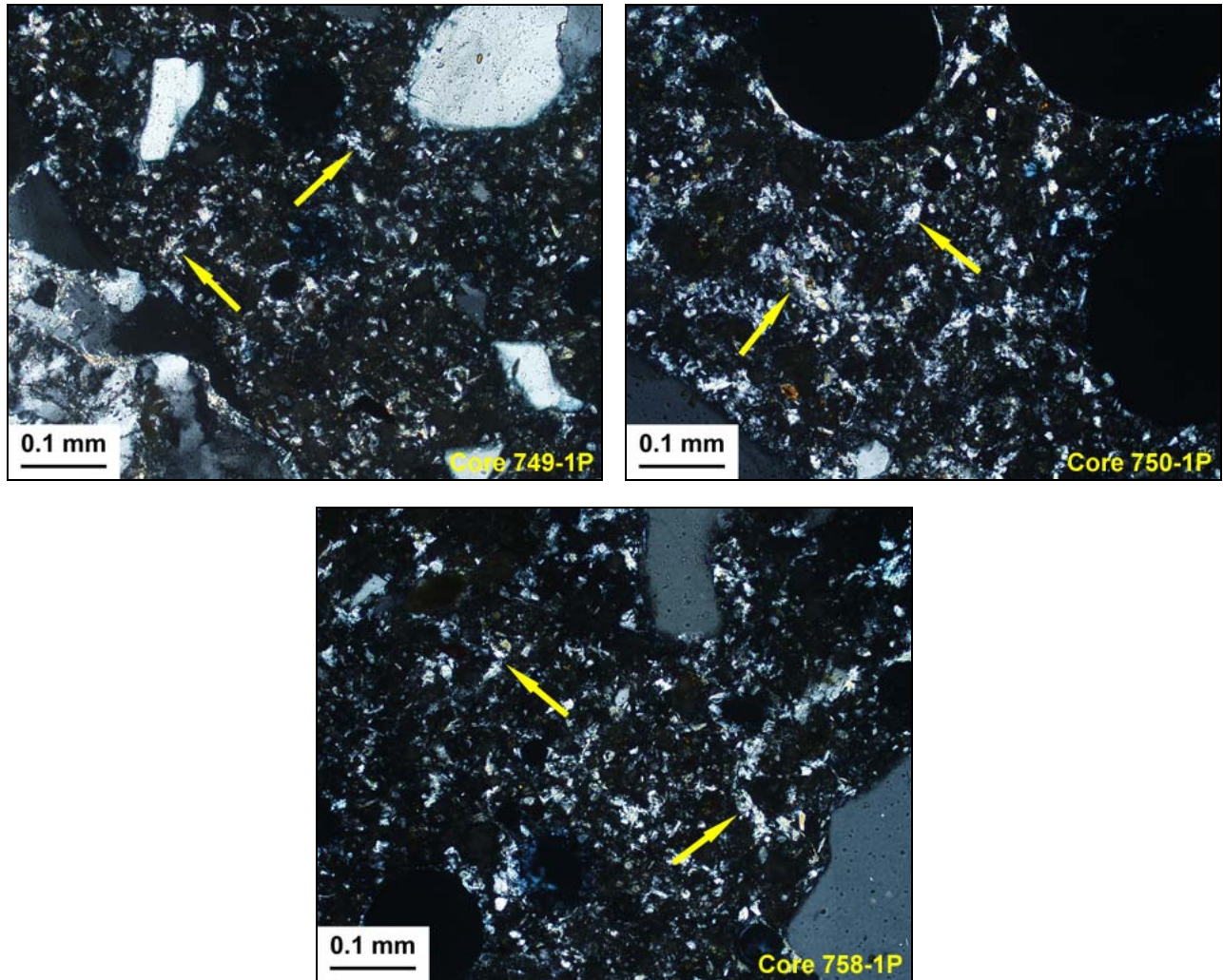


**Figure 16 (cont'd.):** XPL photomicrographs illustrating the occurrence of primary calcium hydroxide produced during the cement hydration.

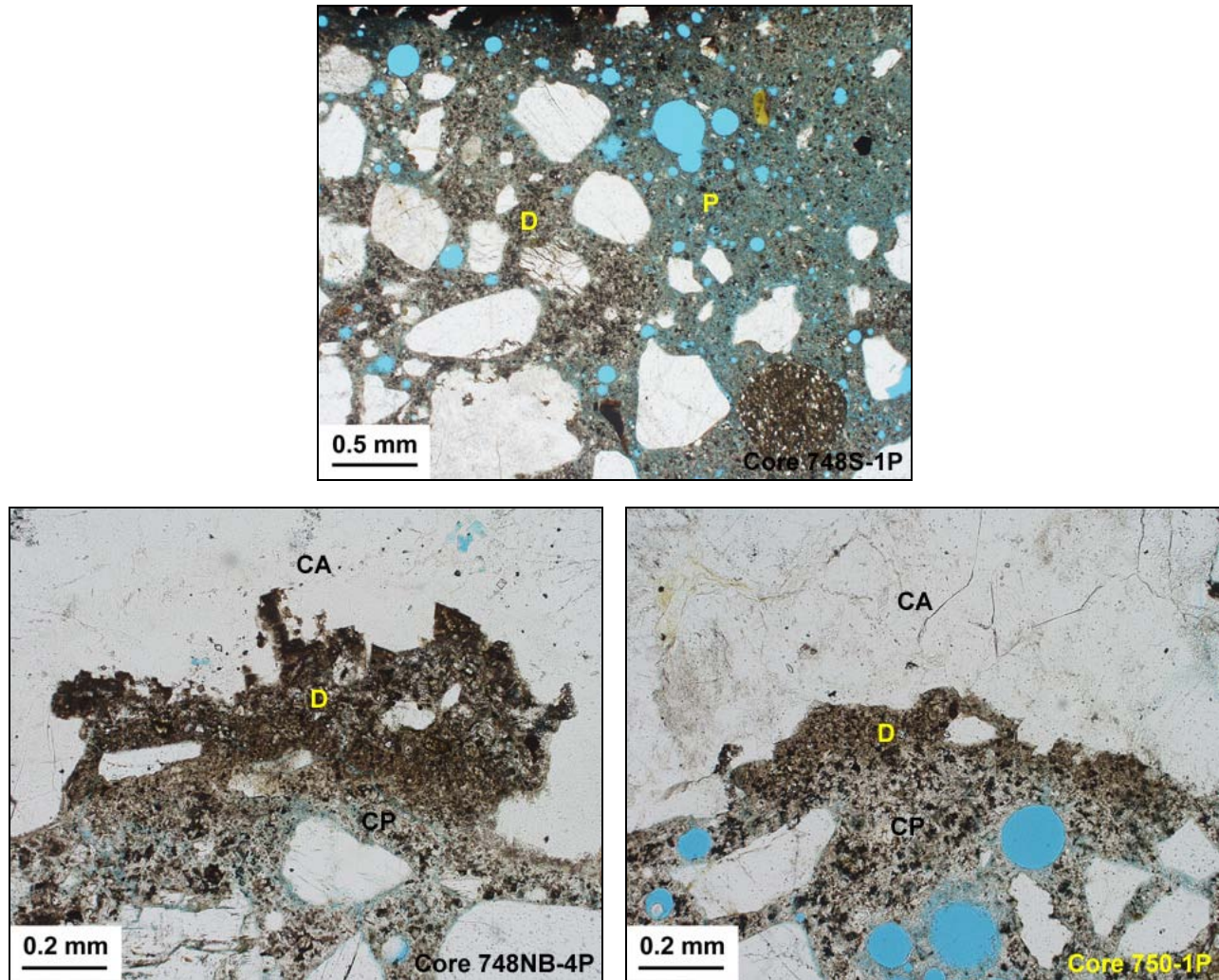


**Figure 17:** (Upper image) Evidence for some bleed water development and migration is only found in Core 748S-1P as shown in this PPL photomicrograph. Note the juxtaposition of denser (D) and more porous zones (P) within the cement paste. The variation in local porosity is evidenced by the difference in the absorption of blue-dyed epoxy used in the sample preparation. The porosity is caused by the presence of evaporable water in the fresh mixture. (Lower PPL images) Thin discontinuous linings of dense cement paste (D) are also found between the “normal” cement paste (CP) and coarse aggregate (CA) in Cores 748NB-4P and 750-1P. These represent small bits of cement that did not fully incorporate with the mix water. However, they are more likely the result of microscopic embayments along aggregate surfaces and not indicative of inappropriate retempering.

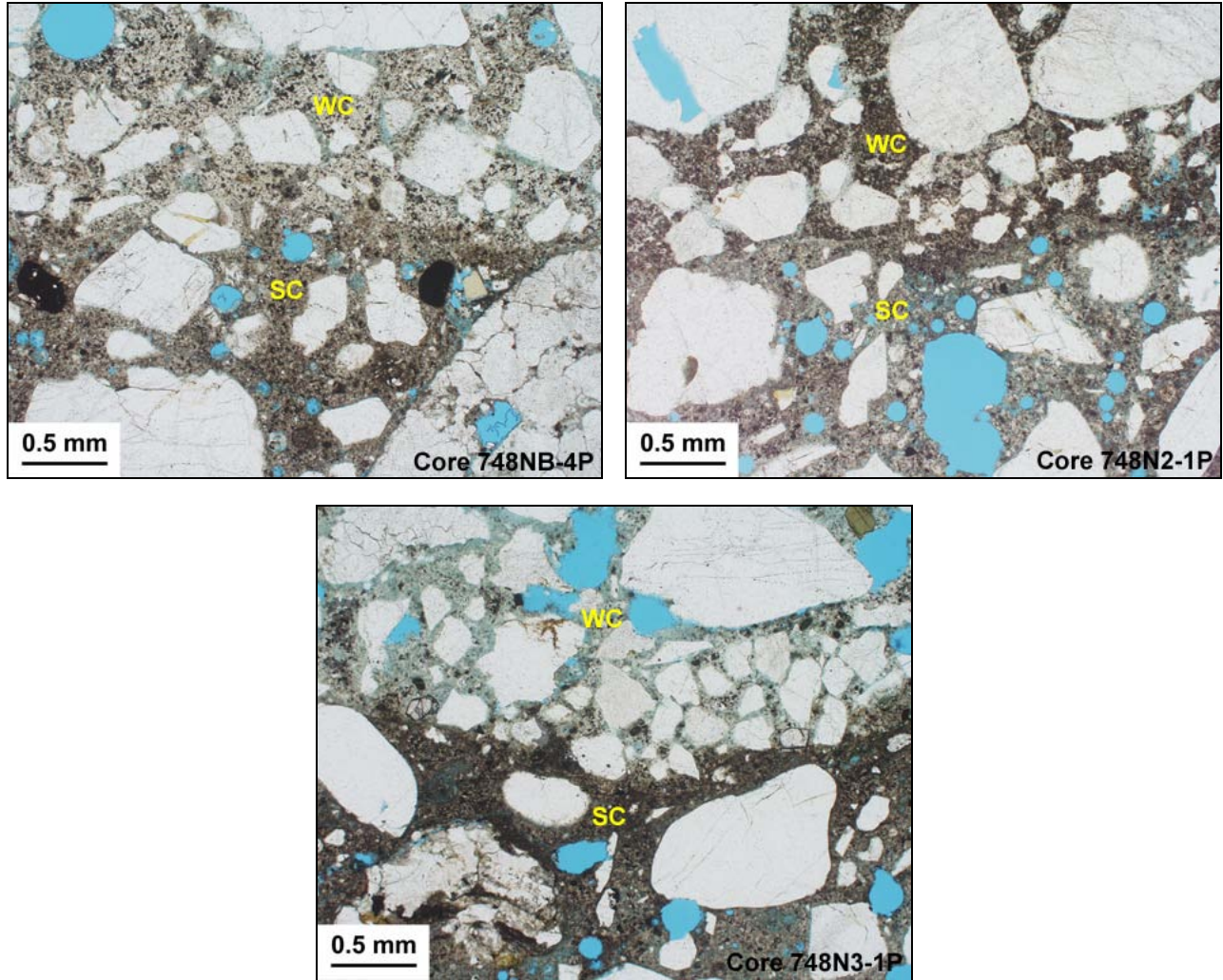


**Figure 18:** PPL photomicrographs illustrating the tight contacts between wear course (WC) and structural concrete (SC) in nine of the ten core samples. A crack (C) intervenes only in Core 749-1P and this is related to later alkali-silica reactions.

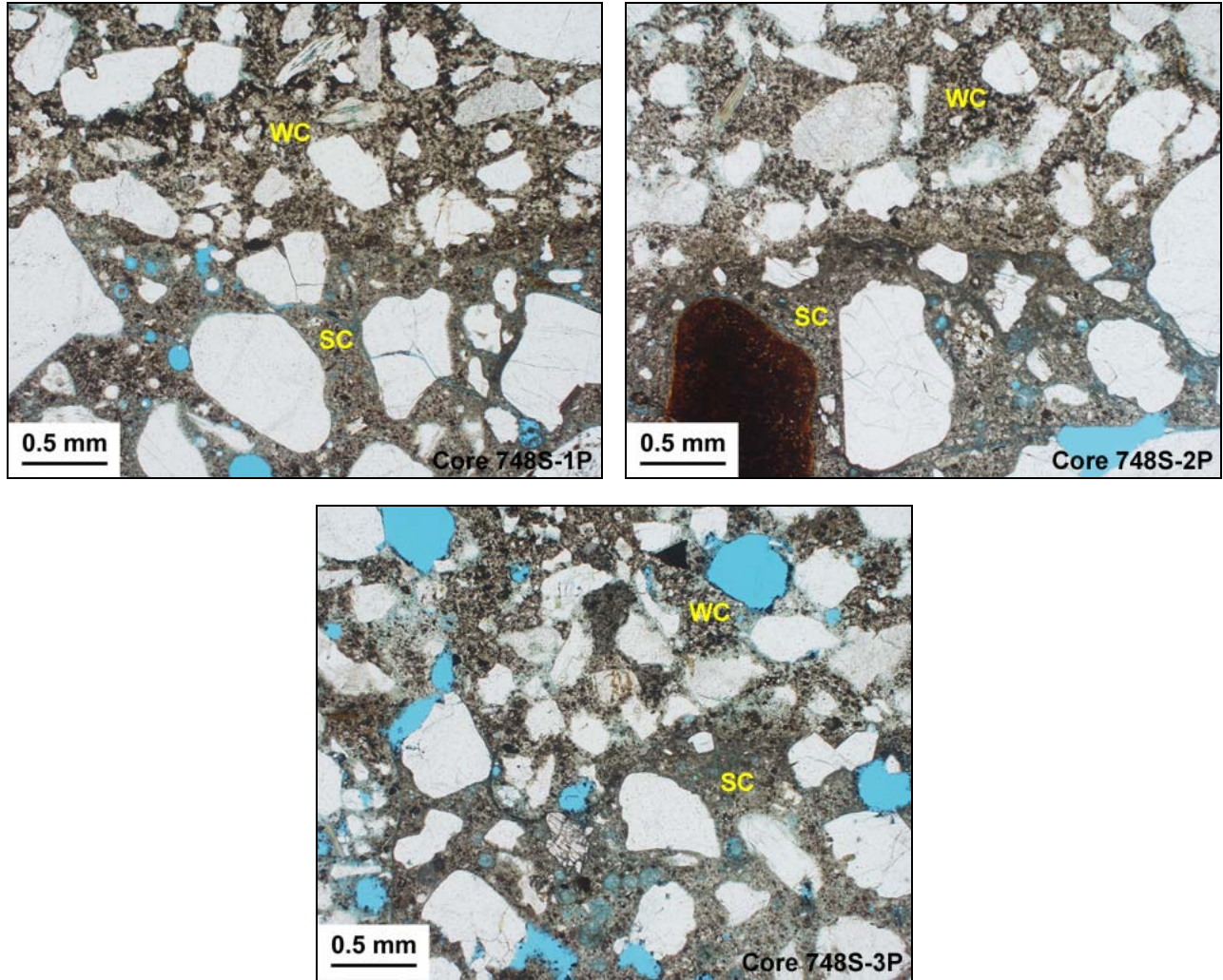


**Figure 18 (cont'd.):** PPL photomicrographs illustrating the tight contacts between wear course (WC) and structural concrete (SC) in nine of the ten core samples.

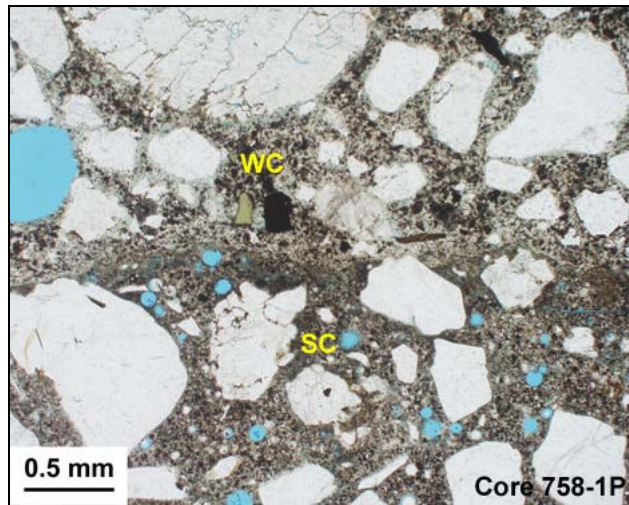
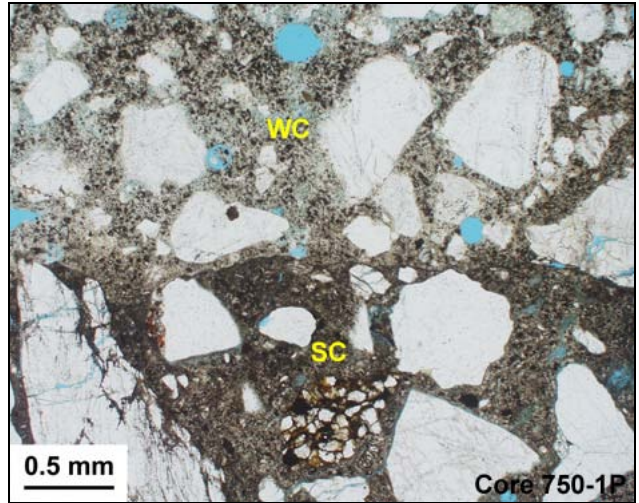
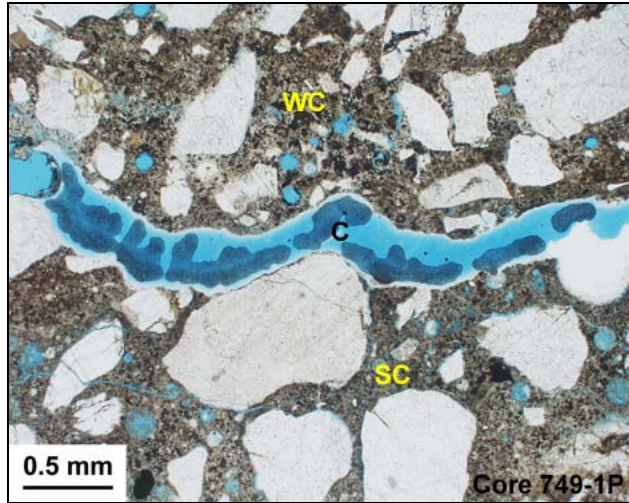


**Figure 18 (cont'd.):** PPL photomicrographs illustrating the tight contacts between wear course (WC) and structural concrete (SC) in nine of the ten core samples.

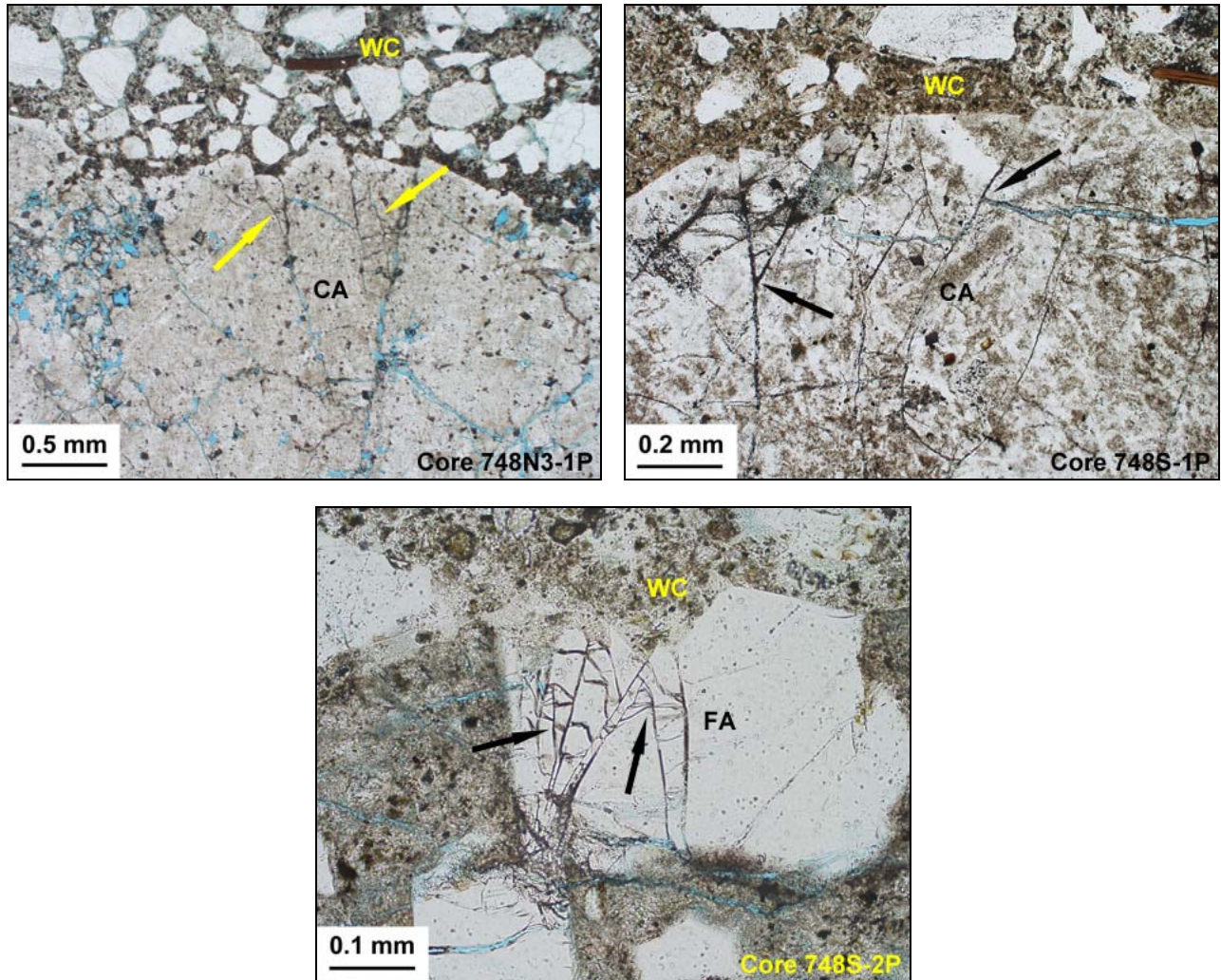


**Figure 19:** PPL photomicrographs illustrating evidence for scarification of the concrete substrate in three of the examined core samples. The arrows indicate “shatter” cracks within coarse aggregate (CA) and fine aggregate grains (FA) that are truncated just below the wear course (WC). The interior of the affected particles are offset by these cracks indicating local deformation of an originally exposed surface.

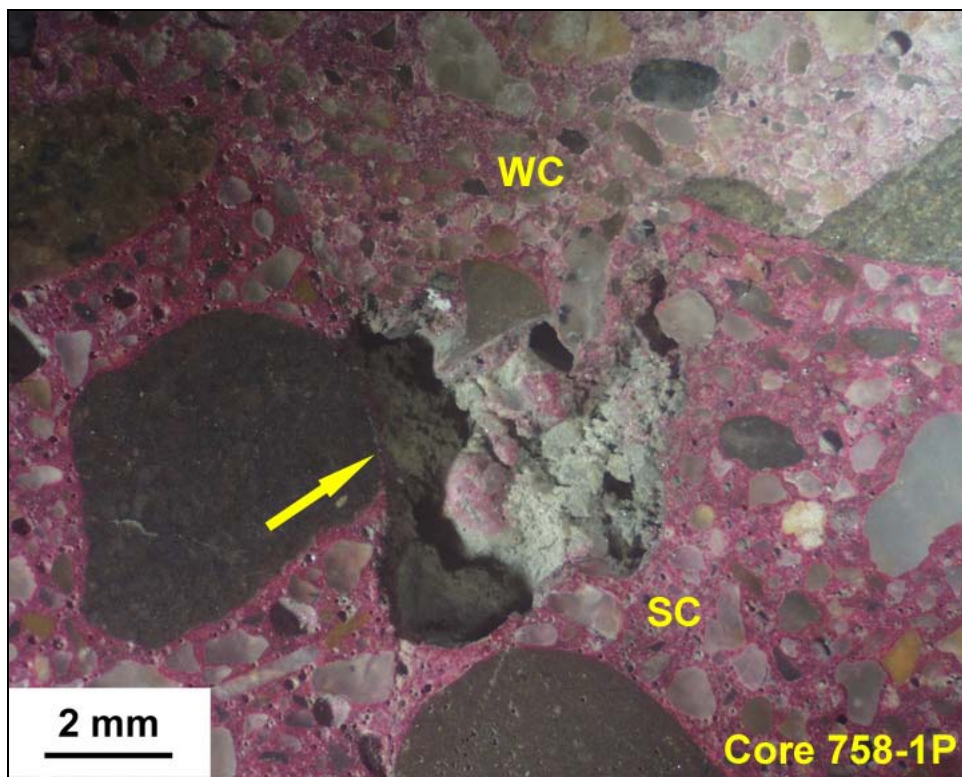


**Figure 20:** Reflected light photomicrograph. In Core 758-1P, thin “fingers” of wear course (WC) appear plastically embedded in the structural concrete (SC).

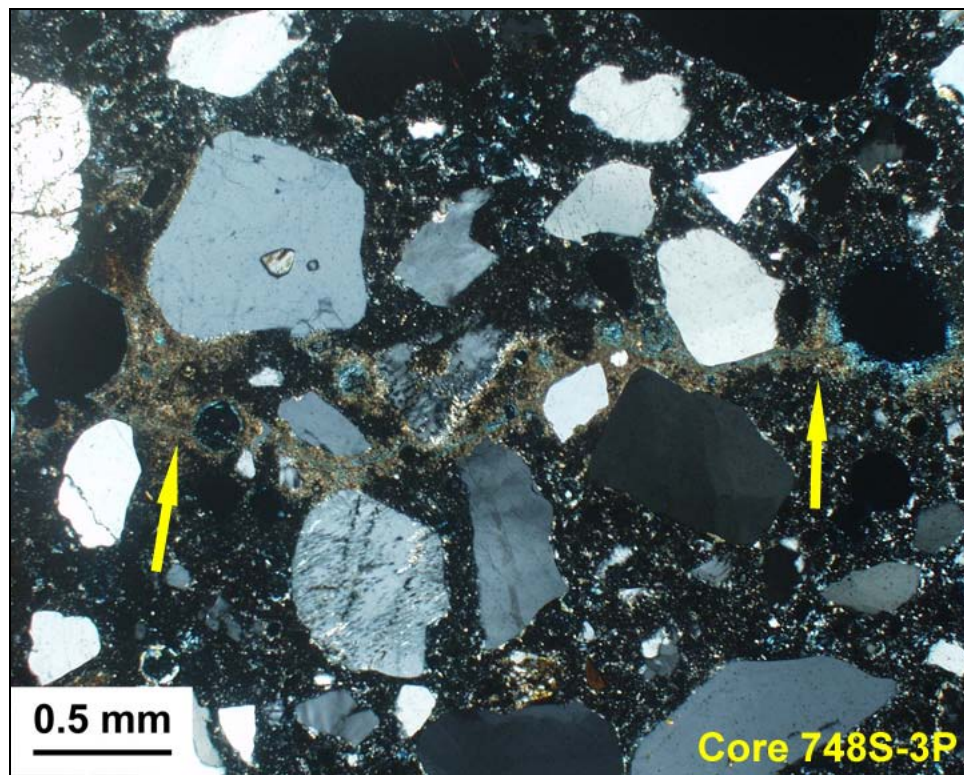


**Figure 21:** Vertical microcracking from the surface of the concrete substrate is only identified in Core 748S-3P. The image is rotated ninety degrees from the actual field orientation in this XPL photomicrograph. The arrows indicate this microcrack which is lined by secondary calcium carbonate. The carbonate appears golden-colored against the uncarbonated cement paste.

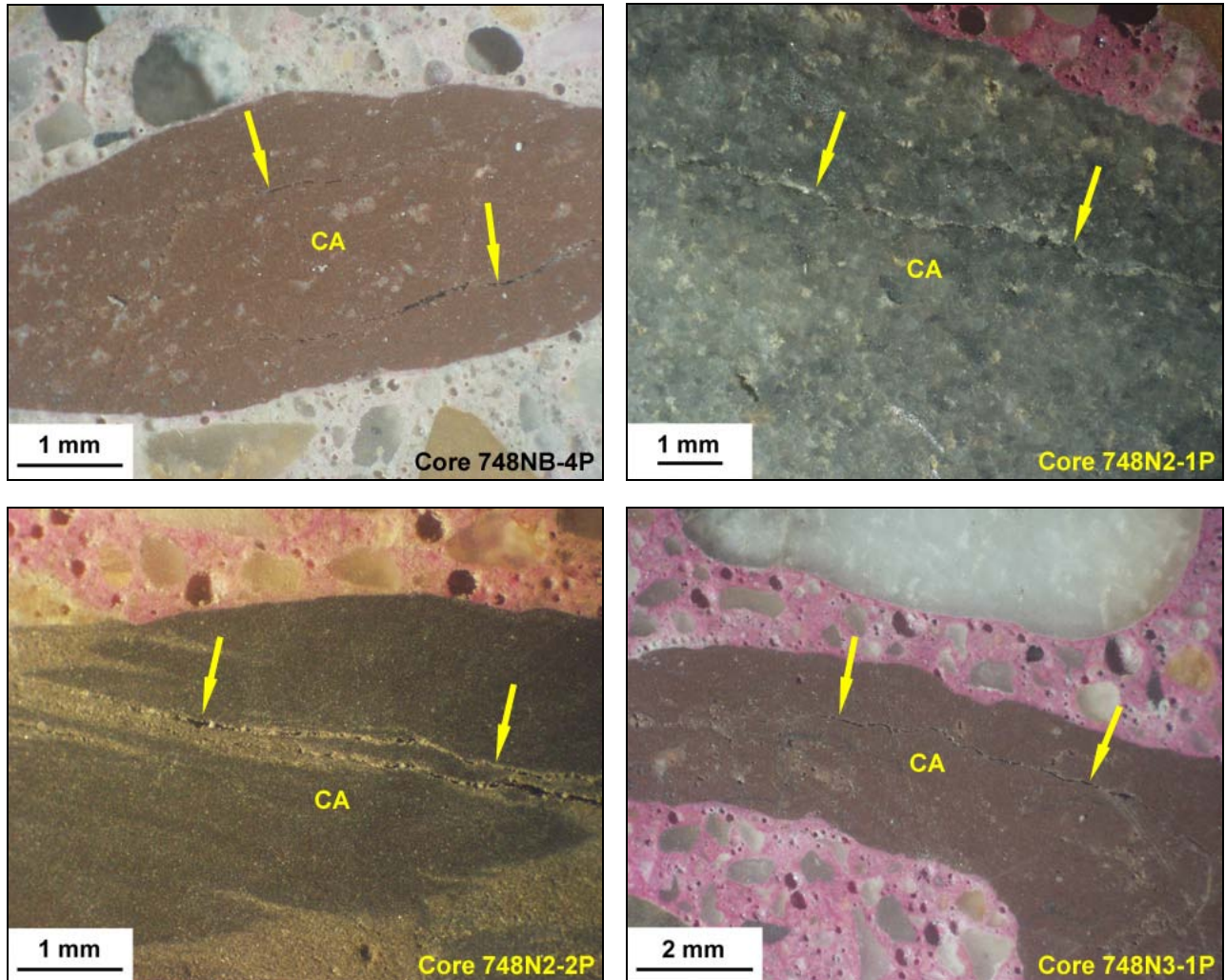


**Figure 22:** Reflected light photomicrographs indicating microcracking visible in honed cross sections of the concrete. The arrows indicate trace microcracks within some of the finer-grained coarse aggregate types (CA). These may be related to some minor dilation occurring during saturated freezing events. The sedimentary rocks are considered more porous than other types of crushed stone aggregate such as limestone, traprock, or granite. In no case do these cracks extend into the adjacent mortar.

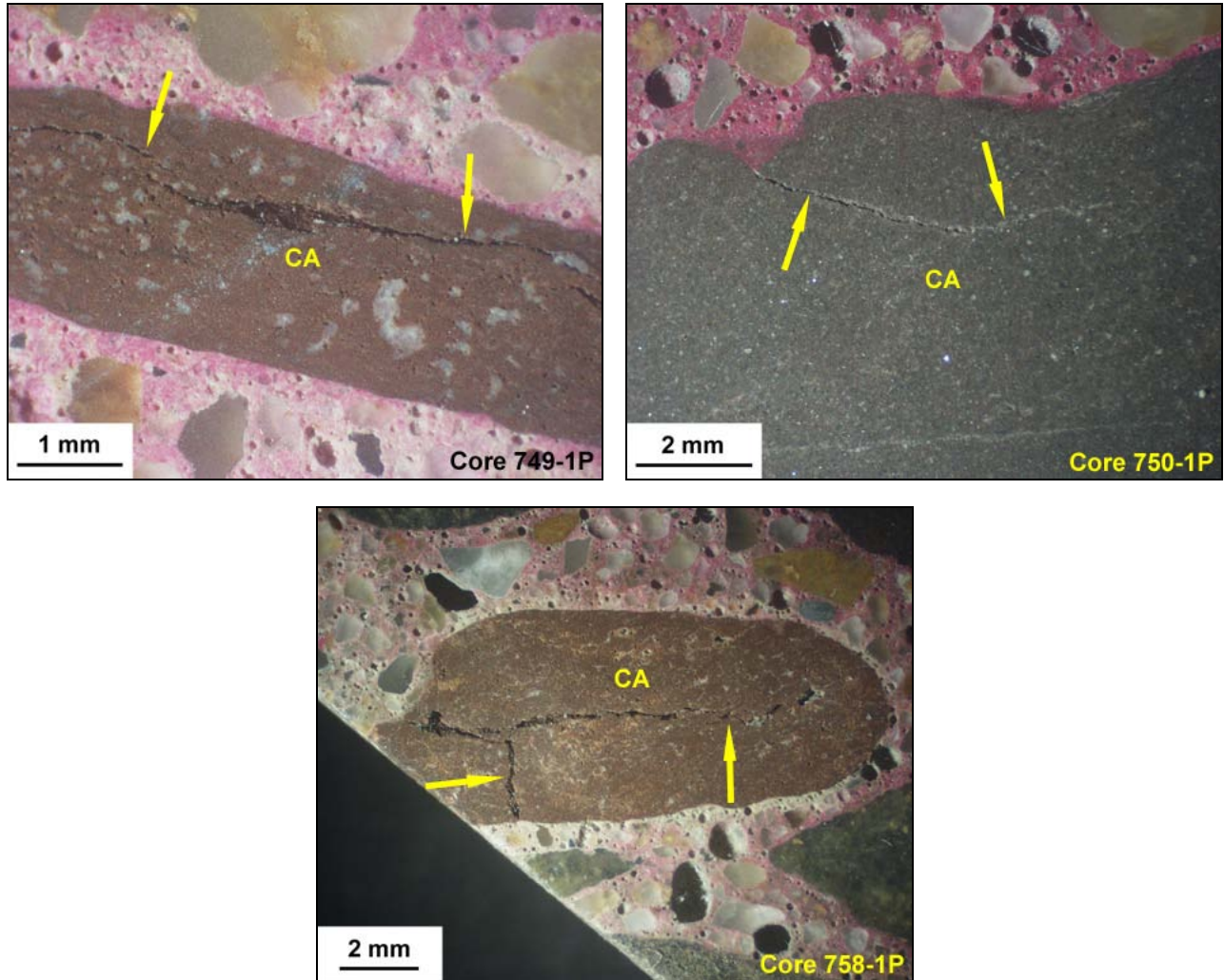
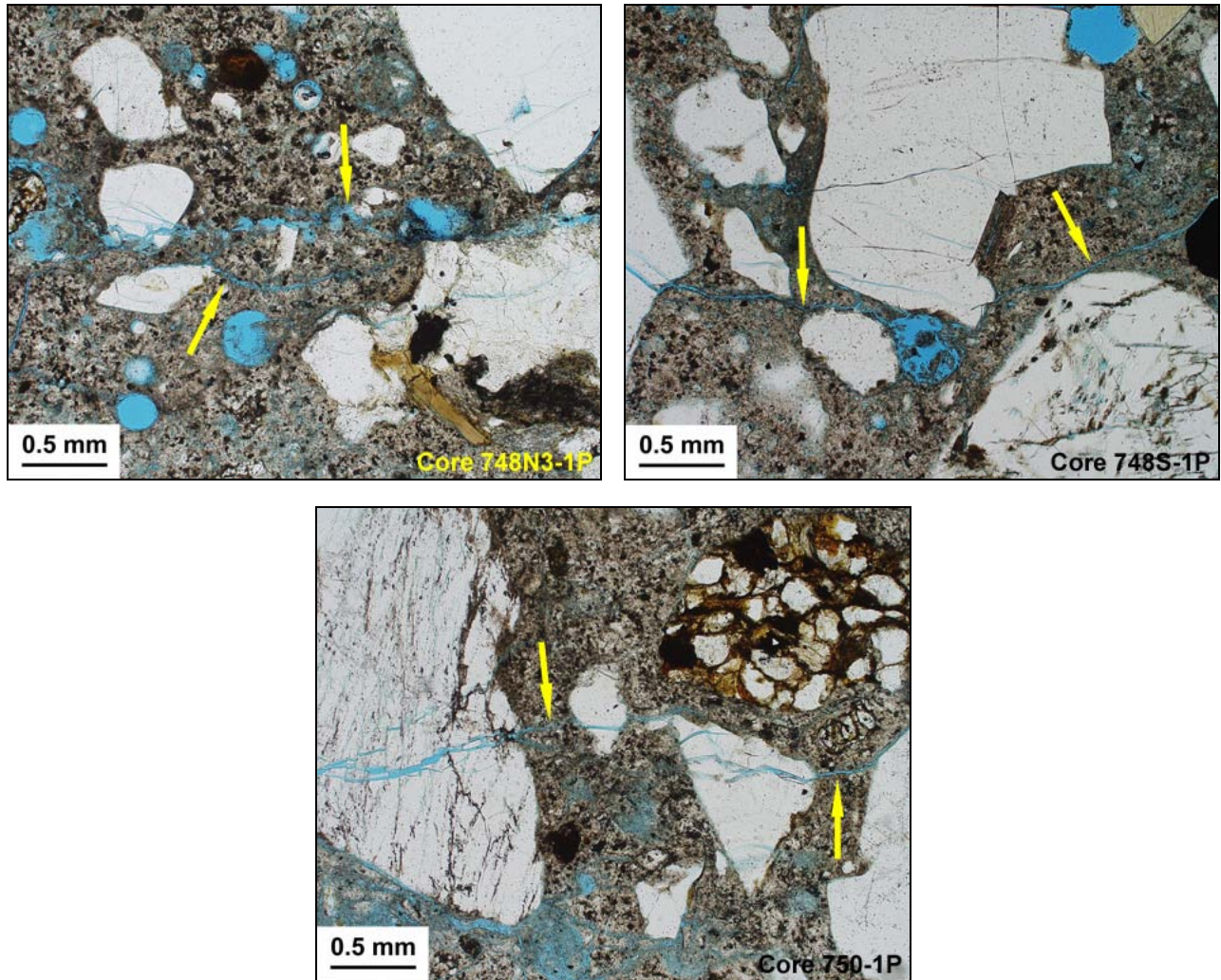
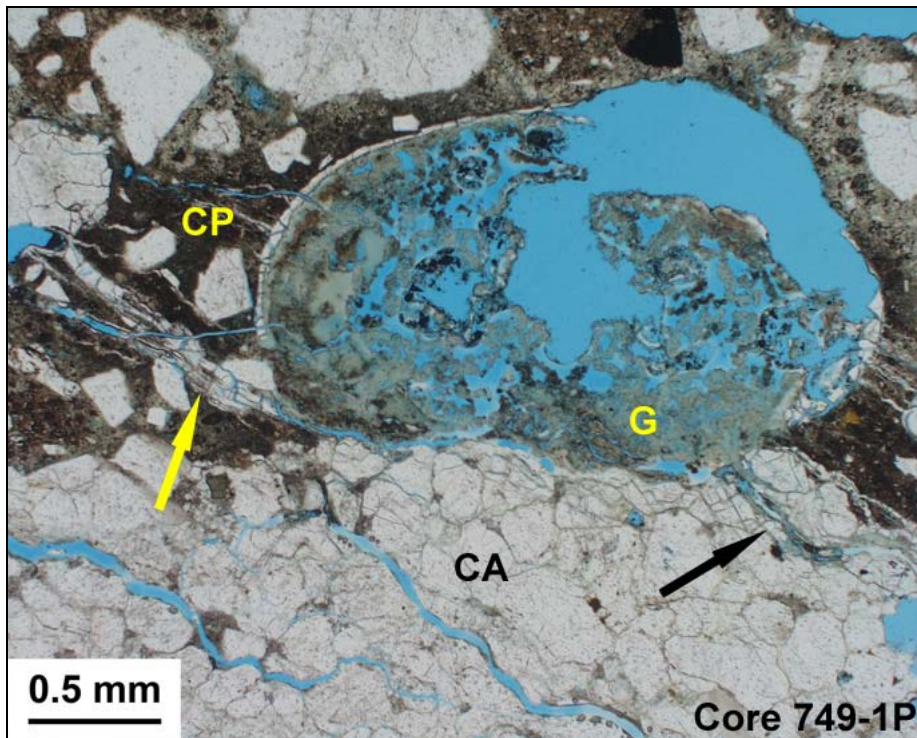
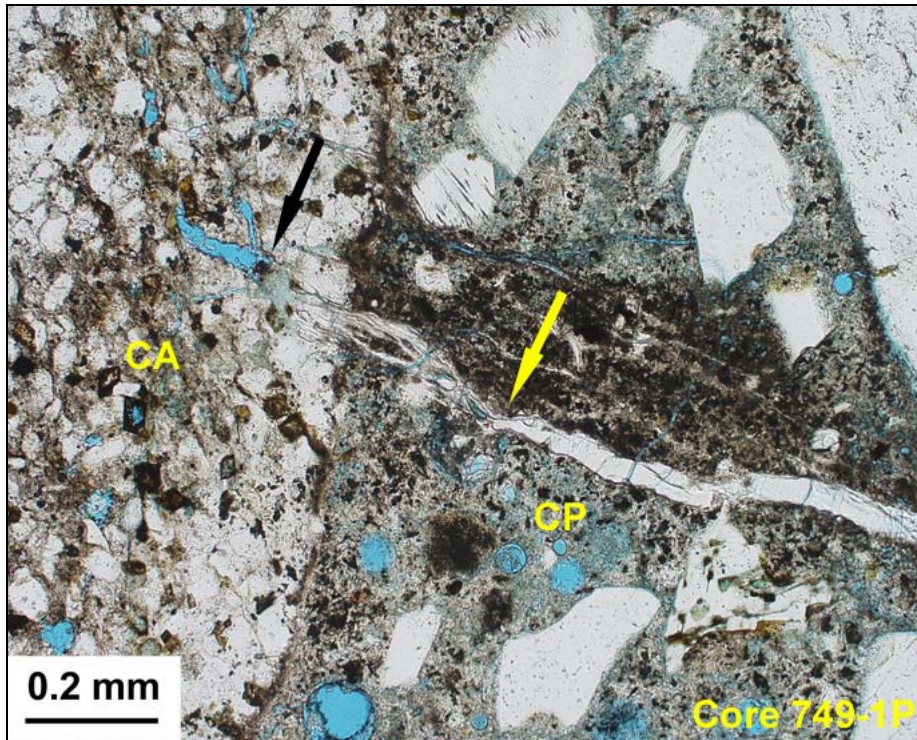


Figure 22 (cont'd): Reflected light photomicrographs indicating microcracking visible in honed cross sections of the concrete.



**Figure 23:** PPL photomicrographs. The arrows indicate minor surface-parallel microcracks just below the upper surface of the structural concrete in Cores 748N3-1P, 748S-1P, and 750-1P. The cracking could be related to some freeze-thaw distress but the evidence is quite scant.



**Figure 24:** Core 749-1P exhibits the most well-developed alkali-silica reaction even if the reaction is only in its early stages and limited to the uppermost 2” of the structural concrete. In the two PPL photomicrographs, the black arrows indicate reaction cracks within coarse aggregate grains (CA). The yellow arrows indicate where these have propagated into the adjacent cement paste (CP). ASR gel plugs are found at the periphery of the reactive stone and ASR reaction gel lines the paste cracks. A large deposit of reaction gel (G) is shown adjacent to the reactive stone in the lower image. The stone in the upper image is a silty argillite and that in the lower image is a quartz arenite.

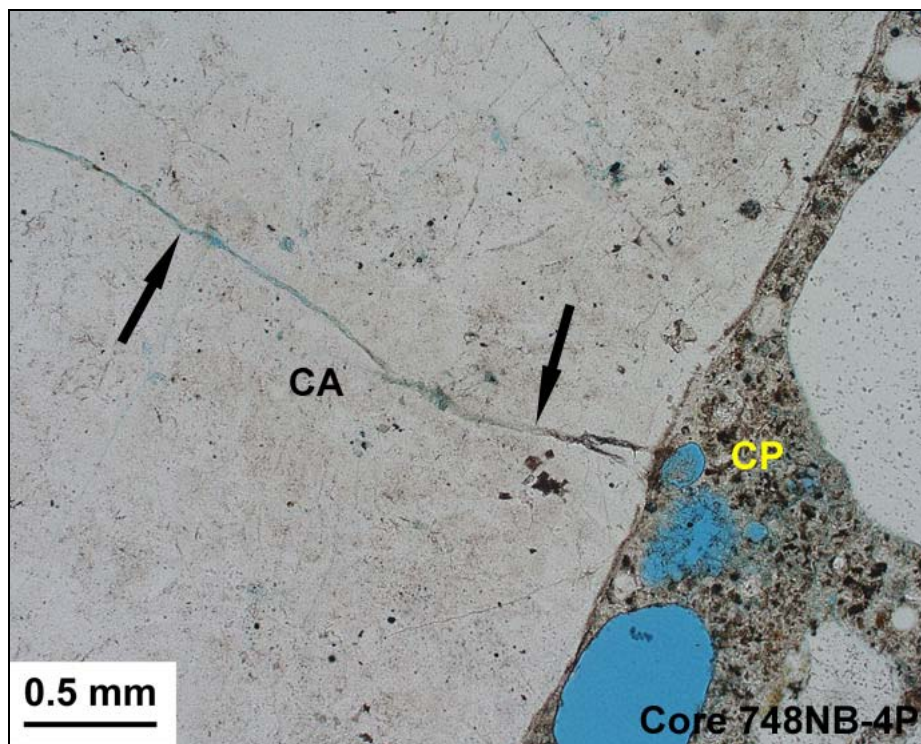
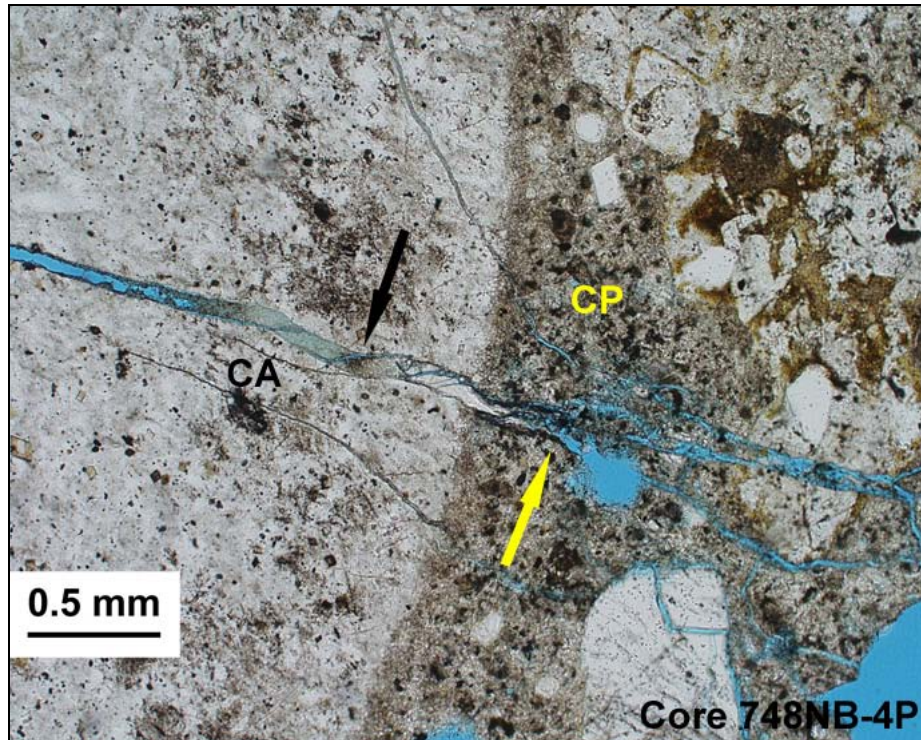


**Figure 25:** Only very minor traces of reaction are detected in Core 748NB-4P as shown by these PPL photomicrographs. In both cases, the black arrows indicate reaction cracks within chert coarse aggregate grains (CA). The yellow arrow indicates where one of these has propagated into the adjacent cement paste (CP). A well-defined ASR gel plug is found at the periphery of the reactive chert in the upper image. No adjacent paste cracking is found in the area shown in the lower image.

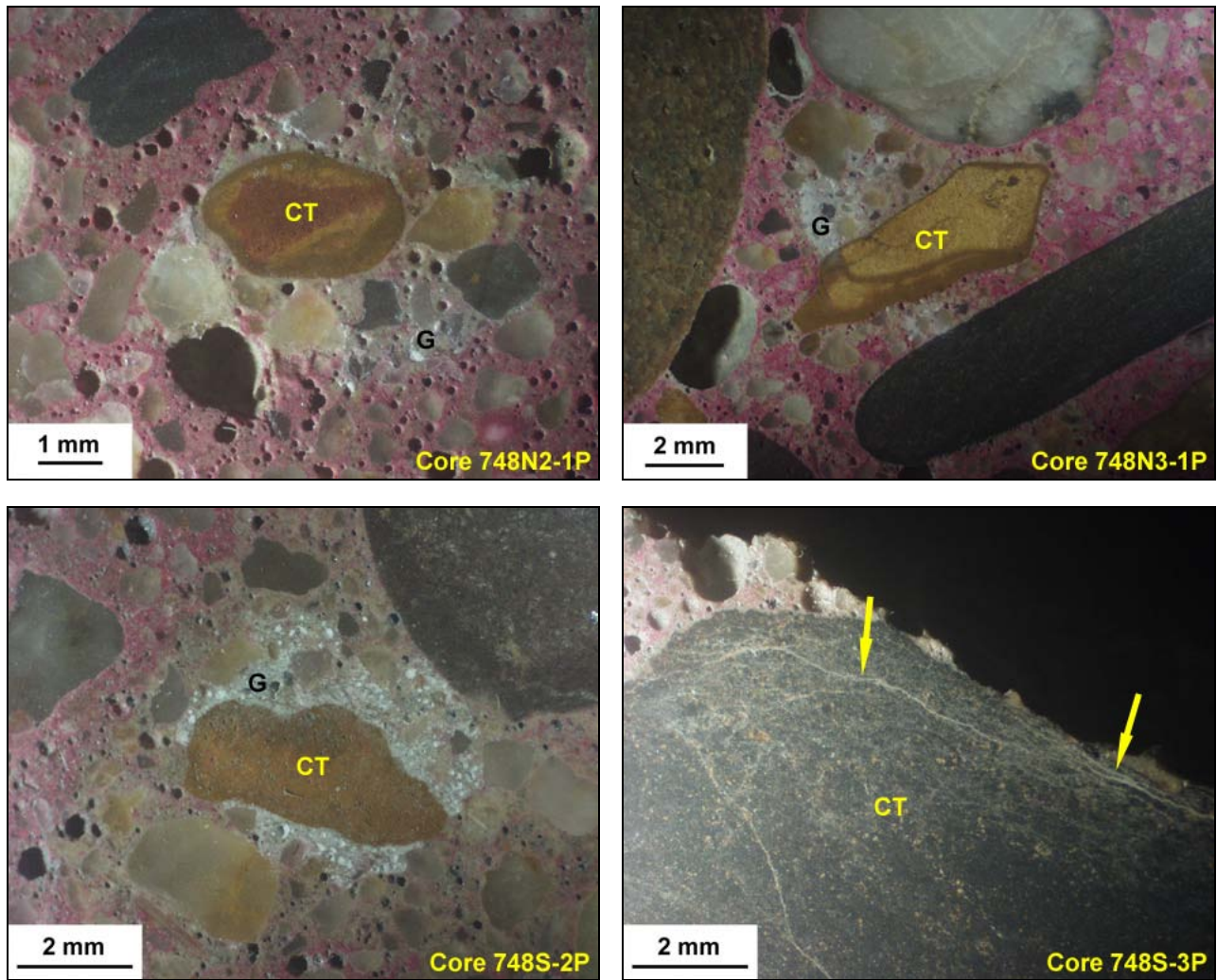


**Figure 26:** Reflected light photomicrographs taken of honed concrete core sections. Very little evidence for ASR reaction is identified in most of the samples other than the early stage reaction in Core 749-1P and the traces in Core 748NB-4P. Other than this, there are some minor exudates of ASR gel (G) in the paste adjacent to chert fine aggregate (CT) in some of the cores. These had not formed previously but rather exuded from the paste after cutting and polishing the core section. In the lower right image, a chert grain is shown with some internal microcracking (arrows). This is observed in Core 748S-3P but nowhere else.

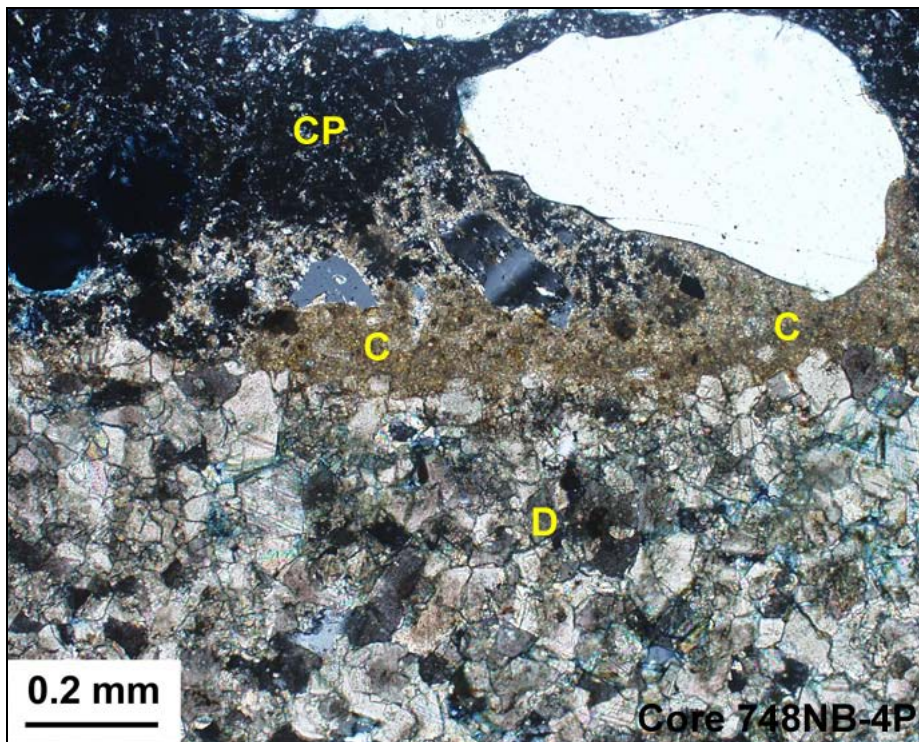
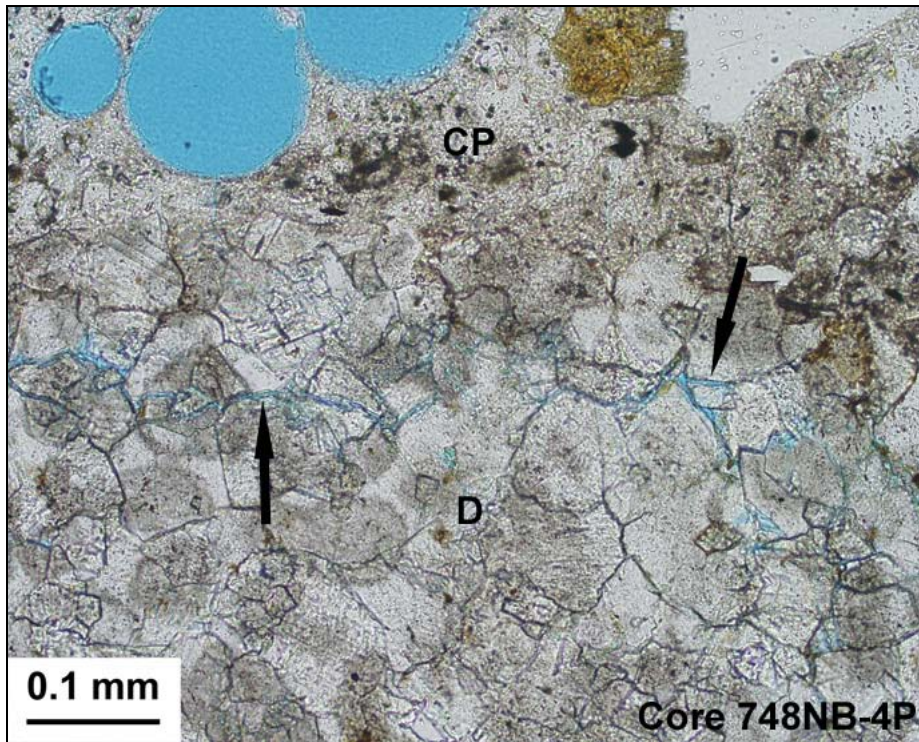


**Figure 27:** Evidence for alkali-carbonate reaction is detected in a single dolostone aggregate (D) present in Core 748NB-4P. In the upper PPL image, the arrows indicate microcracks just beyond the grain periphery. The location of the adjacent cement paste (CP) is labeled for visual reference. In the lower XPL image, the dedolomitization reaction is evidenced by a “bloom” of carbonation (C) that emanates from the dolostone aggregate. Note the golden-color of the carbonated paste juxtaposed against the normal dark color of the cement paste (CP).